



Almousa, Mohammad (2017) Effect of high leaf temperature and nitrogen concentration on barley (*Hordeum vulgare* L.) photosynthesis and flowering. PhD thesis.

<http://theses.gla.ac.uk/8125/>

Copyright and moral rights for this work are retained by the author

A copy can be downloaded for personal non-commercial research or study, without prior permission or charge

This work cannot be reproduced or quoted extensively from without first obtaining permission in writing from the author

The content must not be changed in any way or sold commercially in any format or medium without the formal permission of the author

When referring to this work, full bibliographic details including the author, title, awarding institution and date of the thesis must be given

Enlighten:Theses
<http://theses.gla.ac.uk/>
theses@gla.ac.uk



**Effect of High Leaf Temperature and Nitrogen
Concentration on Barley (*Hordeum vulgare L.*)
Photosynthesis and Flowering**

Mohammad Adel Almousa

**Thesis submitted in fulfilment of the requirements for the
degree of Doctor of Philosophy**

**Institute of Molecular, Cell and Systems Biology School of
Life Sciences**

**College of Medical, Veterinary and Life Sciences University
of Glasgow**

May, 2016

ABSTRACT

The response of plants to abiotic stress factors is a major determinant of the growth and yields of crops. In this study the effects of two separate but related abiotic stress factors on elite spring barley cultivars (*Hordeum vulgare*) were studied; the effects of high leaf temperatures (T_{leaf}) on photosynthesis rates, and the effects of high nitrogen supply on photosynthesis rates and flowering.

A novel method was developed for precisely controlling T_{leaf} within $\pm 0.2^{\circ}\text{C}$ of the set temperature. These experiments confirmed the results of others that increasing T_{leaf} above 36.0°C for 3 hours severely impaired light saturated CO_2 assimilation rates (A_{sat}) by irreversibly suppressing the activity of the C3 cycle by $>80\%$. This suppression was not attributable to stomatal closure, the generation of ROS, or an increase in photorespiration; instead the data were consistent with the hypothesis that limitations imposed by low chloroplast ATP levels. Measurements on whole leaf ATP levels in the light and dark of control and heat stressed leaves, however, were equivocal. Whole leaf ATP levels of light adapted leaves increased with T_{leaf} whereas the levels in dark adapted leaves initially decreased but increased again above 38°C ; most importantly, the difference – an estimate of chloroplast ATP levels - increased with T_{leaf} , an observation that is not consistent with the hypothesis.

The effects of high T_{leaf} was assessed on plants grown in soil and hydroponic solutions over a range of N-supply. Similar responses were observed regardless of the nitrogen status of the plants. Surprisingly, the unit leaf area (ULA)

photosynthesis rates of control (not heat stressed) attached leaves doubled when plants were grown in 16 mM N compared with 0.6 mM N (commensurate with arable soils); detailed analysis of CO₂ Assimilation vs. Internal CO₂ concentration (**A/C_i**) curves showed the carboxylation coefficient (**Φ_{CO₂}**) increased suggesting the ULA capacity of the C3 cycle had been boosted and this correlated well with ULA protein levels. It seems there is a good prospect, therefore, for boosting ULA photosynthesis rates, and hence grain yield, by increasing plant N-status above that currently used in arable production. Increasing N-supply to these levels, however, has detrimental effects on the morphology and development of barley. Increasing N-supply above 0.3 mM induced tillering (increased resource sink strength) as well as yield; above 1.6 mM, however, yields began to decline, flowering was delayed, although tillering (vegetative growth) continued to proliferate. At the highest levels used (16 mM) flowering was completely suppressed; the crown meristem underwent a vegetative to reproductive transition but stem elongation was incomplete – plants rarely progress beyond the 3 node stage. A series of transcript profiling experiments were conducted to establish the mechanisms by which high N-status suppressed flowering. Analysis of the transcriptional activity of key components of the flowering pathway in leaves, coupled with observations on floral spike development suggested flowering was triggered and initiated the development of the inflorescence at the crown meristem, but high N inhibits the development of the floral primordia. A RNA-Seq experiment was undertaken to determine the transcriptome profiles of 2-3 node stage floral primordia in plants grown in 16 mM and 0.64 mM N-supply. These studies were hampered by the poor level of annotation of published barley sequences, but none-the-less several interesting candidate sequences, including a homologue of the Arabidopsis flowering gene *AtAPETELLA2*, were strongly down

regulated; these results from these experiments are discussed in detail. Studies were also undertaken to manipulate sink strength in barley plants by reducing the number of tillers either mechanically (removal) or using 'uniculm' mutants from the Bowman barley accession lines. These experiments have proved to be challenging and progress has been slow; a discussion is provided on how these experiments may be completed.

The ultimate goal of this project is to develop barley lines with an optimized sink strength (tiller number) that will not trigger excessive vegetative growth when plant N-status is high. This should lead to the retention of N in the leaves of the main culm leading to higher ULA photosynthesis rates and hence higher yields. To achieve this, however, these plants will have to be further manipulated so that high plant N-status does not suppress flower development.

Table of Content

ABSTRACT	i
Table of Content	iv
List of Tables	ix
List of Figures	x
ACKNOWLEDGEMENTS	xiii
ABBREVIATIONS	xiv
Declaration	xix
1 Introduction	1
1.1 Food security	1
1.2 Abiotic stress	3
1.2.1 Arid region crop production	4
1.2.2 Leaf Temperature (T_{leaf})	7
1.2.3 Nutrient Availability	9
1.3 Photosynthesis	10
1.3.1 Light Reaction and Electron Transport	11
1.3.2 C ₃ Cycle	13
1.3.3 Reactions In Chloroplasts.	19
1.4 The Effect of Nutrients on Plant Physiology.	21
1.4.1 The Green Revolution	21
1.4.2 Effect of Nitrogen Levels on Crops.	24
1.5 Flowering in Crops	27
1.5.1 Control of Flowering in Cereal crops	27
	iv

1.6	Project Aims	30
2	Chapter 2: Materials and Methods	32
2.1	Growth and Maintenance of Plant Material	32
2.1.1	Growth in Soil.	32
2.1.2	Growth in Hydroponic Solutions	33
2.2	Measurement of Photosynthesis Parameters	35
2.2.1	Infrared Gas Exchange	35
2.2.2	Maximum Photosystem II Quantum Yield (Φ PSII max) and <i>in vivo</i> Electron Transport Rates (ETR) Measurements.	40
2.2.3	Measurement of Photorespiration.	40
2.3	Exposure of Attached Leaves to High T_{leaf}	41
2.3.1	Steady State Post Heat Stress Experiments	41
2.3.2	Pseudo Steady State Heat Stress Experiments	42
2.4	Measurement of Whole Leaf ATP Levels	42
2.4.1	Sample Preparation	42
2.4.2	Luciferin-Luciferase Assay	43
2.4.3	Sample Analysis	44
2.5	Measurement of Growth, Development, and Morphological Parameters	46
2.5.1	Growth Parameters	46
2.6	Development	47
2.6.1	Zadock's Scale for Quantifying Stage of Growth	47
2.6.2	Meristem Development	49
2.6.3	Cell Morphology and Number of Chloroplasts	50
2.6.4	Chlorophyll Content in Barley Leaf	50
2.7	Total Leaf Protein	51
2.7.1	Sample Preparation	51

2.7.2	Assessment of Protein Content Using the Bradford Assay.	51
2.7.3	Protein Gel Electrophoresis	52
2.8	Assessment of <i>VRN 1</i>, <i>VRN 2</i> and <i>VRN 3</i> Expression in Leaves.	53
2.8.1	Genomic DNA Isolation	53
2.8.2	RNA Extraction	53
2.8.3	Quantification of DNA and RNA	55
2.8.4	RNA Treatment with DNase	56
2.8.5	Agarose Gel Electrophoresis of RNA	56
2.9	RNA Sequencing	57
2.10	Statistical Analysis	58
3	Chapter 3: Response of Barley Photosynthesis Rates to Heat Stress.	59
3.1	Steady State Post Heat Stress Measurements	60
3.1.1	High T_{leaf} Effects on Photosynthesis	62
3.1.2	The Effects of T_{leaf} on Photorespiration Rates	69
3.1.3	ATP Levels in Heat Stressed Leaves	78
3.2	<i>Pseudo-Steady State</i> Heat Stress Measurements	82
3.3	Discussion	85
3.3.1	Steady State Heat Stress Experiments	85
3.3.2	Effect of Pseudo Steady State Heat Stress on A_{sat} and g_s	88
3.3.3	Effects of High Nitrogen and T_{leaf} on Photosynthesis Rates and Yields of Barley	89
4	Effect of Nitrogen Supply on Barley Photosynthesis and Development	92
4.1	Introduction	92
4.2	Preliminary Observation on the Effects of N Supply on Barley Morphology.	95
4.3	Photosynthesis	99
4.3.1	Assimilation Rate	99
4.3.2	Electron Transport Rate	102

4.3.3	Maximum Quantum Efficiency of PSII (φ_{PSII})	102
4.4	Growth and Development	106
4.4.1	Barley Growth	106
4.4.2	Zadoks Staging Scale	118
4.4.3	Meristem Elongation	119
4.4.4	Chlorophyll Content	121
4.5	Protein Concentration	123
4.6	Number of Chloroplast	125
4.7	Leaf Thickness	127
4.8	Discussion	130
5	Chapter 5 Transcriptome Profiling of Barley Floral Meristems	139
5.1	Introduction	139
5.2	Transcript Profiling of Barley Floral Meristem	145
5.3	Sequences Down Regulated in High Nitrogen.	152
5.3.1	Expansins.	152
5.3.2	Transcription Factors.	160
5.3.3	Negative Regulators of Translation.	162
5.4	Sequences Up Regulated in High Nitrogen.	164
5.4.1	Transcription Factors.	164
5.4.2	Control of Flowering.	164
5.4.3	Signalling.	165
5.5	Discussion	165
6	Chapter 6 General Discussion	170
6.1	Effect of High T_{leaf} on Photosynthesis	170
6.2	The Effects of Nitrogen Supply on the Growth and Development of Barley	179
6.3	Future Perspectives	184

Appendixes	189
References:	249

List of Tables

Table 2-1 Composition of Modified Hoagland's Solution.....	34
Table 5-1. Summary of Illumina RNA Sequencing of Floral Meristems from Barley cv Belgravia Grown in Moderate and High Levels of Nitrogen.....	146
Table 5-2. List of Selective Highly Abundant Sequences in Floral Primordia of Barley Grown in 0.6 mM Nitrogen	154
Table 5-3. List of Selective Highly Abundant Sequences in Floral Primordia of Barley Grown in 16 mM Nitrogen	158

List of Figures

Figure 1-1 The Transfer of Electrons and Protons in the Thylakoid Membrane During the Light Reaction.	12
Figure 1-2 C3 Cycle	14
Figure 1-3 The C3 Cycle and the Main Injury Sites Affecting A_{sat} .	15
Figure 1-4 Model for the Regulation of Flowering in Cereals.	29
Figure 2-1. Program of Leaf Chamber Conditions use to Obtained CO_2 Response Curves.	37
Figure 2-2. CO_2 Response Curves for Barley.	38
Figure 2-3 Light Response Curve for Barley	39
Figure 2-4. Calibration of Luciferin / Luciferase Assay for ATP Determination.	45
Figure 2-5 A Field Guide to Cereal Staging	49
Figure 3-1. The Effect of High T_{Leaf} and High Light Intensity on CO_2 Assimilation in Barley Leaves.	64
Figure 3-2. The Effect of Elevated T_{leaf} on Steady State in vivo Photosynthetic Electron Transport Rates of Attached Barley Leaves.	66
Figure 3-3. Effects of High T_{leaf} on the Maximum Quantum Efficiency ($\Phi_{\text{PSII max}}$) of Attached Barley Leaves.	68
Figure 3-4. A/Ca and A/Ci Curves of Attached Barley Leaves in 21% and 1% O_2 .	71
Figure 3-5. Light Response Curve of Attached Barley Leaves in Air Containing 21% and 1% Oxygen	73

Figure 3-6. Assessment of R_L Rates in Attached Barley Leaves in Response to Changing Ca and Absorbance.	74
Figure 3-7. The Effect of T_{leaf} on A_{sat} and Photorespiration Rates in Attached Barley Leaves.	77
Figure 3-8. The Effect of Increasing Leaf Temperature on Whole Leaf ATP Content in Barley Leaves.	81
Figure Figure 3-9 . Effects of Increasing T_{leaf} on Measured Pseudo Steady State A_{sat} and g_s in Attached Barley Leaves.	84
Figure 4-1. Effect of Fertilizer Application on the Growth and Development of Soil-Grown Barley.	97
Figure 4-2. The Effect of Nitrogen Application on the Growth of Barley in Hydroponic Solutions.	98
Figure 4-3. The Effect of Increasing N Supply on Hydroponically Grown Barley	100
Figure 4-4. The Effect of Increasing N Supply on Hydroponically Grown Barley	101
Figure 4-5. The Effect of N-Supply on <i>in vivo</i> Photosynthetic Electron Transport Rates (ETRs) of 7 Week-Old Barley.	104
Figure 4-6. Effects of N Supply on Maximum Quantum Efficiency (Φ_{PSII}) of 7 Week-Old Barley.	105
Figure 4-7. Effect of N Supply on the Number of Leaves Per Tiller in 10 Week Old Barley Plants.	108
Figure 4-8. Effect of N Supply on Tillering in 10 Week-Old Barley	110
Figure 4-9. Number of Spikes per Barley Plant Grown in Hydroponic Solutions with Different Levels of N.	111

Figure 4-10. Effect of N Supply on Stem Development in 10 Week-Old Barley.	112
Figure 4-11. Effect of N Supply on Stem Development in 14 Week-Old Barley.	114
Figure 4-12 The Nodes Position and Development of Spike in Barley.	116
Figure 4-13. Effect of N Supply on Grain Production in Barley.	117
Figure 4-14. Effect of N Supply on Barley Staging (Zadok's Scale)	118
Figure 4-15. Effects of Nitrogen Supply on Barely Floral Meristem Development.	120
Figure 4-16. The Effect of N Supply on Leaf Chlorophyll content of 8 Week-Old Barley	122
Figure 4-17. A The Effect of N Supply on Total Leaf Protein Levels in Barley	124
Figure 4-18 Estimates of Chloroplast Number in Barley Leaf Mesophyll Cells.	126
Figure 4-19 Barley Leaf Thickness in Response to Different N Supply	128
Figure 4-20 The Microscopy Images of Barley Leaf and Stem Among Different N Levels.	129
Figure 4-21 Nitrogen Supply Affects Tillering and Flowering in Barley	132
Figure 4-22 Bowman Lines.	136
Figure 5-1. Graphical Representations of Barley Floral Meristem Transcript Profiles from DESSeq2 Package	148
Figure 5-2. Transcriptional Changes of GO Metabolic Function Classes in Barley Floral Meristems Grown in Moderate and High Levels of Nitrogen.	151



وَفَوْقَ كُلِّ ذِي عِلْمٍ عَلِيمٌ

In the name of God, the Most Gracious, the Most Merciful.

“over every possessor of knowledge is one [more] knowing” (*Quran, 12:76*).

ACKNOWLEDGEMENTS

I'm very grateful for my supervisor Dr. Peter J. Dominy for his unfailing and constant support, advice, encouragement and all assistance he provided it to me. I highly appreciated the all valuable discussions we had thought the Ph.D. period about my experiments designs and its outcome. I don't think I have enough words to thank him or to adverse his assistance.

I would also like to thanks, all people of Dominy group especially: Dr. Najla Al Malki, May Wado, Janet Liard, Triona Seditas, Wen Liang, Ruth Hamilton, Theophilus Quashie and all other students and colleague work together with me. For all assistance and even little fever and support they did for me during four years of my project. I am especially thankful for every person in the Bower Building. Many thanks for all of friends who support me during that time. Special thanks to Dr. Mansour Abdullah and Dr. Zakriya Al Mohamad for their incredible support and encouragements during my Ph.D. project.

Last, but not by means least, massive thanks to my parents. The unlimited supports and encouragements by my father and mother from the begging by their particular cares and prayers and wishes. I think there is no word can express thanks to them, what they did was fruitful for me. I express thanks to my dearest wife who has to inspire me and give me emotion and support during my studies. I also thank my daughter Lujain, my sons Adel and Ali for their warm environment they provided for me and their patience during my study period. I would like to thanks my brothers and sisters and all belonging and family. Definitely, I haven't completed this without support from them.

ABBREVIATIONS

A	CO ₂ Assimilation Rate.
ABA	Abscisic Acid.
ADP	Adenosine diphosphate.
AMP	Adenosine monophosphate.
A _{max}	Maximum Photosynthesis Rate.
A _{sat}	Light Saturated Photosynthesis Rate.
ATP	Adenosine Tri Phosphate.
bp	Base pair.
BSA	bovine serum albumin
	Air CO ₂ Concentration. Chloroplast CO ₂ Concentration. Internal
Ca Cc Ci	CO ₂ Concentration.
cDNA	Complementary Deoxyribonucleic Acid.
CO	Constans
dS m ⁻¹	DeciSiemens per meter.
DHAP	Di Hydrogen Adenosine Phosphate.
2D	2 Dimensional Liquid Chromatography / Mass spectrometry.

DNA	deoxyribonucleic acid
dNTP	deoxynucleotide triphosphate
DTT	Dithiothreitol.
D Wt	Dry Weight.
E	Transpiration Rate.
EC	Electrical Conductivity.
EDTA	Ethylenediamine tetra acetic acid.
ETR	Photosynthetic Electron Transport Rate.
FAO	Food and Agricultural Organization of the United Nation.
FBP	Fructose Bisphosphate.
F6P	Fructose 6 Phosphate.
F ₀	Base Fluorescence.
F _m	Maximum Fluorescence
FT	Flowering locus T
F _v	Variable Fluorescence.
F Wt	Fresh Weight.
GABA	γ-4-aminobutyric acid. Glutamate

GAD	Glutamate Decarboxylase.
GB	Gibberellins
gDNA	genomic Deoxyribonucleic acid.
gs	Stomatal Conductance.
gm	Mesophyll Conductance.
ICARDA	International Centre for Agricultural Research in the Dry Areas.
IRGA	Infra Red Gas Analyzers.
kDa	Kilo Daltons.
kHz	Kilo Hertz
LRC	Light Response Curve.
LHCP	Light Harvesting Chlorophyll–Protein Complexes.
MPa	Mega Pascal.
mRNAs	Messenger Ribonucleic acids.
NADP	Nicotinamide Adenine Dinucleotide Phosphate
NADPH	Nicotinamide Adenine Dinucleotide Phosphate-Oxidase.
NCBI	National Centre for Biotechnology Information
NPQ	Non-Photochemical Quenching.

PAR	Photosynthetic Active Radiation.
PCR	polymerase chain reaction
PEP	Phosphoenol pyruvate.
PGA	Phosphoglyceric Acid.
pH	Hydrogen Ion Concentration Unit.
ppm	Part Per Million.
psi	Pounds Per Square inch.
PPFD	Photosynthetic Photon Flux Density.
PSI & PSII	Photosystem 1 & 2.
Rd	Dark Respiration.
ROS	Reactive Oxygen Species
rpm	Revolution Per Minute.
R5P	Ribulose 5 Phosphate.
RT-PCR	reverse transcriptase polymerase chain reaction
RuBisCO	Ribulose Bisphosphate Carboxylase-Oxygenase.
RuBP	Ribulose Bisphosphate.
SDS	sodium dodecyl sulphate

SDS-PAGE	SDS polyacrylamide gel electrophoresis
TAE	Tris-acetate EDTA
TEMED	N,N,N',N'-tetramethylethane-1,2-diamine
T _{leaf} and T _{air}	Leaf and Air Temperature, respectively.
Tris	Tris (hydroxymethyl) aminomethane
UV	ultra violet
VPD	Vapour Pressure Deficits.
v/v	volume/volume
w/v	weight/volume
Γ	CO ₂ Compensation Point.
ΦCO ₂	Carboxylation Efficiency.
ΦPSII	Maximum Quantum Efficiency of PSII (Fv/Fm).
ψH ₂ O	Water Potential.
ψP	Turgor Pressure.
^{Cyt} ψ _s	Cytoplasm Solute Potential.

Declaration

I declare that this thesis for the degree of Doctor of Philosophy has been edited entirely by me and the work presented herein was performed by me unless stated otherwise.

Signature:

1 Introduction

1.1 Food security

Over the last century global food production (agricultural production) has increased dramatically due to the application of better agronomic practices, integrated pest control methods, classical plant breeding, and advance bioengineering technologies (Huang *et al.*, 2006; Pretty, 2008). In particular cereal crop yields have literally doubled during the last 50 years since the beginning of the Green Revolution (Kishore and Shewmaker 1999; Toenniessen *et al.* 2003; Fischer and Edmeades 2010). These achievements are attributed to the ingenuity and efforts of farmers, agronomists, and plant biologists (Mann 1999). It is likely, however, that both increased yields and the acquisition of new arable land will be required to meet the food demands of the 21st Century. Whatever technologies are developed and used, they must be sustainable in the long term (Bassett 2010).

One problem is that food production is not uniformly distributed across the globe due to the diversity of terrain, local climatic conditions, the available germplasm and the local agricultural expertise. Clearly, there is a limit to the amount of land available for food production, and to the theoretical limit on the maximum attainable yield (yield potential) of any given crop (Barrett 2010). At present, global food production is unbalanced; 183 nations in the world depend on food from outside their borders (food imports) and this food comes from those countries with relatively low populations that practice intensive agriculture. Eighty percent of global cereal export is produced in the United States, Canada, Australia, and Argentina (Bureau, 2004;

Marchione and Messer, 2010), but this will not be the case in the next 60 years if the population continues to rise. Overall, based on realistic trends in food supply, it is forecast these countries may no longer be in a position to export food by 2050 (Brown, 2000; Beddington, 2010). In addition to these difficulties the World's population doubled between 1900 and 1960; by 2000, the population had reached 6.8 billion citizens, more than three-and-a-half times the population of 1900. The World Bank and the United Nations FAO document that 1 to 2 billion people are now malnourished due to a combination of the inadequate food supply, low income, and unfair food distribution (Pimentel *et al.* 1997).

In the past the demand for more food was met by increasing the area farmed. Our ancestors appropriated more natural habitat and turned it over to arable production. The germplasm used were landraces of wheat, barley, maize, rice, etc., plants that have their origins in lush tropical and sub-tropical climates. As farming spread into temperate and harsher regions new landraces were selected that performed well and practices such as irrigation, and later fertilizer application, were adopted to increase yields. In others words, the habitats were modified to suit these tropical and sub-tropical domesticated grasses.

Today the best (champion) yields of our major cereals are achieved, not in the regions where these plants evolved for tens of millions of years, but in intensively managed land with different climates often in different continents. Wheat, for example has it's origins in the Middle-East yields 4 to 7 T/Ha, but champion yields of 14 to 16.5 T/Ha are consistently recorded in Northen Europe (Jones 2015; FAO 2016).

Increasing crop production is now constrained by the amount of land that is suitable for agriculture, and by limited water supply and energy requirements. With limited suitable land and suitable elite crops lines to meet this challenge, improved crop yields and production are required (Beddington 2010). The available land for agricultural purposes is controlled by environmental factors such as protection of the remaining tropical rain forest to preserve biodiversity and to ameliorate the effects of green house gases. In addition, there is further pressure from urbanization due to the increase in human population over the next few decades.

However, to develop crops with higher yields, new techniques are required to accelerate progress, as the classical breeding methods are limited in scope and slow to implement. One area of research that has been identified is improving CO₂ assimilation rates in cereals (Khush 2013; Alemayehu et al. 2014; Gu et al. 2014).

1.2 Abiotic stress

Abiotic stresses can limit crop production in arid regions of the tropics and subtropics, where soil water potentials are often low more negative than -1.3 MPa (Lobell and Asner 2003; Sharkey and Zhang 2010). These can reduce plant growth by reducing water availability for crops leading to a decrease in stomatal conductance (**gs**), which controls gaseous exchange between leaves and the surrounding environment to allow CO₂ to be assimilated. However, **gs** responds to factors such as the vapor pressure deficits (VPD), blue light, and CO₂ concentration. High atmospheric VPD decrease **gs** to minimize transpiration and maintain plant cell turgor pressure, which leads to a reduced assimilation rate (**A_{sat}**) due to

deficiency of CO_2 entering chloroplasts of mesophyll cells (Ocheltree *et al.* 2014). A decrease in g_s might lead to a rise in leaf temperature (T_{leaf}) as transpirational cooling would also be impaired (Farquhar and Sharkey 1982).

1.2.1 Arid region crop production

Water is a major factor for achieving high rates of crop production particularly in arid regions and this directly affects yield. In arid and semi arid regions plants grow in harsh environments with low water availability and usually very high air temperatures during daytime. In addition, high soil salinity and high VPD reduce the growth of crops and may lead to death.

In some regions very high day and night temperatures are routinely recorded, for example in Kuwait where the average maximum temperature in July is 45.6°C , and the average T_{air} during July (the hottest month in the Arabian Peninsula) is 38.2°C . The annual average temperature is forecast to rise over the next few decades by $0.4^\circ\text{C}/\text{decade}$ due to Global Climate Change (UNFCCC 2012). That is the case for extreme arid regions where the crop production is very limited, but what are the predictions for the major crop growing in regions of the globe? how will the climate change and how will the established elite crop lines that have been developed to yield well in these regions respond?

It is a testament to the ingenuity of humans that the Green Revolution brought such improvements and is arguably our greatest achievement. The strategy of appropriating more natural habitat for arable production when food supply becomes limiting,

however, is not sustainable. The application of common sense, good genetics, and good agronomy has greatly extended the range of these crops but for a variety of reasons the prospects are poor to extending their range further into the less suited natural habitat that now remain. For example, there are vast tracts of lands in North Africa, South West Asia, the Americas, and Australia that are suitable for cereal production if rainfall was higher. Already 75% of the fresh water consumed by humans is used for food production; doubling food supply by 2050 by simply scaling, doing more of what we already do, will place severe pressure on global water supply, pressures that the planet may not be able to sustain. There are two potential solutions to the water shortage problem. One is to continue to attempt to exploit these arid habitats whilst developing crops that are more water use efficient. This is the high-tech strategy adopted in research programs in the Developed World, one that may be doomed to failure. Crops in arid habitats are also exposed to high temperatures that can quickly and irreversibly damage tissues unless transpirational cooling is significant. Reducing transpiration may conserve water but present the plant with a more acute problem, heat stress. Many wild plants that are native to these arid regions do reduce transpiration but have evolved complex mechanisms and adaptation for coping with high tissue temperatures, but our major crops simply do not possess these.

Another potential solution for growing crops in arid climates may emerge from engineers, not biologists. Two-thirds of the surface of our planet is covered by water; there is no shortage of water. The problem, of course, is most of this water is highly saline and toxic to crops. Technologies exist, however, to de-salinate sea water to a level that is comparable to potable water extracted from rainfall run off. One of the

better technologies, reverse osmosis, uses pressure to force water molecules in sea water through re-cyclable semi-permeable membranes. Commercial – scale reverse-osmosis desalination plants are currently operating in Western Australia and the Middle – East producing potable water at a cost of less than \$0.50 a cubic meter (Zhou and Tol 2005; Zhang and Babovic 2012). This adds less than 20% to the cost of cereal production but further economic efficiencies are likely to arise through technological developments and economies of scale. Perhaps, instead, we should turn our attention to why we don't grow crops in regions where there is sufficient rainfall (Northern Europe, Northern Asia, Canada, for example). Farming here is not practised because of late spring or early autumn frosts which decimate crops. The challenge then becomes one of developing cereal crops that can withstand freezing conditions (as do many wild grasses in these regions), or of shortening their life cycle by deactivating their circadian clocks (wheat, barley and rice lines exist that complete a life cycle in 8 weeks).

Clearly, although the major crops do not yield well in hot arid regions unless extensively irrigated, what thermotolerance and drought tolerance mechanisms have the many species of wild plant that inhabit these regions developed? To address this question, it is perhaps instructive to consider, why plants need water. Water is the matrix in which all bio-catalytic process occurs. It is required to maintain the three-dimensional structure of bio-molecules, and to transport cargo within and between cells from one metabolic site to another. Water is required in plants for cell growth through the mechanisms of turgor-driven cell expansion in the zones of elongation adjacent to the meristems where cell division occurs (Taiz and Zeiger 2006). Water is also required to establish turgor pressure in guard cells to open the

stomatal pore thereby enabling plants to acquire CO₂ for growth (Taiz and Zeiger 2006; Laanemets *et al.* 2013). In addition, turgor is also required to establish an erect habit, particularly in herbaceous, non-woody plants such as cereal crops. Without the ability to stand erect, a plant may in the long term, become out competed once a closed canopy forms above. The rate of water and nutrient ion transport through the xylem from the root to the shoot (transpiration) is also regulated by the turgor pressure of the guard cells, and so the acquisition of mineral ions and other simple solutes is dependent on leaf water potential (Farquhar and Sharkey 1982; Kim *et al.* 2010; Buckley and Mott 2013). Finally, water evaporation from the stomatal pores cools the leaf due to the latent heat of evaporation (Farquhar & Sharkey, 1982).

1.2.2 Leaf Temperature (T_{leaf})

What happens when plants cannot gain sufficient water to maintain an optimal level of hydration? This occurs in many habitats, but is a particularly acute problem for plants growing in high temperatures in arid and semi-arid zones.

Numerous studies have shown that when most herbaceous plants lose 10-20% of their tissue water they wilt severely, and in some cases the plants will not recover upon re-watering. One might predict that upon mild desiccation (>90% hydration state), the guard cells might lose their turgor resulting in stomatal closure thereby minimizing further water loss; but they do not. The vast majority of plants partly close their stomata but water loss to the atmosphere continues resulting in severe wilting. The reason for this can be determined by monitoring leaf temperature as leaves

begin to desiccate. The leaf temperature (T_{Leaf}) of well watered plants in high air temperatures ($>35\text{ }^{\circ}\text{C}$) is often 5-10 $^{\circ}\text{C}$ below air temperature (T_{air}) due to transpiration but as the rate slows (T_{Leaf}) rises. The plant is now faced with several short-term and long-term dilemmas regarding its requirement for water. Partial desiccation will result in an increase in the cytoplasm /vacuole volume ratio and this will further decrease the concentration of solutes in the cytoplasm (osmotic potential Ψ_s); metabolic flux will slow although it is difficult to assess by how much, and this may have longer term consequences for growth and survival. Water loss will also cause a slowing of turgor-driven growth, and the onset of visible wilting symptoms (loss of erect stature); again all of these factors will compromise the plant in the medium-to-long term, but are unlikely to affect plant survival in the short term.

One of the topics addressed in this thesis is the effects of heat stress on photosynthesis rates in barley leaves. The experiments reported will build on the finding of others from our laboratory (Shahwani 2011; Almalki 2014).

1.2.2.1 High T_{leaf}

Increasing leaf temperature, however, is a serious threat to plant survival in both the short and long term. Experiments have shown that elevating leaf temperature of some plants to $38\text{ }^{\circ}\text{C}$ for just ten minutes effectively 'cooks' the leaf (Velitchkova et al. 2013). Re-watering and placement in optimal growth temperatures does not lead to a recovery; the leaf fully desiccates, turns brown and dies. Therefore, it is reasonable to assert that, leaf temperatures of $>38^{\circ}\text{C}$ for a few hours irreversibly damages leaves, causing symptoms that are mistakenly attributed to water deficit.

If this is the case, research effort should be re-focused to determine the mechanism that confers thermal-tolerance on some plants, not drought-tolerance.

Previous studies in our laboratory have shown the primary effect of heat stress is the impairment of carbon flow in the C3 cycle. In these studies, however, heat stress was applied to intact leaves in the dark to remove the effects of photochemically generated reactive oxygen species (ROS) on activity; this approach allowed the direct effect of heat stress on photosynthesis to be studied. Briefly, these studies have shown leaf temperatures (T_{Leaf}) of 38.0°C for 3 hours in the dark suppresses intact leaf CO₂ assimilation rate (A_{Sat}) by > 80%. The corresponding capacity for PS II photochemistry and photosynthetic electron transport is impaired by 40%, the CO₂ supply to the chloroplast is unaffected, but carbon flow through the C3 cycle is inhibited by 85%. The implication is that the primary cause for the observed decline in A_{Sat} is a direct effect of heat stress on the kinetic properties of the C3 cycle. Studies have subsequently shown that carbon flow between Ribose 5-phosphate and Ribulose 1,5-bisphosphate was severely impaired and chloroplastic ATP levels have been implicated (Schrader et al. 2004).

1.2.3 Nutrient Availability

Plants require mineral nutrients in inorganic form for growth. The essential nutrients required for plant growth are nitrogen, phosphorus and potassium. The amount of nutrients available to crops is a major determining factor of yields (Taiz and Zeiger 2010; Marschner and Rengel 2012). Good nutrient management programmes are essential for increasing food availability by raising the yields of crops. N is

assimilated by plant biochemical processes to maintain cellular growth through the supply of essential N-containing biomolecules such as amino acids, proteins, and nucleic acids so it has an important role in determining vegetative growth and yield of plants including crops. The Green Revolution in the last century was achieved in part by better management of nutrient addition to the soil.

A deficiency in N availability to cereals may lead to reduced growth and aberrant development. The deficiency modifies leaf colour to yellow which results in abscission of older leaves and the remaining N is remobilized into younger upper leaves with a light green colour. Stem and tiller hardness increased due to N deficiency and stem colour becomes a darker pink or brown (Taiz and Zeiger 2010).

To study the effects of nutrient availability on plant growth, hydroponic experiment can be used with modified Hogland's nutrient solution. By manipulating the concentration of different elements, the effect of these on plant growth can be assessed

Another theme investigated in this study is the effects of high N supply on vegetative growth, photosynthesis rates and flowering in barley.

1.3 Photosynthesis

The source of organic carbon in our globe is the autotrophic algae and higher plants by fixation of atmospheric CO₂ into organic forms of carbon that build up cell

structures via the C3 cycle. Nutrient availability in the soil and other abiotic factors such as high temperature and CO₂ concentration can control the photosynthesis rates in cereals.

The energy obtained from the sun is the main source of energy that is essential for life on Earth. The process of photosynthesis is the only way living organisms can harvest and utilize the energy of the sun. Viewed simply, photosynthesis is a process that synthesizes carbohydrates by fixing atmospheric CO₂ in presence of solar light. The fixation of CO₂ requires 'high energy' compounds in the form of ATP and NADPH which are produced by splitting water molecules into O₂ and H⁺ to supply 'energized electrons' for transport through the thylakoid membrane in the chloroplast. For convenience, photosynthesis can be divided into two reactions: the Light Reactions or Photochemistry, and Carbon Assimilation (Taiz and Zeigler 2006).

1.3.1 Light Reaction and Electron Transport

Light drives the chemical reaction of photosynthesis through protein complexes imbedded in thylakoid known as photosystem I (PSI) and photosystem II (PSII) (Figure 1-1). Photosystem II (PSII) is activated by light and splits H₂O molecules which results in the release of O₂ gas, and two H⁺ that are released into lumen of the thylakoid, and two 'energised' electrons. The electrons (e⁻) are then transported through the thylakoid electron transport chain down a redox gradient through different acceptors such as quinones (Q_A, Q_B and PQ), the Cytochrome b₆f complex, and plastocyanin (PC) before reducing oxidized PSI (PSI⁺). PSI⁺ is

generated by light and the 'released energized' e^- is transferred through other acceptors finally reducing the soluble flavoprotein ferredoxin-NADP reductase (FNR) which in turn reduces $NADP^+$ to NADPH. The protons in the lumen that were released by PSII oxidation of water, and the protons transported into lumen via the reduction and oxidation of the $Cyt b_6/f$ complex, develops a pH gradient. This gradient (or proton motive force, pmf) drives the ATP synthase complex and ATP is generated in the stroma. Thus, NADPH and ATP, which are required by C3 cycle to assimilate carbon, is generated by light (Baker 2008; Taiz and Zeiger 2010; Nickelsen and Rengstl 2013; Pribil *et al.* 2014).

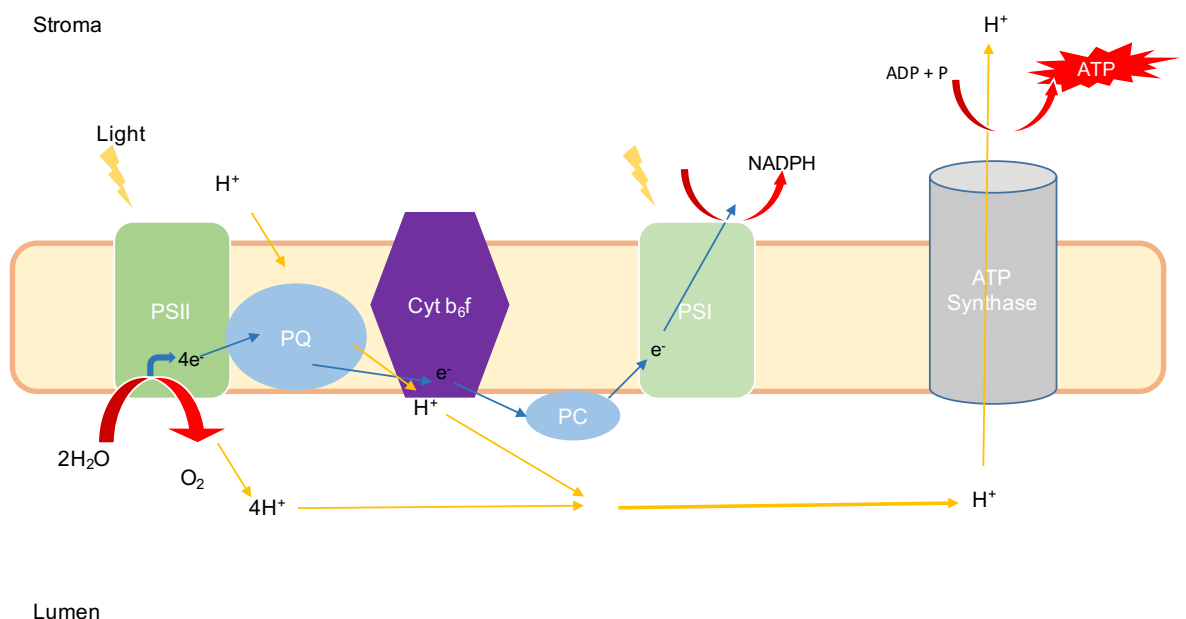


Figure 1-1 The Transfer of Electrons and Protons in the Thylakoid Membrane During the Light Reaction.

After illumination both PSII and PSI become oxidized ($PSII^+$ and PSI^+) and the removed e^- move to the right and pass through redox complexes down a gradient. $PSII^+$ removes e^- from water and regenerates PSII; O_2 is evolved and H^+ are released to the thylakoid lumen. The e^- that are photochemically ejected from PSII pass through PQ, the cytochrome b_6/f complex and PC re-reduce PSI^+ ; as this occurs, H^+ are 'pumped' from the stroma to the lumen. The proton gradient that is established drives the ATP synthase resulting in the generation of ATP.

1.3.2 C3 Cycle

The most important pathway of fixing atmospheric CO₂ to provide carbon skeletons for the synthesis of organic compounds in autotrophs is the C₃ (Calvin-Benson) Cycle. The elucidation of the C₃ Cycle was provided in 1950s by a series of classic experiments (Benson and Calvin 1950; Benson 1951). The reaction shown in Figure 1-2 starts when CO₂ carboxylation take place by binding CO₂ and water with Ribulose 1,5-Bisphosphate (RuBP) to generate two molecules of 3-phosphoglycerate. The carboxylation reaction is catalyzed by Ribulose 1,5-Bisphosphate Carboxylase / Oxygenase (RuBisCO). The second stage is the reduction of 3-phosphoglycerate (3PGA) to Glyceraldehyde 3-phosphate (G3P) through two steps. First, the formation of 1,3-Bisphosphoglycerate (1,3-GBP), by utilizing ATP which was generated in the light reactions, and is catalyzed by 3-phosphoglycerate kinase. Second, the 1,3-GBP is reduced to Glyceraldehyde 3-phosphate by NADPH that is also generated in the light reactions. The third and last phase of the C₃ cycle results in the conversion of some of the G3P into RuBP to support further carboxylation events. This stage also requires ATP generated during the light reactions associated with the thylakoid.

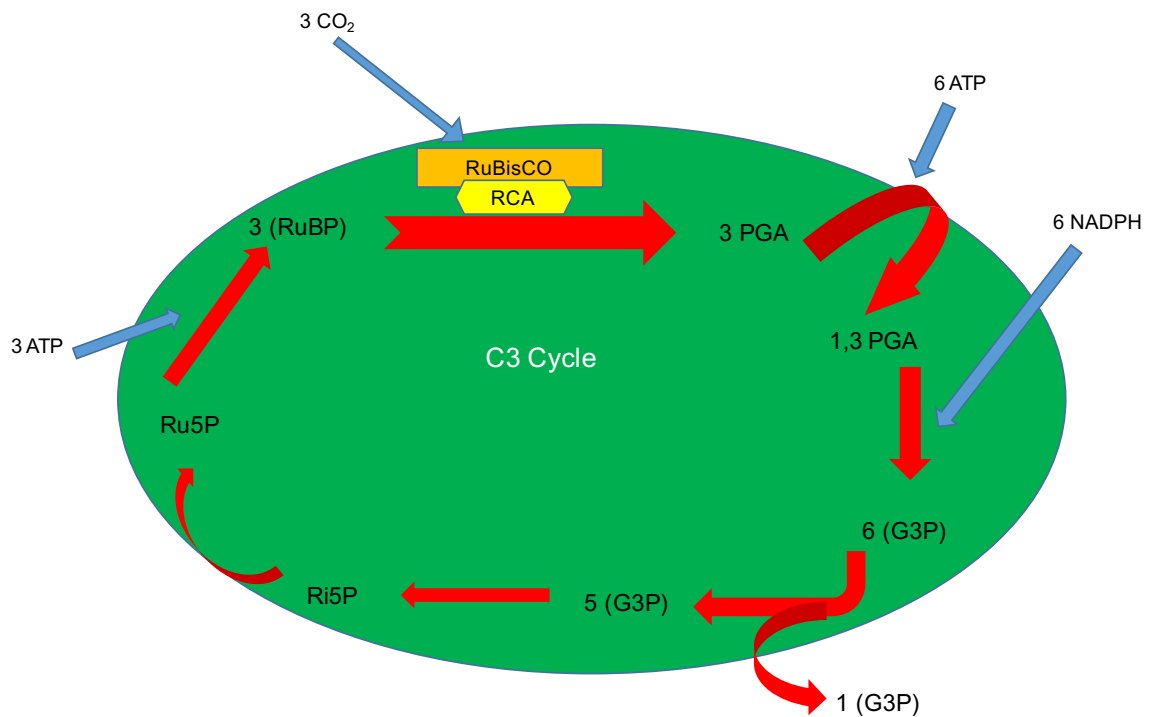


Figure 1-2 C3 Cycle

See text for description

The fixation of atmospheric CO₂ is the key point for studying the effect of abiotic stress on photosynthetic rates and many different factors might be involved. Figure 1-3 shows the different component that regulate the C3 cycle. First, RuBisCO may be sensitive to stress and that can result in limitations of photosynthesis. Second, the enzyme that activates RuBisCO in leaves, is RuBisCO Activase (RCA), may be affected. Third, the regeneration of RuBP, which is dependent on the availability of ATP, may be affected as shown by metabolomics profiling (Shahwany, 2011). The supply of CO₂ through the stomatal pore (stomatal conductance, **gs**) and across the mesophyll cell (mesophyll conductance, **gm**) to the chloroplasts. Finally, photorespiration rates (R_L) that arises from competition between CO₂ and O₂ for binding site on RuBisCO, might also be affected.

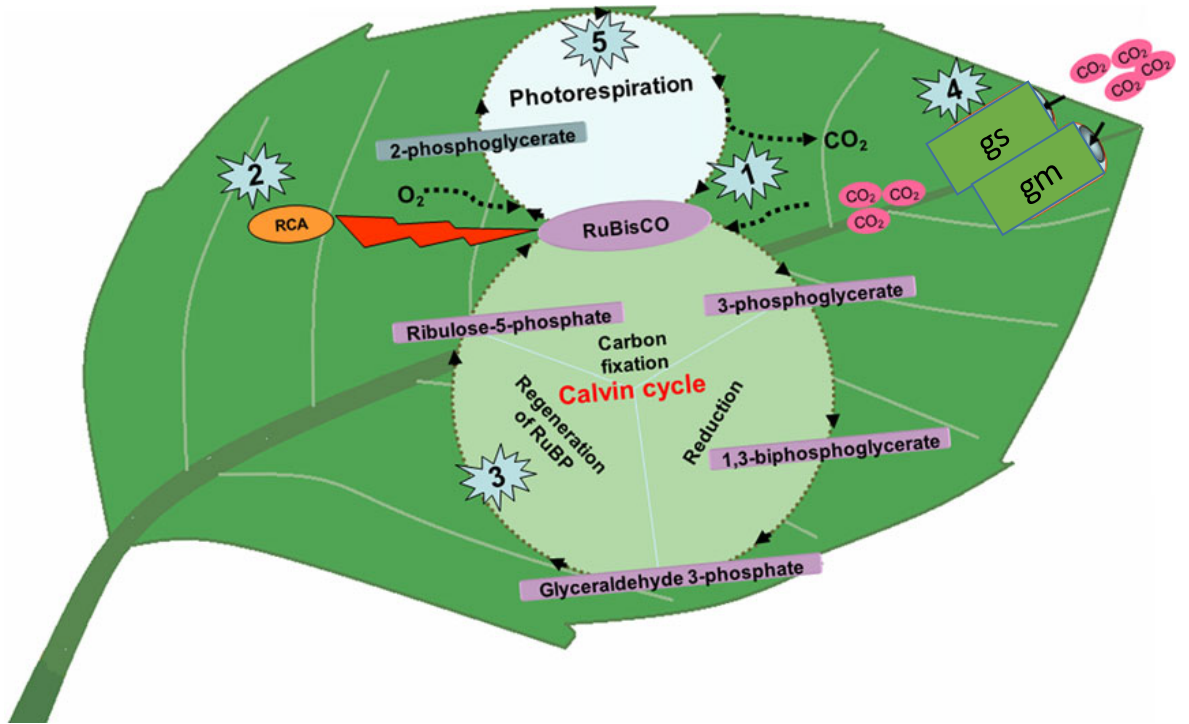


Figure 1-3 The C₃ Cycle and the Main Injury Sites Affecting A_{sat} .

The main three steps of C₃ cycle and the major five locations that might be involved in decreasing of A_{sat} in response to stress. These are: (1) RuBisCO, (2) RCA, (3) Regeneration RuBP, (4) CO₂ transport across stomata and mesophyll cell membrane, and (5) Photorespiration. The modified diagram was adopted from (Singh *et al.* 2014).

1.3.2.1 Regeneration of RuBP

The regeneration of RuBP is essential to allow the C3 cycle to continue and fix CO₂. The regeneration of RuBP may be the most significant factor responsible for the decline of C3 turnover in response to high T_{leaf} (Schrader et al. 2004; Cen and Sage 2005; Kubien and Sage 2008; Sage et al. 2008). The regeneration of RuBP might be limited by the activities of enzymes involved in regeneration of RuBP in the C3 cycle or ATP levels in the chloroplast. Previously at the University of Glasgow, metabolomic studies on the leaves of spring barley cv. Optic indicated leaf 3PGA levels were depleted whilst the pools of precursors for RuBP synthesis were unchanged. These findings suggest that thermal damage acts somewhere between Ribulose 5-phosphate (Ru5P) and 3PGA (Shahwani 2011). This implicates damages to one or more of the following enzymes: Ribose 5-phosphate Isomerase (Ri5PI), phosphoribulokinase (PRK), RuBisCO, RCA, or a decline in ATP levels. Experiments performed by Almalki (2014) indicated the endogenous activities of RuBisCO, Ri5PI, and PRK were not significantly affected by heat stress in leaves that showed >80% thermal inhibition of photosynthesis.

ATP is required as a substrate for PRK for the conversion of Ru5P to RUBP. Currently, it is not clear whether the synthesis of ATP in chloroplasts is impaired by heat stress, as previously hypothesized (Lawlor 2002). Other studies (Sharkey and Seemann 1989) found the amount of ATP in the chloroplast was unchanged under mild water stress while at the same time RuBP declined by 50%. Chloroplast ATP levels may not change in response to high T_{leaf} stress but changes in the ATP/NADPH ratio may affect the metabolic balance of chloroplast mechanisms resulting in impairment of A_{sat} .

1.3.2.2 RuBisCO

RuBisCO is the major enzyme in all phototrophic higher plants, algae, and photosynthetic prokaryotes. On the other hand, rather than fixing CO₂ and turning C3 cycle to generate two molecules of 3-phosphoglycerate, RuBisCO can catalyze an oxygenation reaction to fix O₂ resulting in photorespiration. In optimum condition of saturating light and CO₂ concentration, the amount of RuBisCO in cereal leaves such as rice might be around 35-50% of total leaf protein (Makino et al. 2000). In contrast, RuBisCO accounts for only around 2-6% of the total cell protein in marine phytoplankton (Losh et al. 2013). The activation of RuBisCO requires CO₂, Mg⁺² and RCA to convert RuBP and CO₂ into 3PGA (Lorimer 1981; Uematsu et al. 2012). The kinetics of RuBisCO and mesophyll conductance vary among plant species *In vivo* (Walker et al. 2013).

1.3.2.3 RuBisCO Activase (RCA)

RuBisCO requires activation *in vivo* and this is achieved by an increase in stromal pH, Mg²⁺ concentrations, and redox potential as well as the enzyme RCA which removes RuBP from RUBisCO allowing CO₂ to bind first at the catalytic site. RCA is activated by ATP which then leads to the activation of RuBisCO (Portis et al. 2007). However, overexpression of RCA in rice causes a slight increase in the activation state of RuBisCO with an accompanying decrease in RuBisCO content and **A_{sat}** (Fukayama et al. 2012). In addition, most published research indicate that RCA is thermo sensitive and can limit photosynthesis under moderate and high temperatures (Crafts-Brandner and Salvucci 2000; Carmo-Silva et al. 2012; Carmo-Silva and Salvucci 2013). Others, however, have indicated that moderate heat

stress induces a large subunit isoform of RCA which increases A_{sat} during heat stress; stress doesn't reduce the activity of RCA but can increase A_{sat} (Sage et al. 2008; Wang et al. 2010; Prins et al. 2016). The results obtained from experiments in University of Glasgow determined that RuBisCO (and hence RCA) remained active after heat while A_{sat} decreased by approximately 80% in barley leaves that were exposed to $T_{\text{leaf}} 40\text{ }^{\circ}\text{C}$ (Schrader et al. 2004; Yan et al. 2011). Others have also found no correlation between thermal suppression of photosynthesis and RCA and RuBisCO activity (Yamori and von Caemmerer 2009).

1.3.2.4 CO₂ Supply

In C₃ plants such as wheat, barley and rice, CO₂ diffuses passively from the surrounding air through the stomatal pore, across the intracellular air spaces, and across the cell membrane and cytoplasm and into the chloroplast stroma. The rate of CO₂ uptake is therefore determined by the CO₂ concentration gradient (driving force) between the air (**Ca**) and the chloroplast (**Cc**), and the conduction pathway (comprised of the sum of the boundary layer, stomatal, and mesophyll conductances – **ga**, **gs**, **gm** respectively), but **Cc** and **gs** are the only components that the plant can regulate at the metabolic levels. Factors that affect **gs** include temperature, light intensity, water availability, ABA and CO₂ concentration (Froese and Sehon 1975; Epron et al. 1995; Gillon and Yakir 2000; Cano et al. 2013).

1.3.2.5 Photorespiration

The competition between O₂ and CO₂ on the binding site of RuBisCO was first hypothesized in 1943 by Tamiya & Huzisige who provided no evidence for their

conclusion. Twenty-eight years later evidence was supplied through the *in vitro* experiments of Ogren and Bowes and others (Ogren and Bowes 1971; Lorimer 1981). During water stress, low CO₂ and high light intensity, leads to an increase in photorespiration rates and in addition ROS, one view is that photorespiration protects photosynthesis components from ROS (Voss et al. 2013; Walker et al. 2014). Timm et al. (2015) concluded that an increase in photorespiration resulted in protection and subsequently enhanced assimilation rates in Arabidopsis.

1.3.3 Reactions In Chloroplasts.

ATP is generated in chloroplasts by the process of photophosphorylation which involves the formation of redox generated proton gradients and the action of the ATP synthase (Solhaug et al. 2014; Peltier et al. 2016). More recently, however, a role has been found for secondary redox reactions such as chlororespiration.

1.3.3.1 Chlororespiration

Changes in the redox status of the plastoquinone (PQ) pool of dark-adapted algae was first mentioned by Goedheer (1961). The term 'Chlororespiration' was mentioned by Bennoun in 1982 (Peltier and Cournac 2002). Further evidence was supplied from studies on the competition between cyclic and linear electron transport in algae and cyanobacteria (Dominy and Williams 1987) with changing temperature and light intensity; and this has been confirmed by others (Sage et al. 2008; Wang et al. 2010). In addition, the presence of two NAD(P)H dehydrogenase (NDH) complexes in chloroplasts (NDH-1 and NDH-2) where the NDH-1 is similar to mitochondrial NDH complex has been found (Peltier and Cournac 2002; Peltier

et al. 2016). Chlororespiration is now viewed as a mechanisms to feed 'respiratory' electrons from NAD(P)H into the PQ pool in the dark to produce ATP by chemiosmosis (Cornic and Baker 2012; Peltier et al. 2016).

1.3.3.2 Cyclic Electron Transport

The electron flow from water through PSII and PSI to NADP⁺ or oxygen is termed linear electron transport. The other electron transport pathway in the chloroplast of higher plants and algae (cyclic electron flow, **CEF**) has recently been reviewed (Eberhard et al. 2008; Peltier et al. 2016; Yamori and Shikanai 2016) where electrons flow around the PSI and PQ to increase proton concentration in the lumen without reducing NADP⁺ to NADPH. Abiotic stress is believed induces **CEF** to maintain the ATP/NADPH ratio and maintain ΔpH across the thylakoid. The demand on ATP increases which stimulates **CEF** in response high T_{leaf} , low T_{leaf} , drought, low CO₂ and anaerobic conditions (Endo and Asada 2008; Yamori and Shikanai 2016). While chlororespiration is dependent upon NDH complexes in the thylakoid, **CEF** requires either electron transport through NDH complexes which are known components of the NDH-dependent pathway, or through PGR5-PGRL1 (Yamori and Shikanai 2016). Increasing T_{leaf} leads to an increase in the rate of **CEF** in rice cultivars that is associated mainly with the NDH pathway rather than the FQR complex pathway (Essemine et al. 2016).

1.3.3.3 Water- Water Cycle (Mehler Reaction)

The reaction was identified by Mehler (1951) in chloroplast where the electrons from the photo-oxidation of dioxygen are passed through PSII and PSI and used in a

futile cycle to reduce di-oxygen to produce hydrogen peroxide instead of reducing NADP⁺ (Endo and Asada 2008). The Mehler reaction is thought to act as a safety valve for photosynthetic **ETR** allowing the dissipation of captured light energy when the C3 cycle is down-regulated. The hydrogen peroxide (H₂O₂) generated is subsequently converted to water by the action of catalase to prevent oxidative damage to the chloroplast. In addition, ROS (reactive oxygen species) can inhibit CO₂ assimilation in minutes. However, the rate of the Mehler reaction is initially high upon illumination and before the start of CO₂ assimilation, but gradually returns to basal levels once the C3 cycle is activated (Eberhard et al. 2008; Endo and Asada 2008; Cornic and Baker 2012; Ozgur et al. 2015; Wiczarz et al. 2015) .

1.4 The Effect of Nutrients on Plant Physiology.

The amount of nutrients supplied to plants affects their growth and yield by controlling many different physiological processes, including photosynthesis, flowering, vegetative growth, secondary thickening, and others. The judicious management of fertilizer use is an important factor in attaining high crop yields.

1.4.1 The Green Revolution

There is a compelling case that a new Green Revolution is required to cope the raising food requirements over the next few decades. Through the history of human civilization there have been several green revolutions. The first major revolution was implemented by the Sumerians by constructing water canals from the Euphrates River and using nutrients and irrigation water to maximize the yields of barley and

wheat to 2 T Ha^{-1} . Other green revolutions occurred at similar times in different parts of the globe as humans developed farming as the method for sustaining a population. The second major green revolution occurred in United Kingdom during 18th century. Here revolutionary agronomic methods such as crop rotation using legumes and grasses (called Norfolk rotation) improved the yield of wheat and barley to 2 T Ha^{-1} compare to the common yields in Europe 0.8 Ha^{-1} (Sinclair and Sinclair 2010; Sinclair and Ruffy 2012).

The latest and major Green Revolution occurred between 1950s -1970s. At the beginning of the last century the availability of cheap fertilizer to farmers resulted in major increases in vegetative growth of crops although only modest increases in grain yield. The use of the fertilizers in the first half of the 20th century was the main driver of the green revolution, but subsequently plant breeding played a significant role as well (Borlaug 2007; Sinclair and Sinclair 2010; Sinclair and Ruffy 2012). The highest yield production of wheat currently cultivated in United Kingdom which is around 14 t Ha^{-1} , while rice production in Japan and Philippines reached 11 and 12 T Ha^{-1} respectively (Fischer and Edmeades 2010; FAO 2016). At present the World's population is growing faster than crop yields and crop production. The next Green Revolution, it is argued, will depend on the application of genetics to increasing photosynthesis rates and develop crops that are more tolerant of abiotic stress factors such as extremes of temperature, limited water availability, and increasing atmospheric CO_2 levels (Pretty 2008; Fan et al. 2012; Rakshit et al. 2012; Vermeulen et al. 2012; Komatsu et al. 2013; Yin 2013; Curtis and Halford 2014; Emebiri 2015; Chang et al. 2016).

The Green Revolution has its origins in Mexico just after World War II but through the 1960s and 1970s expanded to other parts of the world. Huge improvements in crop production were attained principally through the development of improved germplasm and the adoption of modern farming practices. The focus on improved germplasm involved the development of dwarf lines and improved resistance to pathogens, especially in wheat and rice (Borlaug 2007). The major dwarf genes that were identified and involved in the Green Revolution were Reduced height (Rht) in wheat, and in rice Slender 1 (Sln1) and semidwarf 1 (sd 1) (Peng et al. 1999; Hedden 2003; Chandler and Harding 2013). Rht and Sln1 are nuclear encoded genes, and their products are transcription factors that include a DELLA protein motif and suppress growth through a downregulation of the transcription of key growth sequences (Hedden 2003; Saville et al. 2012; Chandler and Harding 2013). Sd1 is believed to regulate GA biosynthesis by deactivating GA 20 in rice; GA is normally required to degrade the DELLA transcription factors and stimulate growth, so its absence decreases shoot elongation (Spielmeyer et al. 2002; Khush 2013; Rao et al. 2014). The dwarf and semidwarf shoot phenotype solved the lodging problem, and the corresponding reduced sink (straw) ensured the acquired N increased biomass and N use efficiency resulting in higher yields (Fischer and Edmeades 2010; Sinclair and Rufty 2012; Bennett et al. 2013). The production of wheat in Mexico, for example, was around 0.5 t Ha⁻¹ before the green revolution while it reached 8 t Ha⁻¹ now days (Borlaug 2007). Resistance to a variety of pathogens was enhanced by the identification and introgression of some key alleles (Saville et al. 2012; Chandler and Harding 2013; Boden et al. 2014; Van De Velde et al. 2017).

1.4.2 Effect of Nitrogen Levels on Crops.

Increasing N levels supply results in an increase in A_{sat} in rice and this has been attributed to an increase in RuBisCO content of leaves (Nakano et al. 1997; Makino et al. 2000; Tsutsumi et al. 2014). Tsutsumi and coworkers (2014) found that in rice there was a strong positive correlation between RuBisCO content and N supply regardless of whether the plants were grown hydroponically or in soil (Tsutsumi et al. 2014). Agricultural soils typically contain the equivalent of between 0.5mM and 0.8 mM available N (Marschner and Rengel 2012). The amount of N supplied to a plant may lead to an increase in A_{sat} but excess nutrients may be stored in the leaves, stems, roots, or partitioned to the grain; consequently there are several sinks for these resources (Kirschbaum 2011). Storage of resources (nutrients and carbon) in these different sinks does not necessarily result in an increase in grain yield in crop plants such as barley, wheat and rice. In cereals, RuBisCO is considered as a nitrogen sink in leaves; RuBisCO can account for 30-50% of the total leaf protein, whilst it accounts for only 2-6% in phytoplankton (Makino et al. 1997; Losh et al. 2013; White et al. 2016). The high amount of RuBisCO in leaves can cause a decrease in photosynthesis rates in CO₂ enriched air; photosynthesis rates are normally expected to increase in high CO₂ but transgenic rice containing only 60% of normal levels showed an increase in carbon assimilation compared with controls (Makino et al. 2000). Improving crop production in high concentrations of CO₂ and developing appropriate fertilizer management regimes is an important goal over the next few decades as climate changes; this will help to optimize nitrogen application and decrease leaching of N into lower soil layers and water resources.

The capacity of A_{sat} might be enhanced by increasing the amount of available nitrogen for plant growth which leads in high yields. Thus, the increasing N supply might lead to an increase in crop production and yield depending on what will be achieved by the next green revolution.

Nitrogen is, of course, an essential nutrient for the synthesis of proteins and nucleotides. Soil N is available for acquisition by plants either as nitrate (NO_3^-) or/and in the reduced form as ammonium (NH_4^+). For metabolic assimilation *in planta* N has to be present as NH_4^+ so acquired NO_3^- must first be reduced. This is achieved in non-green plastids in the roots of some plants, or in the chloroplasts in the leaves of others. In these organelles, nitrate reductase converts NO_3^- to nitrite (NO_2^-), and then Nitrite Reductase converts this to NH_4^+ . The ammonium ion can also be taken uptake directly from soil. The assimilation of NH_4^+ into amino acids also occurs in chloroplasts through the action of glutamine synthetase (GS) and the GOGAT (Glutamine-2-oxoglutarate aminotransferase) cycle (Forde and Lea 2007; Tabuchi et al. 2007; Xu et al. 2012). The product of the GOGAT cycle, glutamate, plays a central role in amino acid production as it is the precursor of all other amino acid synthesised in plants (Forde and Lea 2007; Xu et al. 2012).

Several transport mechanisms for the acquisition of N from soils have been identified. The *NRT2.1* gene encodes a NO_3^- transporter that is induced by *NRT1.1*, which is also a NO_3^- transporter. *NRT2.1* expression is also triggered by *NLP7*, a NIN-Like Protein7 (Li et al. 2014c; Medici and Krouk 2014; Ruffel et al. 2014). Furthermore, NRTs have been implicated in loading and unloading NO_3^- from the xylem in root and shoot tissues. The source/ sink relationship controlling NO_3^-

movement within the whole plant is complex. During the seedling and vegetative growth stage young leaves act as the N sink, whilst mature leaves become the N source, particularly during senescence (Dechorgnat et al. 2011; Xu et al. 2012). During leaf senescence amino acids and NH_4^+ are remobilized into new plant organs. Both GS and the GOGAT pathway, and NADH, are required during proteolysis (Tabuchi et al. 2007; Avice and Etienne 2014). As there is a large energy requirement during NO_3^- assimilation into NH_4^+ in plastids, low ATP/NADPH ratios may occur. During photorespiration, some N is lost as NH_4^+ is converted to gaseous NH_3 which is excreted from the plant. Therefore, **CEF** and the Mehler reaction, in addition to photorespiration, may be required to balance energy requirements of the cell. (Tabuchi et al. 2007; Xu et al. 2012; Walker et al. 2014).

The relationship between nitrate assimilation and endogenous activities of the the phytohormones Cytokinins (CK) and Auxin is complex. Nitrate uptake stimulates the biosynthesis of CK in both roots and shoots, but CK also suppresses *NRT* gene expression thereby providing a negative feedback system for nitrogen homeostasis in the plant. CK also directly promote bud growth and branching which will result in an increased nitrogen sink strength (Albacete et al. 2008; Ghanem et al. 2011; Kiba et al. 2011; Kudoyarova et al. 2014) . In contrast, high soil NO_3^- concentrations are sensed by the plant and this triggers an auxin-dependent lateral root initiation (Kiba et al. 2011). In addition, auxin regulates CK biosynthesis thereby adjusting the auxin:cytokinin ratio. A deficiency in CK result in reduced shoot growth and promotes the growth of root. Auxin biosynthesis itself is reduced by another negative feedback regulatory system which leads to a lowering of the auxin:cytokinin ratio. Several studies have demonstrated a close relationship between root:shoot

biomass ratio and auxin:cytokinin activities (Albacete et al. 2008; Ongaro and Leyser 2008; Werner et al. 2008; Xu et al. 2012; Takatani et al. 2014; de Wit et al. 2016).

1.5 Flowering in Crops

The target for researchers is to increase yield production of the crops in general. In barley and all other cereals, this goal needs to be achieved in next few years by increasing the number and quality of the grain whilst cultivating the smallest possible area of agricultural land, that is increase crop production by increasing yields ($T\ Ha^{-1}$) due to low availability of new suitable agricultural lands. Flowering can be induced by abiotic stress whilst the grain yields can be increased by fertilizer application. High yields with short time period between sowing and harvesting may allow multiple harvests per year.

1.5.1 Control of Flowering in Cereal crops

The crown or axillary meristem forms tillers in grasses during the vegetative phase of growth while it forms florets during the reproductive growth phase (Zhang and Yuan 2014). Flowering in plants is a complicated process that can be activated by several separate, and in some cases interacting, pathways. For example, in the model plant *Arabidopsis* flowering can be initiated by photoperiod, age (autonomous), the growth regulator gibberellin (GA), and exposure to low (vernalization) and warm temperature pathways (Wellmer and Riechmann 2010). In monocots inflorescence meristems are generated from the primary stem but

normally some of the secondary stems (tillers) can also develop inflorescences leading to the formation of spikelets and fertile floral organs in cereals. In some respects the flowering in cereals can be considered to be more complicated than other plants such as *Arabidopsis* (Zhang and Yuan 2014).

In spring barley long days are sensed by the phytochrome receptor PHYC in the leaf. The transition from a vegetative to a reproductive crown meristem is controlled by the expression of photoperiod (*PPD1*) and constans (*CO*) genes in the leaf. In barley there are two *CO* proteins, the first *HvCO1* is expressed during flower emergence until initiation, and the second *HvCO2* is highly expressed in late stages of terminal spike production and heading (Song et al. 2015). Furthermore, *CO* and *PPD1* induce *HvVRN3* (the homologue of *FT1* in *Arabidopsis* sp.), but this is not straightforward in barley. The expression of *HvVRN3* is considered to be suppressed by other factors such as *HvVRN2*. In barley leaves *HvVRN2* expression, a suppressor of flowering, can itself be suppressed in favourable conditions by *HvVRN1*. The suppression of *HvVRN2* will allow *HvVRN3* to be expressed in leaves and transferred via the phloem to the crown meristem where it transcriptionally activates *HvVRN1*; this is an absolute requirement for flowering in cereals (Song et al. 2015). The ABCDE model of flower development, first developed in the *Arabidopsis* and *Antirrhinum* (Coen and Meyerowitz, 1991), is also believed to operate in cereals the 'E class' genes are believed to function in floral meristem development which is controlled by two known sub families at *AGL2* and *AGL6*, in addition to floral organs, ovule (integument) and seed development (Dreni and Zhang 2016).

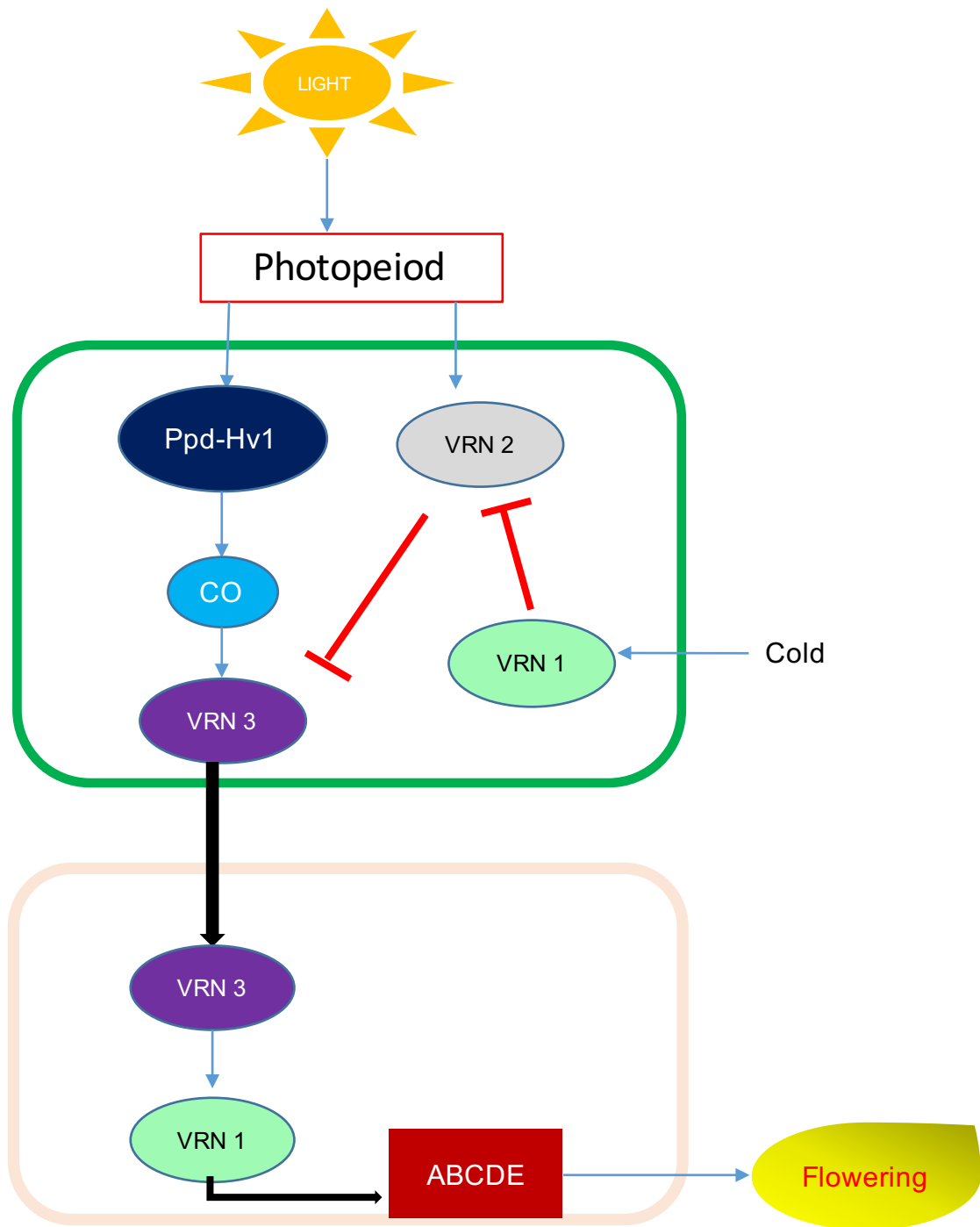


Figure 1-4 Model for the Regulation of Flowering in Cereals.

The circadian clock pseudo-response regulator (PPDH1) which activates the transcription factor CONSTANS (CO), leading to an accumulation of VRN3. VRN3 is a mobile signal that moves through the phloem to the crown meristem where it activates VRN1; this triggers the transition of the vegetative to a reproductive meristem and is required for flowering in cereals through ABCDE box model. In winter lines, flowering in autumn is prevented by the (Long Day) activation of the suppressor of flowering VRN2. VRN1 accumulates in leaves in response to the cold conditions and short days of winter and eventually suppresses VRN2, so that on return to spring, VRN3 accumulates in leaves and triggers flowering in the crown meristem.

In addition to VRN1, VRN2, VRN3 and CO other factors also regulate inflorescence development for example the growth hormone regulator GA. The production of GA will induce flowering in plant meristems. The role of nitrogen supply on flower development is unclear at present, but it is thought to affect VRN3 expression and GA production (Marín et al. 2011; Boden et al. 2014). The inhibition of GA biosynthesis might be controlled by KNOX proteins (Zhang and Yuan 2014), and *ELF3* (Boden et al. 2014). The importance of nitrogen supply in increasing plant growth and yield is well established but the mechanisms that underpin these responses is far from clear. It is obvious that the growth and yield of crops such as barley are badly compromised when N-supply is deficient but very high levels of N-supply suppress flowering whilst boosting biomass accumulation.

1.6 Project Aims

The original aims of this study were to build on earlier work from my host laboratory on the effects of high T_{leaf} on photosynthesis rates. Most of this work was conducted on barley plants grown in N-rich soils (compost) that generated aberrant phenotypes in barley. There were several aims for the work described in this thesis. First, was to confirm these responses were also shown by barley plants grown in normal levels of N-supply exhibiting normal growth phenotypes. Second, to establish whether, in the field where plants are exposed to high irradiance, light-generated ROS in leaves will impose damage on the photosynthetic apparatus before any direct effects of thermal stress. Third, to extend the preliminary observations of previous workers on this project and assess whether changes in whole leaf ATP levels can account for the observed changes in photosynthesis rates. It was hoped that a better understanding of these factors would lead on to a series of experiments where thermal tolerance in leaves of barley could be manipulated to improve yields under

high temperatures. The results from this section of the project, however, suggested this would not be achieved easily and so further experiments were abandoned. What was observed during this phase of the project, however, were interesting effects of N-supply on photosynthesis rates, and it was decided to set new aims and pursue this line of enquiry. Specifically, how does high N-supply promote tillering and suppress flowering in spring barley? Why do unit leaf area (ULA) photosynthesis rates increase with increasing N-supply. How does high N-supply suppress flowering in barley. Finally, can Φ_{CO_2} , (a measure of C3 cycle efficiency), and hence A_{sat} , be increased without suppressing the development of fertile florets? To address these question a better understanding is required of the N sensors and signalling pathways that lead to the three observed phenotypic responses (increase in A_{sat} and tillering, suppression of flowering).

2 Chapter 2: Materials and Methods

2.1 Growth and Maintenance of Plant Material

2.1.1 Growth in Soil.

Spring barley (*Hordeum vulgare* L.) of cultivars Belgravia or Optic (malting barley) were obtained from Nickerson Limagrains Limited (Rothwell, Lincolnshire, UK) and Syngenta Seeds Limited (Cambridge, UK). Seeds were germinated damp paper towels for 5-7 days and seedlings transferred into 2-Liter pots containing a mixture of compost and perlite (1:5). The seedlings were placed in controlled environment growth room (16/ 8 hour Day/ Night photoperiod, light intensity $300 \mu\text{moles.m}^{-2}.\text{s}^{-1}$, 23/18 °C temperature, humidity 60%).

In some experiments plants were germinated as described above and placed in 5L pots containing 15% top soil and 85% sand, and subsequently supplemented with a NPK fertilizer (3:1:2) at a final rate of 0, 2, 10, 20 and 47 g m⁻² of N; fertilizer was added at the 4-week and 8-week stage in two equal amounts (N application of 10 g m⁻² soil is equivalent to 100 kg / Ha, levels that are similar to those used in arable production). Pots were placed in a growth room (photoperiod of 16 / 8 hour, Light / Dark and 22°C / 16°C).

2.1.2 Growth in Hydroponic Solutions

Spring barley (*Hordeum vulgare* L.) of cultivars Belgravia or Optiac were germinated (Section 2.1.1) and transferred after 7 days into 20L plastic tanks. Seedlings were secured in a 300 mm length of 40 mm dia. domestic plastic pipe and eight of these were secured into holes cut into a piece of expanded polystyrene sheet (400 x 600 mm). This assembly was then inserted, roots down, into one of the 20 L plastic tanks which was filled with 15L of modified aerated Hoagland's solution ensuring the seedling roots were immersed. The tanks were then placed in a 22°C glasshouse supplemented with LED lighting providing an additional irradiance of $200 \mu\text{mol m}^{-2} \text{s}^{-1}$ PPFD to the seedlings (14/10 hr Day/Night cycle). Solutions were replaced once every week. The tank, pipe, and polystyrene assembly was opaque to prevent light ingress to the roots. This assembly also ensured all plants grew upwards for 200 mm before emerging from the cut end of the pipe; this proved to be beneficial particularly for plants grown in high N-supply that were prone to a prostrate growth habit due to little secondary cell wall thickening. Root aeration was achieved by aquarium air pumps. The hydroponics solutions used were based on Hoagland's recipe except that all salts containing nitrogen (ammonium and nitrate) were removed and removed balancing ions made up with sodium or chloride salts, and nitrogen was added back to the desired level using ammonium nitrate. This approach ensured the composition of the different Modified Hoagland's solutions differed only in the amount of NH_4NO_3 added. The recipe for Modified Hoagland's solution is presented in Table 2-1.

Table 2-1 Composition of Modified Hoagland's Solution

The amount of nutrients in milliLitres of stock solutions to added to water for a final 15 L volume. Full-strength of Hoagland's solution contains 16 mM nitrogen.

Nutrient	Stocks Concentration	Concentration of N (mM)							
		16	6.4	3.2	1.6	0.64	0.32	0.16	0.08
KH ₂ PO ₄	1.0 M	7.5	7.5	7.5	7.5	7.5	7.5	7.5	7.5
Mg SO ₄ .7H ₂ O	2.0 M	15	15	15	15	15	15	15	15
H ₃ BO ₃	50 mM	15	15	15	15	15	15	15	15
MnCl ₂ .4H ₂ O	500 µM	15	15	15	15	15	15	15	15
ZnSO ₄ .7H ₂ O	200 µM	15	15	15	15	15	15	15	15
CuSO ₄ .5H ₂ O	200 µM	15	15	15	15	15	15	15	15
H ₂ MoO ₄ .H ₂ O	700 µM	15	15	15	15	15	15	15	15
Fe Na EDTA	45 µM	15	15	15	15	15	15	15	15
NH ₄ NO ₃	1.0 M	112.5	45	22.5	11.2	4.5	2.3	1.1	0.6
K Cl	1.0 M	90	90	90	90	90	90	90	90
CaCl ₂ .2H ₂ O	0.5 M	120	120	120	120	120	120	120	120

2.2 Measurement of Photosynthesis Parameters

2.2.1 Infrared Gas Exchange

The measurements of photosynthesis on barley leaves were taken by using infrared gas analysers (IRGAs; LCpro+, ADC Bioscientific Ltd., Hoddesdon, Herts., UK) fitted with a rectangular narrow leaf chamber (window area of 5.8 cm²). Mature attached leaves were carefully placed in the leaf chambers ensuring no damage occurred and the full area of the chamber was covered. Illumination was provided by the LCpro LED unit; CO₂ supply, air temperature, and humidity were controlled by LCpro console.

2.2.1.1 CO₂ Response Curves

Assimilation of CO₂ with changes in air CO₂ concentration, *i.e.* **A/C_a** curves, were collected using standard procedures (Farquhar *et al.*, 1980). Using this approach useful photosynthetic parameters can be calculated and from estimates of the intracellular space CO₂ concentration (**C_i**), **A/C_i** plot can also be constructed. This approach effectively removes any stomatal control of assimilation rate.

Unless otherwise stated, mature leaves were sealed in LCpro+ leaf chamber and a program run with saturating light (>600 μmol photons .m⁻² .s⁻¹ PPF), 5 mmol humidity mol⁻¹ air, and ambient Ca (380 μmol CO₂ mol⁻¹ air) for 20 minutes to ensure the leaf was capable of achieving good rates of photosynthesis (*i.e.* over 10 μmol CO₂ . m⁻² . s⁻¹). If this was achieved all leaf chamber parameters were held constant

and **Ca** was adjusted from 0 to 1200 $\mu\text{mol CO}_2 \text{ mol}^{-1}$ air in incremental steps (0, 10, 20, 50, 100, 200, 300, 400, 500, 600, 800, 1000 and 1200) of 15 minutes. A typical control program is presented in Fig 2-1 and the corresponding **A/Ca** and **A/Ci** responses shown in Figure 2-2.

2.2.1.2 Light Response Curve

Immediately after completing a CO_2 response curve, the IRGAs were normally programmed to perform a Light Response (**A/I**) curve on the same section of leaf. All leaf chamber parameters were held constant (**Ca** 380 $\mu\text{mol CO}_2 \text{ mol}^{-1}$ air, humidity 5 mmol mol^{-1} air, constant **T_{air}**) but incident light intensity was incrementally changed from 0 to 1000 $\mu\text{mol photons} \cdot \text{m}^{-2} \cdot \text{s}^{-1}$ PPF) in 15 steps to provide the following leaf absorbances (0, 9, 17, 44, 87, 174, 261, 358, 435, 522, 696 and 870 $\mu\text{mol m}^{-2} \cdot \text{s}^{-1}$, PPF).

Figure 2-3 presents a typical light response curve from barley. From this curve, several important photosynthetic parameters can be extracted, such as the apparent quantum yield of photosynthesis (α), the maximum photosynthesis rate (**A_{max}**), light-saturated photosynthesis rate in normal air (**A_{sat}**), and the dark respiration rate (R_d). A standard absorbance factor of 0.86 was used to estimate absorbed light, correcting for losses from reflectance and transmission; the absorbed light energy is considered to be divided equally between the two photosystems (von Caemmerer 2013).

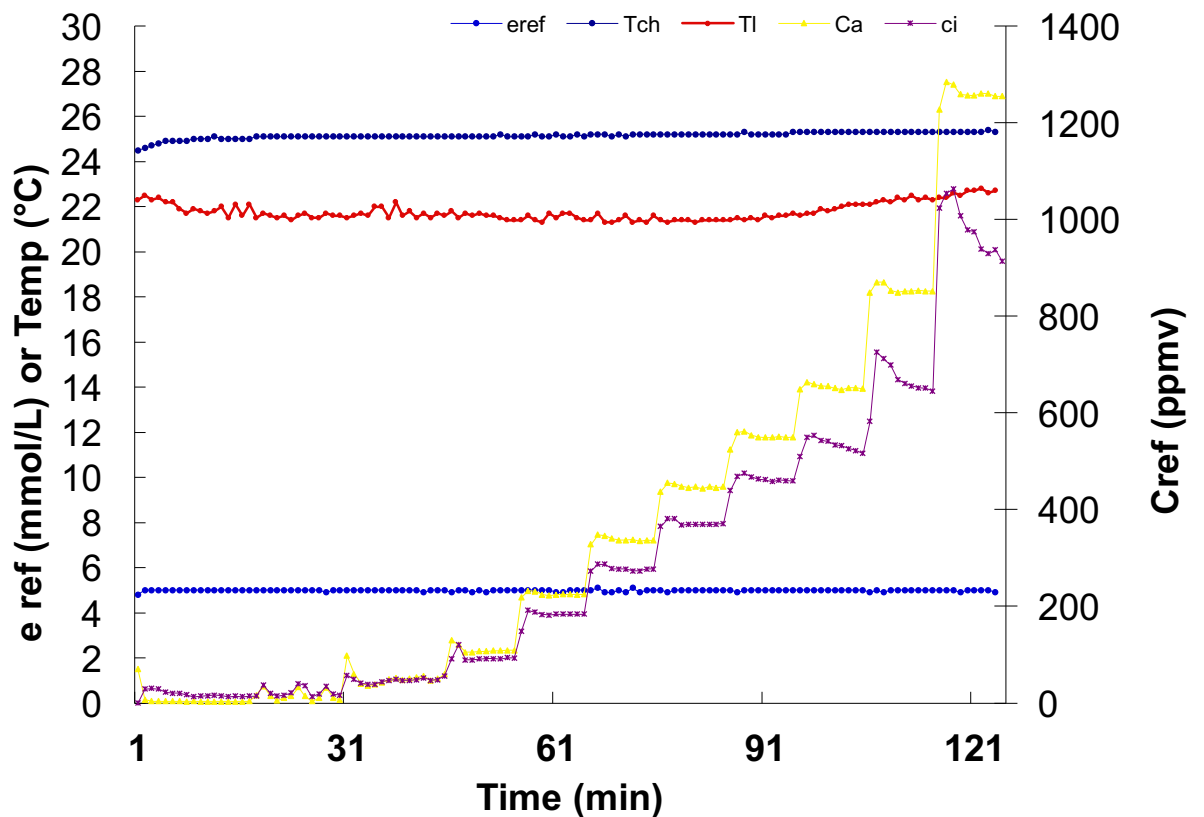


Figure 2-1. Program of Leaf Chamber Conditions use to Obtained CO₂ Response Curves.

The readings of IRGA were taken every one minute during the experiment to obtain CO₂ response curves. Light illumination was fixed at 600 $\mu\text{mol photons} \cdot \text{m}^{-2} \cdot \text{s}^{-1}$ (PPFD). T_{ch} is the temperature of the leaf chamber; T_{l} is T_{leaf} , which is the temperature of leaf surface; e_{ref} , air humidity; C_{a} and C_{i} , CO₂ concentration in the air and in the intercellular leaf spaces.

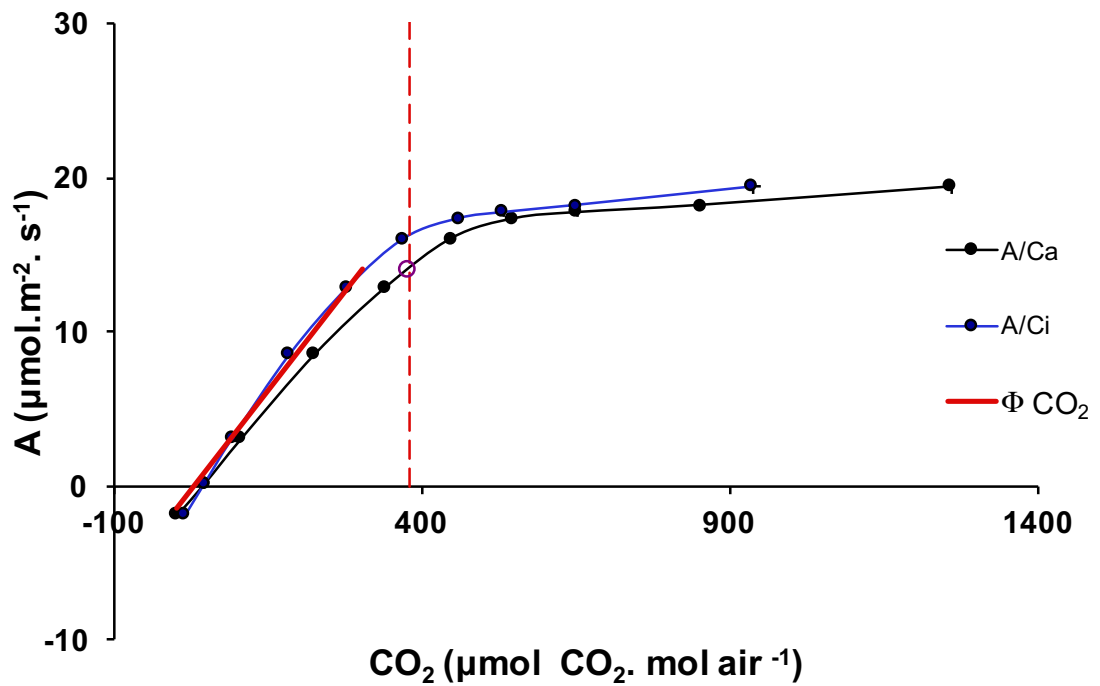


Figure 2-2. CO₂ Response Curves for Barley.

The barley leaf was sealed in LCpro leaf chamber with conditions described in Figure 2-1. The solid blue line is the relationship between net CO₂ assimilation (**A**) and the internal CO₂ concentration (**C_i**). Black solid line is the relationship between net CO₂ assimilation (**A**) and the air CO₂ concentration (**C_a**). Red Solid line Φ_{CO_2} (carboxylation efficiency) from the initial slope of the A/C_i curve. Red vertical dashed line ambient CO₂ (380 $\mu\text{mol CO}_2 \cdot \text{mol}^{-1} \text{air}$).

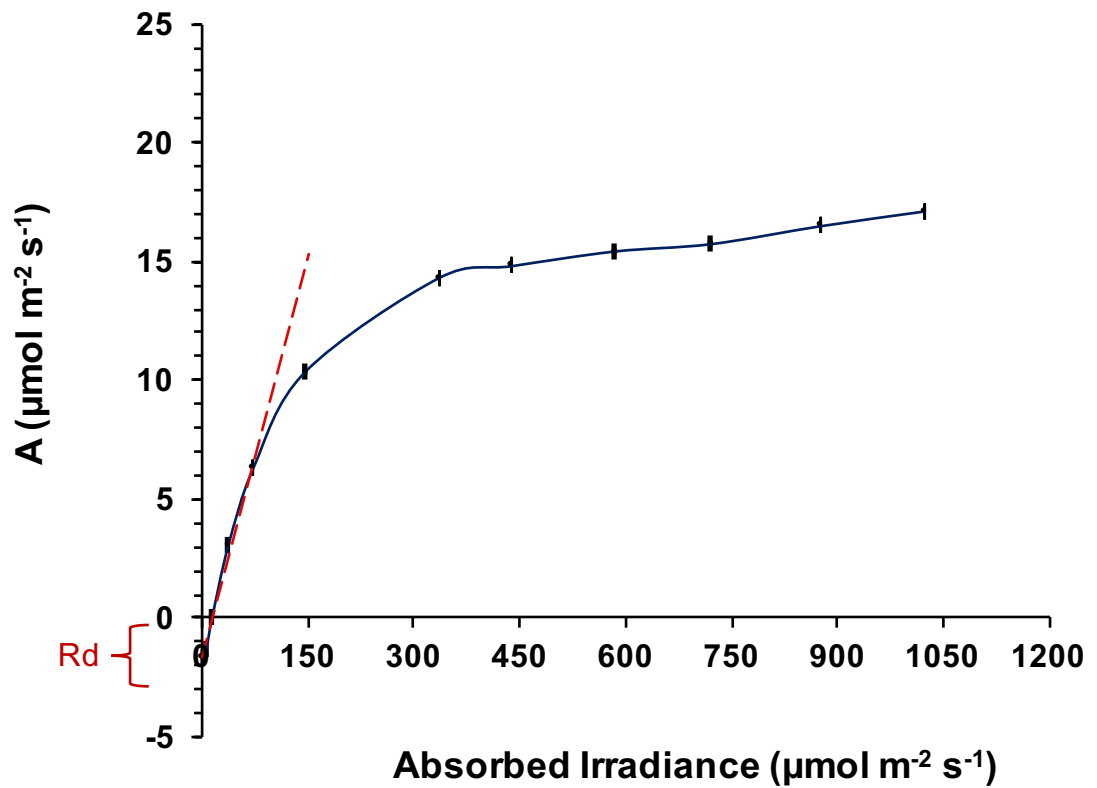


Figure 2-3 Light Response Curve for Barley

The barley leaf was sealed in LCpro leaf chamber with conditions described in Figure 2-1. Where the solid blue line is the relationship between net CO_2 assimilation (**A**) and light absorbance (PPFD). The CO_2 concentration was ambient air ($380 \text{ mol}^{-1} \text{ air}$) and $5 \text{ mmol} \cdot \text{mol}^{-1}$ humidity. The response curve is shown A_{sat} for barley c.v. Belgravia.

2.2.2 Maximum Photosystem II Quantum Yield ($\Phi_{\text{PSII max}}$) and *in vivo* Electron Transport Rates (ETR) Measurements.

The modulated chlorophyll fluorescence measurements were obtained by using PAM fluorometer (PAM2000H Walz, Effeltrich, Germany) fitted with a 2030-B Leaf Clip. Irradiation was provided by the internal internal actinic light source or from an external quartz-halogen light source fitted with a fiber optic light guide (Zeiss KL 1500). Measurements were made on PSII quantum efficiency of dark adapted ($\Phi_{\text{PSII max}}$), and light adapted leaves (Φ_{PSII}) to determine the electron transport rate **ETR**. Attached leaf samples were left in the dark for at least 30 minutes before measurements on maximum photochemical efficiency were made ($\Phi_{\text{PSII max}}$); *in vivo* **ETR** were measured at steady states at least 5 minutes after the onset of irradiation.

2.2.3 Measurement of Photorespiration.

Initially, attempts were made to measure a full CO₂ Response curves (Section 2.2.1.1) in normal air (21% O₂) adjusted for different CO₂ content, and then again with modified air (1% O₂) adjusted for different CO₂ content. This approach generated erratic data, probably because the attached leaf was exposed to partial anaerobic conditions for over two hours. To circumvent this problem leaves were then exposed to a given level of CO₂ in normal air followed by exposure to the same CO₂ level in modified air; the process was then repeated at a different CO₂ level. This method was shown to be an improvement on the previously described method, but still the results were erratic. For this reason, it was decided to reduce the time of exposure of leaves to modified air by measuring assimilation rates at ambient

CO₂ levels (380 μmol CO₂ mol⁻¹ air) first in normal air (21% O₂) and then for 20 minutes in modified air (1% O₂). The different air compositions were prepared using Mass Flow Controllers (GFC, Aalborg) with nitrogen and oxygen gas cylinders; to deliver mixtures to the LCpro+ IRGAs of 79% of N₂ and 21% of O₂, and 99% N₂ and 1% O₂ in the low level of O₂; CO₂ was added to these air streams by the IRGAs to provide 380 μmol CO₂ mol⁻¹ air stream. In these experiments light levels were maintained at 600 μmol photons .m⁻². s⁻¹, humidity was 5 mmol mol⁻¹air, and T_{air} was held at 25°C.

Photorespiration was calculated as the difference between A_{sat} in normal (21% O₂) and modified (1% O₂) air.

2.3 Exposure of Attached Leaves to High T_{leaf}

2.3.1 Steady State Post Heat Stress Experiments

Mature attached leaves were placed on an aluminium plate that was attached to the thermal block of a PCR machine (PTC-200, Peltier Thermal Cycle, MJ Instruments). The attached leaf was covered with a neoprene pad (120 x 70 mm) to ensure thermal insulation; bead thermocouples were placed both under and above the leaf to record T_{leaf} during the incubation period. The PCR machine was then programmed to hold a constant temperature for the desired period (normally 3 hours). The temperatures recorded with the thermocouples showed no thermal gradients across the leaves and measured temperature did not vary by more than ± 0.3°C of the set temperature. After the incubation period, attached leaf sections were placed into the IRGA leaf chambers and photosynthesis parameters measured. Normally, heat stress was applied to leaves in the dark. Where heat

stress was applied in the light, a neoprene pad with a 15 x 70 mm rectangular hole and covered in cling film was placed over the attached leaf which was irradiated with a cool white light source providing $600 \mu\text{mol photons} \cdot \text{m}^{-2} \cdot \text{s}^{-1}$ PPFD at the leaf surface. T_{leaf} was monitored throughout the incubation period using bead thermocouples and again temperatures did not vary by more than $\pm 0.3^\circ\text{C}$ from the set temperatures.

2.3.2 Pseudo Steady State Heat Stress Experiments

The effect of continuous exposure to heat on Barley leaf physiological parameters that related to photosynthesis was measured. Barley cv. Optic was used in this experiment. The whole plant was placed in Sanyo Growth Cabinet, which is programmed to manage air temperature inside it. The reason is the IRGA can control leaf temperatures at $\pm 5^\circ\text{C}$ of room temperature. First, measure the assimilation rates at control room temperature (25°C) for 30 minutes, then increased the cabinet temperatures to 35, 37, 38, 39, 40, 41, 42 and 43 (± 0.4) $^\circ\text{C}$ of T_{leaf} . The conditions were ambient CO_2 ($380 \mu\text{mol CO}_2 \text{ mol}^{-1}$ air) and saturating light ($560 \mu\text{mol photons m}^{-2} \text{ s}^{-1}$) for 210 minutes and the new steady state A_{sat} and g_s measured.

2.4 Measurement of Whole Leaf ATP Levels

2.4.1 Sample Preparation

The intact leaves of barley were attached to a PAM fluorometer to measure *in vivo* **ETRs** before exposing the leaf to heat stress at the following temperatures: 25, 30,

35, 36, 37, 38 and 40 °C for three hours in the dark. Then each leaf was either incubated in dark or under 660 $\mu\text{mol m}^{-2} \text{s}^{-1}$ PAR of light intensity for 20 minutes in normal air at 25°C. During light incubation the **ETRs** were measured again. Then, after 20 minutes of light or dark incubation, the leaves were flash frozen in liquid nitrogen. This step was performed rapidly under constant light or dark conditions (<1s) to ensure endogenous ATP pools were not perturbed. The leaf samples were then ground in liquid nitrogen to a fine powder and ca. 50 mg samples (measured to ± 0.1 mg precision) were added to an Eppendorf tube containing 1.000 mL of hot distilled water in a water bath at 95°C and incubated for 5 minutes. The leaf extracts were then centrifuged at 12,000g for 5 minutes at 4°C and the supernatants transferred into fresh tubes. Previous experiments had demonstrated this process ensured ATP pools did not change during sample preparation; the high temperatures ensured phosphatase activity in the samples was inactivated immediately upon thawing. These samples were then stored at -80°C until required.

2.4.2 Luciferin-Luciferase Assay

The ATP assay was measured by using Molecular Probes' Molecular Probes ATP Determination Kit (A22066, Invitrogen, Ltd. 3 Fountain Drive Inchinnan Business Park Paisley PA4 9RF, United Kingdom). The Luciferase buffer for ATP assay was prepared as recommended by the manufacture in 10 mL total amount that contained 0.5 mM D-luciferin, 25 mM Tricine buffer pH 7.8, 1mM DTT, 125 mg/mL firefly luciferase, 100 μM EDTA and 5mM MgSO_4 . The recombinant firefly luciferase and its substrate D-luciferin estimated ATP levels in 96 flat-bottomed well, black microtiter plates. The assay was run by using Luminoskan Ascent Microplate

Luminometer (Thermo Ficher). The Luminometer was connected to a computer and Ascent software version 2.6 was used for controlling data collection and the analysis of the data. The samples were loaded into the microtiter plate by adding 10 μ L of a sample in each well in triplicate to minimize errors arising from sample handling. The reactions were started by the addition of 100 μ L of luciferase buffer to each well. A standard curve was generated each day using stock ATP (0, 0.1, 0.5, 1, 5, 10, 15 and 25 pmol of ATP).

2.4.3 Sample Analysis

The luciferin – luciferase assay reaction half-life is short so the signal rapidly decays exponentially; this means that the time lapse after starting the assay and measuring the signal is critical. For this reason, after samples had been loaded into the microtiter plates, the luciferase buffer was added one column at a time using an 8-channel multipipette (*i.e.* 1 column of samples on the 8 x 12 = 96 well plate). The differences in time between buffer additions was standardized as 10s. After collecting the signal decay curves for all samples, the data were analyzed in a spreadsheet by plotting the Log_{10} of signal against the time (seconds); this produced straight lines near time=0, and the off-set (+ 10 s intervals) time-corrected signals were estimated by extrapolating back to t=0s. The amount of ATP in each sample was then determined from the standard curves (Fig 2-4)

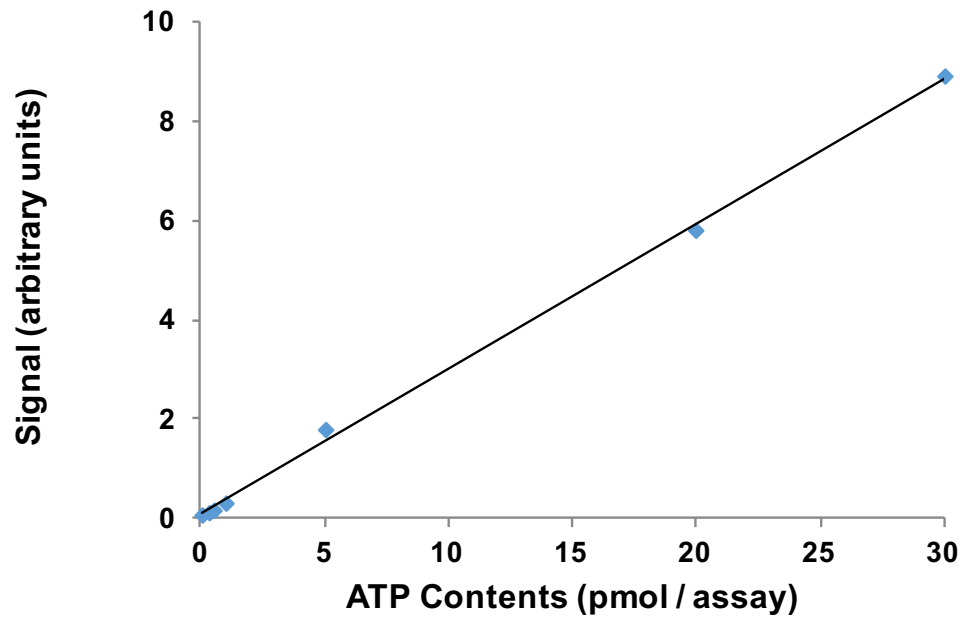


Figure 2-4. Calibration of Luciferin / Luciferase Assay for ATP Determination.

Standard curves for ATP was generated by adding a series of ATP concentrations ranging from 0.1 to 10 picomoles added to a 110 μL reaction containing 1.25 $\mu\text{g}/\text{mL}$ of firefly luciferase, 50 μM D-luciferin and 1 mM DTT in 1X Reaction Buffer (100 μL total volume). Luminescence was measured immediately after luciferin addition for 10 min using a luminometer (arbitrary units) and corrected for time-dependent signal decay by extrapolation to time zero (see text for details).

2.5 Measurement of Growth, Development, and Morphological Parameters

2.5.1 Growth Parameters

Measurements included the number of leaves, grains, and spikes per tiller and per plant. The number of tillers including the main stem was counted at each plant at each N concentration. The number of nodes in each tiller was assessed externally, and the distance between nodes was also measured to determine the spike elongation.

2.6 Development

2.6.1 Zadock's Scale for Quantifying Stage of Growth

The development of whole plants was assessed every second or third day using Zadock's Growth Staging scale (Zadoks et al. 1974) which is detailed below:

Scale	Description	Scale	Description
	Germination		Booting
0	Dry seed	40	-
1	Start of imbibition	41	Flag leaf sheath extending
3	Imbibition complete	45	Boots just swollen
5	Radicle emerged from seed	47	Flag leaf sheath opening
7	Coleoptile emerged from seed	49	First awns visible
9	Leaf just at coleoptile tip		Inflorescence emergence
	Seedling growth	50	First spikelet of inflorescence visible
10	First leaf through coleoptile	53	1/4 of inflorescence emerged
11	First leaf unfolded	55	1/2 of inflorescence emerged
12	2 leaves unfolded	57	3/4 of inflorescence emerged
13	3 leaves unfolded	59	Emergence of inflorescence completed
14	4 leaves unfolded		Anthesis
15	5 leaves unfolded	60	Beginning on anthesis
16	6 leaves unfolded	65	Anthesis half-way
17	7 leaves unfolded	69	Anthesis completed
18	8 leaves unfolded		Milk development

19	9 or more leaves unfolded	70	-
	Tillering	71	Kernel watery ripe
20	Main shoot only	73	Early milk
21	Main shoot and 1 tiller	75	Medium milk
22	Main shoot and 2 tillers	77	Late milk
23	Main shoot and 3 tillers		Dough development
24	Main shoot and 4 tillers	80	-
25	Main shoot and 5 tillers	83	Early dough
26	Main shoot and 6 tillers	85	Soft dough
27	Main shoot and 7 tillers	87	Hard dough
28	Main shoot and 8 tillers		Ripening
29	Main shoot and 9 or more tillers	90	-
	Stem Elongation	91	Kernel hard (difficult to divide with thumbnail)
30	Pseudo stem erection	92	Kernel hard (no longer dented with thumbnail)
31	1st node detectable	93	Kernel loosening in daytime
32	2nd node detectable	94	Overripe, straw dead and collapsing
33	3rd node detectable	95	Seed dormant
34	4th node detectable	96	Viable seed giving 50% germination
35	5th node detectable	97	Seed not dormant
36	6th node detectable	98	Secondary dormancy induced
37	Flag leaf just visible	99	Secondary dormancy lost
39	Flag leaf ligule/collar just visible		

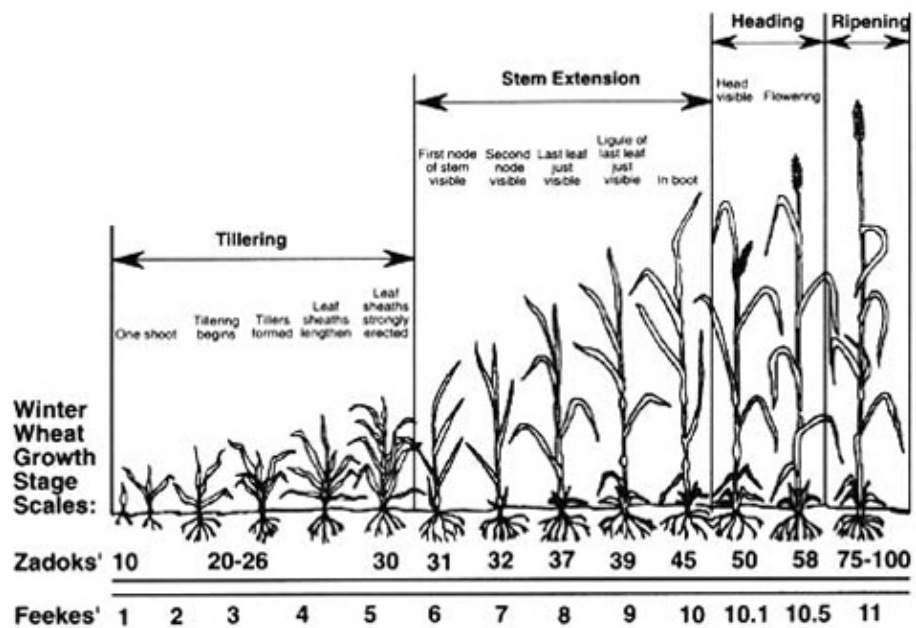


Figure 2-5 A Field Guide to Cereal Staging

The Zadock's scale is shown at different stages adopted from (Alley et al. 2009).

2.6.2 Meristem Development

The main stem of plants grown under each N concentration was removed from the hydroponic solution and then dissected to reveal the crown meristem. The position of the meristem varies between plants depending on age and the concentration of N-supply. The stems were dissected under a stereo dissecting microscope using a fine blade scalpel and forceps to remove all materials surrounding and protecting the meristems. Images of the meristems were taken using a Dino-Eye Digital Eye Piece Camera (AM7023(R4), ANMO Electronics Corporation) attached to the C-mount on the microscope. The camera was connected to a PC and controlled by DinoCapture 2.0 software version 1.5.12.

2.6.3 Cell Morphology and Number of Chloroplasts

The leaf thickness was measured under the microscope by preparing cross sections of the leaf. The number of chloroplasts in each cell was measured under the microscope as well.

2.6.3.1 Preparation of Thin Cross Sections of Leaves, Stems, and Meristems

Samples were cut from plants and immersed overnight in 3% glutaraldehyde to fix tissues. After this period, the samples were dehydrated by placing in a series of ethanol solutions (100 mL; 60% 80% and 100%) for 1 hour. The samples were then mounted in liquefied wax at 50°C and cooled to room temperature to induce solidification. The samples were then trimmed into blocks and mounted on a microtome and thin sections cut (<100 µm). Thin sections were then recovered, mounted on glass slides, stained with Toluidine Blue for 20 – 60 minutes, washed and cover slips fixed into position. Samples were then viewed using a light microscope at X50 – X250 magnification.

2.6.4 Chlorophyll Content in Barley Leaf

The amount of chlorophyll in barley leaves grown at different N levels was measured by using a portable Hansatech CL-01 Chlorophyll Content meter (Hansatech Instruments Ltd, Norfolk, UK).

2.7 Total Leaf Protein

2.7.1 Sample Preparation

Total leaf protein was assessed by cutting 3 leaf discs using a #3 cork borer (dia. 6 mm). The discs were then ground in liquid nitrogen in Eppendorf tubes, 1.00mL of ice cold acetone added to the leaf powder, and the samples incubated in the dark at -20 °C for 24 hours. After the incubation period, the leaf extracts were centrifuged at 15,000g for 15 minutes at -10 °C and the supernatants discarded. The pellets were washed with ice cold acetone and centrifuged again; this step was repeated until the pellets were colourless. The final pellets were allowed to air dry at room temperature for 10 minutes and then stored.

2.7.2 Assessment of Protein Content Using the Bradford Assay.

The concentration of the total leaf protein was measured by using Bradford dye method (**5000006**, Bio-Rad, UK) according to the manufacturer's instructions. The extraction buffer contained; 25 mM Tris, 75 mM NaCl, 5mM EDTA, 5 mM EGTA, 5% glycerol, 0.05% Nonidet Np, and deionized water was added to 100 mL volume. An 800 µL aliquot of the buffer was added to the samples and the solutions were then vortexed and centrifuged at 15,000g for 15 minutes at 4 °C and the supernatant transferred into fresh tubes. A calibration curve was constructed each day using five concentrations of bovine serum albumin (BSA) standards. The assay starts by adding 200 µL the dye to 800 µL of sample and incubating the tube for 5 minutes to allow the reaction to complete. The absorbance was then measured at 595 nm.

2.7.3 Protein Gel Electrophoresis

Leaf proteins were separated using SDS- polyacrylamide gel electrophoresis (SDS- page). Total leaf protein was prepared (Section 2.7.1) and diluted 1:2 with sample buffer (1.25 mL 0.5 M Tris-HCl pH6.8, 2.5 mL glycerol, 2 mL 10% SDS, 0.2mL 0.5% Bromophenol Blue, and 3.55 mL deionized water). A total of 950 μ L of solution was mixed with 50 μ L of 1mM DTT just prior to use). The samples were then heated to 95 °C for 5 minutes to denature secondary and tertiary structure just prior to loading into the wells. The resolving gel consisted of 10% acrylamide/bisacrylamide whilst the stacking gels were 6%. The resolving gel contained 1,5M Tris-HCl pH 8.8, 4 mL of 30% Acrylamide/Bis, 50 μ L 10% APS and 5 μ L TEMED. The Stacking gel contain 0.5 M Tris-HCl pH 6.8, 2.7 mL of 30% Acrylamide/Bis, 50 μ L 10% APS and 10 μ L TEMED .The proteins were separated by using Running Buffer (Resolving buffer contain: 3.04 g of Tris base, 14.4g glycine, and 1g SDS) and 200 V for approximately 1 hour or until the loading dye reached the bottom of the gel. To determine the molecular weight of the proteins, unstained molecular weight marker (P7703, New England Biolabs) were used. Coomassie Brilliant Blue staining was used for SDS- PAGE gels. The gels were incubated for 30 to 60 minutes in 0.1% Coomassie Brilliant Blue, 45% methanol and 10% acetic acid with shaking. The gels were then destained in 45% methanol and 10% acetic acid overnight. The gels were subsequently scanned after distaining.

2.8 Assessment of *VRN 1*, *VRN 2* and *VRN 3* Expression in Leaves.

2.8.1 Genomic DNA Isolation

Barley leaves were harvested and ground to a fine powder using liquid nitrogen in prechilled mortar and pestle. Approximately 50 mg of leaf powder were transferred into 1.5 mL microfuge tubes and 500 μ L Extraction Buffer (200 mM Tris-HCl pH 7.5, 250 mM NaCl, 25 mM EDTA and 0.5% SDS) was added, and the samples mixed by repeated pipetting; these samples were incubated at room temperature for 30 minutes. The samples were then centrifuge at 15,000g for 5 minutes at room temperature and 400 μ L of the supernatants transferred into new tubes and mixed with 400 μ L Isopropanol; the tubes were then centrifuged again at 15,000g for 2 minutes at room temperature. The isopropanol was discarded and the pellets washed with 75% iced cold ethanol. The pellets were then allowed to air dry for 30 minutes before resuspension in 200 μ L Extraction Buffer and incubation at room temperature for 1 hour.

2.8.2 RNA Extraction

2.8.2.1 RNA Extraction by using TRI-Reagent.

The total extraction done by using Tri-reagent (T9424 - TRI Reagent®, Sigma-Aldrich Chemical Co. Ltd., Dorset, UK). About 100 mg of frozen powder (Section 2.8.1) was transferred into microfuge tubes. Approximately 1 mL TRI-reagent was added and vortexed briefly. The samples were then centrifuge at 12,000g for 10

minutes at 4 °C and the supernatants transferred to a fresh microfuge tubes and incubated on ice for 5 minutes. Then, 200 µL of chloroform was added to the tubes and shaken vigorously for 15 seconds, and incubated on ice for 10 minutes. The tubes were centrifuged again at 12,000g for 15 min at 4 °C and then incubated on ice for a further 10 minutes. The top colourless supernatants containing RNA were transferred to new, fresh tubes and mixed with 500 µL isopropanol. The samples were incubated on ice for 10 minutes and then centrifuged at 12,000 g for 15 min at 4 °C, and the supernatants were discarded. The remaining pellet, containing total RNA ,was washed by adding 1 mL of ice-cold 75% ethanol and mixed by vortexing, and centrifuged at 7,500 g for 5 minutes at 4 °C. The pellets were then allowed to air dry at room temperature. Then the samples were re-suspended in 30 µL of DEPC water and the pellets dissolved at 55-65 °C for 30 minutes.

2.8.2.2 Meristems RNA Extraction Using Hot Phenol Method

Freshly dissected meristems were ground in liquid nitrogen to a fine powder and 50-100 mg transferred to Eppendorf tubes. A 500µL aliquot of freshly prepared hot (80°C) Phenol Extraction Buffer (0.1M LiCl, 0.1M Tris HCl, 10mM EDTA, and 1% SDS) was added to the samples and vortexed for 30 – 40 seconds. Then 250µL of chloroform: isoamyl alcohol (IAA) (23:1) was added and samples, vortexed again for 30 seconds, and stored on ice. Samples were then centrifuged at 13,500g for 5 minutes at room temperature and the aqueous supernatants transferred to fresh microfuge tubes and incubated on ice for 5 minutes. The total volume of each sample collected was carefully measured and an equal volume of 4M LiCl was added, vortex, and then incubated overnight in ice in a cold room. After this

incubation step the samples were centrifuged at 13,500g for 10 minutes at 4 °C. The supernatants were discarded and the pellets were re-suspended by adding 250µL of DEPC treated water and vortexed until dissolved. A tenth volume (25µL) of 3M NaAcOH (pH5.2) and 2 volumes (500µL) of cold (-20°C) absolute ethanol was added, the samples mixed well by vortexing, and then incubated at -20°C at least for 2 hours. The samples were then centrifuged at 13,500g for 10 minutes at 4°C, the supernatants discarded, and the pellet washed with pre-cold 70% ethanol (made with DEPC treated water). Samples were then centrifuged again at 13,500g for 10 minutes at 4°C. The ethanol was removed with care by using nuclease free tips, and the pellets allowed to air dry at room temperature, before re-suspension in 20-50µL of DEPC-treated water.

2.8.3 Quantification of DNA and RNA

Nucleic acid concentration in samples was estimated using nano-drop (Nanophotometer Peral, Imlen). A 2 µL aliquot volume of the sample was calibrated against a water blank and the absorbance measured at 230nm, 260 nm and 280 nm. According to (Sambrook and W Russell 2001), the concentration was obtained by measuring absorbance at 260 nm where the absorbance of 1 mean 50 µg/mL of DNA and 38 µg/mL of RNA. The purity of the samples was measured by the ratio of 260/280.

2.8.4 RNA Treatment with DNase

The RNA samples were treated with RNAase-free DNase to remove DNA (DNA-free, Ambion® ThermoFischer; Cat No. AM1907) according to the manufacturer's instructions. Briefly, about 5 µg of RNA were incubated with 4 units of DNase I and 1 x DNase buffer at 37°C for 1 hour. The reaction was stopped by addition of DNase Inactivation Reagent to the reaction mix. The samples were incubated for 5 minutes at room temperature and centrifuged at 12,000g at room temperature and the pellets were discarded.

2.8.5 Agarose Gel Electrophoresis of RNA

Where required, integrity of RNA was checked by agarose gel electrophoresis. One 1 µg of RNA (see section 2.6.1.5) was separated on a 1.5 (w/v) agarose gel containing 10 % formaldehyde and 1 x MOPS buffer, pH 7.0 (20 mM MOPS, 5 mM sodium acetate, 1 mM EDTA (Sambrook and Russell, 2001)). Before loading, the RNA was mixed with 1 % (v/v) formaldehyde, 30 % (v/v) formamide, 1 x MOPS pH 8.0, and 0.1 volumes of ethidium bromide as a staining agent. RNA mixtures were heated at 65 °C for 10 minutes, cooled on ice, then mixed with 0.2 volumes of loading dye (Promega UK, Ltd., Southampton, UK) then loaded on the MOPS gel. Electrophoresis was performed in 1 x MOPS buffer pH 7.0 for 2 hours at 100 V and visualized by UV illumination. RNA integrity was assessed by the presence of defined bands.

2.9 RNA Sequencing

Frozen powder for each of the extracted meristem total RNA samples was removed from the -80°C freezer (Section 2.8.2.2) and dissolved in 15 µL DEPC-treated water to give a total RNA content of 1.8 – 3.5 µg. These were 3 biological replicates of 2- to-3 node stage meristems from plants grown in High (16 mM) and 3 from Moderate (0.64 mM) N-supply. These samples were then sent to the Glasgow Polyomics facility at the University of Glasgow for processing. Briefly, this involved a quality control check using an Agilent 2100 Bioanalyser, and polyA RNA isolation and cDNA synthesis using a standard TruSeq total RNA kit (Illumina Inc.). The cDNA samples were then fragmented in *ca.*100 bp lengths and unique adapter pairs ligated to each of the six cDNA samples to provide multiplexing capability. The samples were then mixed and loaded onto a flow cell for analysis using an Illumina NextSeq 500 DNA sequencer. Over 400 million 100bp reads were obtained providing over 200 million paired end reads; these were sorted by the multiplex adapters into six data sets (3 High and 3 Moderate N-supply) each containing 30-35 million paired end reads. All subsequent data analysis was performed on the University of Glasgow Galaxy server (Love et al. 2014). Each of the six data sets were then 'trimmed' to remove multiplex adapter and nonsense sequence using the Trimmomatic package (Bolger et al. 2014) and a quality control further checked performed using FastQC (Blankenberg et al. 2010). The output from FastQC was then piped into the Kallisto package (Bray et al. 2016) and the reads aligned to the barley 'cDNA' reference genome consisting of known cDNAs, coding sequences, DNA, non-coding RNA, and peptides

(ftp://ftp.ensemblgenomes.org/pub/plants/release-32/fasta/hordeum_vulgare). The aligned reads of all six data sets were then piped into the DESeq2 package for transcript quantification and statistical analysis using the barley cDNA annotation file (Love et al. 2014).

2.10 Statistical Analysis

Data were analyzed using Minitab ver 17 statistical package. The Analysis of Variance General Linear Model (GLIM) was used in most cases and where appropriate data Log_{10} or square root transformations were applied to ensure the data sets conformed to a Normal Distribution. Differences between levels of experimental factors were assessed using Tukey's *a posteriori* tests. In some cases where the explanatory variables were continuous, regression lines were fitted using the GLIM Covariance routine.

3 Chapter 3: Response of Barley Photosynthesis Rates to Heat Stress.

The effects of high leaf temperatures (T_{leaf}) on photosynthesis rates of attached barley leaves was measured using two different methods; attached leaf gas exchange using IRGAs and pulse modulated chlorophyll fluorescence. Two sets of experiments were performed.

In the first measurements **A/Ci** curves (see Section 2.2.1) were constructed to assess important physiological parameters of attached leaves just prior to, and just after, a 3-hour period of controlled T_{leaf} (25.0 to 40.0°C, $\pm 0.2^\circ\text{C}$); this allowed a comparison of the effects of T_{leaf} on steady state photosynthesis rates at 25°C on the same section of attached leaf. These experiments will henceforth be referred to as *Steady State Post Heat Stress* measurements.

In the second set of experiments attached leaves were enclosed in the leaf chamber of an IRGA and T_{leaf} was initially held at 25°C for 30 min to assess photosynthesis rates. T_{leaf} was then increased to either 35.0, 37.0, 38.0, 39.0, 40.0, 41.0, 42.0 or 43.0°C $\pm 0.7^\circ\text{C}$ in normal air, and then A_{sat} and other important parameters, were then measured at these elevated temperatures. These experiments also allowed the effects of T_{leaf} on photosynthesis rates to be assessed but here measurements were made at each T_{leaf} (*cf.* 25.0°C in the post heat stress experiments) on the same section of leaf. The advantage of this approach is that the effects of T_{leaf} on photosynthesis rates at high leaf temperatures can be assessed. The disadvantage,

however, is that leaves were at pseudo-steady state; T_{leaf} was held for 180 minutes at each elevated temperature and measurements were then made whilst further damage may have been imparted. These experiments will henceforth be referred to as *Pseudo-Steady State Heat Stress* measurements.

3.1 Steady State Post Heat Stress Measurements

Previous studies in our laboratory suggested T_{leaf} of 38.0°C for 3 hours in the dark suppresses intact leaf light saturated leaf CO₂ assimilation rates (A_{sat}) by 80% in the C3 cereal barley and in the C4 crop maize, regardless of the geographical origins of the cultivar (tropical or temperate). In that study it was reported that the corresponding capacity for PS II photochemistry and *in vitro* photosynthetic electron transport was impaired by 40%, the CO₂ supply to the chloroplast was unaffected, but carbon flow through the C3 cycle was inhibited by 85%. The interpretation of these experiments was that the primary cause for the observed decline in A_{sat} was a direct effect of heat stress on the kinetic properties of the C3 cycle (Almalki 2014). Almalki (2014) went on to show that carbon flow between Ribose 5-phosphate and Ribulose 1,5-bisphosphate was severely impaired, and a high temperature-induced decrease in chloroplast ATP levels leading to a reduction in carbon flow through Phosphoribulokinase (see Figure 1-2) was implicated (Almalki 2014).

The findings from that study are compelling but do not support a considerable body of literature that implicates the enzyme RuBisCO Activase (RCA) as the primary site of thermal damage to photosynthesis (Salvucci 2004; Salvucci and Crafts-Brandner 2004; Carmo-Silva and Salvucci 2012; Evans 2013; Galmés et al. 2014). For this

reason it was decided to undertake a series of experiments to check the validity of the findings of previous work in the Arnott laboratory at the University of Glasgow. There are four areas of some concern regarding the experimental approach used by Almalki (2014) that require further clarification. First, Post Heat Stress experiments were conducted on intact leaves heat stressed for three hours in the dark. The rationale for this approach was to remove any effects of photochemically generated reactive oxygen species (ROS) on photosynthetic activity; by heat stressing leaves in the dark the direct effect of elevated leaf temperature alone on photosynthesis could be studied. To state this potential problem in another way, does the presence of ROS exacerbate thermal injury to A_{sat} of plants grown in the field as mentioned in the literature (Kosová et al. 2014)? Second, the evidence for thermally induced changes in leaf ATP levels were reported to be preliminary and not extensive. To ensure these conclusions of Almalki (2014) are consistent and robust, further analyses is required. Third, a decline in A_{sat} can arise from a decline in gross photosynthesis rates or from an increase in respiration and photorespiration. It seemed prudent, therefore, to assess the effects of T_{leaf} on the rates of photorespiration and respiration, and on and photosynthesis. Finally, the barley plants used previously in the Arnott laboratory were grown in compost, a medium that is used extensively in our institute for growing the model dicot *Arabidopsis*. Whilst the weedy species *Arabidopsis* superficially appears to show no phenotypic response to growth in nitrogen rich soil, cereal crops do show gross abnormalities (profuse tillering, increased levels of leaf protein, prostrate habit – little secondary thickening, reduced fecundity, etc.,). The uptake of excess nitrogen and its accumulation in leaves as storage protein may present a particular problem; RuBisCO is reported to be one of the major nitrogen storage proteins in leaves, and

therefore it is conceivable the results of Almalki (2014) on the effects of heat stress on RuBisCO activity in barley leaves were compromised by the aphysiological levels of RuBisCO that might have accumulated in those plants. Again, it seems prudent to re-assess the findings of Almalki (2014) on phenotypically 'normal' barley plants grown in physiologically relevant levels of nitrogen. In addition, proteins related to nitrogen metabolism are downregulated by heat stress (Ashoub et al. 2015).

3.1.1 High T_{leaf} Effects on Photosynthesis

Barley plants were grown in physiologically relevant levels of nitrogen (Section 2.1.1) and exposed to the heat stress (Section 2.3.1) as described in the Materials and Methods chapter. In all cases measurements were first made prior to heat stress to ensure the section of leaf under study exhibited a high rate of photosynthesis determined by gas exchange ($> 10 \mu\text{mol CO}_2 \text{ m}^{-2} \text{ Leaf s}^{-1}$; Section 2.2.1) or electron transport rate determined by chlorophyll fluorescence measurements ($> 100 \mu\text{mol electrons m}^{-2} \text{ Leaf s}^{-1}$; Section 2.2.2); subsequently, heat stress was applied and the relevant photosynthetic parameters determined.

3.1.1.1 Gas Exchange Measurements

Figure 3.1 presents the results from a series of Post Heat Stress experiments on attached barley leaves grown in physiologically relevant levels of nitrogen. A_{sat} declined markedly when T_{leaf} exceeded 37°C for 3 hours in the dark, and temperatures of 40.0°C caused approximately 80% inhibition. These findings are entirely consistent with those reported by previous experiment in Arnott laboratory

(Hüve et al. 2011). It appears that a similar profile of thermal inactivation of A_{sat} occurs regardless of the nitrogen status of the plant.

Attached leaves were also exposed to the same temperature regimes but incubated in saturating levels of white light ($560 \mu\text{mol photons m}^{-2} \text{s}^{-1}\text{PAR}$), however, results showed an almost identical pattern (Fig 3.1). The thermal profile of the decline in A_{sat} of attached barley leaves in response to high T_{leaf} is almost identical regardless of whether incubation was carried out in the dark or in saturating light.

Anova analysis using the GLIM routine of Minitab 17 and Tukey's *post hoc* test showed no significant interaction between factors Light and Temperature (Fig. A-1). Analysis of the main factor Light also failed to generate a significant difference ($p=0.989$), but main effect Temperature was highly significant ($p < 0.001$). Tukey's *post hoc* comparisons test revealed 40°C produced a significant ($p < 0.05$) reduction in A_{sat} when compared with a temperature of 37°C and below.

To conclude, the results of these experiments on heat stress in the dark of plants grown in soil/sand mixtures with physiologically relevant levels of N are similar to those of plants grown in N-rich compost. There is no evidence, therefore, that the nitrogen status of leaves affects the thermal sensitivity of photosynthesis rates in barley. Further, exposure to high light during heat stress caused no more damage to photosynthesis rates than heat stress alone and it appears, therefore, that any thermal suppression of A_{sat} observed in field-grown barley plants will arise from a direct effect on the photosynthetic apparatus and not from light-generated ROS.

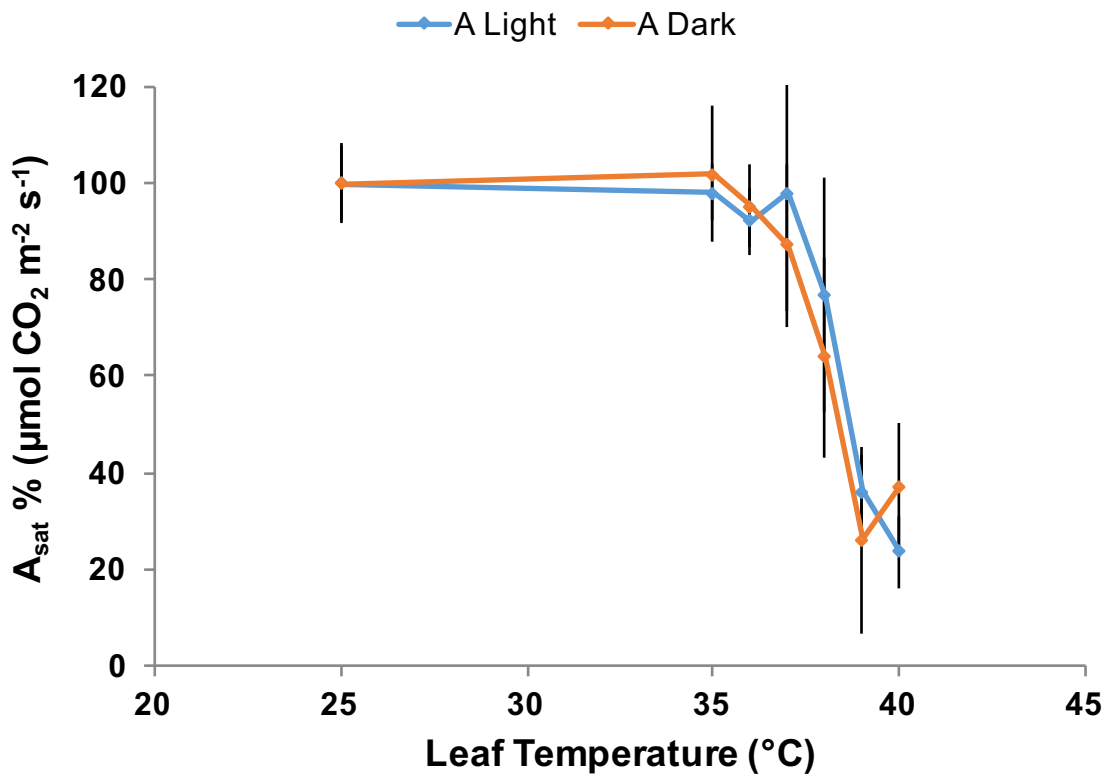


Figure 3-1. The Effect of High T_{Leaf} and High Light Intensity on CO_2 Assimilation in Barley Leaves.

The 4th attached leaf of barley (cv. Optic) were marked with a fine pen and placed in the leaf chamber of an IRGA to measure A_{sat} at 25.0°C in normal air (380 $\mu\text{mol CO}_2 \text{ mol}^{-1} \text{air}$) and saturating light (560 $\mu\text{mol photons m}^{-2} \text{ s}^{-1} \text{PAR}$). Only leaves that showed an A_{sat} rates of over 10.0 were subsequently used. The marked sections of the attached leaves were then exposed to a range of T_{Leaf} (25, 35, 36, 37, 38, 39 and 40°C (± 0.2 °C) for three hours in high light (560 $\mu\text{mol photons m}^{-2} \text{ s}^{-1} \text{PAR}$) or the dark. Assimilation rates A_{sat} were subsequently measured using ambient CO_2 (380 $\mu\text{mol CO}_2 \text{ mol}^{-1} \text{air}$) and saturating levels of light (560 $\mu\text{mol photons m}^{-2} \text{ s}^{-1} \text{PAR}$) and a T_{leaf} 25.0°C. The values represent the average (\pm SE) of $n=5$ independent intact leaves. The 100% rate for dark stressed leaves was equivalent to value of 14.4, while that for light stressed leaves was 14.0 $\mu\text{mol CO}_2 \text{ m}^{-2} \text{ s}^{-1}$.

3.1.1.2 *in vivo* Electron Transport Rate Measurements

The photosynthesis rates of attached leaves can also be estimated from pulse amplitude modulated chlorophyll fluorescence measurements of *in vivo* electron transport rates (Baker 2008). These measurements on Post Heat Stressed attached leaves provide a second independent and rapid method to assess the effects of high T_{leaf} on photosynthesis rates. It is important to emphasize, however, that measurements on *in vivo* **ETR** provide information on the consumption of photochemically-generated reducing potential by whole leaf processes, and not just the reduction of CO_2 (*i.e.* reduction of NO_3^- , SO_4^{2-} , *etc.*, and the Mehler reaction). Figure 3-2 presents estimates of steady state photosynthetic **ETRs** of attached leaves heat stressed in the dark using the methods described earlier (see Legend of Figure 3-1). A strong, significant ($p < 0.001$; Appendix A-2) decrease in **ETR** was observed at T_{leaf} above 37.0°C , where the inhibition of **ETR** began to take place. After exposure to 40.0°C *in vivo* **ETRs** had declined to approximately 15% of their pre-stress levels ($p < 0.001$; Appendix A-2). These data are consistent with those from the gas exchange A_{sat} measurements (Fig 3-1), photosynthetic transport in barley leaves is severely impaired by over 80% after a 3 hour exposure to T_{leaf} 38.0°C .

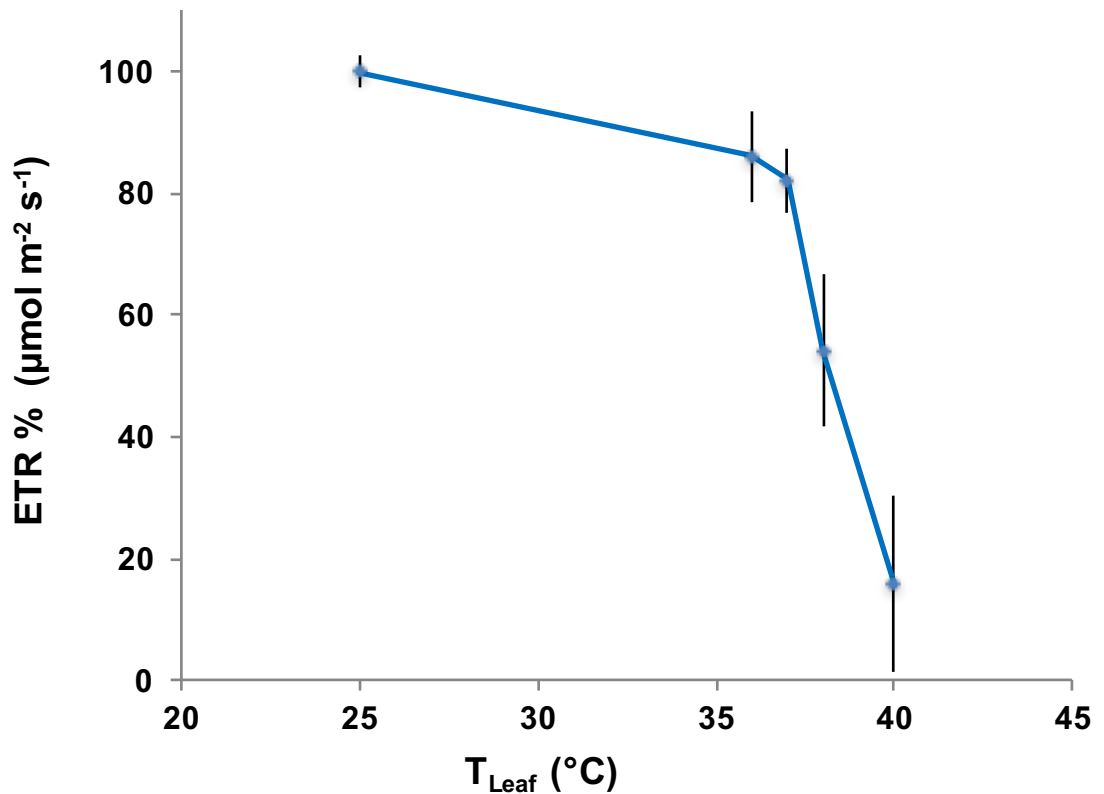


Figure 3-2. The Effect of Elevated Tleaf on Steady State in vivo Photosynthetic Electron Transport Rates of Attached Barley Leaves.

Sections of fully expanded 4th or 5th emergent attached leaves were exposed to air (380 μL CO₂ L⁻¹ air) at 25°C and saturating light (580 μmol m⁻² s⁻¹ PAR) for 20 minutes to establish maximum steady state photosynthesis rates. *In vivo* **ETR** was then measured using pulse amplitude modulated fluorescence. These measurements were taken as the maximum (100%) rates of **ETR**. The same section of attached leaf was then exposed to one of a range of temperatures (25, 36, 37, 38 or 40°C ±0.3°C) in the dark for three hours (Section 2.2.2). After this period the **ETR** of the treated attached section of leaf was reassessed as described above. The data points are the average and SE of n= 27 for 25°C, n=10 for 36°C and 37°C, and n=17 for 38°C and 40°C. 100% is equivalent to 173.4 μmol m⁻² s⁻¹.

3.1.1.3 Photosystem II Photochemical Efficiency (Φ_{PSII})

Photosystem II (PSII) is particularly sensitive to damage from photoinhibition and photobleaching and it seemed sensible, therefore, to assess the effects of high T_{leaf} on the stability of PSII. Modulated fluorescence can easily be used to measure the maximum efficiency of *in vivo* PSII photochemistry, that is the transfer of electrons from the electron donor (a tyrosine residue on the D2 protein) through the PSII reaction center special pair of chlorophyll molecules (P680) through to the primary electron acceptor quinone (Q), *i.e.* Y161 \rightarrow P680 \rightarrow Q. (Yamamoto et al. 2014; Allahverdiyeva et al. 2015; Yamori and Shikanai 2016).

The maximum quantum efficiency photosystem II (Φ_{PSII}) was measured using modulated chlorophyll fluorescence to determine the effect of high T_{leaf} on photosystem II photochemical processes. Changes in Φ_{PSII} with increasing T_{leaf} were found but this was only approximately a 10% reduction at 38.0°C and 50% at 40.0°C (Figure 3-3). This compares with a concomitant 60% and >80% decrease in A_{sat} (Figure 3-1), and a 70% decrease in *in vivo* ETR (Figure 3-2), over the same temperature range.

The results shows that A_{sat} and ETR declines at lower temperatures with increasing T_{leaf} (Eberhard et al. 2008; Ventrella et al. 2008; Malnoe et al. 2014; Zhang et al. 2014; Chauvet et al. 2015; Liu and Last 2015) than Φ_{PSII} , and the thermal damage to photosystem II photochemical processes are unlikely to account for the observed decline in whole leaf photosynthesis.

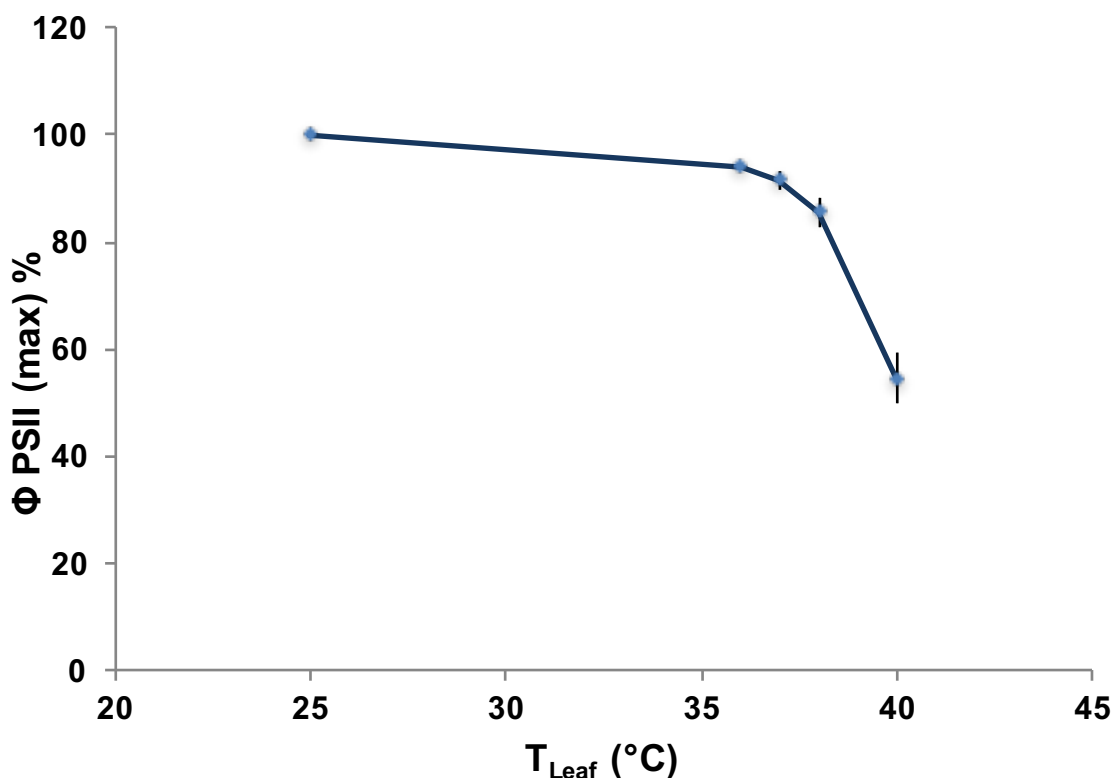


Figure 3-3. Effects of High Tleaf on the Maximum Quantum Efficiency (Φ_{PSII} max) of Attached Barley Leaves.

Attached fully expanded 4th and 5th emergent leaves were treated by exposure in the dark to a range of temperatures using a thermal block for three hours (Section 2.3.1). Leaves were then left in air at 25°C in the dark for 20 minutes to recover and then Φ_{PSII} was measured using pulse amplitude modulated fluorescence. Heat stress was 25°, 36°, 37°, 38° and 40°C ($\pm 0.2^\circ\text{C}$). Each data point is the average and SE of n= 27 (25 °C), n= 10 (36° and 37 °C), n= 17 (38° and 40°C). 100% is equivalent to 0.767 Fv/Fm ratio.

3.1.2 The Effects of T_{leaf} on Photorespiration Rates

The major carboxylation enzyme of the C3 cycle, RuBisCO, binds the 5-carbon sugar ribulose 1,5-bisphosphate (RuBP) and CO_2 , in which case it catalyzes carboxylation, or O_2 , in which case it catalyzes oxygenation – the breakdown of RuBP and the release of CO_2 through the process of photorespiration (Lorimer 1981; Archontoulis et al. 2012; Voss et al. 2013; Gandin et al. 2014; Walker et al. 2016). Thus, CO_2 and O_2 compete with each other for the binding site on RuBisCO. Increasing the rate of photorespiration is reported to affect the yield of crops (Pick et al. 2013). RuBisCO catalyzes the assimilation of atmospheric CO_2 as Ribulose 1,5-bisphosphate (RuBP) is converted into two molecules of 3-phosphoglycerate (3PGA). Alternatively, oxygenation of RuBisCO (photorespiration) converts RuBP to 3PGA and 2-phosphoglycolate (2-PG). The plant's photorespiration is viewed as an attempt to recovery of some of the 2-PG but this is only 50% efficient (Pick et al. 2013).

One possibility to explain the observed decline in A_{sat} with increasing the T_{leaf} is that high temperatures increase photorespiration rates rather than induce a decline in photosynthesis (carboxylation). To assess this possibility, methods were developed to measure the effects of T_{leaf} on photorespiration directly. These experiments involved measuring gas exchange in leaves at 21% O_2 and 1% O_2 levels; the latter is reported to suppress photorespiration allowing gross photosynthesis rates to be measured. In normal air with a 21:79 mix of $\text{O}_2:\text{N}_2$ plus CO_2 normal A/Ca and A/Ci responses were measured (Fig 3-4). A_{sat} in normal air ($380 \mu\text{mol CO}_2 \text{ mol}^{-1} \text{ air } 21:79$ % $\text{O}_2:\text{N}_2$) were approximately $13 \mu\text{mol CO}_2 \text{ m}^{-2} \text{ s}^{-1}$, and total respiration rates (dark

respiration plus photorespiration, $R_d + R_L$) were approximately $-2.0 \mu\text{mol m}^{-2} \text{s}^{-1}$ (Figure 3-4 A). In contrast, A_{sat} in modified air ($380 \mu\text{mol CO}_2 \text{ mol air}^{-1}$; 1:99 % $\text{O}_2:\text{N}_2$) was $\sim 17 \mu\text{mol CO}_2 \text{ m}^{-2} \text{s}^{-1}$ and total respiration rates were approximately $-1.0 \mu\text{mol CO}_2 \text{ m}^{-2} \text{s}^{-1}$ (Figure 3-4 A).

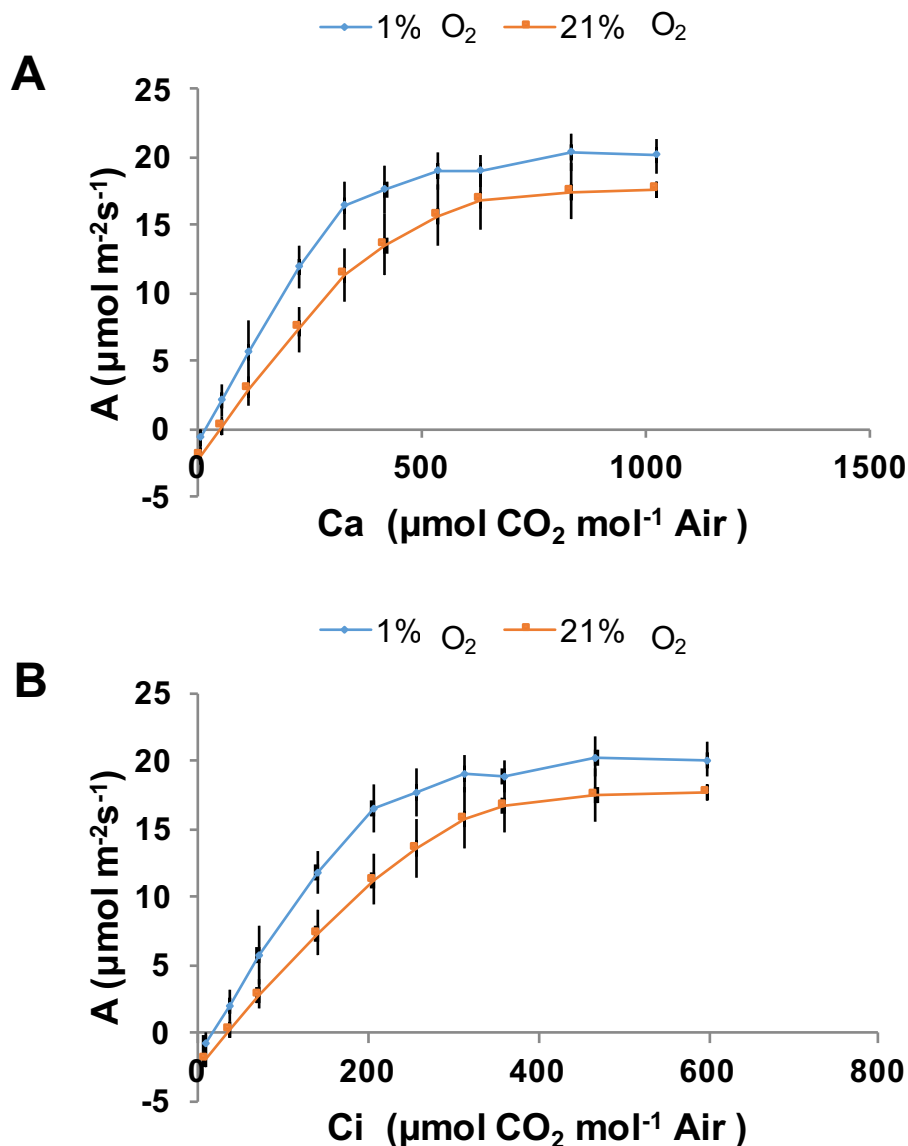


Figure 3-4. A/Ca and A/Ci Curves of Attached Barley Leaves in 21% and 1% O₂.

Fully expanded 4th attached leaves were placed in the leaf chamber of an IRGA and exposed for 20 minutes to incremental increases in CO₂ concentration (0, 50, 150, 300, 380 (ambient), 450, 550, 700, 850 and 1100 $\mu\text{mol CO}_2 \text{ mol}^{-1} \text{ air}$), saturating levels of white light (560 $\mu\text{mol photons m}^{-2} \text{ s}^{-1}$ PAR); T_{leaf} was 25.0 ± 0.4 °C throughout. After assessing the steady state rate of carbon assimilation in normal air (21:79 O₂:N₂) the ratio of O₂:N₂ was adjusted using mass flow controllers to 1:99 but the CO₂ level was maintained. Panel A, **A/Ca** curve; panel B, **A/Ci** curve (see Section 2.2.3). The values represent the average (\pm SE) of n=5 independent leaves of cv. Belgravia.

At first sight these data appear contradictory. Photorespiration (R_L) should decrease with increasing CO_2 as O_2 experiences increasing competition for the binding site on RuBisCO, but in all of the experiments performed to date the opposite is true; R_L increased with increasing CO_2 (cf. $-2 \mu\text{mol m}^{-2} \text{s}^{-1}$ at zero CO_2 , $-4 \mu\text{mol m}^{-2} \text{s}^{-1}$ at $380 \mu\text{mol CO}_2 \text{ mol}^{-1}$ air and above). The reason for this is not entirely clear but may be associated with the inability of the C3 cycle to generate sufficient quantities of the other substrate of RuBisCO, RuBP, when external CO_2 levels (C_a) are low.

Similar discrepancies were obtained when light response curves were measured in normal and modified air (Figure 3-5). In the dark, respiration rates in normal air (21:79 $O_2:N_2$ mixtures) were approximately $-2.0 \mu\text{mol CO}_2 \text{ m}^{-2} \text{ s}^{-1}$, where as in modified air (1:99 $O_2:N_2$ mixtures) they were approximately $-0.5 \mu\text{mol CO}_2 \text{ m}^{-2} \text{ s}^{-1}$ (Figure 3-5). Presumably in low light the capacity of chloroplasts to generate enough RuBP to support photorespiration is compromised and this accounts for the low R_L rates observed below an absorbance of $200 \mu\text{mol m}^{-2} \text{ s}^{-1}$ PAR.

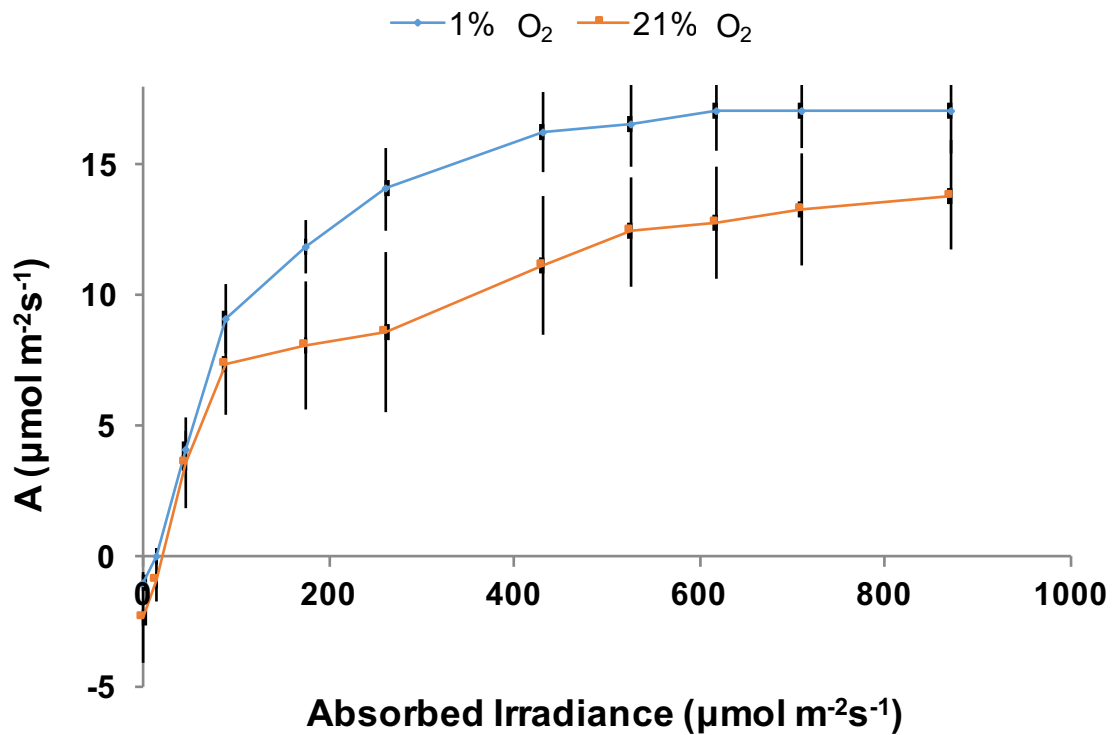


Figure 3-5. Light Response Curve of Attached Barley Leaves in Air Containing 21% and 1% Oxygen

The 4th attached leaf was placed on gas exchange (IRGA) leaf chamber and exposed to different light intensity (0, 20, 50, 100, 250, 400, 500, 560, 650, 800 and 950 $\mu\text{mol photons m}^{-2}\text{s}^{-1}$), ambient CO₂ concentration (380 $\mu\text{mol CO}_2 \text{ mol}^{-1}$ 21:79 mixture), T_{leaf} was 25 °C and concentration of Oxygen manipulated by mass flow controllers to adjust the amount of O₂ and N₂ supplied to IRGA. The values represent the average (\pm SE) of n=4 independent leaves of c.v. Belgravia.

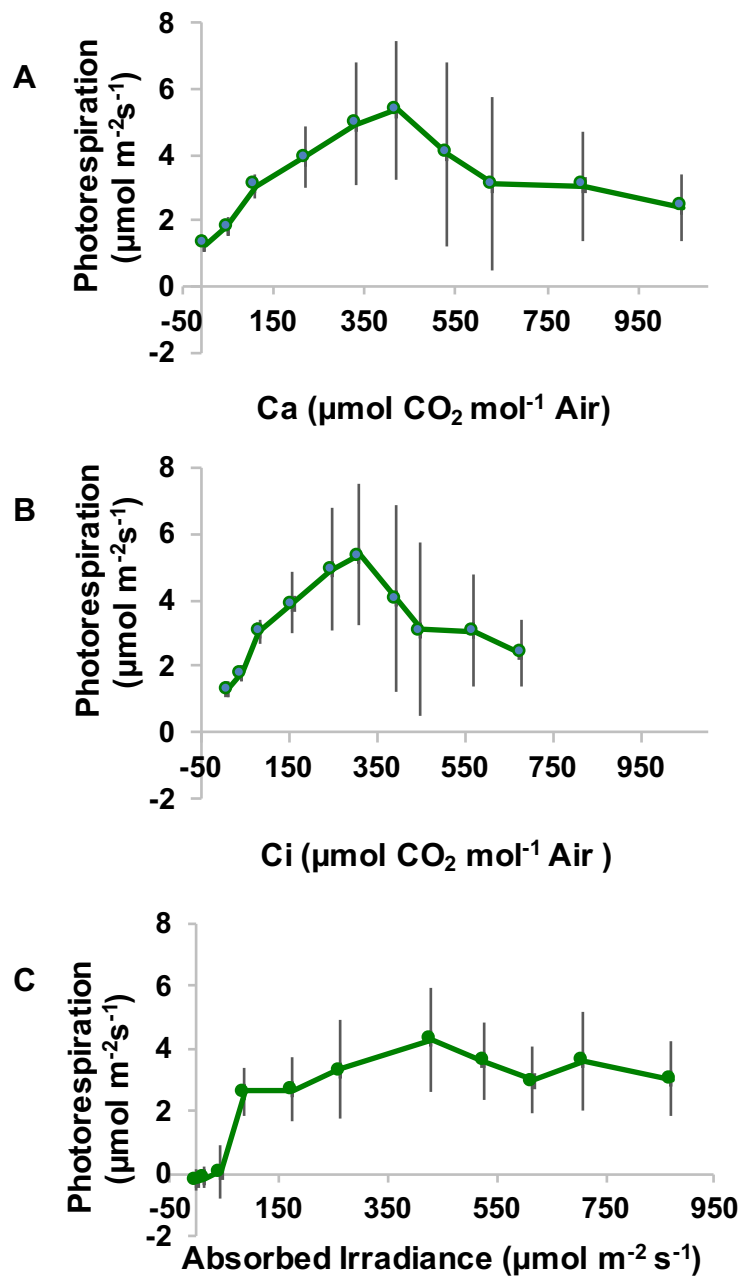


Figure 3-6. Assessment of R_L Rates in Attached Barley Leaves in Response to Changing C_a and Absorbance.

Panel A. Photorespiration rates of attached barley leaves ($T_{\text{leaf}} 25.0^\circ\text{C} \pm 0.4^\circ\text{C}$) in response to changing C_a . These data were collected using the methods described in Figure 3-4; the data were calculated as the A_{sat} rates in modified air (1% O_2) minus A_{sat} in normal air (21% O_2). Panel B; data from Panel A plotted against C_i . Panel C; Photorespiration rates of barley leaves ($T_{\text{leaf}} 25.0^\circ\text{C} \pm 0.4^\circ\text{C}$) in response to changing leaf absorbance. These data were collected using the methods described in Figure 3-5; photorespiration rates were calculated as A_{sat} rates in modified air (1% O_2) minus A_{sat} in normal air (21% O_2). The values represent the average (\pm SE) of at least $n=4$ independent leaves of cv. Belgravia.

The methods used to assess photorespiration rates in attached leaves (Figure 3-6) have been used routinely in many studies. The data in Figure 3-6 do show sensible trends in photorespiration rates with increasing **Ca** and leaf Absorbance, and provide sensible values in normal air (ca. $5 \mu\text{mol CO}_2 \text{ m}^{-2} \text{ s}^{-1}$, about one-third of the corresponding observed **A_{sat}** or one quarter of gross photosynthesis rates), but the high levels of variance incurred in these non-stressed leaves will probably make it difficult to draw firm conclusions on photorespiration rates in heat stressed leaves. For this reason, another method for assessing photorespiration rates was developed.

This alternative method was designed to measure **A_{sat}** in normal air (21% O₂) for 15 minutes followed by **A_{sat}** measurements in modified air (1% O₂). The intention of using this method was to avoid the accumulation of the products of anerobiosis that might build up in tissues after repeated cycles exposed to 21% and 1% O₂ over a full range of **Ca** or light intensity. The disadvantage of this approach, however, is that estimates of photorespiration can only be assessed at ambient levels of **Ca** ($380 \mu\text{mol CO}_2 \text{ mol}^{-1} \text{ air}$); none-the-less, this approach was considered to be the best way forward.

Figure 3-7 shows this modified method was successful in reducing the variance within the observed values of photorespiration allowing the effects of **T_{leaf}** to be assessed with some precision. No significant changes in photorespiration rates were observed when **T_{leaf}** was increased from 25°C to 36°C. Increasing **T_{leaf}** above 36°C caused photorespiration to rise by approximately 50% (from ca. 2 to 3 μmol

CO₂ m⁻² s⁻¹) but this was not statistically significant (Appendix A-3). This modest change in photorespiration, however, was accompanied by a major decrease in **A_{sat}**, consistent with the decline observed before (Figure 3-1). Photorespiration rates did not increase above ca. 3 μmol CO₂ m⁻² s⁻¹ in any of the heat stress treatments, and it is concluded, therefore, that the major suppression in **A_{sat}** observed in attached leaves exposed to **T_{leaf}** above 36°C is not attributable to an increase in photorespiration but to a decrease in carbon assimilation.

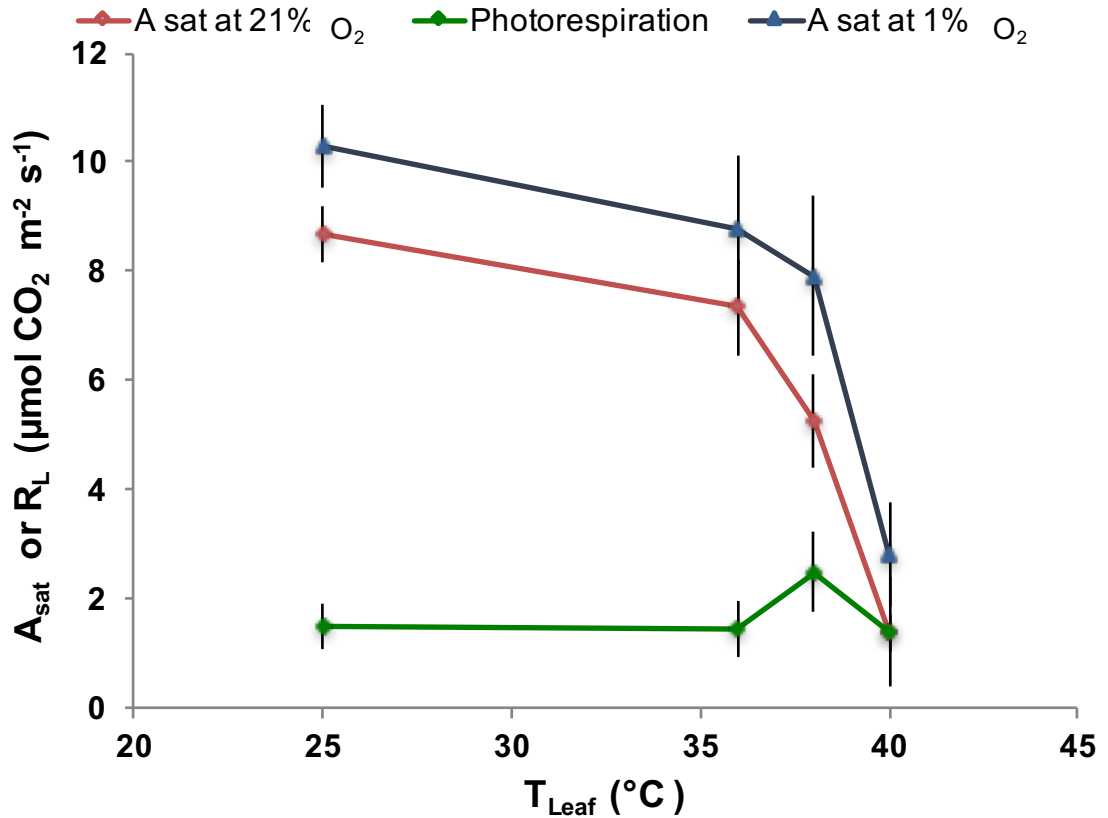


Figure 3-7. The Effect of T_{leaf} on A_{sat} and Photorespiration Rates in Attached Barley Leaves.

Healthy, sections of fully expanded 4th attached barley leaves demonstrating high initial rates of A_{sat} ($>9 \mu\text{mol CO}_2 \text{ m}^{-2} \text{ s}^{-1}$) were marked and then heat stressed by placement on a thermal block in the dark to 25.0, 36.0, 38.0 and 40.0 °C (± 0.2 °C) for 3 hours. The A_{sat} values from the same leaf sections was then re-assessed after 10 minutes in normal air (21:79 O₂:N₂, plus 380 $\mu\text{mol CO}_2 \text{ mol}^{-1}$ gas mix) and saturating white light (580 $\mu\text{mol m}^{-2} \text{ s}^{-1}$ PAR). The gas mix was then adjusted to modified air (1:99 O₂:N₂, plus 380 $\mu\text{mol CO}_2 \text{ mol}^{-1}$ air) and A_{sat} measured again after 10 minutes. The values represent the average (\pm SE) of $n > 7$ independent leaves of Barley.

3.1.3 ATP Levels in Heat Stressed Leaves

Previous preliminary studies in our laboratory had indicated the decline in A_{sat} with increasing T_{leaf} was accompanied by a decrease in whole leaf ATP levels (Almalki 2014). To confirm this observation further experiments were conducted on the attached leaves of barley plants grown in physiologically relevant levels of nitrogen exposed to a range of T_{leaf} in the dark for 3 hours. Treated leaves were then exposed to normal air at 25°C and saturating levels of white light ($560 \mu\text{mol m}^{-2} \text{s}^{-1}$ PAR) for 20 minutes to achieve maximum A_{sat} . Steady state A_{sat} was confirmed by assessing *in vivo* ETR rates using modulated fluorescence (Section 3.1.1.2), and then leaves were rapidly frozen in liquid nitrogen. Care was taken to keep the leaves fully illuminated throughout the procedure to ensure endogenous ATP levels were maintained until the tissue was fully frozen. Preliminary experiments using a thermal imaging camera demonstrated T_{leaf} decreased from 25°C to below -30°C (the low temperature limit of the camera) in less than 1s. Unfortunately, it is not possible to assess chloroplast ATP levels in attached leaves, only whole leaf ATP levels. Adenylate levels in leaves change very rapidly (< 1s) with modest changes in irradiance, and it is not possible, therefore, to obtain meaningful results from chloroplasts isolated from treated leaves (Sulpice et al. 2007). For this reason whole leaf ATP levels were measured in the light and dark and the difference taken as an estimate of *in vivo* chloroplast ATP levels. Briefly, attached leaves were heat stressed as described earlier (Section 3.1.1.1) and then adapted to saturating light or dark conditions for 20 minutes in normal air (25°C); *in vivo* ETR and NPQ were measured during this period to confirm of thermal effects on photosynthesis rates. Leaves were then flash frozen in liquid nitrogen, the samples recovered, ground to a fine powder in liquid nitrogen, and then stored at -80°C until required. ATP was

extracted from frozen samples by rapidly immersing approximately 20 mg sample (measured to 0.1 mg precision) into 1 mL of hot water (90°C) to inhibit phosphatase activity. The samples were incubated with shaking for a further 5 min before centrifugation for 5 minutes at 4°C. The supernatant was removed and the luciferin-luciferase bioluminescence assay was performed using a luminometer (Section 2.4). The amount of ATP in the samples was calculated from standard curves generated each day using a series of known ATP concentrations.

In light adapted leaves the amount of ATP increased with T_{leaf} from ca. 2 nmol g⁻¹ FWt at 25.0°C to ca. 5 nmol g⁻¹ FWt at 40.0°C (Figure 3-8). In contrast, samples from dark adapted leaves showed a decrease in whole leaf ATP levels when T_{leaf} was increase from 25.0°C (ca. 7.5 nmol g⁻¹ FWt) to 38.0°C (ca. 2.0 nmol g⁻¹ FWt); at higher temperatures, however, whole leaf ATP levels increased to over 22 nmol g⁻¹ FWt. Anova analysis of the ATP data revealed a highly significant interaction between Light and Temperature ($p < 0.001$) preventing further analysis of the main effect using a Factorial model (Appendix A-3). Covariance analysis of ATP data using factor Light alone revealed a highly significant correlation ($p = 0.008$) with positive slope of approximately 1.1°C. Anova analysis of the ATP data for dark incubated samples using factor Temperature alone also showed a highly significant effect ($p < 0.001$) and Tukey's *post hoc* test revealed significant differences ($p = 0.05$) at 40°C (Appendix A-3).

These results, however, are not consistent with those measured previously at Glasgow (Almalki 2014). In those experiments whole leaf ATP levels of control leaves (25.0°) were found to be approximately 3 times higher in light adapted leaves

than in dark adapted leaves (7.5 *cf.* 2.5 nmol g⁻¹ FWt). Further, in those experiments the Light-minus-Dark levels of ATP, which was taken as an estimate of chloroplast ATP levels, declined from *ca.* 5.5 to 3.0 nmol g⁻¹ FWt as **T_{leaf}** increased from 25.0° to 40.0° C (Almalki 2014). Possible reasons for these discrepancies are discussed later.

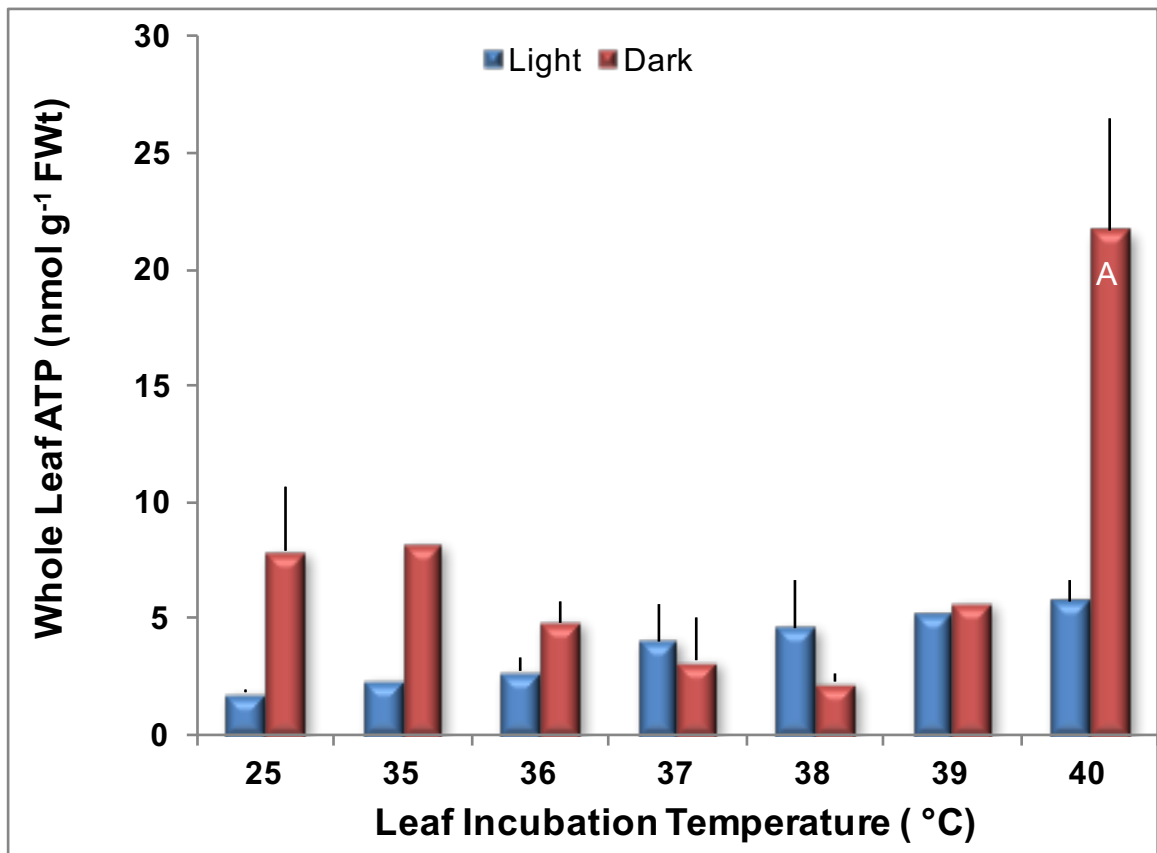


Figure 3-8. The Effect of Increasing Leaf Temperature on Whole Leaf ATP Content in Barley Leaves.

Fully expanded attached 3rd or 4th leaves of healthy barley plants were first incubated in the dark for 3hr on a thermal block set at 25.0, 36.0, 38.0 or 40.0°C (\pm 0.2°C). After this period leaves were incubated for a further 20 minutes in normal air ($380\mu\text{mol CO}_2 \text{ mol}^{-1}$ air) at 25°C either in the dark or in saturating white light ($580\mu\text{mol m}^{-2} \text{ s}^{-1}$ PAR). Leaf tissue was then rapidly frozen in liquid nitrogen, ground to a fine powder, and ATP levels determined using the luciferin-luciferase bioluminescence assay (Section 2.4.2). The values are the average and SE for $n=7$ independent biological replicates at each temperature (7 light, 7 dark). Prior to heat stress the *in vivo* ETR of each leaf was assessed to ensure the leaves were capable of high rates of photosynthesis and only those with values greater than $100\mu\text{mol m}^{-2} \text{ s}^{-1}$ – approximately equivalent to A_{sat} of $>10\mu\text{mol CO}_2 \text{ m}^{-2} \text{ s}^{-1}$ were used.

3.2 *Pseudo-Steady State Heat Stress Measurements*

Prior exposure to high T_{leaf} caused a decline in A_{sat} and this decrease might be due to several factors. These are: light harvesting capacity and energy transfer to the reaction centers (photosystem I and photosystem II); **ETR** and ATP/ NADPH synthesis; the activity of the C3 cycle enzymes; CO_2 concentration in the chloroplast (**Cc**) which is dependent on stomatal conductance (**gs**) and mesophyll conductance (**gm**). In this part of the project the effects of high T_{leaf} on pseudo steady state photosynthesis rates were studied.

Stomatal aperture can be controlled by blue light, CO_2 and ABA concentration and is mediated by changes in guard cell turgor pressure (Farquhar and Sharkey 1982). Open stomata allow CO_2 uptake for photosynthesis and water vapor efflux by transpiration. At night, however, and under drought stress conditions and high air temperatures, stomata are reported to close. High temperatures may cause a decrease in turgor pressure which results in stomatal closure to conserve water (Farquhar and Sharkey 1982).

In order to investigate the effect of transient changes in T_{leaf} on A_{sat} and **gs** gas exchange measurement were made on plants placed in a controlled environment growth chamber set to different air temperatures (T_{air}). High T_{air} will tend to drive high T_{leaf} which can be measured with $\pm 0.3^\circ\text{C}$ precision, but not controlled as precisely as it can using a thermal block (Section 3.1). Mature leaves were sealed in a the leaf chamber of an IRGA and exposed to normal air ($380 \mu\text{mol CO}_2 \text{ mol}^{-1}$ air) and saturating white light ($580 \mu\text{mol m}^{-2} \text{ s}^{-1}$ PAR) for 20 minutes and then

Pseudo Steady State photosynthetic parameters measured at 23°C (these included **A_{sat}**, **gs**, **Ci**, **E**, and **T_{leaf}**; only leaves demonstrating high rates of **A_{sat}** ($> 10 \mu\text{mol CO}_2 \text{ m}^{-2} \text{ s}^{-1}$) were subsequently used. After this period the temperature of the cabinet and the leaf chamber was increased from 25°C and held at a set elevated values for 180 minutes whilst photosynthesis parameters indicated above were measured again. Figure 3-9 shows the pseudo steady state changes in **A_{sat}** and **gs** in response to increasing **T_{leaf}**. In these experiments a significant effect of temperature on **A_{sat}** was observed ($p < 0.001$; Appendix A-4) above 40°C.

In contrast, **gs** increased abruptly and significantly ($p < 0.005$) when **T_{leaf}** exceeded 37°C (~0.60 to 1.20) but declined to control levels at 40°C and above (Appendix A-4). Even at 43°C, however, **gs** was greater than $0.3 \text{ mol m}^{-2} \text{ s}^{-1}$, the threshold level below which **gs** begins to exert a major influence on carbon assimilation (Figure 3-9). The implications are that the large decline in **A_{sat}** at high **T_{leaf}** are not attributable to **gs** limitations of CO₂ supply to the chloroplast as has often been reported (Flexas et al. 2014; Sharma et al. 2014).

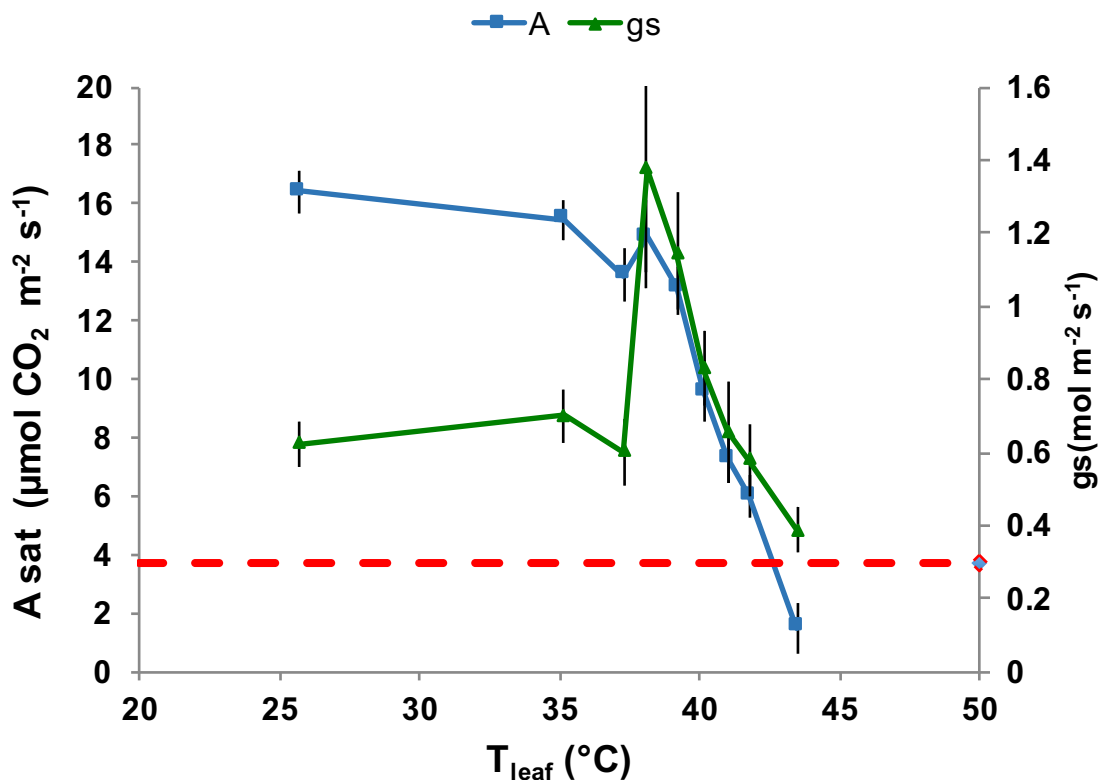


Figure Figure 3-9 . Effects of Increasing T_{leaf} on Measured Pseudo Steady State A_{sat} and g_s in Attached Barley Leaves.

Pots containing barley plants were placed in a controlled environment growth cabinet set initially to 25°C. Fully expanded 4th attached leaves were placed in a leaf chamber attached to an IRGA and exposed to T_{leaf} of 25, 35, 37, 38, 39, 40, 41, 42 and 43 (± 0.4) °C. The leaves were exposed to normal air (380 $\mu\text{mol CO}_2 \text{ mol}^{-1} \text{ air}$) and saturating white light (580 $\mu\text{mol photons. m}^{-2} \text{ s}^{-1} \text{ PAR}$). Leaves were first held at 25°C for 30 minutes and *Pseudo Steady State* photosynthesis parameters measured. The cabinet temperature was then increased to one of the indicated temperatures for 210 minutes and the new steady state A_{sat} and g_s measured (see Section 2.3.2). The broken red line indicates the threshold level ($\sim 0.3 \text{ mol m}^{-2} \text{ s}^{-1}$) below which g_s begins to exert a major influence on carbon assimilation (Appendix A-19). The values represent the average ($\pm \text{SE}$) of $n=3$ at 38, $n>7$ at 35 and 37, $n>10$ at 25, 39 and 43, $n>17$ at 40, 41 and 42°C, independent leaves of cv. Optic.

3.3 Discussion

3.3.1 Steady State Heat Stress Experiments

The results presented in the Section 3.1.1 indicate there are no differences in the thermal suppression of A_{sat} when stress is imposed in saturating light or in the dark. It would appear, therefore, that light generated ROS produced during heat stress events in field-grown barley can be ignored (Figure 3-1). The direct effects of heat stress ($T_{\text{leaf}} > 36^{\circ}\text{C}$) on carbon assimilation rates, however, are profound.

Further, the results presented in Section 3.1.2 indicates there was no significant increase in photorespiration rate that might be responsible for the inhibition of A_{sat} in response to heat stress even at high T_{leaf} of 40°C and above. The conclusion is that the observed suppression of A_{sat} (and ϕCO_2) arises from a direct effect of high T_{leaf} on the turnover rate of the C3 cycle. (Shikanai 2010). In addition, the $\Phi_{\text{PSII max}}$ did not change until T_{leaf} reached 38°C and above, whereas it has been reported that no change occurred below 43°C ; clearly, the changes in A_{sat} reported here can not be attributed to changes in $\Phi_{\text{PSII max}}$ (Lazár and Ilík 1997; Kalaji et al. 2011).

Previous metabolomics studies by Shahwani (2012) on barley leaves indicated high T_{leaf} caused a severe blockage in C3 cycle carbon flow between in the C3 cycle between Ri5P and 3PGA, but none of the enzymes involved in this conversion was affected (Al-Malki 2014). The only remaining possibilities to account for the combined observations of changes in A_{sat} and the metabolite profile is a decline in the concentration of CO_2 concentration in the chloroplast (C_c) or a decrease in chloroplast ATP levels preventing the efficient synthesis of RuBP by the

phosphoribulose kinase. Direct measurements on the effect of increasing Ca on photosynthesis rates in heat stressed leaves suggested the physical CO₂ diffusion pathway was not affected (Al-Malki 2014; this study) leaving changes in the chloroplast ATP levels as the only remaining possibility to account for the combined observations of the effects of high T_{leaf} on whole leaf metabolite profiles and photosynthesis rates. Careful analysis on the effects of high T_{leaf} on whole leaf ATP levels, however, were not consistent with this view. Whole leaf ATP levels increased with T_{leaf} in post heat stressed leaves incubated for 20 minutes in the light (Fig 3-8) whilst concomitant measurements on in vivo electron transport rates showed a strong decline (Fig 3-2). If whole leaf ATP levels are reliable estimates of the levels in chloroplasts, it is difficult to attribute the observed decline in A_{sat} to low turnover rates of PRK due to insufficient levels of ATP. A different pattern of whole leaf ATP levels was observed when post heat stressed leaves incubated for 20 minutes in the dark (Fig 3-8). In unstressed leaves (25°C) ATP levels were significantly higher when incubated in the dark than in saturating light (Fig 3-8) and declined T_{leaf} ; above 38°C, however, ATP levels increased to well above the levels found in controls. No major changes in dark respiration were observed over the temperature range (Almalki 2014; this study, data not presented; AtKin et al. 2005) (Almalki 2014; this study, data not presented; AtKin et al. 2005) and of course in the dark photophosphorylation cannot occur, so the complex pattern of change in dark adapted heat stressed leaves must arise from changes in the consumption of whole leaf ATP, not its generation. These conclusions are similar to those other who showed the amount of cytosolic ATP might be higher in the dark (Krömer et al. 1988; Gardstrom 1993). In addition, exposure of leaves to more extreme stress has been reported to increase ATP production (Kosová et al. 2014)

The Mehler reaction (water- water cycle) is believed to operate in vivo in chloroplasts, and this may in part contribute to the anomalous changes in whole leaf ATP. The Mehler reaction involves electron flow from water, through PSII and the Cyt b6/f complex but instead of reducing P700+ in the reaction centre of PSI, they reduce water in the stroma to hydrogen peroxide (which is subsequently converted back to water by the action of chloroplast catalase activity). This process results in the synthesis of ATP through chemiosmosis but does not generate reducing potential in the form of ferredoxin or NADPH; cyclic electron flow around PSI might also occur and produce a similar effect (Munekage et al. 2004; Endo and Asada 2008; Shikanai 2010, 2014; Peeva et al. 2012). In addition, chlororespiration might be involved in this increasing chloroplast ATP levels during dark at high T_{Leaf} (Peltier and Cournac 2002; Nixon and Rich 2007). Furthermore, (Clarke and Johnson 2001) investigated the role of the Mehler reaction and cyclic electron flow in maintaining thylakoid membrane function under high T_{leaf} in barley and concluded the Mehler reaction was not as important as CEF.

Other studies have found changes in chloroplast ATP levels are inversely correlated with drought-induced changes in photosynthesis rates (Lawlor and Khanna-Chopra 1984; Paul et al. 1995; Tezara et al. 1999); a decrease in photosynthesis rates resulted in an increase in whole leaf ATP as consumption, but not production, increased. Others, however, found water stress limited photosynthesis rates and the ratio of PGA to triose phosphate declined, but concluded ATP was not responsible (Sharkey and Badger 1982; Sharkey and Seemann 1989).

3.3.2 Effect of Pseudo Steady State Heat Stress on A_{sat} and g_s

These experiments confirm a direct effect of high T_{leaf} on A_{sat} , and also showed that stomata do indeed open in response to moderate heat stress (37°C-40°C). Above this temperature, however, stomata close but not to the extent that CO_2 supply to the chloroplast limits photosynthesis. Raising T_{leaf} above 35°C, however, has the opposite effect, stomata open, presumably to increase transpiration and reduce T_{leaf} ; this is a novel observation. The conclusion is that when T_{leaf} is above 35°C, preventing a further increase in T_{leaf} is more important than conserving water.

In these experiments attached leaves were exposed to heat stress while irradiated with saturating levels of light and these observations support the results shown in Figure 3-1 where the ROS not causing the inhibition of A_{sat} . In contrast, Figure 3-9 shows the severe damages to A_{sat} take place when T_{leaf} reached 43°C or above when the A_{sat} declined in 65%, and the inhibition of A_{sat} is 89% when T_{leaf} is 44°C. These results inconstant with the findings in Figure 3-1, where the inhibition of A_{sat} is 80% when the T_{leaf} equal to 40°C. The reasons might be due to exposing only part of an attached leaf to high T_{leaf} using a heating block (in Section 3.1.1.1) where the function of stomata in cooling was limited. While, in this Section (3.2), the whole plant was exposed to high temperature ($\pm 6^\circ\text{C}$ of T_{leaf}), and changes in stomatal function will affect leaf temperature. Exposure of barley leaves to T_{leaf} above 45°C has been reported to cause inhibition of PSII that were attributed to redox changes in the plastoquinone pool (Čajánek et al. 1998; Bukhov and Carpentier 2000; Egorova and Bukhov 2002; Kaa et al. 2008).

3.3.3 Effects of High Nitrogen and T_{leaf} on Photosynthesis Rates and Yields of Barley

The increasing T_{leaf} might lead to a decline in A_{sat} for no identified reasons on which is the sensitive component causing the damage. Furthermore, the majority of literature blaming RCA as a thermosensitive protein (Salvucci 2004; Carmo-Silva et al. 2012; Henderson et al. 2013; Gontero and Salvucci 2014). In order to find the role amount of protein that might be acting as source of protein and could enhance photosynthesis rates, the effect of nitrogen supply need to be identified. Thus, both N levels and T_{leaf} are abiotic stress if increased or decreased at certain levels to the plants.

The effect of N supply on photosynthesis rates and the yield of barley need to be studied. Moreover, the next two chapters will investigate the impact of N supply on physiology and flowering in barley.

Earlier experiments conducted at Glasgow University on the effects of T_{leaf} on barley photosynthesis rates were conducted on plants grown in N-rich compost (Almalki 2014). These plants were exposed to N levels that were probably 30 times higher than those experienced by plants growing in well-fertilized agricultural soil and showed several growth abnormalities. It is conceivable, therefore, that the responses reported by Almalki (2014) were artefacts that arose from exposure of plants to a physiologically high levels of N. This possibility was investigated by repeating the experiments on plants grown in different levels of N (hydroponics or soil/sand mixtures) that generated plants with phenotypes

that are commonly found in field grown plants (3- 5 tillers and 1- 3 floral spikes per plant, etc.). The results from these experiments on the effect of T_{leaf} on photosynthesis rates, however, did not differ from those reported by Almalki (2014), and it is concluded that N- Supply did not generate experimental artefacts.

In summary, raising T_{leaf} to over 36°C for 3 hours severely, and irreversibly, suppresses A_{sat} in the elite barley cultivars Optic and Belgravia. Similar responses were found in a previous study (Al-Malki) where sub-tropical and temperate barley (C3) lines (landrace 'Local' from SE Asia, and Optic, respectively) and maize (C4) cultivars (Katamani from NE Africa and Sundance, respectively). Further analysis from A/C_i curves and on g_s measurements confirmed the decline in A_{sat} is attributable to a direct effect of high temperatures on the turnover of the C3 cycle (Shahwani, 2011; Almalki, 2014; experiments reported in this chapter). Metabolomics profiling (Shahwani 2011) and measurements on the activities of key C3 cycle enzymes (Almalki 2014) suggests the flow of carbon through RuBisCO is greatly affected but this could not be attributed to the activities of Ri5P Isomerase, phosphoribulose kinase, RuBisCO itself, or RuBisCO activase. In addition, the supply of CO₂ to RuBisCO did not appear to be greatly affected. Heat stress might cause changes in the levels of many proteins in the leaf including those involved in photosynthesis (Rollins et al. 2013)

Chloroplast ATP levels could affect carbon flow in the C3 cycle, but it is not possible to measure these directly. Instead, whole leaf ATP levels were

measured immediately after heat stress and significant changes were observed. In saturating light whole leaf ATP levels increased significantly with T_{leaf} implying metabolic consumption of ATP may decline with temperature; there was no evidence that ATP production increased (Almalki, 2014; experiments reported in this thesis), these results are inconsistent with the hypothesis that T_{leaf} decreases chloroplast ATP levels and this impairs carbon flow through phosphoribulose kinase to generate the RuBisCO substrate RuBP (Figure 3-8). A high T_{leaf} -induced decline in chloroplast ATP levels can not be discounted, however, as only whole leaf ATP levels have been measured. Unfortunately, there are no reliable methods for measuring *In vivo* chloroplast ATP levels in the light and so this issue remains unresolved. It is conceivable that other chloroplast factors such as ionic balance, pH, co-factors are affected by high T_{leaf} and these suppress the activity of the C3 cycle. Further experiments are required to resolve this possibility.

4 Effect of Nitrogen Supply on Barley

Photosynthesis and Development

4.1 Introduction

Barley is grown in many different geographical locations around the globe that includes temperate and subtropical climates, the Nordic countries, at high altitudes in Peru, in the African Sahel (Ullrich 2011), and in arid region with a harsh environment such as Kuwait (Almenaie et al. 2013). Clearly, barley demonstrates an ability to tolerate abiotic stress such as cold, drought, and salinity. Barley lines have been developed to exploit local climatic conditions and consequently winter and spring lines have been selected (Landraces) or developed (cultivars). Spring barley is sown in March when soil temperatures are at least 5°C although optimum soil temperature may be between 15 and 24 °C. Early planting results in an earlier harvest with good quality grain and avoidance of thermal and drought stresses that can be experienced in mid- and late summer (Robertson and Stark 2003). Winter barley lines are normally sown in autumn, at least one month before the onset of any frost; this strategy allows the benefit of vigorous vegetative growth due to plentiful rainfall during the autumn/ winter/ early spring, allowing high yields in early summer before the onset of extreme summer temperatures and drought (Allen-stevens 2013).

Barley is to used as animal feed (55-60%), for malting (30-40%), as food (2-3%) for direct human consumption, and 5% for seed (Ullrich 2011). The nitrogen

requirement for winter and spring barley is different so the nutrient management programme for the two systems requires modification. Winter lines require about 220 kg Ha^{-1} of N compared to 190 kg Ha^{-1} of N in spring lines; these applications, however, have to be decreased by 20-30% to attain good quality malting barley. Furthermore, the malt barley is normally grown in spring, with the vast majority of winter lines providing feed for livestock. Malting barley typically contains 10 – 13.5 % of protein and 60-60 % starch but care with N application is required to ensure the quality is maintained (Schwarz and Li 2011; Ullrich 2011; Allen-stevens 2013). In England, around 30% of malting barley is grown over the winter. The cultivation of good quality winter malting barley ensures a dual-purpose product yielding grain suitable for animal feed and for malting purposes. (Robertson and Stark 2003; Ullrich 2011; Allen-stevens 2013)..

Previous studies at Glasgow University have indicated high T_{leaf} affects the activities of the key enzymes of the C3 cycle , and this accounted for the observed thermal suppression of A_{sat} (Almalki 2014). Specifically, carbon flow through RuBisCO in attached leaves appeared to be suppressed, an observation that is consistent with several publications in the literature that had identified RuBisCO Activase (RCA) as the temperature sensitive component (Section 1.3.2). However, in contrast to these *in vitro* studies on RuBisCO and RCA, the work of Almalki (2014) clearly showed *in vivo* RuBisCO activity, and therefore RCA activity, was unaffected and could not account for the observed decline in whole leaf photosynthesis rates. The experiments of Almalki, however, were conducted on barley plants grown in potting compost, a very nitrogen-rich medium (~30 times higher than found in agricultural soils). These elevated levels of N cause severe phenotype abnormalities in cereals

(suppressed flowering, excessive tillering, reduced secondary wall thickening, excessively broad and elongated leaves, *etc.*) and are reported to lead to the accumulation of several major leaf proteins, including RuBisCO, which serves as a long term nitrogen store (Tsutsumi et al. 2014) .

It is conceivable, therefore, that the apparent high *in vivo* activities of RuBisCO extracted from heat stressed leaves observed by Almalki (2014) was an artefact. It is possible that when luxury levels of N are available, two pools of RuBisCO develop. One contributes to endogenous carbon fixation and is severely affected by heat stress; the other, the larger of the two pools, does not contribute to *in vivo* CO₂ assimilation, is not significantly affected by heat stress, but does contribute to the activity measurement *in vitro*. For this reason, it was decided to re-assess the effect of high T_{leaf} on barley plants grown over a range of N-supply. The experiments reported in Chapter 3 have shown, however, that this was not the case. Similar effects of high T_{leaf} were found on photosynthesis rates regardless of whether plants were grown in N-rich medium or exposed to N levels commensurate with those found in agricultural settings. During these experiments, however, some unusual, unexpected, and very interesting phenotypical responses were observed, and this prompted a change in focus of the research direction. The results of experiments prompted by this change of focus are reported in this chapter and Chapter 5.

Nitrogen is a major essential nutrient for plant growth and is required for the synthesis of amino acids, nucleic acid, and chlorophyll (Miller et al. 2007). Increasing N levels supply results in an increase in A_{sat} in rice and this has been attributed to an increase in RuBisCO (Nakano et al. 1997; Makino et al. 2000; Tsutsumi et al.

2014) . Tsutsumi et al. (2014) found that in rice there was a strong positive correlation between RuBisCO content and N supply regardless of whether the plants were grown hydroponically or in soil. Increasing soil N levels induced many developmental responses in barley plants grown in soil (Figure 4-1) and similar effects were observed when they are grown over a range of N-supply in hydroponic solutions (Figure 4-2). Agricultural soils typically contain the equivalent of between 0.5mM and 0.8 mM available N (Marschner and Rengel 2012).

4.2 Preliminary Observation on the Effects of N Supply on Barley Morphology.

For the reason outlined above a series of experiments was conducted using Barley (*Hordeum vulgare* cvs. Belgravia and Optic) grown over a range of N supply to re-assess the effects of high T_{leaf} on the thermal suppression of photosynthesis rates. In these experiments plants were grown in a nutrient depleted mixture of 15:85 top soil: sand to which NPK was added in two equal portions at the 4 week and 8-week stage (Figure 4-1). In addition, plants were also grown in hydroponics using a modified Hoagland's solution. Here, all salts containing N were removed and where appropriate the levels of other ions were increased to the levels specified in the Hoagland's recipe; this constituted Hoagland's Basal Media to which N in the form of ammonium nitrate was added (See Section 2.5.1.2 for full experimental details). Using this approach only N-supply changed between the hydroponic solutions. Up to eight plants were grown in 15L of Basal Hoagland's Media supplemented with ammonium nitrate. The pH, NO_3^- , and NH_4^+ levels were monitored every second day to ensure the hydroponic solutions were stable, and fresh solutions were

prepared every week (Figure 4-2). It was clear from both the soil and hydroponic experiment plants grown in low N were stunted, unicum (produced only one stem), showed an erect habit (demonstrated by some secondary cell wall thickening of stems), and flowered. With increasing N supply plants were larger, more tillers developed, and larger flowers appeared. At the highest levels of N supply, biomass increased dramatically, tillering was profuse, and at the very highest levels in hydroponic flowering was suppressed and plants failed adopt an erect habit (Figure 4-1 and 4-2). Further, measurements on A_{sat} of control (non-heat stressed leaves) suggested a strong positive correlation with N supply. This observation was very interesting; A_{sat} is a measure of the light saturated rates of carbon assimilation expressed on a per unit of leaf area (ULA) basis; that is an estimate of the ULA carboxylation processes in leaves. The preliminary conclusions are that the carboxylation processes of photosynthesis in normal agricultural soils is limited by the supply of N, and increasing N supply above those normally applied in an agricultural setting will boost ULA photosynthesis rates. This chapter reports on a series of experiments that were conducted to assess the effects of a wide range of N supply on the growth and development of barley.

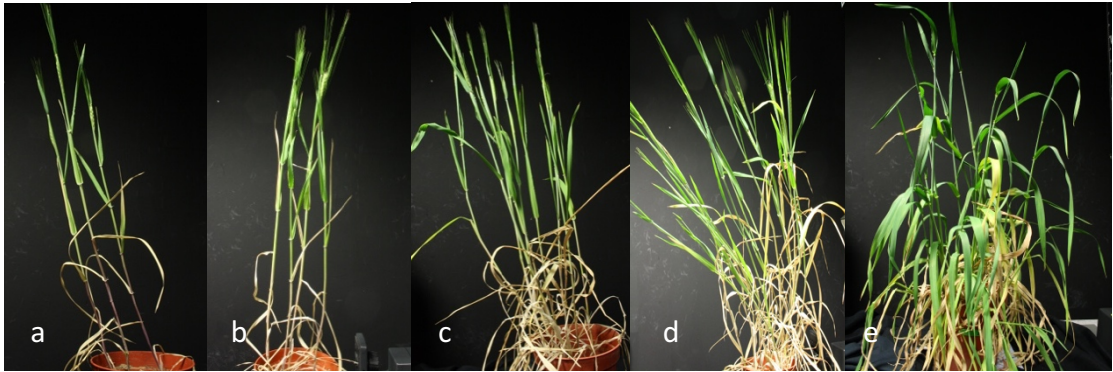


Figure 4-1. Effect of Fertilizer Application on the Growth and Development of Soil-Grown Barley.

Seeds of *Hordeum vulgare* cv. Optic were germinated on moist filter paper and planted in 5L pots containing 15% top soil (Levington Organic Blend, The Scot Miracle-Grow Co. Salisbury House Weyside Park, Catteshall Lane, Godalming, Surrey GU7 1XE, UK) and 85% agricultural sand and supplemented with a NPK fertilizer (3:1:2). The pots were placed in a growth room (photoperiod of 16 / 8 hour, Light / Dark and 22°C / 16°C). The images are from plants after 10 weeks. Nitrogen applications were as follows: 0, 2, 10, 20 and 47 g / m² of N (Section 2.5.1.1). Half of the indicated level of fertilizer was added at the 4 weeks' stage and the remainder at the 8-week stage. N application of 10 g m⁻² soil is equivalent to 100 kg / ha, levels that are similar to those used in arable production.

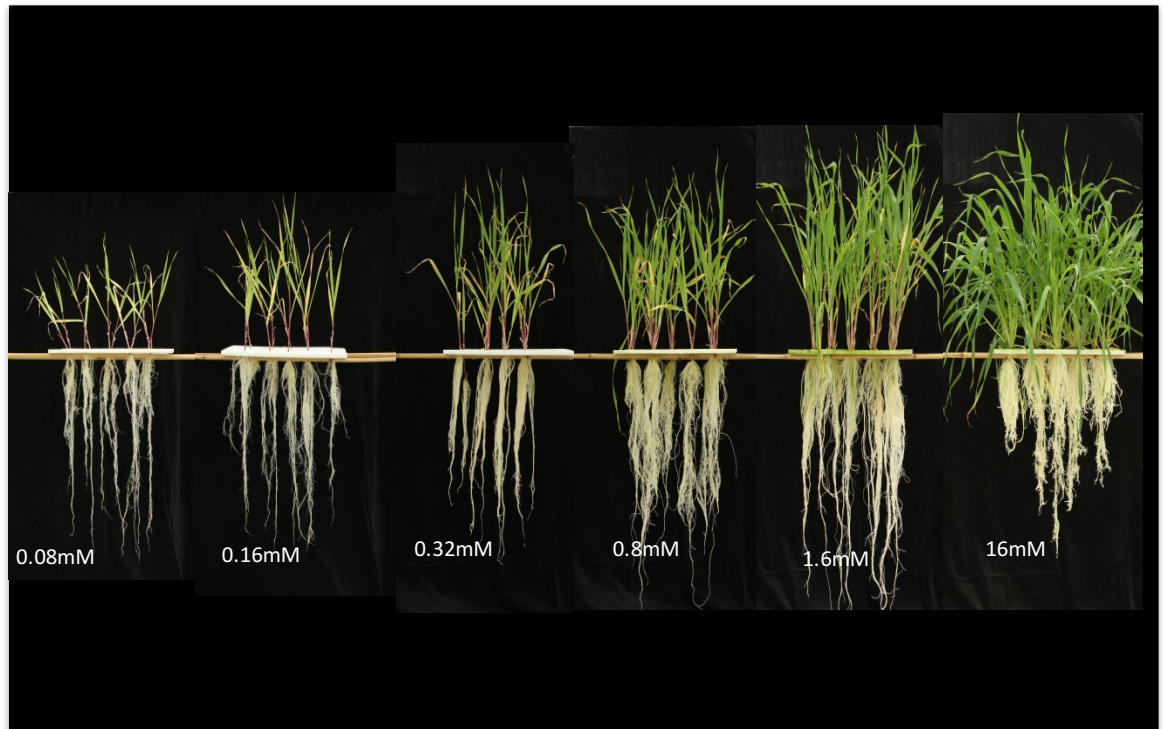


Figure 4-2. The Effect of Nitrogen Application on the Growth of Barley in Hydroponic Solutions.

Hordeum vulgare cv. Optic plants were grown for 5 weeks in full-strength Basal Hoagland's Medium adjusted to contain the indicated N levels; fresh solutions were prepared every week (Section 2.5.1.2). Increasing N supply (as ammonium nitrate) above 0.16 mM induced tillering; at levels above 1.6 mM plants failed to go on to flower and remained in the vegetative state for the duration of the experiment (11 weeks). Nutrient replete agricultural soils are reported to contain 0.5-0.8 mM N (Marschner and Rengel 2012).

4.3 Photosynthesis

4.3.1 Assimilation Rate

Measurements of A_{sat} from leaves of these plants showed an increase with N supply (Figure 4-3 for cv. Optic and 4-4 for cv. Belgravia). A/C_i plots were constructed from A_{sat} versus C_a curves to remove the effect of stomatal control on photosynthesis, and the resulting carboxylation coefficient, Φ_{CO_2} , a measure of the turnover efficiency of the *in vivo* C3 cycle activity, was plotted against N-supply. The results are unequivocal; for both cultivars there is a highly significant ($p < 0.001$; Appendix A-6 and A-7) linear increase in C3 cycle activity with the log of N-supply that appears to not be attributable to stomatal changes. The important points to note here is that both A_{sat} and Φ_{CO_2} are expressed on a unit leaf area basis. To state this conclusion another way, in typical agricultural soils (0.5- 0.8 mM N) the photosynthesis rates of light saturated barley plants in air appear to be limited by the amount of available N, possibly the concentration of C3 cycle enzymes.

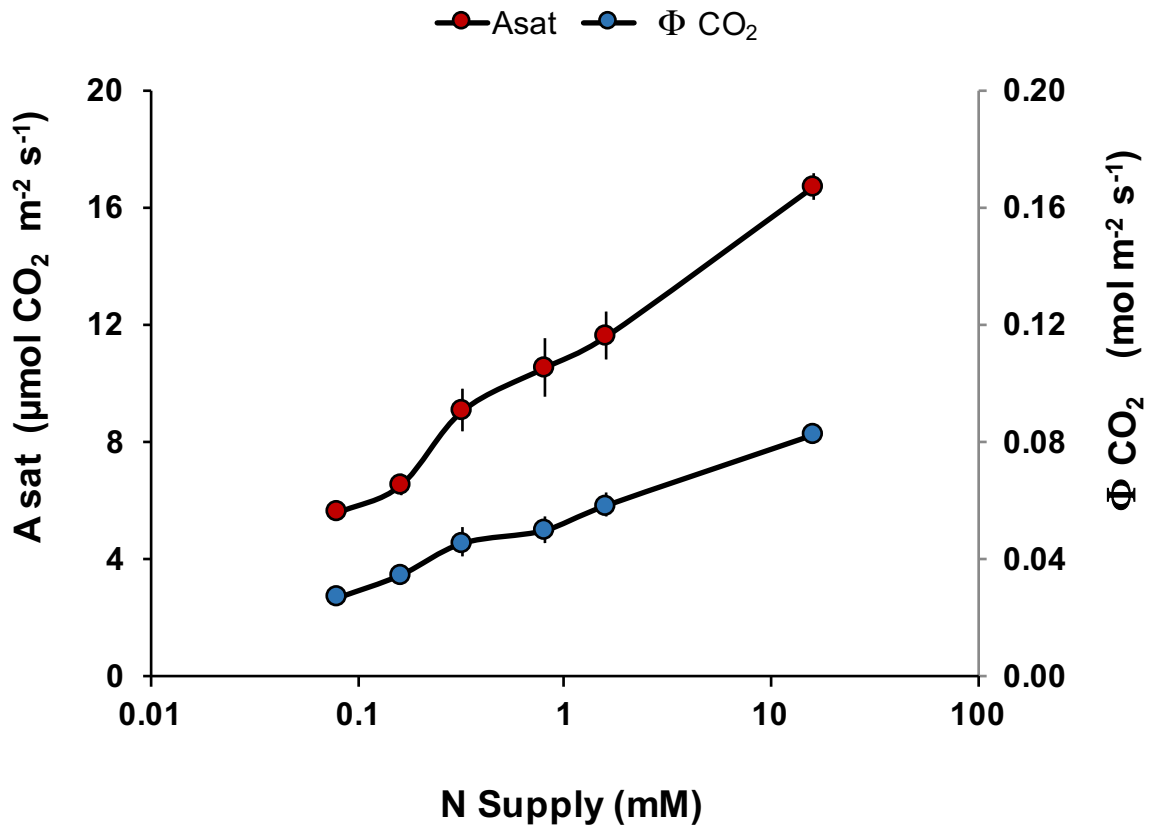


Figure 4-3. The Effect of Increasing N Supply on Hydroponically Grown Barley

Plants were grown for 5 weeks in full-strength Hoagland's solution adjusted to contain the indicated N levels; fresh solutions were prepared every week. Light saturated levels ($560 \mu\text{mol m}^{-2} \text{s}^{-1}$ PAR) CO₂ assimilation rates in air ($380 \mu\text{mol CO}_2 \text{mol}^{-1}$ air), A_{sat} , were estimated from A/C_a curves measured from fully expanded attached leaves; the Carboxylation Coefficients, Φ_{CO_2} were estimated from the initial slopes of the corresponding A/C_i plots (each data point is the average (\pm SE) of $n > 4$ biological replicates of barley cv Optic).

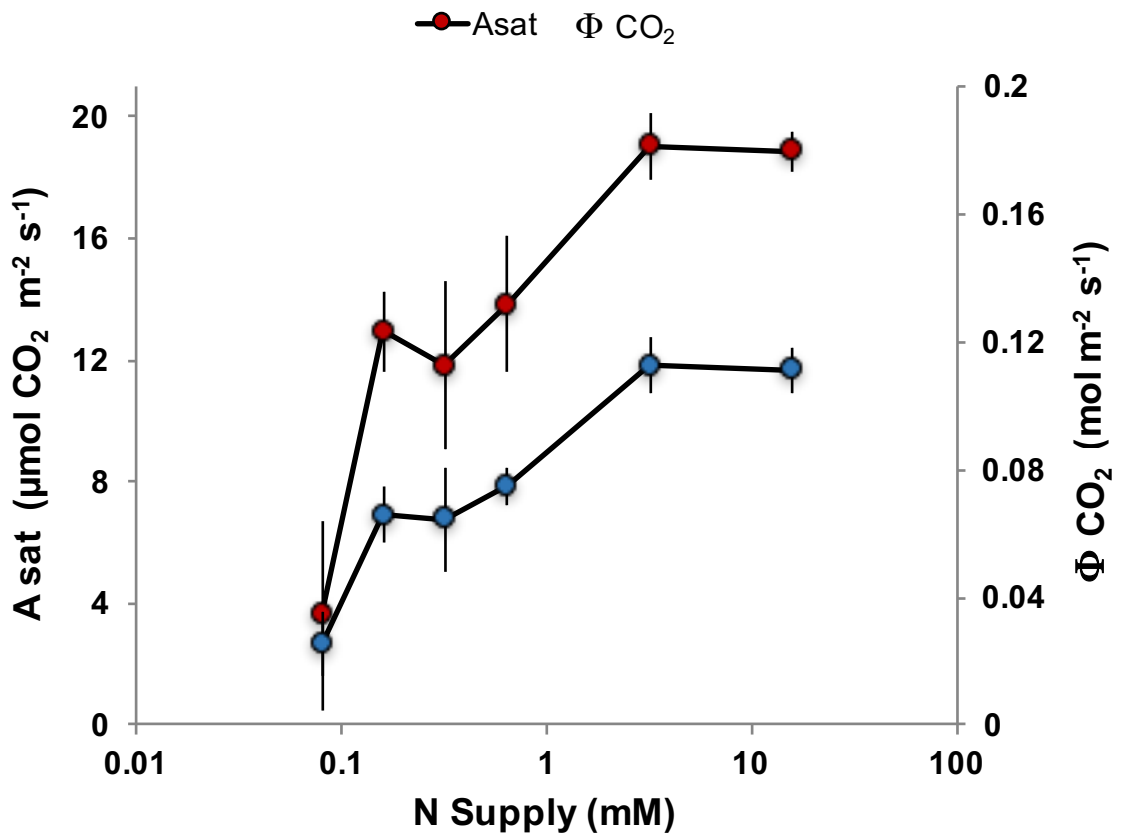


Figure 4-4. The Effect of Increasing N Supply on Hydroponically Grown Barley

Plants were grown for 6 weeks in full-strength Hoagland's solution adjusted to contain the indicated N levels; fresh solutions were prepared every week. Light saturated levels (560 $\mu\text{mol m}^{-2} \text{s}^{-1}$ PAR) CO₂ assimilation rates in air (380 $\mu\text{mol CO}_2 \text{ mol}^{-1} \text{ air}$), A_{sat} , were estimated from A/C_a curves measured from fully expanded attached leaves; the Carboxylation Coefficients, Φ_{CO_2} were estimated from the initial slopes of the corresponding A/C_i plots (each data point is the average (\pm SE) of $n > 5$ biological replicates of barley cv. Belgravia).

4.3.2 Electron Transport Rate

Figure 4-5 presents values of steady state photosynthetic electron transport rates (**ETR**s) of attached leaves of hydroponically grown barley estimated by modulated chlorophyll fluorescence measurements. The ULA **ETR**s constantly increased significantly ($p < 0.001$; Appendix A-8) with N supply in a fashion similar to that observed by gas exchange measurements (Figs. 4.3 and 4.4). The results in Figure 4-5 indicate that the high N enhanced **ETR**. The **ETR** at 0.08 mM of N is approximately $56 \mu\text{mol electrons m}^{-2} \text{s}^{-1}$. This rate doubled across the N supply range and reached $126 \mu\text{mol electrons m}^{-2} \text{s}^{-1}$ at 16 mM of N. The efficiency of **ETR** is an important parameter of photosynthetic activity which suggests healthy plant growth can be expected. These data are consistent with those from A_{sat} measurements, photosynthetic transport in barley leaves increases when N supply is increased.

4.3.3 Maximum Quantum Efficiency of PSII (Φ_{PSII})

The effect of N supply on photosystem II photochemical processes was determined by measuring Φ_{PSII} . Changes in Φ_{PSII} with increasing N supply showed a very slight increase over the range used. Values of Φ_{PSII} considered to be indicative of healthy, non-stressed leaf tissue (0.7 – 0.8; Baker, 2008) were observed at all levels of N supply (Figure 4-6). In conclusion, N supply has no major effect on Φ_{PSII} and the efficiency of photosystem II photochemical processes.

The results of this section indicate that ULA photosynthesis rate determined by two independent methods (A_{sat} and ϕ_{CO_2} from gas exchange measurements and *in vivo* **ETR** rates from modulated chlorophyll fluorescence) approximately tripple when N supply is increased from 0.08 to 16 mM. In contrast, measurements on ϕ_{PSII} was approximately constant across different N concentrations providing no evidence that primary photochemical reactions were affected.

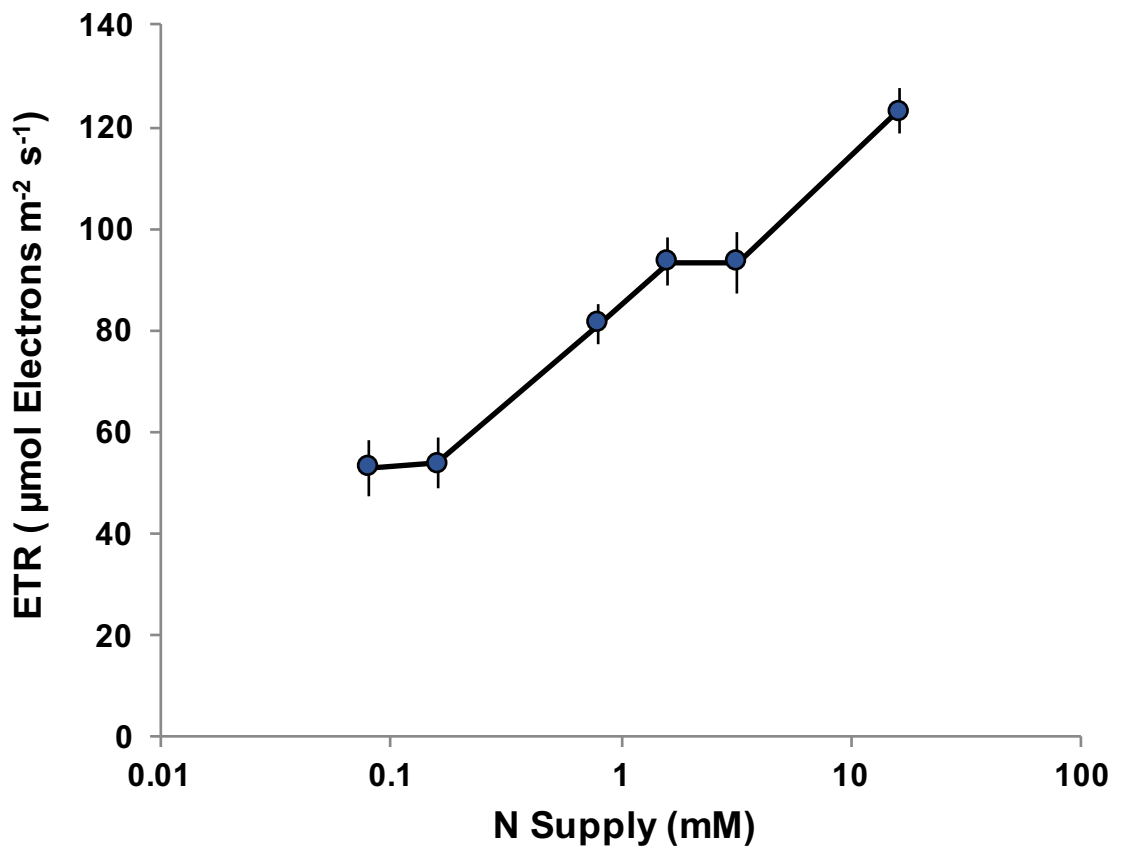


Figure 4-5. The Effect of N-Supply on *in vivo* Photosynthetic Electron Transport Rates (ETRs) of 7 Week-Old Barley.

Plants were grown in Hydroponic solution at different range of N-supply 0.08, 0.16, 0.32, 0.64, 1.6, and 16 mM of N (Section 2.5.1.2). Leaves were incubated in the dark for 20 minutes and then steady state **ETRs** were measured using pulse amplitude modulated fluorescence at 25°C, Light saturated levels (560 µmol m⁻² s⁻¹ PAR) immediately. Values are averages (± SE) of n= 6 measurements on leaves of separate plants, cv. Belgravia.

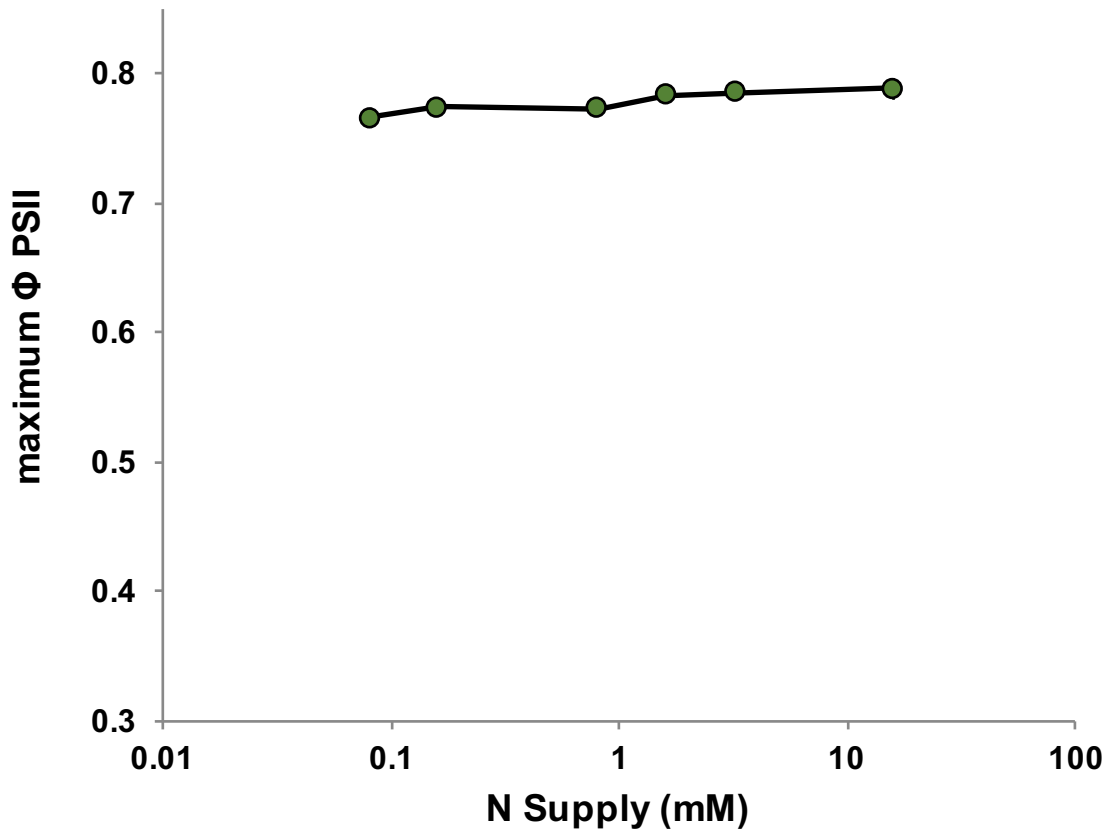


Figure 4-6. Effects of N Supply on Maximum Quantum Efficiency (Φ_{PSII}) of 7 Week-Old Barley.

Plants were grown in Hydroponic solution at different range of N-supply 0.08, 0.16, 0.32, 0.64, 1.6, and 16 mM of N (Section 2.5.1.2). Leaves were incubated in dark, then Φ_{PSII} was measured immediately using pulse amplitude modulated fluorescence at 25°C and Light saturated levels (560 $\mu\text{mol m}^{-2} \text{s}^{-1}$ PAR; Section 2.1.3). Values are average (\pm SE) of n= 6, cv. Belgravia.

4.4 Growth and Development

The effects of N supply on the growth and development of barley is not noticeable for the first four or five weeks after transferring seedlings into hydroponic solutions containing different levels of N-supply but after this period clear morphological differences become apparent (Section 4.2). Apart from major differences in the extent of tillering and spike initiation, at high levels of N supply leaves became broader and longer. For this reason, it was decided to quantify growth staging (the timing of development) and seed set/ harvest parameters.

4.4.1 Barley Growth

After exposure for five weeks to the different N supply regimes clear differences in the number of leaves per tiller became apparent (Figure 4.7 A & B). When grown in soil the average number of leaves / tiller was 8 with no supplemental N and this declined significantly ($p < 0.001$, Anova; $p < 0.001$ Kruskal-Wallis non-parametric test ; Appendix A-9) to approximately 6 with the addition of up to 47 g N / m² (Fig 4.7 A). A similar pattern was observed when plants were grown in hydroponic solutions with values of ca. 7 leaves / tiller at 0.08 mM N declining to 5 or 6 at 16 mM N (Fig 4.7 B) but neither Anova nor the Kruskal-Wallis test showed significance (Appendix A-9). These data indicate that the soil / sand mixture used in these experiments contained less than 0.08 mM N. Typical additions of N to arable land are within the range of 100 to 180 kg / ha (or 10 – 20 g / m²) and this is consistent with the claim that good agricultural soils contain 0.5-0.8 mM N (Marschner and Rengel 2012).

The effects of N supply on the number of tillers / plant are shown in Fig. 4-8. Tiller number / plant increased significantly ($p < 0.001$, Anova and $p < 0.001$ Kruskal-Wallis test; Appendix 10) from 1 in soil with no N additions up to ca. 7 at 47 g / m^2 (Fig 4-8 A). For cv. Optic grown in hydroponics no tillering was initiated until N supply exceeded 0.32 mM , after which tillering continually increased significantly ($p < 0.001$, Anova and $p < 0.001$ Kruskal-Wallis test; Appendix 10) up to ca. 17 at the highest N level of 16 mM . In contrast, in cv. Belgravia tillering increased significantly ($p < 0.001$, Anova and $p < 0.001$ Kruskal-Wallis test; Appendix 10) to over 5 / plant at 0.32 mM N supply and over 20 per plant were observed at 16 mM (Fig 4-8 B & C). These data clearly indicate tillering is promoted strongly when plants are exposed to high levels of N supply. Again, in the range of 0.64 to 1.2 mM N barley developed 5-8 tillers / plant, and this is similar to plants grown in well-fertilized fields.

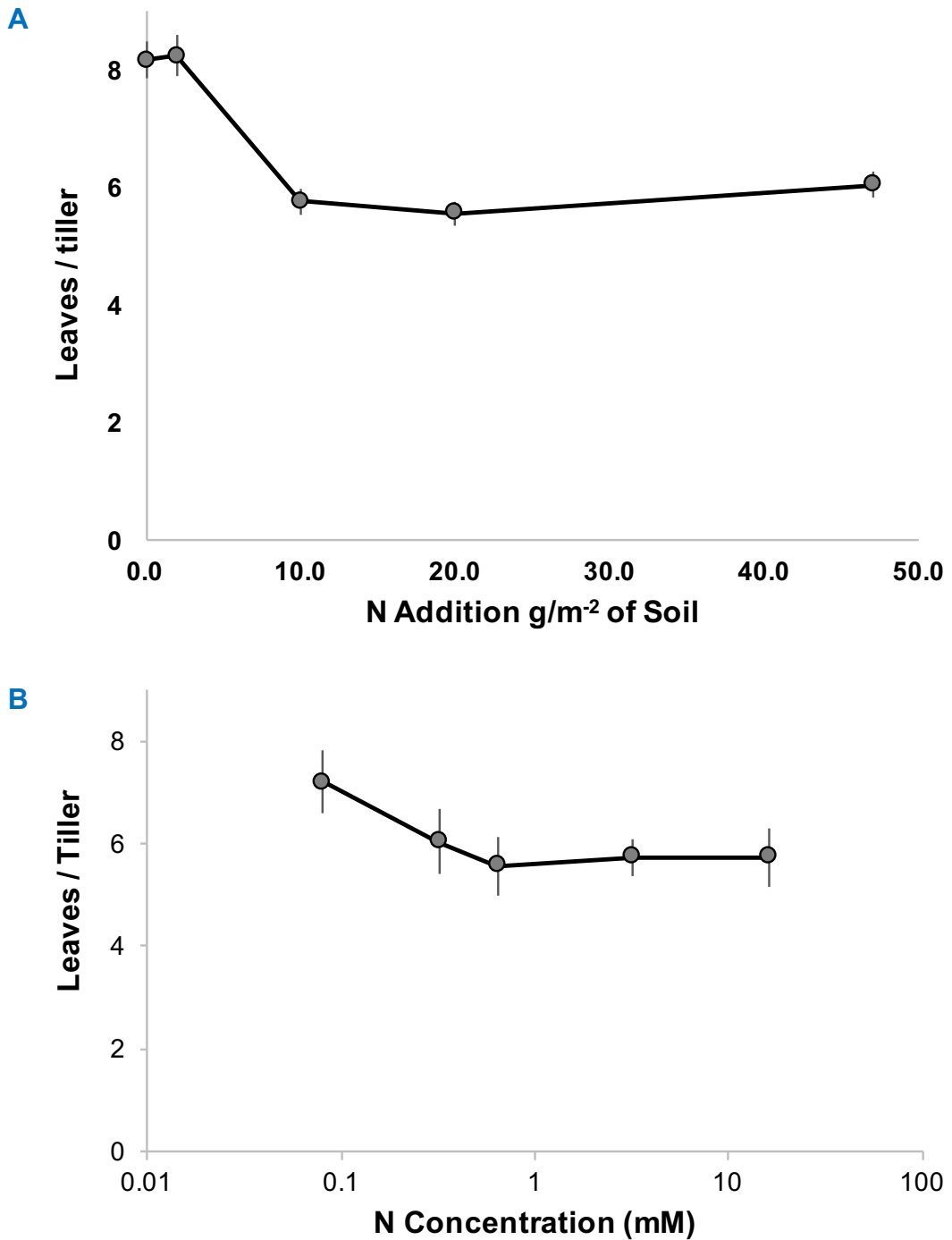


Figure 4-7. Effect of N Supply on the Number of Leaves Per Tiller in 10 Week Old Barley Plants.

Hordeum vulgare seedlings (cv. Optic) were grown as mentioned in Section 2.5.1.2 and assessed after 10 weeks. Panel A, soil-grown plants; the fertilizer application rates of N were 0, 2, 10, 20 and 47 g m⁻². Panel B, hydroponically-grown plants; the N concentrations were 0.08, 0.32, 0.64, 3.2 and 16 mM. Values are average (\pm SE) of $n \geq$ plants cv. Belgravia.

Figure 4-9 shows the number of floral spikes / plant was approximately 1 or slightly less at 0.08 mM N supply (where plants developed only 1 tiller – i.e. they were unicum) but between 0.16 and 0.32 mM N floral spike initiation was triggered. In this experiment the maximum number of spikes was observed at 1.6 mM N (ca. 3.8 / plant) but no spikes were visible in 10 week-old plants when grown in 3.2 mM N supply (Fig 4-9; Appendix A-11). On further analysis dissection of the main tillers showed some spike development had occurred at the higher levels of N but this development was obscured by the surrounding leaf sheath. After 10 weeks maximum spike length was observed in 0.32 mM N (ca. 32 cm) but growth was progressively and significantly ($p < 0.009$) suppressed at higher N levels (Fig. 4-10 A; Appendix A-12). The number of nodes in 10 week-old plants was approximately 3 but this did not change significantly ($p > 0.05$) with N supply (Fig. 4-10B; Appendix A-12).

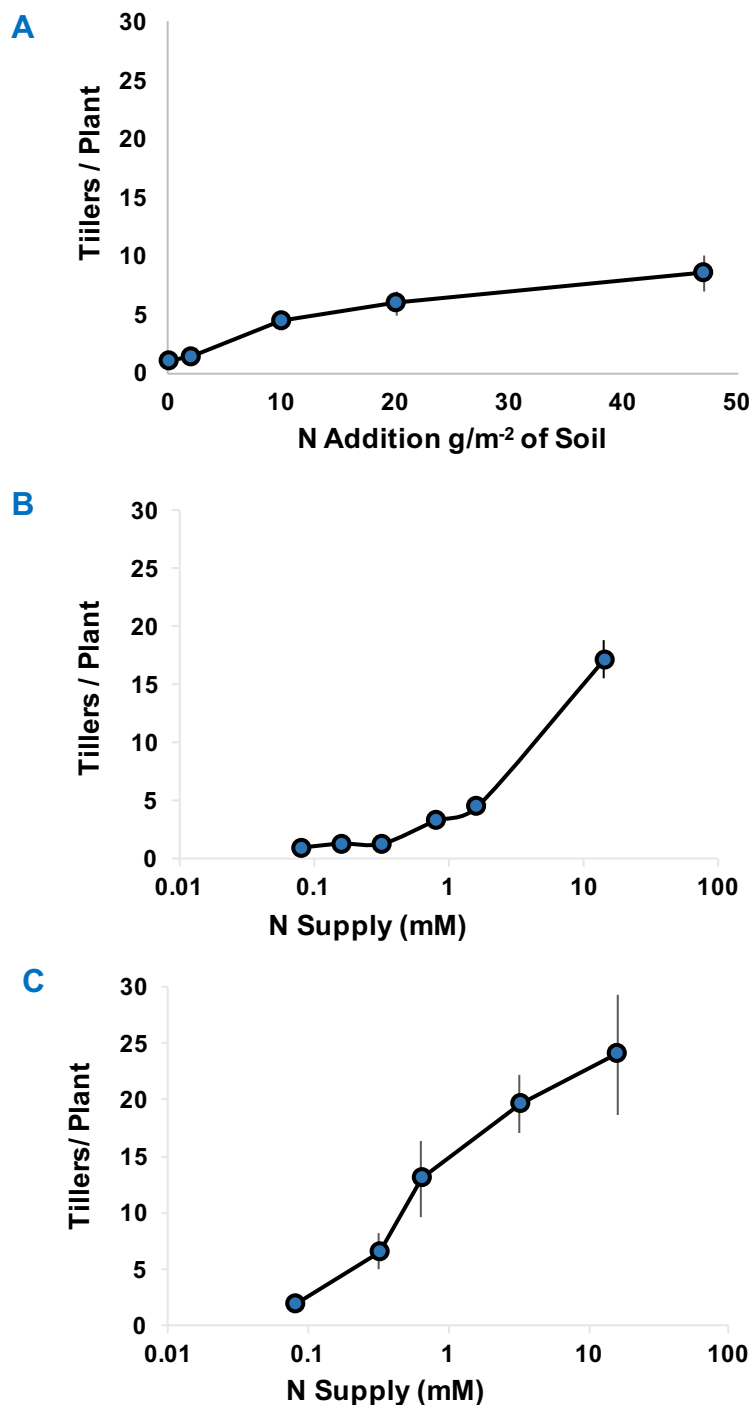


Figure 4-8. Effect of N Supply on Tillering in 10 Week-Old Barley

Seven-day-old *Hordeum vulgare* cvs. Belgravia or Optic seedlings were transferred to soil or hydroponic solutions and grown for 10 weeks (Section 2.5.1).

Panel A, soil-grown plants (Section 2.5.1.1); values are average (\pm SE) of $n=6$ plants of cv. Optic. Panel B, hydroponically-grown Optic plants (Section 2.5.2); values are average (\pm SE) of $n=9$ plants cv. Optic. Panel C, hydroponically-grown Belgravia plants (Section 2.5.1.2); plants were assessed after 10 weeks; values are the average (\pm SE) of $n \geq 4$ plants.

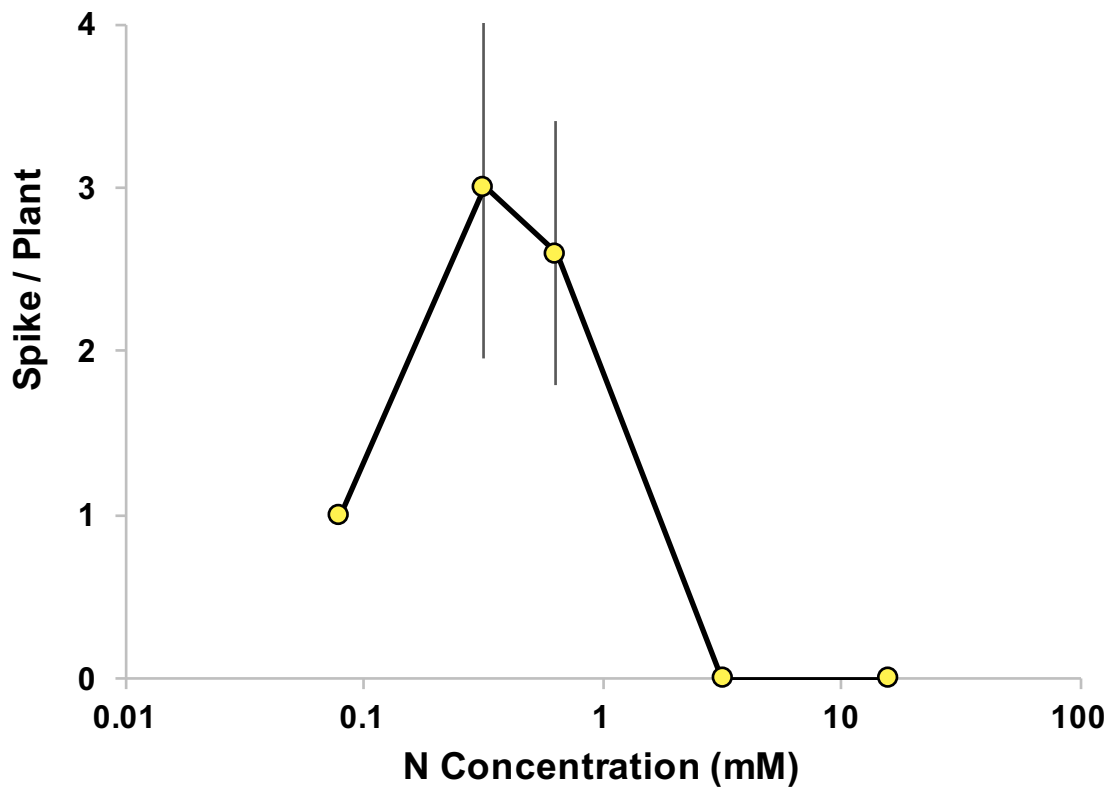


Figure 4-9. Number of Spikes per Barley Plant Grown in Hydroponic Solutions with Different Levels of N.

Seven-day-old *Hordeum vulgare* were transferred to hydroponic solutions containing a range of N concentrations (0.08, 0.16, 0.32, 0.64, 0.8, 1.6, 3.2 and 16 mM; Section 2.5.1.2. Plants were grown in the glasshouse for a further 10 weeks and the number of floral spikes counted; values are the average (\pm SE) of $n=8$ plants.

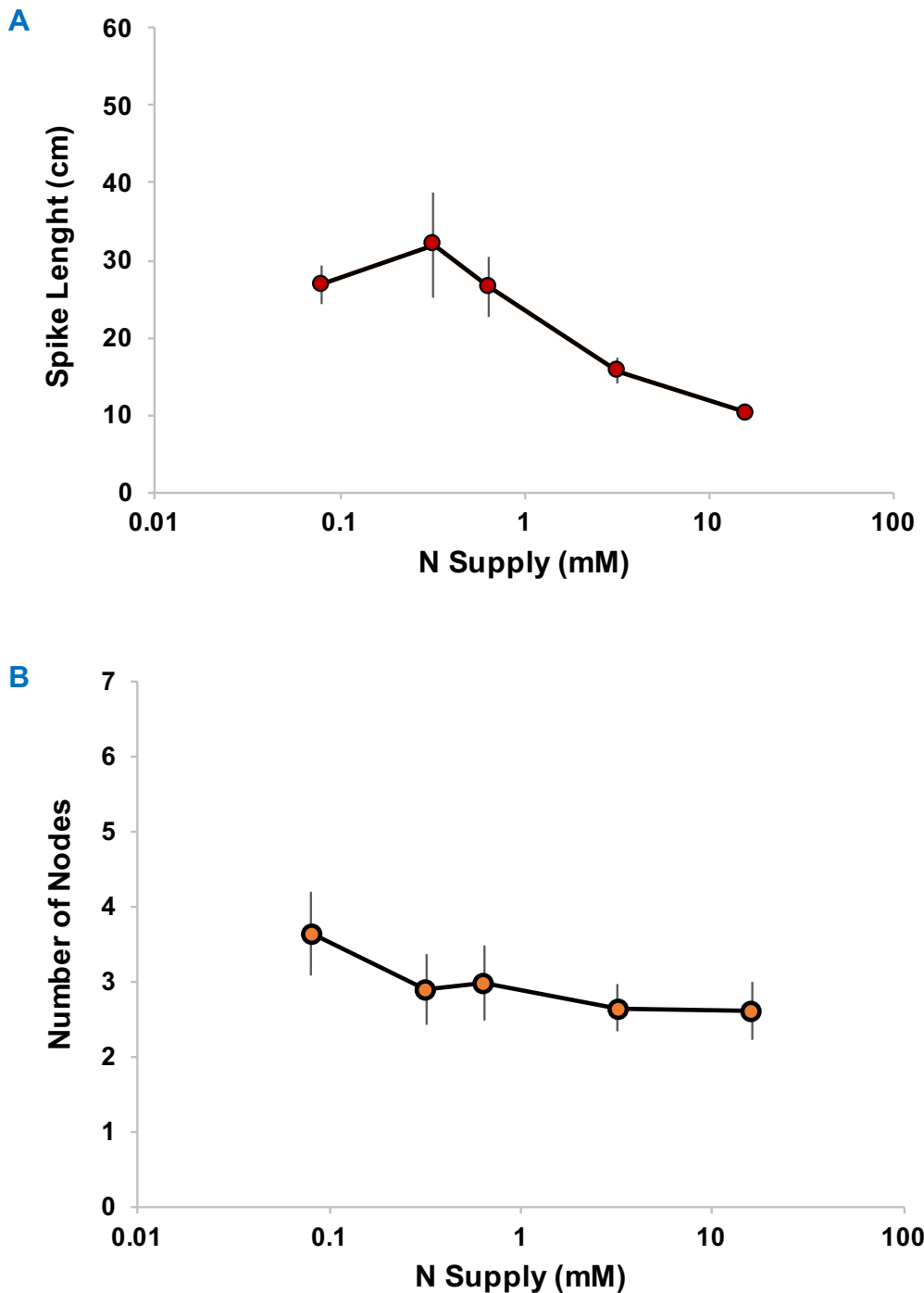


Figure 4-10. Effect of N Supply on Stem Development in 10 Week-Old Barley.

Seven-day-old *Hordeum vulgare* cv. Belgravia were transferred to hydroponic solutions containing a range of N concentrations (0.08, 0.32, 0.64, 3.2 and 16 mM; Section 2.5.1.2). Plants were grown in the glasshouse for a further 10 weeks and then harvested and dissected. Panel A, stem elongation. Panel B, the number of nodes. Values represent the average (\pm SE) of $n \geq 4$ barley plants.

After 14 weeks, however, spike length had increased to over 50 cm for plants in 0.64 mM N but this decreased sharply at higher levels; no spikes were observed in 16 mM N although flowering and seed set had occurred at 0.64 mM and below (Fig. 4-11 A; Appemdix 1-13). Node number has also increased between 10 and 14 weeks; five or six nodes had developed at 3.2 mM N or below, but at 16 mM only 2 nodes were observed suggesting high nitrogen supply arrested spike development at the two or three node stage (Fig. 4-11 B; Appendix A-12). The dissected stem of 13 week barley showing the nodes and internode position across stem of hydroponically grown barley (Fig. 4-12).

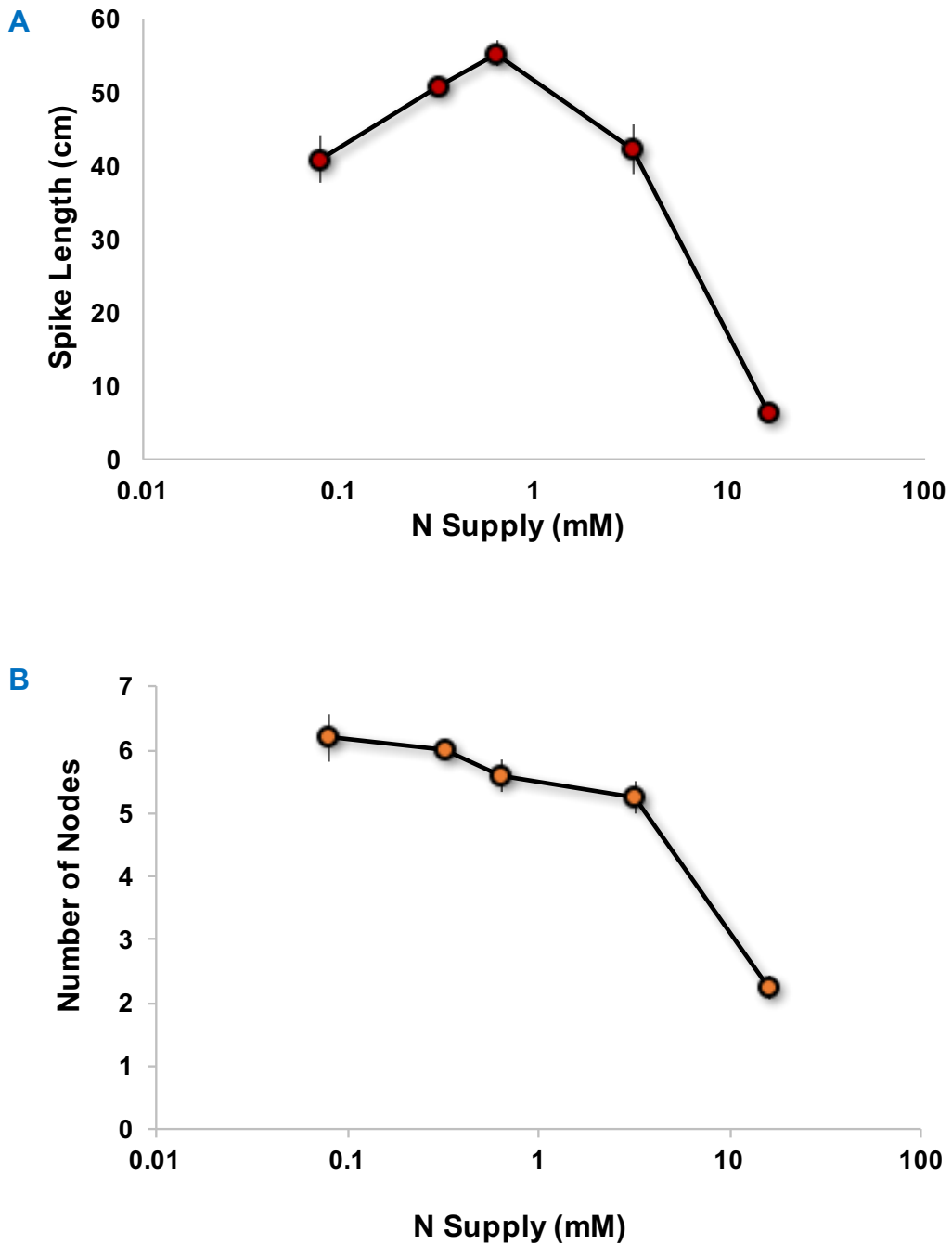


Figure 4-11. Effect of N Supply on Stem Development in 14 Week-Old Barley.

Seven-day-old *Hordeum vulgare* cv. Belgravia were transferred to hydroponic solutions containing a range of N concentrations (0.08, 0.32, 0.64, 3.2 and 16 mM; Section 2.5.1.2). Plants were grown in the glasshouse for a further 14 weeks and then harvested and dissected. Panel A, stem elongation. Panel B, the number of nodes. Values represent the average (\pm SE) of $n \geq 4$ barley plants.

Increasing N supply to soil or hydroponically grown barley plants had a profound effect on grain production. Figure 4-13 shows that grain yield decreased significantly ($p < 0.001$; Appendix A-14) when soil was supplemented with N levels of above 2 g / m² (equivalent to 20 kg / Ha) and was completely abolished at 47 g / m² (equivalent to 480 kg / Ha; Fig 4-13 A). The number of grain produced in soil grown plants peaked at 20 g / m² additions (200 kg / Ha; Fig 4-13 C; Appendix A-14).

Similar trends were observed in hydroponically grown plants (Fig 4-13 B & D; Appendix A-14). The maximum number of grain / plant was observed at 1.6 mM N but seed weight was slightly reduced (Fig 4-13 C; Appendix A-14). These data suggest the best grain yield in hydroponically grown plants would be achieved between 0.64 and 1.6 mM N supply.

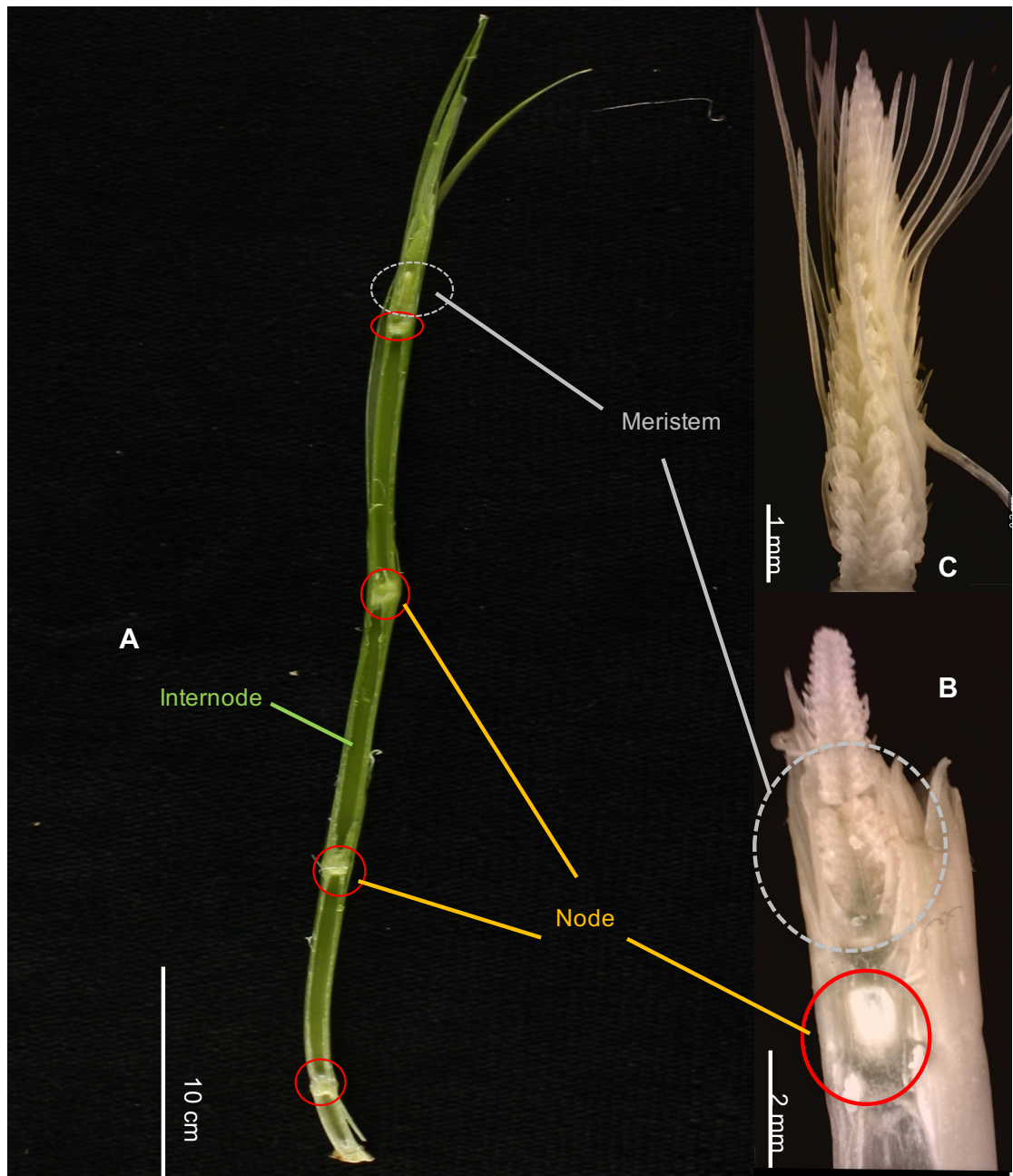


Figure 4-12 The Nodes Position and Development of Spike in Barley.

Barley (*H. vulgare* cv. Belgravia) was grown in hydroponic solution (Section 2.5.1.2). The 13-week old dissected stem (A) showing the nodes, internodes and the floral meristem emerged on the 4th node. In (B), the floral meristem emerged from the node is presented, where the node is marked by red circle (○) and the meristem marked with grey dashed circle (○). The mature floral meristem and spikelet formation shown in (C).

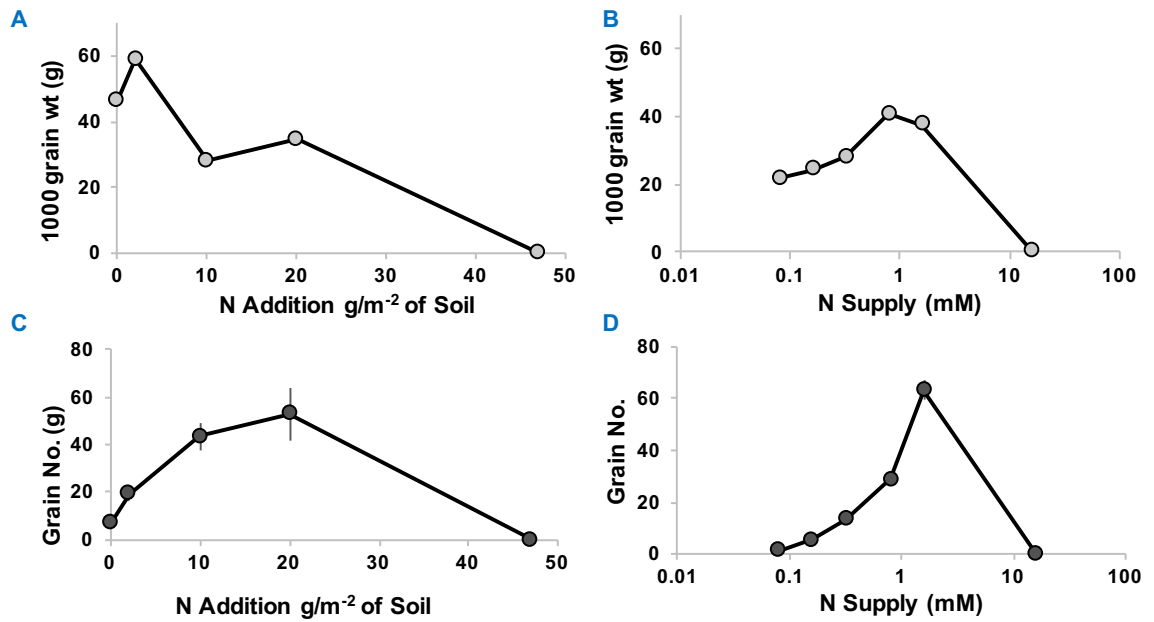


Figure 4-13. Effect of N Supply on Grain Production in Barley.

Plants grown as mentioned in section 2.5.1.1 at different amount of fertilizer phenotypes can be distinguished in this Figure. The age of plant at harvesting was 11 weeks can be seen in graph A which show the weight of 1000 grain and graph C show the number of grains. Plants grown at different concentration of N as mentioned in section 2.5.1.2. Panel B and D show barley seedlings (cv. Optic) were grown in hydroponic solutions as described in Table 2-1 until seed had set. Increasing N supply from 0.08 to 1.6 mM resulted in a 50-fold increase in grain yield attributable to both an increase in gains / spike (10-fold) and spikes / plant (5-fold). Above 1.6 mM available N supply, however, flowering was completely suppressed and plants remained in a vigorous state of vegetative growth. Values represent the average (\pm SE) of $n > 8$ plants

4.4.2 Zadoks Staging Scale

The Zadoks Scale (Figure 4.14) can be used to assess the timing of developmental staging from germination until grain ripening. Thus, the lowest levels of N supply (0.08 mM) delayed time to seed maturity by 5 to 7 days when compared with 0.16, 0.32, 0.64 and 1.6 mM N supply. The exceptions were the plants grown above 1.6 mM N which failed to progress beyond the stem elongation stage (Zadock's score of 30-40) and further reproductive development was arrested.

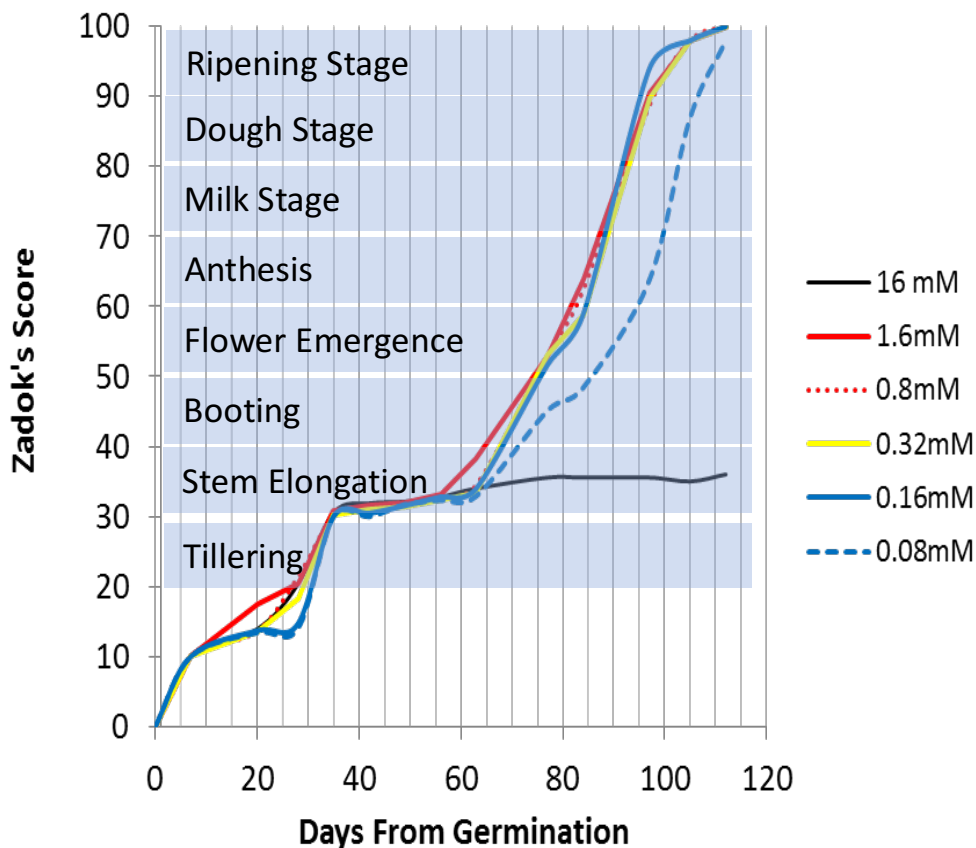


Figure 4-14. Effect of N Supply on Barley Staging (Zadok's Scale)

Barley seedlings (cv. Optic) were placed in full-strength Hoagland's solutions containing the indicated levels of N and grown in the glasshouse until the seed had fully ripened; fresh solutions were prepared every week (Section 2.6.1). Development was scored every 2-3 days on 8 plants at each concentration using the Zadok's scale.

4.4.3 Meristem Elongation

The effects of N supply on the initiation of flowers was determined by examining dissected shoot meristems using a stereo dissecting microscope. The results shown in Figure 4-15 give an overview on how N levels affected the growth and development of the shoot meristem in spring barley. In moderate levels of N supply (0.32 and 0.64 mM) meristems continued to develop beyond the 5 week stage and rudimentary awns were observed by 8 weeks (Fig 4-15). In contrast, at the lowest levels (0.08 mM), although the meristems had grown in size, floret development and awn production was not less pronounced probably due to the low availability of N. At higher levels of N supply (3.2 And 16 mM), however, further growth of the meristems was suppressed at 7 and 8 weeks (*cf* 0.64 mM).

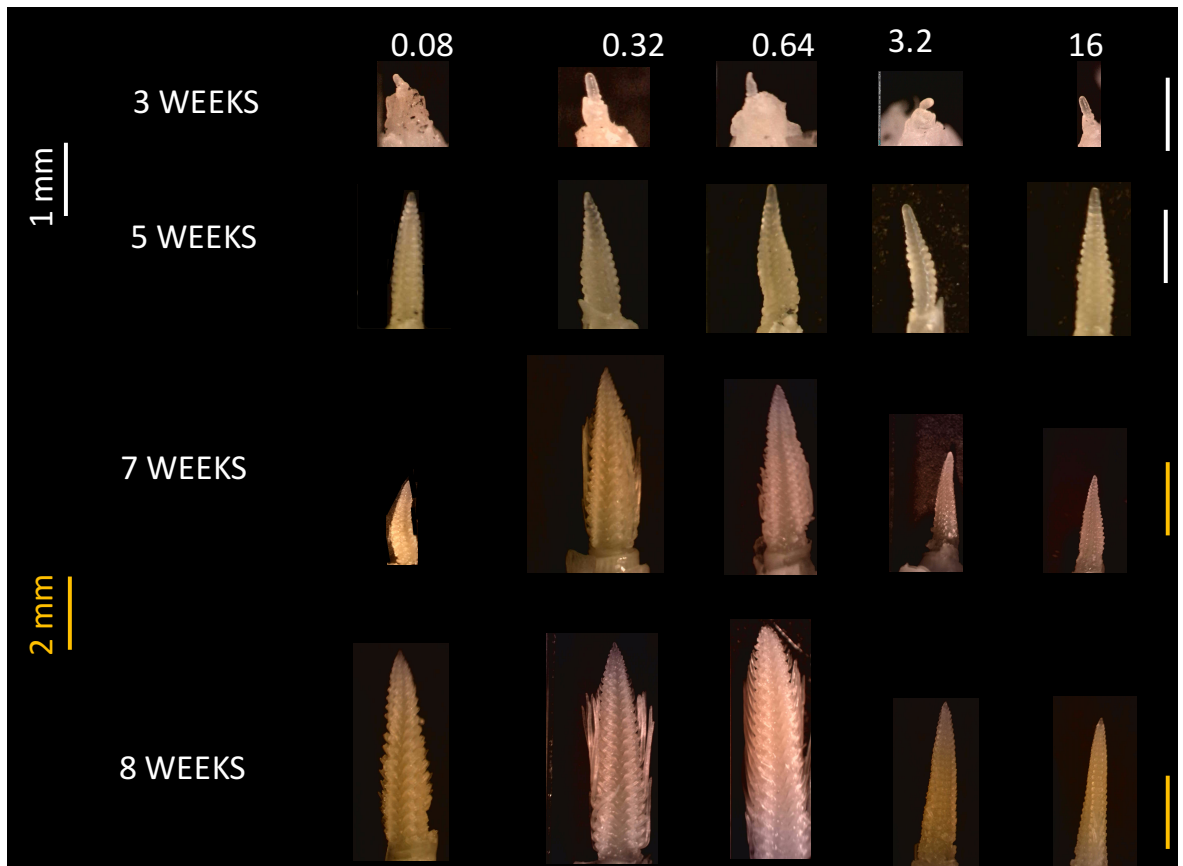


Figure 4-15. Effects of Nitrogen Supply on Barely Floral Meristem Development.

Seven-day-old *Hordeum vulgare* cv. Belgravia were transferred to hydroponic solutions containing a range of N concentrations (0.08, 0.32, 0.64, 3.2 and 16 mM; Section 2.5.1.2). Plants were grown in the glasshouse for up to a further 9 weeks. Plants were harvested and dissected at the indicated times to reveal the floral meristem (Section 2.6.2). The scale bar is 1 mm for white bars, and 2 mm for yellow bars.

4.4.4 Chlorophyll Content

The increase in photosynthesis rates with increasing N supply shown in Figs. 4-3 and 4-4) might arise from an increase in chlorophyll content. To test this possibility the levels of chlorophyll in fully expanded 6th emergent leaves were determined. The data presented in Figure 4-16 indicates that leaf chlorophyll concentration did increase significantly ($p < 0.001$; Appendix A-15) with increasing concentration, from ca. 4.5 to 10 (arbitrary units) across the range of N supply used, and this might account for the concurrent increases in photosynthesis rates.

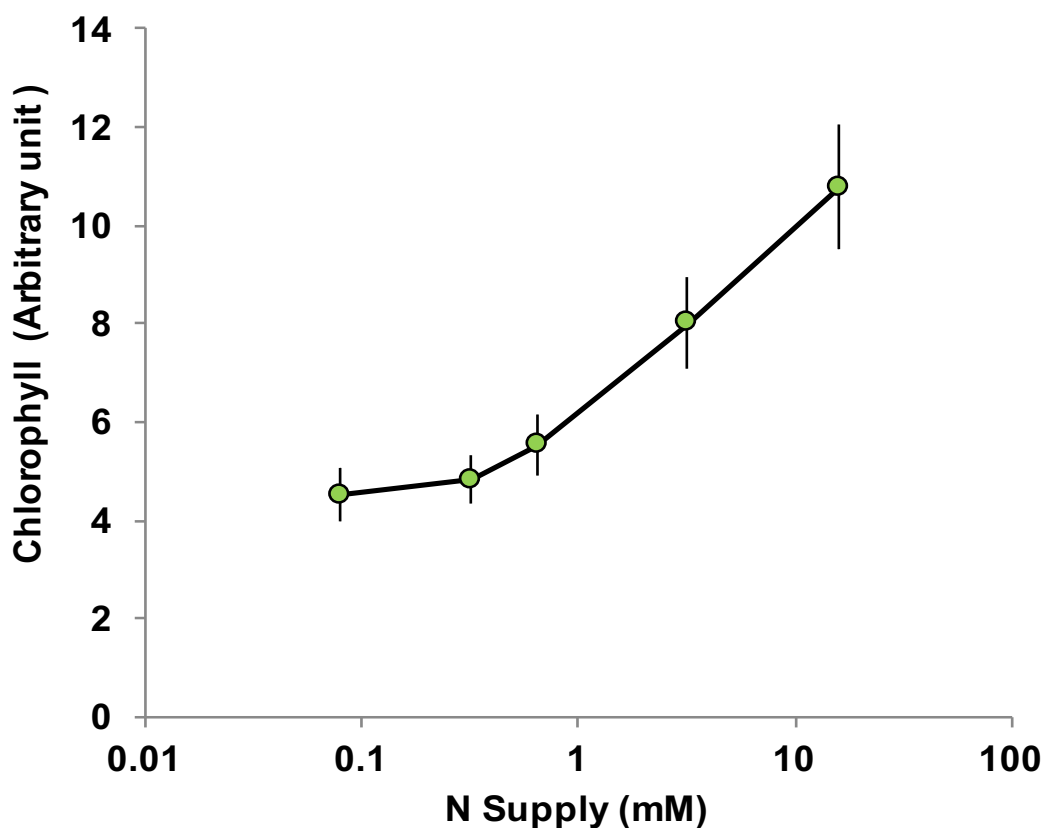


Figure 4-16. The Effect of N Supply on Leaf Chlorophyll content of 8 Week-Old Barley

The concentration of chlorophyll in barley leaves was measured *in vivo* using a portable chlorophyll content meter (Section 2.6.5). The 6th attached leaf was examined to determine the chlorophyll concentration among different nitrogen levels. Values represent the average (\pm SE) of n=10 plants

4.5 Protein Concentration

A hypothesis was presented in the Introduction that the increase in ULA A_{sat} and Φ_{CO_2} observed with an increase in N supply could be attributable to an increase in the soluble protein levels in leaves, specifically the levels of C3 Cycle enzymes in the chloroplast. To test this hypothesis total protein levels in mature, fully expanded 4th to 6th leaves of cv Belgravia was assessed. These data are presented in Fig. 4-17. Total ULA protein levels increased from approximately 1.6 g m⁻² to 5.2 g m⁻² over the N concentration range used ($p < 0.001$; Appendix A-16) indicating 3-fold increase on an area basis.

Other leaf area parameters were measured to assess whether N supply affected leaf morphology or A_{sat} directly. These included estimates of chloroplast number per cell and leaf thickness; these data are presented in Section 4.6 and 4.7.

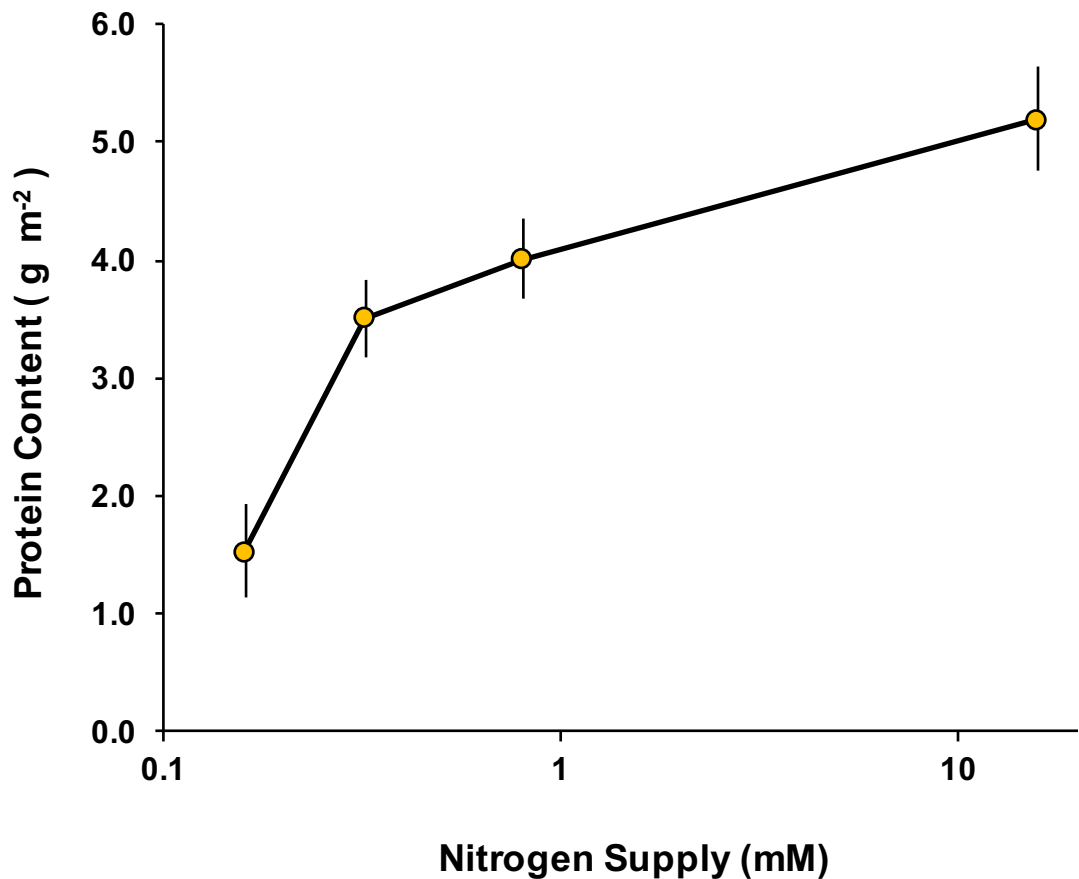


Figure 4-17. A The Effect of N Supply on Total Leaf Protein Levels in Barley

Plants were grown for 5 weeks in hydroponics over a range of N supply as described in Figure 4-2. After 5 weeks 3 leaf discs were cut from each of 4 fully expanded 4th -6th leaf and total leaf protein extracted in an SDS buffer, precipitated in acetone at -20°C overnight and re-suspended in the extraction buffer. Protein levels were determined using the Biorad Protein Assay using BSA standards (Section 2.7). Total leaf protein is expressed per m² of leaf. The data are the averages and SE of n=4 biological replicates.

4.6 Number of Chloroplast

The number of chloroplast in leaf mesophyll tissues with increasing N-supply was estimated by counting the plastids visible in random cell cross-sections using a confocal microscope. These data are presented in Fig 4-18. Increasing N-supply produced a significant increase in chloroplast number where an Anova test was used ($p=0.004$; Appendix A-17). Further analysis using Tukey's *post-hoc* test revealed no significant change over the 0.08 to 0.32 mM range ($p > 0.05$) but significant differences were observed at 0.8 mM and above ($p < 0.05$; Appendix A-17) when compared with the lower concentrations. Over the full range chloroplast numbers increased from *ca.* 10 *ca.* 15 per cell cross section. Scrutiny of the residuals from the Anova analysis, however, suggested these data may not have been normally distributed in which case Anova tests are invalid. For this reason a less sensitive non-parametric (distribution-free) statistical test, Kruskal-Wallis, was used. When a K-W test was used a probability of $p=0.053$ was calculated which is approximately equivalent to a 1 in 19 chance (*cf.* the normal 1 in 20) that the changes observed occurred randomly. Although the usual limit of significance accepted by biologists is $p < 0.05$, a probability of $p=0.053$ is very close to this limit. Had more replicates been used significance may have emerged using this less sensitive, non-parametric test. Taking this point into consideration, and given the high level of significance generated by Anova test, it would seem reasonable to conclude N-supply dose increase chloroplast number by approximately 50% over the range used.

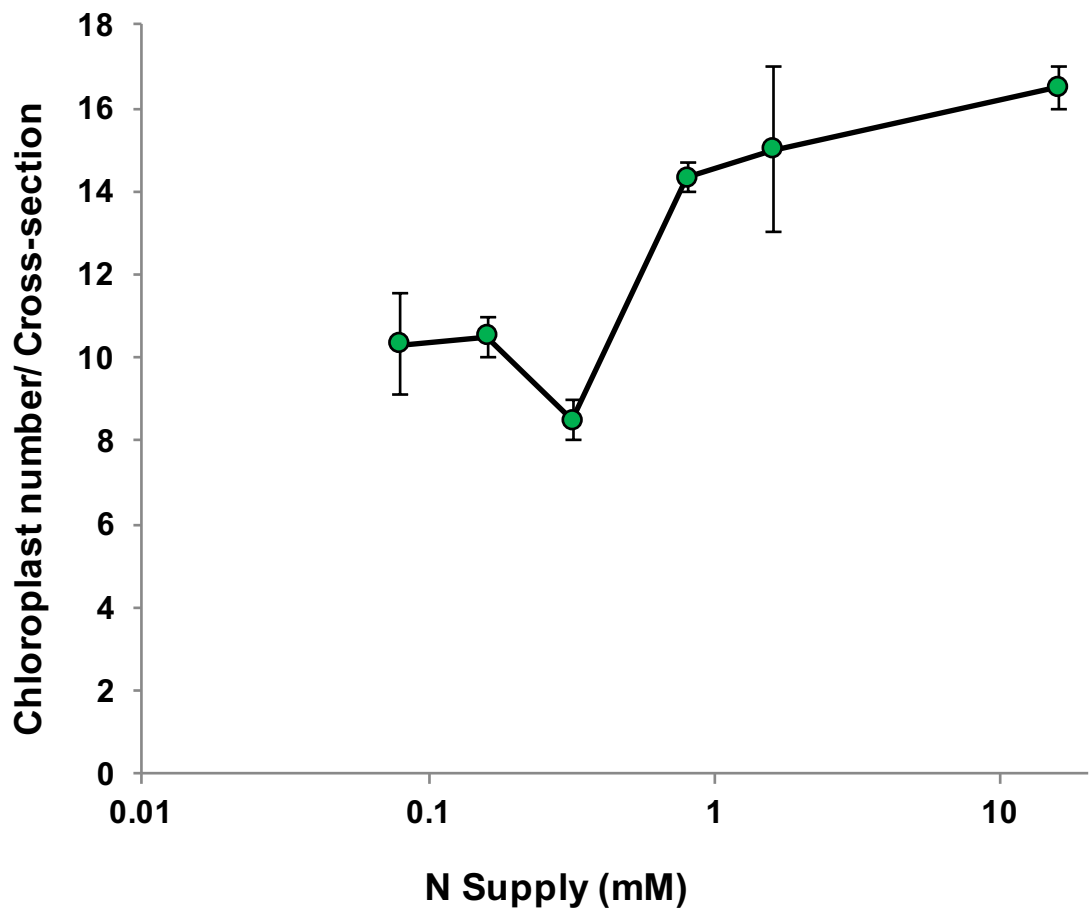


Figure 4-18 Estimates of Chloroplast Number in Barley Leaf Mesophyll Cells.

The leaves of 7 weeks old barley were harvested and examined under a confocal microscope and the number of visible chloroplasts cross section in random cross sections of the mesophyll cells was determine (Section 2.6.3). Values represent the average (\pm SE) of n= 4

4.7 Leaf Thickness

An increase in A_{sat} and ϕ_{CO_2} with N-supply may have arisen from an increase in the number of cells per unit leaf area, *i.e.* leaf thickness. Fully expanded mature leaves (5th and 6th) were harvested and immediately fixed in formaldehyde and cross-sections prepared (Section 2.6.4). Estimates of leaf thickness were then made using a microscope. Figure 4-19 presents these data and Figure 4-20 show leaf sections used in measurements. Increasing N-supply from 0.08 to 0.8 mM produced a significant ($p < 0.001$; Appendix A18) increase in leaf thickness (from *ca.* 60 to *ca.* 120 μm) but no further increase was observed at higher N concentrations.

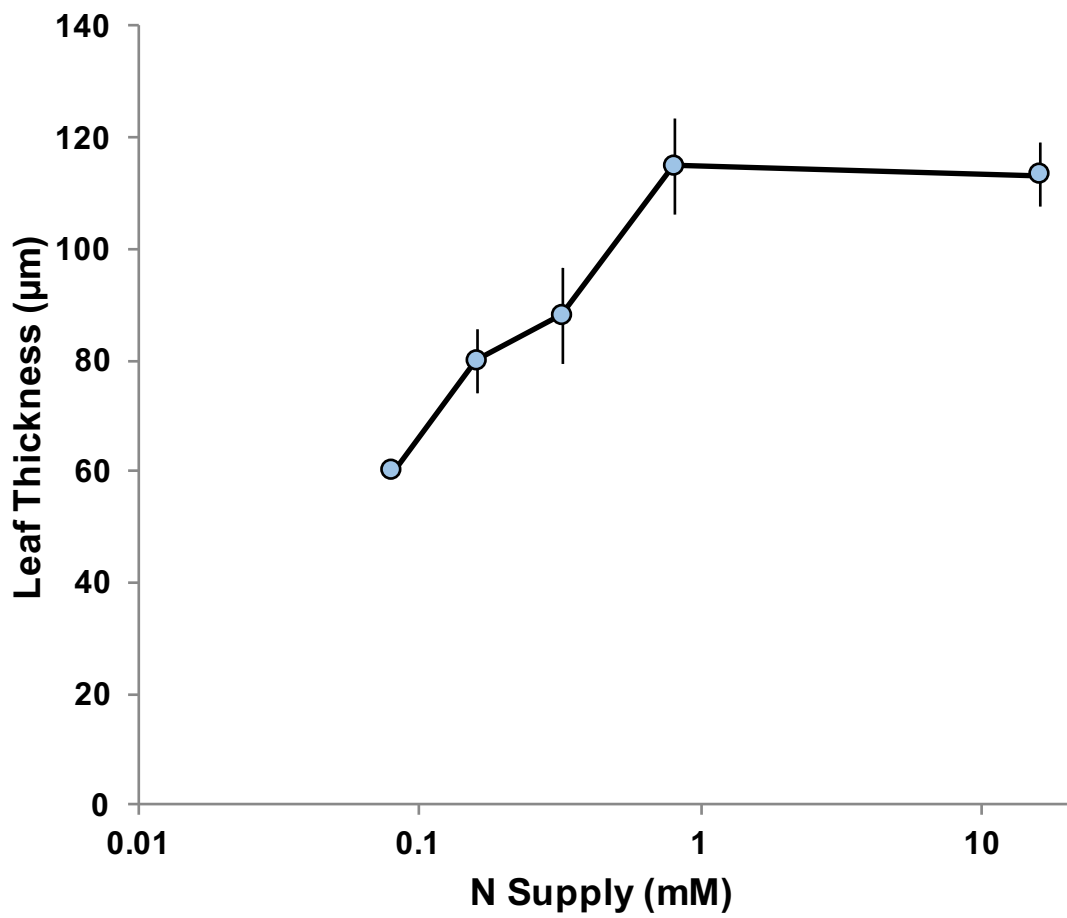


Figure 4-19 Barley Leaf Thickness in Response to Different N Supply

The leaf of 7 weeks old barley was harvested and dissected and examined under the microscope to determine the length between upper and lower epidermis of the leaf. Values represent the average (\pm SE) of $n=3$

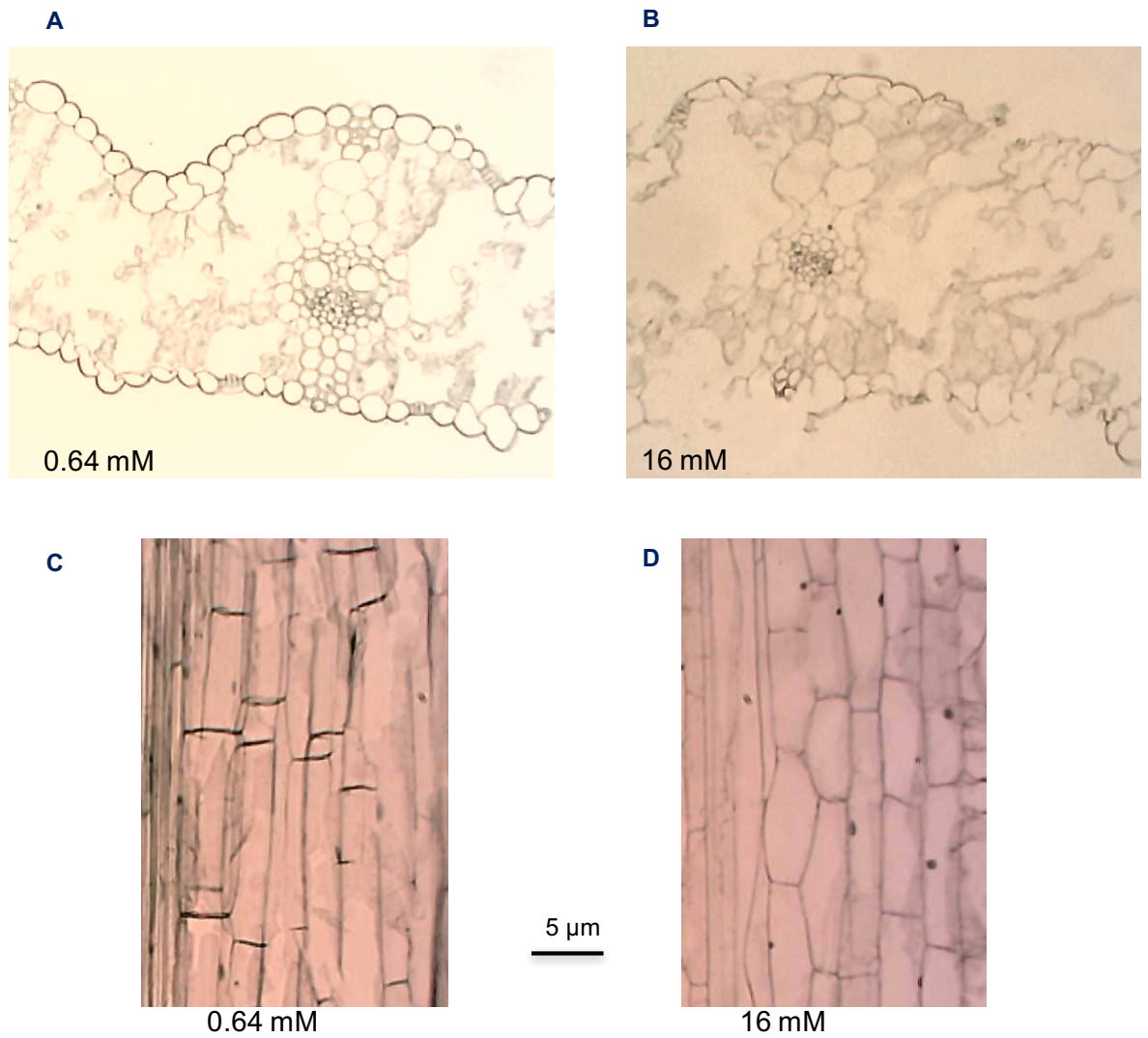


Figure 4-20 The Microscopy Images of Barley Leaf and Stem Among Different N Levels.

The cross section of leaf grown under 0.64 mM of N (A) and 16 mM barley leaf (B). the both image was taken for the second vascular bundle from the midrib. The stem cells (bottom images) was examined under a light microscope by preparing longitudinal section.

4.8 Discussion

Increasing N-supply above the levels normally encountered in agricultural soils (0.3-0.8mM N) appears to significantly increase Φ_{CO_2} (Fig. 4-3 and 4-4) suggesting yield improvements should arise by increasing N fertilizer input. High levels of N-supply, however, significantly suppresses flower development (Fig. 4-9 to 4-14), and increases tillering (Fig. 4-8) providing competing carbon sinks for developing grains. Similar results were obtained when plants were grown in N-deplete soils supplemented with N, or hydroponic solutions (Fig 4-8 and 4-13).

These barley traits are summarized in Fig. 4-21. These findings suggest barley has two endogenous nitrogen sensors. One is triggered when N-supply exceeded 0.3mM a proliferation in tillering. The other is triggered when N- supply exceeds ca. 3.0 mM and leads to the suppression of flowering. Both traits of tillering and flower development will have profound effects on grain yields and it seems that modern elite lines of barley have been selected and bred from Landraces that performed well in this limited range of N-supply (0.3-3.0 mM). A better understanding of these two N-sensors might result in the prospect of manipulation of these processes, resulting in plants with higher ULA photosynthesis rates, reduced tillering (vegetative sinks), and enhanced flowering, and thus higher planting densities and high grain yields. Supplying barley with high level of N leads to late flowering and lower yield (Hall et al. 2014).

Several experiments were conducted in an attempt to manipulate tillering. These included use of 'uniculm' mutants from the barley Bowman collection (BW205, BW207, BW 494, and the parental line (BW3) but these mutants (Fig 4-22) proved

to have very low fertility generating only two or three seeds per plant. Only two seeds from each mutant was sent from the barley stock center (James Hutton Institute, Scotland) due to the low fertility issue, and it became apparent that it would take several years to generate the 100-200 seed required to complete the initial experiments. None-the-less, seed bulking is progressing at Glasgow and these experiments will be undertaken.

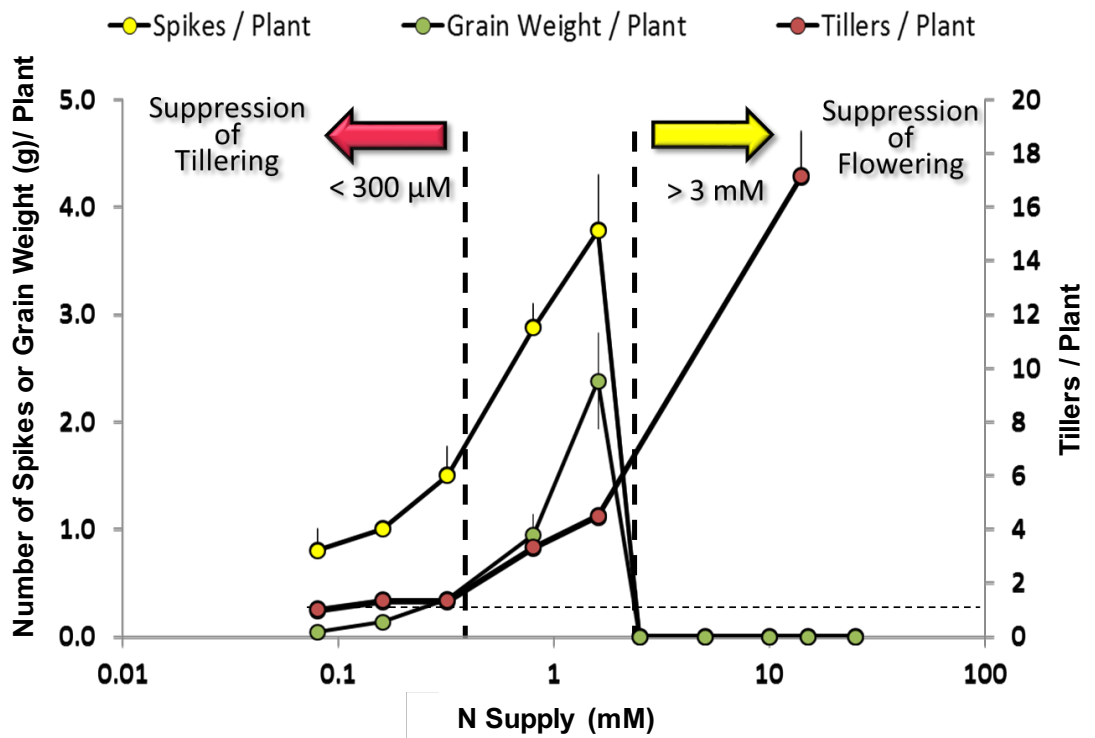


Figure 4-21 Nitrogen Supply Affects Tillering and Flowering in Barley

The effect of different N levels on tillering and flowering in barley. The number of tillers per plant is one (horizontal dashed line) until N-supply exceeds 0.032 mM. affect which it increases to ca. 17 at 16 mM; the dashed left vertical line indicates the N-level that triggers tiller proliferation. The number of spikes per plant and grain yield increases progressively as N-supply is increased from 0.08 to 1.6mM, but declines sharply after that and no seed set was observed at this time from 3.2 to 16 mM. The right vertical dashed line indicates the N-levels that triggers the suppression of flowering responses.

An alternative approach to reduce tiller number was attempted whereby new tillers were surgically removed with a sterile scalpel and wounds sealed with petroleum jelly. Despite best attempts, however, infection proved to be a major problem and this approach was also abandoned.

Focus was then directed towards identifying in which tissues and at what stage of development high levels of N-supply suppressed flowering. In the introduction (Section 1.5) the flowering pathway in small grained cereal crops was outlined. Briefly, photoperiod (Long Days) triggers flowering; this is sensed in the leaves by the circadian clock initiating the CONSTANS-dependent synthesis of VRN3, a mobile transcription factor that shows sequences homology to the Arabidopsis activator of flowering FLT. VRN3 is translocated from the leaf via the phloem to the crown meristem where it activates the synthesis of VRN1, a MADS box transcription factor, that triggers the transition of the meristem to cease producing only vegetative primordia (leaves and tillers) to producing floral primordia and undergo development through the ABCDE pathway. The question to address 'is where does high N-levels suppress flowering; in the leaf (perception), translocation of VRN3 in the phloem, or in the crown meristem (transition to a reproductive meristem or floral development)?'.

Measurements on spike length and number of nodes of cv. Belgravia with time showed that flowering progressed normally at all levels of N-supply up to the 10-week stage (Fig 4-10). Between 2 and 3 nodes had developed and some spike growth had occurred at the highest N levels even though the spikes had not emerged through the leaf sheaths. By 14 weeks (Fig 4-11) spikes had emerged at 3.2 mM N and below but not at 16 mM. Careful dissection and analysis of the stems

of these plants revealed the number of nodes had increased from 2-3 to 5-6 over the 10-week to 14-week period for plants grown in all concentrations of N except for those grown in 16mM. At this concentration spike elongation and development did not progress beyond the 2 node stage.

Leaf N content has been implicated in controlling chlorophyll content and leaf thickness (Cohu et al. 2014; Li et al. 2014a; Tsutsumi et al. 2014). Leaf thickness and chlorophyll content have also been reported to affect photosynthesis rates (Eberhard et al. 2008; Zhu et al. 2010; Li et al. 2013; Cohu et al. 2014; van Campen et al. 2016). Thus, increases in photosynthesis and enhanced absorbance of irradiance are likely consequences of increased N supply (Pandey and Kushwaha 2005; Cohu et al. 2014; van Campen et al. 2016) which could result in improved yields (Zhu et al. 2010; Yuan 2017).

Taken together, these observations suggest the high N-dependent suppression of flowering in barley is associated with the effects of N on floral development (ABCDE pathway) and not on the perception of photoperiod in the leaf, or the downstream signaling events that occur in the leaf (synthesis of CONSTANS and VRN3), the translocation of VRN3 to the crown meristem, or the VRN1-dependent transition of the crown meristem from purely vegetative to reproductive phase.

The experiment have informed a decision to investigate the signaling events that lead to the suppression of flowering in high N-grown plants by comparing the transcription of the floral meristem of six-week old (2 node stage) plants grown in 0.64 and 16 mM N-supply. The results of these experiments are presented in chapter 5.

In the Introduction evidence was presented to show that nitrogen stimulates the biosynthesis of plant growth regulators such as Cytokinins (CK) and Auxin. For reasons that are not entirely clear, the expression of the NRT class of nitrate transporters stimulate the biosynthesis of CK in roots and shoots, and this directly promotes bud growth and branching. In contrast, increasing N uptake by plants result in decreasing activity of auxin in the tissues (Albacete et al. 2008; Ghanem et al. 2011; Kiba et al. 2011; Kudoyarova et al. 2014). Cytokinins are also reported to inactivate the production of auxin and GA. GA and auxin repress CK biosynthesis (Balazadeh et al. 2014; Matías-hernández et al. 2016). High N levels inhibit the functional activity of auxin transporters which result in the accumulation of auxin in root tips and the induction of lateral root growth (Kiba et al. 2011).

Auxin regulates floral meristem development in the cereal crops by inducing cell elongation (Zhang and Yuan 2014). In addition, CK promote the reproductive stage through meristem enlargement where cell division occurs, thereby increasing meristem size and activity. Grain yield increases in response to rising CK activity (Zhang and Yuan 2014; Matías-hernández et al. 2016). The role of gibberellins in controlling flowering is important as well as CK and auxin. In leaves GA induce flowering by degrading DELLA proteins which represses *VRN3 (FT)*. Furthermore, in meristems, GA operates in parallel with, or possibly down stream of, *FT* to accelerate flowering (Cheng et al. 2004; Boden et al. 2014; Chen et al. 2014; Fjellheim et al. 2014; de Wit et al. 2016; Matías-hernández et al. 2016).

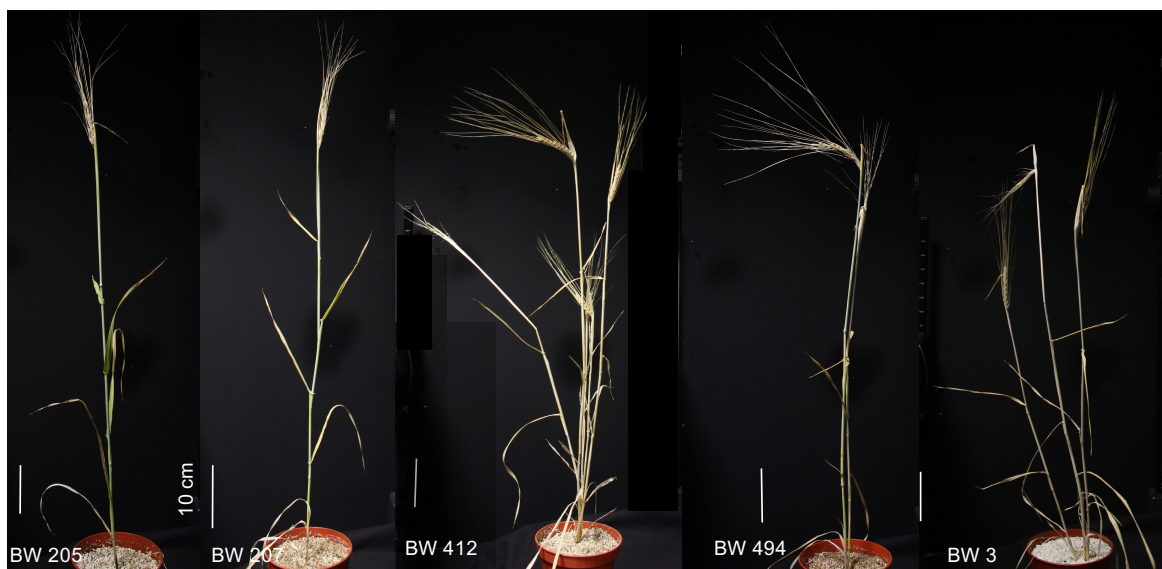


Figure 4-22 Bowman Lines.

The barley cv. Bowman (BW3) and its mutants BW 205, BW 207, BW 412 and BW 494 showed that low number of tillers even in parent line (BW 3). The unculm lines BW 205 and BW 207 produce single stem and low tillering line (BW 494).

The spike elongation which is controlling flowering by developing floral meristem through increasing number of nodes and the distances between these nodes had been regulated by N supply levels. The N supply decrease the spike length among high N levels (Figures 4-10 and 4-11). This elongation also affects on spike production in the plant where the lower number of nodes and shorter length of the stem may result in flower suppressing.

The meristems development was affected by N supply, where increasing N levels delay meristem development and elongation. Pictures of Figure 4-15 show that phenomena. What is the role of N that causing that delay? Indeed, (Boden et al. 2014) indicates that the immaturity and delay in further development in barley meristems might be due to a decline in gibberellin production.

Studies on wheat grown in soil pots showed that the increasing N levels induce tillering and increase yield (Hussain et al. 2006). These results are not compatible with what we found in this project. The increases N level induce tillering but suppress flowering.

The photosynthesis rates increased with increasing nitrogen content in the growth medium which also supported by (Zhang et al. 2013), the results shown in Figure 4-3 and 4-4 indicates the increasing of A_{sat} and ϕ_{CO_2} in responses to N level for barley grown in hydroponic solution.

Comparison between soil and pots experiment for barley done by (Tavakkoli et al. 2012) on salt stress that shows the same results when applying different concentration of N on hydroponic and soil pots grown barley which are similar to what we found in our data.

5 Chapter 5 Transcriptome Profiling of Barley

Floral Meristems

5.1 Introduction

Chapter 4 describes a series of experiments that were undertaken to characterize the effects of very high rates of N-supply on the growth, development, and yields of barley. The conclusions were that high N-supply can double ULA CO₂ assimilation rates and potentially result in higher yields. These yield benefits may not be realised, however, unless the nitrogen-induced promotion of tillering and the suppression of flowering can be prevented. Studies reported in Chapter 4 suggested High Nitrogen does not affect early events in the flowering pathway that occur in the leaf, but hinders flower development at the 2-to3 node stage in the crown meristem once flowering has been triggered. It is also conceivable that current yields in barley are affected in part by the levels of nitrogen applied to fields in intensively managed systems. It is clear, therefore, that a better understanding is required of the mechanisms by which high levels of N supply limits seed production. To address this issue it was decided to compare the full transcript profiles of the developing floral spikes of meristems at the 2-to-3 node stage of *Hordeum vulgare* (L.) cv. Belgravia plants (five-to-six week stage) grown in 0.64 mM (Moderate) and 16 mM (High) N-supply hydroponic solutions. Full experimental procedures for the growth of material and the preparation of total RNA are presented in Section 2.5.1.2 and 2.8.2.2.

Two methods are routinely used for assessing the full transcriptome profile of tissues; DNA Microarrays and high throughput Next Generation Sequencing

(NGS) technologies. Both methods rely on the preparation of high quality total RNA from tissues and the subsequent generation of cDNA which is then used to hybridize to the microarray probes, or is then sequenced. The Affymetrix GeneChip Barley Genome Array was constructed from a collaboration between the barley research community and Affymetrix and became available for general use in 2003. The community submitted EST sequences from 84 libraries providing approximately 400,000 raw sequences, and from the NCBI/GenBank non-redundant databases. About 350,000 of these were considered to be of suitable quality and clustering analysis revealed 53,030 unigenes were represented; 25,500 of these had complete 3' ends and were subsequently used in the array construction. Agilent Technologies also manufacture a barley 4 x 44K array on a single glass slide. Despite the relative simplicity of use of DNA Microarrays, NGS has begun to supplant microarray technology; many feel sequencing cDNA generated from transcripts provides an additional level of confidence for quantification.

Several NGS technologies are available for undertaking expression profiling. Broadly, sample preparation for each of these technologies is similar. Template DNA is fragmented and oligonucleotide adapters are ligated to the ends of the fragments; these modified fragments are then spatially separated by ligation to an inert solid surface, a unique position on a glass slide or a unique silicon bead. The individual DNA fragments are then amplified by the PCR to generate spatially separated clusters of the amplified sequence (to improve signal strength) and followed by a second synthesis step when sequencing reactions are performed. The different technologies rely on different chemical reactions used to assess the DNA sequence of these clusters in a step-wise manner. Four technologies are

routinely used at present; these are Pyrosequencing, Sequencing by Synthesis, Sequencing by Ligation, and Ion Semiconductor (Ion Torrent) Sequencing.

Pyrosequencing relies on the one-base-at-a-time addition of modified nucleotides (A,C,G, or T) to the synthesised DNA fragment from the template. To read the n^{th} base of every fragment on the solid support array (slide or bead), it has to be incubated and then washed sequentially with each of the four modified bases in turn. The addition of a modified nucleotide base results in the release of pyrophosphate which is then used to generate ATP. The successful addition of a base (say, A) to any one cluster is recorded by using the synthesised ATP to generate chemiluminescence using the Luciferin / Luciferase system; no chemiluminescence from a cluster would signify the next base is not an A. All reagents are then washed away and the next modified base and DNA polymerase is added (C for example), and the Luciferin / Luciferase assay repeated. Once all four of the bases have been used to determine the n^{th} base, these newly incorporated bases are modified to allow the addition of the $n^{\text{th}}+1$ base and the process is repeated. Pyrosequencing can produce reads of approximately 1kb but there is a relatively high error rate when there are runs of polynucleotides, and the costs are relatively high. It can generate up to 1 million reads per run each with *ca.* 700 bp (*i.e.* up to 0.7 Gb per run) at a cost of *ca.* \$10,000 US. As Pyrosequencing provides long reads it is capable of effective *de novo* sequencing of cDNAs (transcripts) and would not require an assembly of reads by matching to a reference genome. The low number of transcript reads (1 million) coupled with the current poor annotation of the barley genome makes this method less attractive than other NGS technologies for transcript profiling.

Another popular technology is Ion Semiconductor (Ion Torrent) Sequencing. This method is similar to Pyrosequencing in that four reactions (one for each base) are run and assessed to determine the identity of the n^{th} base before the terminal base is activated to allow the $n^{\text{th}}+1$ base to be added. Adaptors are added to the template DNA strand (ca. 100-150 bp) and each molecule is attached to a single well a semiconductor plate; the template sequence is then amplified to increase signal strength. DNA polymerase, and one of terminator bases (A,C,G, or T) is added. The major difference is that with the addition of each base a H^+ is released and this is detected as a pH change by the semiconductor base. It is therefore, a four-cycle, one base one-base-at-a-time DNA synthesis method, similar to pyrosequencing.

DNA Sequencing by Synthesis is another technology that is routinely used in NGS projects. These methods also rely on one-base-at-a-time synthesis of a new DNA strand using short single strand DNA templates (ca. 100-150 bp), DNA polymerase, and terminator bases that are labelled with a fluorescent dye. Here the n^{th} base is attached and read during one reaction cycle as each of the four terminator bases is ligated to one of four specific dyes; the identity of the added terminator base is established from its colour. After scanning and reading the immobilized DNA clusters using a laser, the support matrix is thoroughly washed, a 3' hydroxyl group is added to the newly added n^{th} base enabling the addition $n^{\text{th}}+1$ base, and the process is repeated. Illumina (Solexa) technology is the most widely used providing up to 3 billion reads of up to 150 bp (450 Gb) at a cost of ca, \$0.10 US per million bases. The Polyomics facility at Glasgow University operates an Illumina NextSeq 500 instrument that provides up to 400 million reads of sequences of ca. 100 bases (40 Gb data). The technology allows samples to be

multiplexed and offers the advantages of paired end reads. Using this technology it is possible to sequence up to 200 million fragments and should provide a sufficient depth of sequencing to allow a quantitative assessment of the changes in the transcriptome of the developing florets of plants grown in high and moderate levels of N.

More recently Nanopore Sequencing technology has emerged that is inexpensive and capable of rapid sequencing of both RNA and DNA. This method relies on feeding long chain single stranded DNA (or RNA) molecules through a nanoscale hole (typically 1 nm diameter) inserted in a ceramic membrane of high electrical resistance; the pores are either proteins (e.g. α -haemolysin) or solid state (graphene or SiO₂). A low voltage is then applied across the membrane and a small electrical current passes between the buffers on either side. Once threaded through the nanopore, the DNA molecule spontaneously passes through. Each of the four bases has a different physical size and this affects the current flowing through the pore. By measuring the change in current with time the sequence of DNA can be read. Oxford Nanopore Technologies claim each pore is capable of reading 250 bases per second of DNA fragments that are up to 5kb long although the company claims fragments of 250kb can be sequenced. The MinION instrument uses a single cartridge containing 512 pores and can sequence 45Gb in 48 hours. The PromethION instrument is a vastly parallel system containing 48 cartridges each containing 3,000 pores; this instrument is therefore capable of sequencing 12Tb in 48 hours. The accuracy of single reads (1D) is relatively low (~90%) but 2D reads are reported to be >99% (Oxford Nanopore Technologies, 2016) (Nanopore Technology 2016) . Glasgow Polyomics has invested in a MinION system and it is currently under trial. At the time of writing, therefore, the

system was considered to be too novel and it was decided not to proceed with this technology.

A physical map of the barley genome cv. Morex was published in 2012 (Consortium 2012). The haploid genome size was reported to be 5.1 Gb with more than 3.90 Gb of sequence anchored to a high-resolution genetic map. Using a deep whole-genome shotgun assembly, complementary DNA deposited in the public databases, and deep RNA sequence data, a framework was constructed that revealed 79,379 putative transcript clusters, with 26,159 identified as 'high-confidence' genes with homology to other plant sequences. There was evidence for a considerable amount of alternative splicing and post-transcriptional regulation. One problem with the barley genome map, however, is that it was – and still remains – poorly annotated (http://plants.ensembl.org/Hordeum_vulgare/Info/Index). The normal procedure for analysing RNA-Seq data from the Illumina platform (which produces a high number, here over 400 million, of relatively short 100 base reads) is to first align the sequences to the genome and discard those reads that do not align. Unaligned sequences could arise for a number of reasons; there could be errors in the original published genome sequence or in the Illumina read of the fragment. It is also possible unaligned sequences arise from significant variation at the DNA level between the cultivar under investigation and the sequences cultivar Morex. Finally, it is conceivable that the alignment algorithms become confused between alignments to authentic genes and the many pseudogenes that are present in organisms such as barley with a low ratio of coding to non-coding genomic DNA (approximately 0.5%, *cf.* Arabidopsis with ~17%). For this reason, in this current study it was decided to align the RNA-Seq reads to barley genes identified from the barley sequenced

cDNA, coding sequence, non-coding RNA, and proteins (available from: ftp://ftp.ensemblgenomes.org/pub/plants/release-32/fasta/hordeum_vulgare). It was hoped that by removing over 99% of the non-coding genome sequence alignments would be more rapid and stringencies could be set to be more tolerant of inter-varietal mismatches.

5.2 Transcript Profiling of Barley Floral Meristem

For these experiments two concentrations of N-supply were chosen, a Moderate Level (0.64 mM) to reflect plants that flower grown in good agricultural soils, and a High Level (16 mM) representing 'super-luxury' levels of N. briefly, seeds of cv. Belgravia were germinated and seedlings grown in modified Hoagland's solution in the glasshouse for 5 weeks (see Section 2.5.1.2); at this stage, both sets of plants had undergone stem elongation to the 2 or 3 node stage with a rudimentary floral spike of approximately 5 mm length. Plants were removed and the developing spikes rapidly dissected and instantly stored in liquid nitrogen. Once a sufficient number of immature spikes were collected, total RNA was extracted for analysis. In total 3 biological replicates of over 1µg from each concentration were prepared. The samples were analysed for quality and then sent to the Glasgow University Polyomics facility for RNA-Seq analysis using an Illumina NextSeq 500 instrument. Complimentary DNA was prepared from each of the six samples and then 100 bp fragments produced. Adapters unique for each sample were ligated to both ends of the fragments and the six samples then mixed and loaded onto the NextSeq 500. In total over 400 million paired end multiplexed reads were obtained (*i.e.* 200 million fragments were sequenced). These data were then filtered for suitable quality using the FastQ algorithms (Blankenberg et al. 2010) and then the Kallisto algorithm (Bray et al. 2016) was used to align reads to the downloaded

reference cDNA genome. Differential abundance calculations and p-values were calculated using the DESeq2 algorithm mounted on the University of Glasgow Galaxy server (Love et al. 2014). A summary of these data are presented in Table 5-1.

Table 5-1. Summary of Illumina RNA Sequencing of Floral Meristems from Barley cv Belgravia Grown in Moderate and High Levels of Nitrogen

Sample	Read1	Read2	Trimmed Read1	Trimmed Read2	Aligned	Percent Aligned
0.64 #1	37,781,644	37,781,644	34,402,954	34,402,954	22,952,966	60.75%
0.64 #2	32,860,640	32,860,640	30,191,273	30,191,273	20,072,826	61.08%
0.64 #3	40,323,292	40,323,292	36,877,309	36,877,309	26,035,838	64.57%
16 #1	38,090,836	38,090,836	34,836,701	34,836,701	24,785,305	65.07%
16 #2	33,559,673	33,559,673	30,084,899	30,084,899	21,684,042	64.61%
16 #3	39,160,069	39,160,069	36,032,947	36,032,947	24,580,458	62.77%
Total	221,776,154	221,776,154	202,426,083	202,426,083	140,111,435	63.14%

Read1 and Read2 are +ve and -ve strand sequences. Trimmed reads are the number of reads after quality control filtering. Aligned reads are the number of reads that were assigned to the reference 'genome' (genes, cDNAs, proteins, etc.).

Between 60.75 and 65.07% of the reads in each sample were aligned to the 62,584 sequences in the reference genome database and in total 51,181 transcripts were found in at least one of the samples. Disappointingly, approximately 35-40% of the reads, therefore, could not be aligned possibly for the reasons given above.

The data were then filtered for significant differences between the two treatments

using p-values of < 0.05 (Anova Tests) yielding 2286 transcripts. These were then further filtered to identify transcripts that were either more than 3-fold more abundant in High Nitrogen (16 mM) or in the Moderate Nitrogen (6.4 mM). This generated a data set of 995 transcripts ($p < 0.05$, > 3 -fold change) in the Moderate N samples and 281 transcripts ($p < 0.05$, > 3 -fold change) in the High N samples. These two data sets, Upregulated in High N and Upregulated in Moderate N are presented in the Appendix as Table A-1 and Table A-2. Figure 5-1 presents some of the graphical output from DESeq2 analysis of these data; these plots are broadly consistent with those predicted and provide confidence that real differences exist between the treatment (Love et al. 2014).

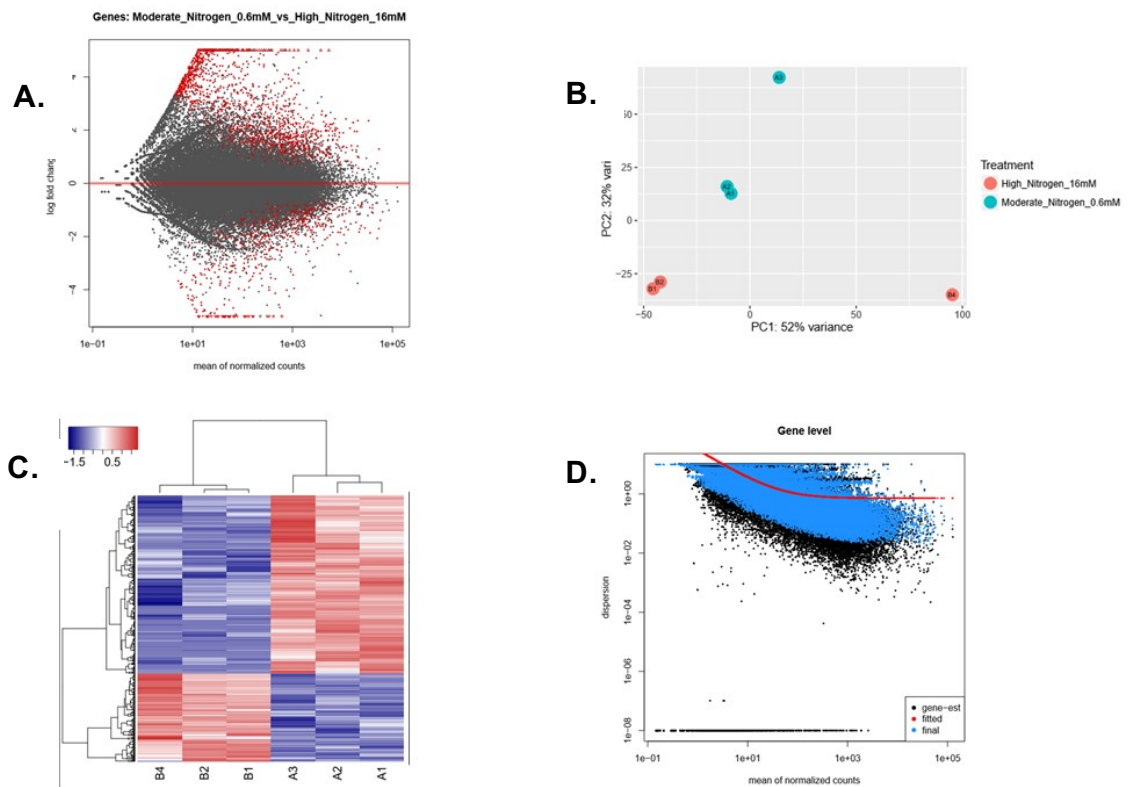


Figure 5-1. Graphical Representations of Barley Floral Meristem Transcript Profiles from DESeq2 Package

A; the plot shows the log₂ fold changes from the treatment over the mean of normalized counts, *i.e.* the average of counts normalized by size factors. **B;** Principle Component Analysis (PCA) plot, the 6 samples shown in the 2D plane spanned by their first two principal components. This type of plot is useful for visualizing the overall effect of experimental covariates and batch effects. **C;** sample-to-sample distances represented as a Heatmap; the Euclidean distances between the samples are calculated from the regularized log transformation. Red are 'upregulated' and blue 'downregulated' sequences. **D;** Dispersion plot showing gene-wise estimates (black), the fitted values (red), and the final maximum a posteriori estimates used in testing (blue). Samples A1-A3 and B1-B4 are biological replicates of samples grown in 0.64 and 16 mM N, respectively. For full details see (Love et al. 2014).

After these procedures, the normal approach would be to automate an interrogation of the databases with the transcript identity codes and extract a variety of information on their biochemical function, metabolic function, cellular location, conserved protein domain (pfam) motifs, BLASTn and BLASTp similarities, etc. However, when this was attempted very little annotation was retrieved so little additional information was provided. On further investigation with Dr Graham Hamilton, the Lead Bioinformatician at the Glasgow Polyomics Unit, this might be due to the very low annotation for barley sequences, or to an interface problem between DESeq2 output and propriety annotation retrieval programs. For this reason, it was decided to progress by manually downloading what annotation could be found and these data are also included in Table A-1 and A-2.

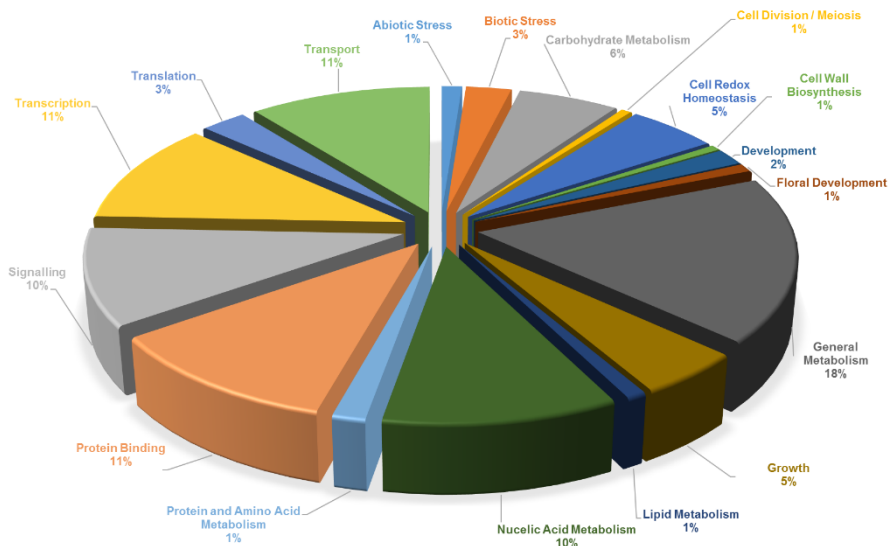
With detailed annotation, including information on biochemical function, metabolic function, and cellular and tissue location it is possible to perform Gene Ontology (GO) analysis providing further insight into the sequences that might be important in the High Nitrogen-induced suppression of flowering in barley. From the sparse annotation in Tables A-1 and A-2, however, it is clear that GO analysis was not feasible at this stage; further annotation will be required and this will involve complex analysis using a variety of programs on each of the 1276 identified sequences (995 +281). A discussion on how this might be achieved is included at the end of this chapter.

Without the advantages of an automated GO analysis, it was decided to use a manual approach to attempt to characterize the differentially abundant transcripts in the two N treatments. Each of the differentially abundant 1276 sequences described above were then used to manually interrogate the public databases

(ENSEMBL) using BLASTp and BLASTn. Where ever possible, GO annotations were added to each sequence. Pie charts were then constructed using the 18 most common GO Metabolic Function classes found and these are presented in Figure 5-2.

The data presented in Fig 5-2A can be viewed as those metabolic processes that are upregulated ($P < 0.05$, more than 3-fold) in the 0.6 mM samples (*cf* 16 mM samples). Alternatively, these same sequences could be viewed as Controls that reflect 'normal' levels of expression, in which case Fig 5-2A could be viewed as those metabolic processes that are downregulated in High Nitrogen (16 mM) and it is this approach that will be used here. Comparing the changes in metabolic function classes in Fig 5-2A and B it appears that High Nitrogen supply perturbs Protein and Amino Acid Metabolism (7% increase *cf* 1% decrease), Translation (5% increase *cf* 3% decrease), as well as Growth (0% increase *cf* 5% decrease), and Development (5% increase *cf* 2% decrease). Major changes were also observed in sequences involved in Abiotic stress (5% increase *cf* 1% decrease) and Cell Redox Homeostasis (9% increase *cf* 5% decrease). In addition, Carbohydrate metabolism (1% increase *cf* 6% decrease), and various transport processes (5% increase *cf* 11% decrease) were also found in the High Nitrogen (16 mM) samples. Taken together these data indicate that exposure to High Nitrogen dramatically affects protein synthesis in the reproductive meristem, which may in part account for the transcriptional suppression of sequences involved in growth and development of the floral primordia. At the same time carbohydrate metabolism and the transport of metabolites appears to be shut down presumably as resources are no longer required to support the growth of the floral spike.

A



B

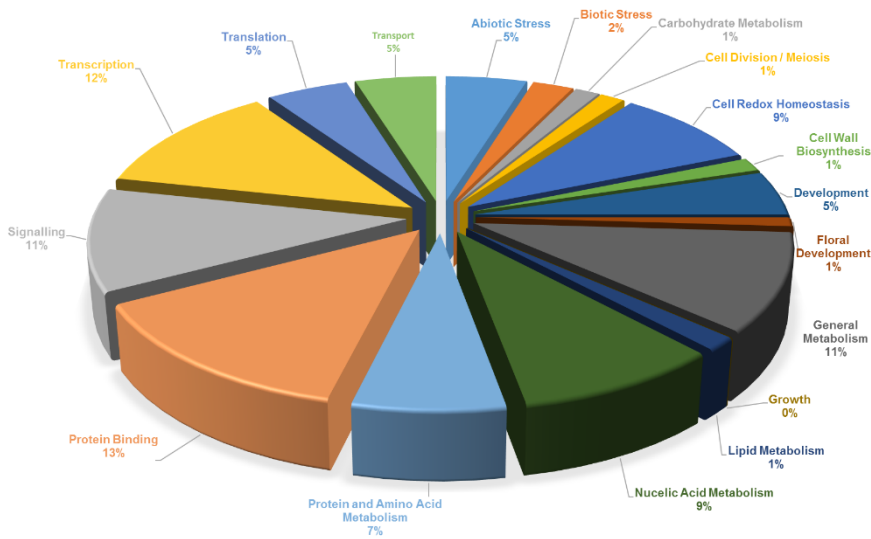


Figure 5-2. Transcriptional Changes of GO Metabolic Function Classes in Barley Floral Meristems Grown in Moderate and High Levels of Nitrogen.

Plants were grown to the 5-to-6 week stage (2nd -to-3rd node) in hydroponic solutions containing Moderate (0.64 mM) and High (16 mM) N supply (see Section 2.5.1.2). Floral primordia were dissected, rapidly frozen, and total RNA extracted for RNA-Seq analysis by Illumina paired-end high throughput sequencing (see Section 2.9). Significant ($p < 0.05$) differentially abundant sequences were identified that were >3-fold down (A) or >3 fold up (B) in the High N sample and where possible, placed into 18 Metabolic Function classes.

Other classes of GO Metabolic Function showed large and significant changes in the sequences expressed but these tended to be compensated by a reciprocal change in members of the same class. For example, 12% of the 'upregulated' and 11% of those 'down regulated' sequences in High Nitrogen were associated with Transcription. Similar antiparallel changes were observed within the Go Metabolic Function classes of Signaling, Cell Division / Meiosis, Floral Development, and Protein Binding.

Tables 5-2 and 5-3 present further GO Biochemical Function and Metabolic Function details gleaned from manual searches of selected sequences in the public databases. Details on some of the more interesting sequences that should be investigated further are discussed below.

5.3 Sequences Down Regulated in High Nitrogen.

5.3.1 Expansins.

The first and fourth most down regulated sequences in the High N samples (up regulated in Moderate N) appear to be Expansins (Table 5-2; 917 and 318 fold change) which are involved in growth. Expansins are extracellular proteins that become activated on cell wall acidification (by p-type H⁺-ATPases) and result in carefully regulated cellulose microfibril (cell wall) loosening. This is accompanied by an increase in cell turgor pressure and leads to pressure-driven cell growth. This normally occurs in zones immediately behind meristems resulting in an up to 100-fold increase in cell volume. After expansion, the p-type ATPases are inactivated, the cell wall pH rises leading to an inactivation of Expansins and rigidification of the cellulose microfibrils. The observation that transcription of two

key splice variants of the Expansin gene MLOC 65431 is significantly ($p < 7.2 \times 10^{-15}$) and hugely downregulated (>318-fold) in floral meristems where growth of the spike is arrested and floral development curtailed makes good sense. Further, homologues in rice (Expansin A-7) have been implicated in the rapid expansion of the rice floral spike (Shin et al. 2005). What is not clear, however, is how high levels of nitrogen suppresses the expression of MLOC 65431.

Table 5-2. List of Selective Highly Abundant Sequences in Floral Primordia of Barley Grown in 0.6 mM Nitrogen

Gene ID	P adj	Chromosome	Fold Change	GO: Biochemical Function	GO: Metabolic Function
MLOC_65431.2	1.9E-24	5	917	Similar to Expansin-A7 in <i>Oryza sativa</i> . May cause loosening and extension of plant cell walls by disrupting non-covalent bonding between cellulose microfibrils and matrix glucans. May be required for rapid internodal elongation.	Development
MLOC_15842.2	9.1E-25	4HL u/o	648	Negative Regulator of Translation, Endohydrolysis of the N-glycosidic bond at one specific adenosine on the 28S rRNA	Translation
MLOC_73247.2	3.7E-21	5	564	Pentatricopeptide (PPR) repeat-containing protein /	Transcription
MLOC_65431.1	7.2E-15	5	318	Expansin-like CBD	Development
MLOC_2933.1	1.1E-12	5	191	GRAS type transcription factor	Transcription
MLOC_73247.3	4.0E-12	5	177	Pentatricopeptide (PPR) repeat-containing protein /	Transcription
MLOC_34924.2	1.0E-10	6	147	Expressed protein/ Transmembrane helical	Transcription
MLOC_2934.2	1.1E-10	5	146	NAD(P)-binding domain	Transcription
MLOC_43830.6	1.1E-09	2	146	<i>CLY1</i> : AP2 /transcription factor activity, sequence-specific DNA binding	Transcription

Gene ID	P adj	Chromosome	Fold Change	GO: Biochemical Function	GO: Metabolic Function
MLOC_64932.2	2.2E-10	4	139	Elongator complex protein 5/ Tetratricopeptide-like helical domain	Transcription
MLOC_55424.1	3.5E-10	4	130	60S acidic ribosomal protein P0	Translation
MLOC_37780.1	1.6E-08	7	115	SANT/Myb domain	Nucleic Acid Metabolism
MLOC_81053.7	2.1E-08	3	115	SLT1 protein or Gnk2-homologous domain	General Metabolism
MLOC_15842.1	5.0E-09	4HL u/o	114	Negative Regulator of Translation	Signalling
MLOC_23441.1	2.5E-10	4HL u/o	106	Negative regulation of translation, rRNA N-glycosylase activity/ rRNA N-glycosidase; Catalytic Activity:Endohydrolysis of the N-glycosidic bond at one specific adenosine on the 28S rRNA.;Belongs to the ribosome-inactivating protein family.	Translation
MLOC_71332.1	3.0E-07	3	96	<i>Gam1/Gamyb</i> : transcription factor activity / Flower development / Transcriptional activator of gibberellin-dependent alpha-amylase expression in aleurone cells. Involved in pollen and floral organs development	Floral Development
MLOC_24033.1	2.5E-15	morex contig 163507	95	<i>RPS12</i> : Ribosomal protein S12	Translation
MLOC_53531.1	5.9E-07	5	70	Gene silencing by RNA	Nucleic Acid Metabolism

Gene ID	P adj	Chromosome	Fold Change	GO: Biochemical Function	GO: Metabolic Function
MLOC_67531.1	8.1E-27	7	67	Sucrose:fructan 6-fructosyltransferase , Belongs to the glycosyl hydrolase 32 family	Carbohydrate Metabolism
MLOC_51326.1	1.3E-06	6	66	O-methyltransferase COMT-type	Transcription
MLOC_52439.4	1.4E-06	5	66	SANT/Myb domain	Nucleic Acid Metabolism
MLOC_76615.2	4.9E-06	2	64	Asymmetric cell division/ serine-type endopeptidase activity	Growth
MLOC_5291.8	8.6E-06	6	62	Gravitropism/ photoperiodism, flowering	Growth
MLOC_63998.2	6.3E-06	3	56	Ribonuclease T2 activity (Catalysis of the two-stage endonucleolytic cleavage to nucleoside 3'-phosphates and 3'-phosphooligonucleotides with 2',3'-cyclic phosphate intermediates)	Translation
MLOC_60198.2	1.1E-04	3	40	MYB-CC type transcription factor, LHEQLE-containing domain	Transcription
MLOC_4381.2	1.8E-04	7	39	Pollen development/ trichome differentiation/ leaf development /	Transcription
MLOC_54911.4	9.5E-04	1	29	Cell wall organization / Defense	Growth
MLOC_5849.2	5.5E-06	2	26	SANT/Myb domain protein 37 [Source:Projected from Arabidopsis thaliana (AT5G23000) TAIR;Acc:AT5G23000] / myb domain protein 37 [Source:Projected from Arabidopsis thaliana (AT5G23000) TAIR;Acc:AT5G23000]	Nucleic Acid Metabolism
MLOC_54352.1	3.7E-03	7	24	KAO1: Ent-kaurenoic acid oxidase 1 / gpr5 (gibberellins biosynthesis)	Growth

Gene ID	P adj	Chromosome	Fold Change	GO: Biochemical Function	GO: Metabolic Function
MLOC_4290.2	4.4E-03	6	22	S-adenosyl-L-methionine-dependent methyltransferases superfamily protein (shoot system development/ methylation)	Growth
MLOC_55676.2	1.1E-02	1	18	DnaJ-like protein C11, C-terminal/ vegetative to reproductive phase transition of meristem	Growth

Sequences were filtered using the criteria of significant difference ($p < 0.05$) and changes of over three-fold (*cf.* plants grown in 16 mM N). This yielded a dataset of 995 sequences. These have been ordered in the table above on 'fold-change'; the values presented are the ratios of abundance in 0.6 mM samples compared with 16 mM samples (i.e. a 100 fold change increase here could be viewed as a 100 fold suppression in the 16 mM sample). GO Biochemical Functions and GO Metabolic Functions were obtained by manual BLASTp and BLASTn searches of the databases.

Table 5-3. List of Selective Highly Abundant Sequences in Floral Primordia of Barley Grown in 16 mM Nitrogen

Gene ID	<i>P</i> adj	Chromosome	Fold Change	GO: Biochemical Function	GO: Metabolic Function
MLOC_21665.1	2.8E-26	6	908	Protein of unknown function	
MLOC_61992.1	4.6E-09	6	149	NB-ARC domain/ Leucine-rich repeat domain, L domain-like	Protein Binding
MLOC_62925.3	1.1E-08	7	122	Pentatricopeptide repeat (PPR) superfamily protein	General Metabolism
MLOC_16403.1	2.1E-18	6	104	InterPro:F-box_dom_cyclin-like: Protein degradation	Floral Development
MLOC_4344.4	8.1E-08	7	103	NB-ARC domain/ Leucine-rich repeat domain, L domain-like (in the L domain from members of the epidermal growth-factor receptor (EGFR) family)	Transcription
MLOC_56325.1	1.5E-07	6	93	Protein kinase superfamily protein	Signalling
MLOC_56074.1	1.6E-53	5	87	BHLH (basic helix-loop-helix) / oxidoreductase activity	Transcription
MLOC_53617.2	2.7E-07	3	85	Z-finger Transcription factor - SUMOylated	Transcription
MLOC_10815.3	1.4E-07	7HS u/o	83	Transcription Factor	Transcription

Gene ID	P adj	Chromosome	Fold Change	GO: Biochemical Function	GO: Metabolic Function
MLOC_34862.1	9.2E-07	5	80	Protein folding, protein transport	Transport
MLOC_55587.11	1.5E-06	5	77	Tetratricopeptide repeat (TPR)-like superfamily protein: RNA degradation?	Nucleic Metabolism Acid
MLOC_71346.10	9.5E-07	2	77	Translation	Translation
MLOC_14088.1	2.7E-06	4	73	Vesicle-mediated transport,	Transport
MLOC_51271.2	2.0E-06	2HL u/o	71	DNA-directed RNA polymerase activity	Transcription
MLOC_11726.3	5.2E-06	2	30	Kinase	Signalling
MLOC_46130.5	6.3E-03	morex contig 285871	21	Metabolic process/ pollen development	Development
MLOC_62829.3	5.3E-06	3	8	Cytochrome P450, family 90, subfamily D, polypeptide 1/ brassinosteroid biosynthetic process/ leaf development/ petal development/ stamen development	Floral Development

Sequences were filtered using the criteria of significant difference ($p < 0.05$) and changes of over three-fold (*cf.* plants grown in 16 mM N). This yielded a dataset of 281 sequences. These have been ordered in the table above on 'fold-change'; the values presented are the ratios of abundance in 16 mM samples compared with 0.6 mM samples (i.e. a 100 fold change increase here could be viewed as a 100 fold suppression in the 0.6 mM sample). GO Biochemical Functions and GO Metabolic Functions were obtained by manual BLASTp and BLASTn searches of the databases.

5.3.2 Transcription Factors.

The abundance of several transcription factors were highly suppressed by growth in High Nitrogen. For example, MLOC 2933 was significantly ($p < 1.1 \times 10^{-12}$) down regulated (191-fold) in High Nitrogen and has putatively been annotated as a GRAS transcription factor. The family of GRAS proteins (GAI, RGA, SCR) share a variable N terminus and a highly conserved C terminus that contains five recognizable motifs. Proteins in the GRAS family are involved in gibberellin (GA) signaling known to be involved in many aspects of plant growth and development. Plant homologues of GRAS proteins include the *Arabidopsis thaliana* SCARECROW (SCR) protein which regulates cell division in the cortex/endodermal cells during root development and the SCARECROW-LIKE (SCL) protein. In addition, the *Arabidopsis thaliana* GIBBERELLIN-ACID INSENSITIVE (GAI) and REPRESSOR OF GA1 (RGA) are two closely related proteins involved in gibberellin signaling. The *Arabidopsis thaliana* SHORT ROOT (SHR) protein which is required for cell division and the formation of the endodermis. In addition, the *Solanum lycopersicon* (tomato) protein LATERAL SUPPRESSOR (LS), controls the formation of lateral branches during vegetative development. It is tempting to speculate that MLOC 2933 may be involved in floret branching in barley and that high levels of nitrogen suppress its action resulting in the arrest of floral development (InterPro; <https://www.ebi.ac.uk/interpro/>).

MLOC 37780, MLOC 52439, and MLOC 5849 encode SANT/Myb transcription factors and these were also highly down regulated in High Nitrogen ($p < 1.4 \times 10^{-6}$; >26-fold). The SANT domain occurs in nuclear receptor co-repressors and has

been implicated in chromatin-remodeling complexes. SANT domains show structural similarities to the DNA binding domain of Myb transcription factors; both possess tandem repeats of three alpha-helices arranged in a helix-turn-helix motif containing an aromatic amino acid (Aasland et al. 1996). The observation that the expression MLOC 37780, MLOC 52439, and MLOC 5849 are so strongly suppressed in the developing flowers of barley by High Nitrogen suggests they play an important role in floral development, possibly at the epigenetic level. It is now well established that flowering time is in part regulated by epigenetic factors in both monocots and dicots. In biennial *Arabidopsis*, flowering in the first year is suppressed by the transcription factor FLOWERING LOCUS C (*FLC*). During this period the chromatin structure associated with *FLC* is open (euchromatin) allowing expression. After exposure to a period of cold acclimation, however, two long non-coding RNAs (lncRNAs), *COOLAIR* and *COLD AIR*, are transcribed and these bind to a Vernalization Response Element (VRE) located in the first intron of the *FLC* gene (Heo and Sung, 2011). These lncRNAs then recruit the Polycomb Repressor Complex 2 (PRC2) which leads to the methylation of key residues in the N-terminus of Histone H3 proteins of nucleosomes (principally trimethylation of lysine 27, H3K27me3) which causes closure of the structure to form heterochromatin. With *FLC*, the suppressor of flowering, embedded in heterochromatin, transcription is no longer possible and flowering can be initiated (Sung and Amasino 2004; Dubin 2015; Hepworth and Dean 2015).

Vernalization is also required to initiate flowering in winter cereals, but here it is the transcription of the promoter of flowering in the crown meristem, *VRN1*, that is under epigenetic control. Before vernalization *VRN1* buried in heterochromatin due to the

trimethylation of Histone H3K27 (H3K27me₃); the markers for condensation are believed to reside in the first intron of *VRN1*. Vernalization results in the demethylation of H3K27, opening up the heterochromatin and enabling transcription (Szűcs et al. 2007; Oliver et al. 2009).

Further studies are required to clarify their role in flowering in barley and to discover how high levels of nitrogen supply suppresses their action. Another Myb-like transcription factor was also highly suppressed by High Nitrogen. MLOC 60198 is a Myb-CC -like protein that was downregulated 40 fold ($p < 1.1 \times 10^{-4}$). Myb-CC domains are found upstream of the C terminus and are characterized by a highly conserved LHEQLE amino acid sequence motif. No further details on their function are available.

MLOC 43830 shows homology to AP2-like (APETELLA2) ethylene-responsive transcription factors in Arabidopsis. APETELLA2 play a central role in Arabidopsis growth and development the protein encoded by At4g36920 has been shown to be essential for floral organ identity and establishment of floral meristem identity (Krogan et al. 2012). The AP2 protein from Arabidopsis also contain ethylene binding (ERF) domains that can bind to the GCC-box.

5.3.3 Negative Regulators of Translation.

Three sequences involved with translation were down regulated in the High Nitrogen samples. Two of these were splice variants of MLOC 15842 ($p < 5.0 \times 10^{-9}$, >114-fold), and MLOC 23441 ($p < 2.5 \times 10^{-10}$, 106 fold). Both of these sequences have been

implicated in the suppression of translation suggesting the synthesis of at least some protein sequences may have been upregulated in the High Nitrogen samples. These findings suggest the regulation of flowering may occur at the transcriptional as well as the translational level.

5.3.3.1 Control of Flowering.

Four sequences were identified that show homology to sequences that have been implicated in flowering in angiosperms and were significantly down regulated in High Nitrogen. These were MLOC 5291 ($p < 8.6 \text{ E-}06$, 62 fold), MLOC 4381 ($1.8 \text{ E-}04$, 39 fold), MLOC 54352 ($p < 3.7 \text{ E-}03$, 24 fold), and MLOC 55676 ($p < 0.01$, 18 fold). MLOC 5291 has been implicated in gravitropism and photoperiodic responses related to flowering. MLOC 55676 contains a Dna J -like (C11) domain; originally these proteins were considered to be prokaryotic molecular chaperones of the 40KDa class, but it is now known they are present in all eukaryotes, and over 80 have been identified in *Arabidopsis thaliana* (InterPro; IPR024586). Specifically, homologues of MLOC 55676 are implicated in the vegetative-to-reproductive phase transition of the meristem. Clearly, the role of High Nitrogen on the strong suppression of this sequence in floral primordia requires further investigation, but at present it is unclear how nitrogen exerts this effect. MLOC 4381 shows homology to sequences that have been implicated in pollen, trichome, and leaf development in *Arabidopsis*. The proposal that homologues of this sequence are involved in the development of three different organs is interesting and suggests it may be a general regulator of cell division or growth. Finally, the protein encoded by MLOC 54352 appears to function as an *Ent*-kaurenoic acid oxidase and involved in gibberellin (GA) biosynthesis. GA, of course, has long been known to be involved

in plant growth and development, in part by accelerating the breakdown of DELLA protein which are transcriptional suppressors of growth (Sun and Gubler 2004; Boden et al. 2014). Interestingly, MLOC 71332, homologues of the *Gam1/Gamyb* transcription factors mentioned above, have been implicated in GA signalling.

5.4 Sequences Up Regulated in High Nitrogen.

5.4.1 Transcription Factors.

Four barley sequences were significantly highly upregulated in the floral primordia of High Nitrogen grown plants that show some homology to other plant sequences annotated as transcription factors. These were MLOC 56074 ($p < 1.6E-6$, 87 fold); MLOC 53617 ($p < 2.7 E-7$, 85 fold); MLOC 10815 ($p < 1.4 E-7$, 83 fold); MLOC 51271 ($p < 2.0 E-6$, 71 fold). MLOC 56074 has a BHLH motif whilst MLOC 53617 contains a zinc-finger motif and also contains a putative SUMOylation domain. No further annotation was found for the other two putative transcription factors but when compared with their expression levels in the floral primordia of Moderate Nitrogen-grown plants, their high abundance (over 70 fold) coupled with their high level of significance ($p < 2.0 E-6$) suggests they may be strong negative transcriptional suppressors of floral development.

5.4.2 Control of Flowering.

Homologues of MLOC 46130 and MLOC 62829 are implicated in flowering. The former was upregulated 21-fold in High Nitrogen ($p < 6.3E-3$), may be involved in pollen development, but exactly how these proteins function in the flowering

pathway is not known. MLOC 62829 was upregulated 8 fold in High Nitrogen floral primordia ($p < 5.3 \text{ E-6}$) and appears to be a P450 Cytochrome protein involved in brassinosteroid biosynthesis. Members of this class of protein have been implicated in petal and stamen development. It is unclear why over expression of proteins involved in brassinosteroid biosynthesis and the promotion of floral development would lead to a suppression of flowering.

5.4.3 Signalling.

Two sequences have been tentatively annotated as kinases; MLOC 56325 and MLOC 11726. The former was upregulated 93 fold ($p < 1.5 \text{ E-7}$) and the latter 30 fold ($p < 5.2 \text{ E-6}$). The strong and significant up regulation of these two sequences lends further support to the suggestion that High Nitrogen induced suppression of flowering is controlled at the transcriptional and post-transcriptional level. Two other sequences, MLOC 16403 (an F-box like protein involved in protein degradation, $p < 2.1 \text{ E-18}$, 104 fold) and MLOC 55587 (a tetratricopeptide repeat protein with putative RNA degradation activity, $p < 1.5 \text{ E-06}$, 77 fold) lends further support to this notion.

5.5 Discussion

The finding from the comparative RNA-Seq analysis of data collected from the floral primordia of barley plants grown in Moderate Nitrogen (0.64 mM) and High Nitrogen (16 mM) suggest highly significant changes occur at the transcriptional and post-transcriptional level that could account for the suppression of flowering. Several

sequences were highly up regulated whilst others were highly down regulated in the floral primordia at the 2-to-three node stage of High Nitrogen grown plants. It is unfortunate that more detailed annotation of barley sequences is not available as this would have led to a more detailed discussion on the possible mechanisms by which floral development is arrested. The model for floral development, the ABCDE model, in dicots has come from detailed analysis of *Arabidopsis* and *Antirrhinum* (Dreni and Zhang 2016). The model proposed for flower development in cereals has in part been based on the more detailed dicot model as homologues of some of the major sequences involved are found in monocots, but it is also clear that there are major differences in the flowering pathways of the two groups of flowering plants. None-the-less, the ABCDE model of floral development has been tacitly adopted in cereals until more detailed analysis refines or refutes it. Regardless, in neither monocots or dicots is a complete understanding of floral development pathway available and further detailed genetic analysis will be required to achieve this (Bai et al. 2016; Dreni and Zhang 2016; Wu et al. 2017).

Unfortunately, a full analysis of these data were not possible within the time frame of this study. In part, this was due to the poor annotation of the barley genome which is possibly a reflection of the relatively small global community who work on barley. Regardless, with time further annotation should become available and the data presented in this study can be analyzed again to provide more insight. Another reason that a more in-depth analysis of the RNA-Seq data has not been provided is the failure to pipe the output of the RNA-Seq data from DESeq2 into the Trinotate package (<https://trinotate.github.io/>) that automates sequence annotation. Trinotate has been developed by the Trinity consortium (Haas et al. 2013); the major

difference between packages that perform RNA-Seq analysis using reference genomes (such as DESeq2, Cufflinks, Bowtie, etc.) and Trinity is that the latter performs *de novo* assembly of reads into transcripts which are then counted and quantified for differences between the treatments. To achieve *de novo* transcript assembly a very high number of reads are required, and a computer with a very large amount of RAM to assist with the assemblies. At this stage it is not clear whether the 200 million reads obtained in this study are sufficient, or whether the University of Glasgow Galaxy server has the raw computing power to undertake this task. Attempts were made to pipe the output from Deseq2 (which aligns to a reference genome) into Trinotate (that expects output from *de novo* transcript assembly) but the import failed and it is unclear at this stage why this has occurred. No doubt this problem will be resolved over the coming months but at the time of writing no code to assist with this problem has been posted on the Galaxy community forums.

Cell growth in plants is effected by the force of turgor pressure acting on cell walls where intermolecular forces between the extracellular matrix have been reduced by the action of Expansins (EXP); the activity of EXP are regulated by cell wall pH (Shin et al. 2005; Cosgrove 2015). As mentioned above, *EXPA* and *EXPB* stimulate the growth of different plant organs such as root growth (*EXPB1*, *EXPB2*, *EXPA4* and *EXPB23*), leaf initiation (*EXPA1*), guard cells (*EXPA1* and *EXPA4*), stem elongation (*EXPB3*, *EXPB4*, *EXPB6* and *EXPB11*), and reproduction (Marowa et al. 2016). Expansin expression can be induced by indole-3-acetic acid (Marowa et al. 2016), ethylene (Li et al. 2014b) and GA (Li et al. 2014b; Xu et al. 2016). In addition, Expansin expression may be regulated by biotic and abiotic stress factors (Ding et

al. 2008; Cosgrove 2015). Expansins involved in the development of floral structures such as *EXPA1* are active at the early stages of floral bud development. *EXPA2*, 7 and 10 are active in all floral organs of rice, whereas *EXPA4*, 5, 6, 13, 16, 18, 25, 26 and 29 are involved in floral initiation and development in rice (Shin et al. 2005; Marowa et al. 2016).

One of the sequences down regulated under high N levels is Pentatricopeptide repeat (PPR) proteins which is one of the largest protein family in plants. PPR are required for many essential processes including RNA editing, RNA splicing, translation, and the restoration of fertility. PPRs play a role in responses to abiotic stress as well as plant development with tissue-specific expression at different developmental stages (Schmitz-Linneweber and Small 2008; Barkan and Small 2014; Wei and Han 2016).

DELLA proteins are members of the GRAS family of transcription regulators (Hedden 2003; Chandler and Harding 2013). In addition to DELLA, other subfamilies of the GRAS family are Scarecrow (SCR) in *Arabidopsis* mesophyll sheath; Nodulation Signaling Pathway 1 (OG-NSP1) which is involved in the biosynthesis of strigolactone in rice; Lateral Suppressor (OG-LS) which functions as Monoculum1 in rice; Nodulation Signaling Pathway 2 (NSP2) which interacts with DELLA; Phytochrome A Signal Transduction (PAT) that includes CIGR2; SCL3 which promotes GA signaling and represses DELLA proteins; Dwarf and Low-Tillering (DLT) in rice; (Hirsch and Oldroyd 2009; Li et al. 2016; Sun et al. 2016; Cenci and Rouard 2017).

High level of N up regulate Tetratricopeptide repeat (TPR)-like superfamily of proteins which are regulatory sequences involved in many processes in the cell such as Auxin signalling, targeting, and import of proteins into the peroxisome, chloroplast, and mitochondria. In addition, TPRs have also been implicated in chloroplast development and greening (Hu et al. 2014; Zhang et al. 2015).

6 Chapter 6 General Discussion

The original aims of this project were threefold. First, to confirm whether earlier findings on the effects of high leaf temperature (T_{leaf}) on leaf photosynthesis rates of barley grown in a physiologically high levels of nitrogen were also applicable to plants grown in nitrogen levels encountered in agricultural soils. Second, to confirm the preliminary finding from our group that high T_{leaf} impaired carbon assimilation by reducing chloroplast ATP levels which subsequently impaired the synthesis of RuBP, a substrate for RuBisCO. Third, to assess the prospects for engineering thermal tolerance of high temperatures in crops.

6.1 Effect of High T_{leaf} on Photosynthesis

A series of experiments is reported in Chapters 3 and 4 where barley plants were grown either in soil or in hydroponics over a range of N-supply. Using this approach plants with a phenotypes similar to those of plants grown on arable farms were subjected to a range of T_{leaf} . Leaf gas exchange and chlorophyll fluorescence measurements were made to assess the effects of heat stress on various photosynthesis parameters and the findings were unequivocal; similar responses were observed regardless of whether plants were grown in moderate (*i.e.* comparable with arable production) or artificially high (*i.e.* 16 mM) levels of nitrogen. In barley, elevating T_{leaf} to 38°C for three hours severely and irreversibly suppresses light saturated photosynthesis rates measured by two independent methods, leaf gas exchange and chlorophyll fluorescence. These observations are in some respects similar but also notably different from the studies reported by others.

Careful analysis of **A/Ci** curves (Figure 3-1) provides further evidence that the capacity of the C3 cycle to fix carbon is compromised by high T_{leaf} , and that this does not arise by stomatal limitations of CO₂ uptake. The suppression of photosynthesis reported in Chapter 3 occurred at temperatures 2-4°C lower than that described elsewhere and was also irreversible (Frolec et al. 2008) compared with full recovery within an hour, (Hüve et al. 2011). It is not clear why these differences have arisen. It could be due to the different species of plant used, in this study barley compared with cotton and tobacco (Crafts-Brandner and Salvucci 2000, 2002). Alternatively, it might be due to the methods used. One of the major difficulties with exposing attached leaves to a consistent and uniform T_{leaf} in the effect of transpirational cooling which might be patchy across the leaf (Baker 2008). T_{leaf} is determined by the combined processes that heat and cool leaves. The heating processes include short (visible light) and long wave (infra-red) radiation (radiative processes), and T_{air} (if T_{air} is above T_{leaf}) coupled with air speed at the surface of the leaf (conductive / convective processes). The cooling processes include mainly long wavelength radiative losses, and T_{air} (if T_{leaf} is above T_{air}) and air speed (conductive and convective processes), plus transpiration. In most experiments in the literature where attached leaf measurements have been made, T_{air} in the leaf chamber was controlled usually within the limits of $\pm 1-2^{\circ}\text{C}$ of the set temperature. The reason for this fluctuation is that whilst T_{air} and airspeed can be controlled, and radiative losses are governed by T_{leaf} and the laws of physics, stomatal conductance and transpirational cooling are controlled by the plant. This problem is exacerbated by fluctuations in **gs** during the period of heat stress. What has been reported in the literature, therefore, is the average T_{leaf} and a review of the literature shows that T_{leaf} is averaged and the incurred variance in T_{leaf} , which

might be as high as 2°C, is simply ignored. It is for this reason that the Post Heat Stress experiments were designed (Chapter 3-2). In these experiments attached leaves were placed on a thermal block in the dark and covered with a neoprene pad for thermal insulation. Careful analysis with multiple thermocouples demonstrated that a uniform T_{leaf} could be imposed on the attached leaf section that varied less than 0.3°C between leaves. Further, as these experiments were performed in the dark in a small volume of still air, radiative heating and transpirational cooling was effectively eliminated. It is reasonable to conclude, therefore, that the thermal profile of the effects of high leaf temperatures on photosynthesis rates provided in Chapter 3 are a better representation of events than those presented in the published literature.

One criticism that could be levelled at the Post Heat Stress experiments described in Chapter 3 relates to the exposure of leaves to high temperatures in the dark. Whilst this approach may show the direct effect of high T_{leaf} on attached leaves, in the field where plants are normally exposed to high T_{air} and high irradiance, other factors such as light-generated reactive oxygen species (ROS) may also cause significant damage before the reported thermal effects are apparent. To explore this possibility leaves were exposed to saturating levels of irradiance (approximately $600 \mu\text{mol m}^{-2} \text{s}^{-1}$ PAR) for 3 hours whilst held over a range of T_{leaf} . The effects on photosynthesis rates were almost identical to those observed on leaves treated in the dark, and it can be concluded that up to this light level damage to the photosynthetic apparatus appears to arise from a direct effect of high temperature on a component or components of the C3 cycle. It could be argued that plants that are exposed to $T_{\text{leaf}} > 36^\circ\text{C}$ are likely to be exposed to full sunlight, which at midday

in the height of summer may be as high as 1500 or 2000 $\mu\text{mol m}^{-2} \text{s}^{-1}$ PAR depending on the latitude. The levels of irradiance used in Chapter 3 were approximately a third of these maximal levels, and it could be argued that had higher levels been used ROS-induced damage might have been observed at those intensities. Whilst this remains a possibility, it should be stressed these are maximal levels of irradiance that peak at midday at the height of summer. Further, significant amounts of ROS would still be generated at 600 $\mu\text{mol m}^{-2} \text{s}^{-1}$ PAR when photosynthetic electron transport rates are impaired. Measurements of photosynthetic electron transport rates also show a large decline at 38°C in which case absorbed light could not be dissipated through normal chloroplast metabolism (C3 cycle, nitrate reduction, *etc.*), through the Mehler reaction, or through the ascorbate/glutathione cycle. Under these conditions the density of excited chlorophyll molecules in the light harvesting complexes would have increased leading to the formation of triplet excited chlorophyll and then singlet oxygen, a very potent oxidant that causes severe damage to tissues. An argument could be made to repeat these experiments using very high levels of irradiance (*e.g.* 2000 $\mu\text{mol m}^{-2} \text{s}^{-1}$ PAR) to test if ROS damage is significant. An alternative approach would be to assess the temperature profile of photosynthesis of plants growing in the field that are exposed to both high T_{leaf} and very high irradiance. These experiments would have the advantage of making meaningful measurements on barley plants exposed to natural conditions, but might be compromised by attempts to interpret a data set where T_{leaf} cannot be held constant and consequently suffers from large inherent variance (see above).

A decline in light saturated photosynthesis rates (A_{sat}) might arise from a direct suppression of high T_{leaf} on carbon assimilation, or by a direct stimulation in photorespiration. Previous work comparing the metabolite pools of control and heat stressed attached barley leaves suggested the C3 cycle is perturbed and that carbon flow between Ribose 5-phosphate and 3-phosphoglycerate was impaired (Almalki 2014). These observations suggest that an increase in photorespiration does not account for the decline in A_{sat} with high leaf temperature. Similarly, other reports where photorespiration was measured on attached leaves suggested it was not a significant factor on the decline in carbon assimilation (Crafts-Brandner and Salvucci 2002), but it was pointed out above that the temperature profiles of these experiments were somewhat different from those presented in this thesis. None-the-less it seemed sensible to check the possibility that high T_{leaf} affects carbon assimilation rates by perturbing photorespiration. Established methods for estimating rates of photorespiration involve determining A/C_a (and hence A/C_i) curves from attached leaves exposed to normal air (21% oxygen – 210 mmol O_2 mol⁻¹ air, variable CO_2) where there is significant competition between CO_2 and O_2 for binding sites on RuBisCO, and modified air (1% O_2 – 10 mmol O_2 mol⁻¹ air, variable CO_2) where there is much less competition; the difference between these two readings can be taken as the rate of photorespiration. These methods proved to be unsuitable for attached barley leaves. Often over 30 minutes was required to attain steady state CO_2 assimilation readings and when exposed to 1% oxygen, this may have induced severe anaerobiosis. For this reason, measurements were made on attached leaves exposed first to normal air (380 $\mu\text{mol } CO_2$ and 210 mmol O_2 mol⁻¹ Air) for 20 minutes followed immediately by exposure to modified normal air (380 $\mu\text{mol } CO_2$ and 10 mmol O_2 mol⁻¹ Air) for a similar period. In this way steady state

readings could be achieved but clearly it was not possible to construct **A/Ca** or **A/Ci** curves and assess the rates of photorespiration over a range of CO₂/O₂ ratios. The findings from these experiments were unequivocal; although high **T_{leaf}** did result in a small increase in photorespiration between 37° and 40 °C, it accounted for only 15% of the observed 80-90% decline in **A_{sat}**. The conclusions are that high **T_{leaf}** directly affects the C3 cycle and has only a minor effect on photorespiration.

In the Introduction (Chapter 1) it was stated that previous work at Glasgow University on the effects of high **T_{leaf}** on photosynthesis had suggested carbon flow between Ri5P and RuBP in the C3 cycle was affected but the two enzymes involved in catalysing this conversion, Ribose 5-phosphate Isomerase (Ri5PI) and Phosphoribulose Kinase (PRK) were almost fully active after heat stress (Almalki 2014). Further work in that report, and new work presented in this thesis (Chapter 3) has confirmed the supply of CO₂ to the chloroplast was not affected, and this left only one possibility to account for a decrease in carbon flow from Ri5P to RuBP, the concentration of ATP in the chloroplast. Preliminary measurement reported in Almalki (2014) suggested high **T_{leaf}** did indeed result in a decline in estimates of chloroplast ATP levels *in vivo* but this needed to be checked. In those experiments estimates of chloroplast ATP levels were made by calculating the difference between the steady state levels measured in the light and the dark. Whilst this method did suggest a decline in chloroplast ATP levels with increasing **T_{leaf}**, the experiments were incomplete as only differences were reported. For this reason, these preliminary experiments were repeated and extended in an attempt to confirm the role of ATP supply on the C3 cycle. The experiments reported in Chapter 3 did not confirm this hypothesis, however. First, in the light whole leaf ATP levels

increased significantly with increasing T_{leaf} suggesting there should have been sufficient chloroplast ATP to support the PRK-dependent conversion of Ru5P to RuBP. Second, the levels of whole leaf ATP in control attached leaves in the dark were higher than in the light; this is in direct contrast with the preliminary data of Almalki (2014) who showed the converse. It is unclear why these discrepancies have arisen. ATP levels within a cell are of course the sum of those in the chloroplasts, the mitochondria, and the cytoplasm; the assumption with these experiments is that mitochondrial and cytoplasmic levels do not change between the light and dark, and the difference therefore reports light-generated ATP in the chloroplast. This is clearly a crude assumption and caution must be applied when interpreting the results from these experiments. Also, it should be stressed that what measured was whole leaf steady state levels of ATP in the light and in the dark. ATP concentration may change because the capacity to generate or consume ATP changes, and this is also a complicating factor when interpreting these data. The increase in light adapted whole leaf ATP levels with increasing T_{leaf} (Figure 3-11) might have arisen, therefore, from an increase in the capacity to generate ATP or from a decrease in the consumption of ATP, or both. Although not measured in this current study, Almalki (2014) did measure over a range of T_{leaf} the dark decay in the apparent F_0 level of chlorophyll fluorescence after a period of illumination; this is considered to reflect the capacity of the thylakoid membrane to develop and sustain a proton motive force (pmf; Baker 2008). The conclusion from these experiments was that in leaves where A_{sat} was severely suppressed by high T_{leaf} , the pmf was comparable to that found in control, non-stressed leaves. What was not clear from these experiments, however, is whether the ATPsynthase was fully functional and able to use the established pmf to generate ATP in the chloroplast.

The fact that ATP levels increase in light adapted leaves with T_{leaf} suggests that if there was sufficient ATP in the stroma to support the activity of PRK (and PGK) at 25°C, there certainly should have been a sufficient level at higher temperatures. This leads to the conclusion that chloroplast ATP levels in the light do not impair the generation of the substrate RuBP required for RuBisCO activity leading to the suppression of A_{sat} . It would appear that on closer analysis there is no evidence to support the hypothesis of Almalki (2014) that low stromal ATP levels account for the observed decline in photosynthesis rates at high leaf temperatures.

The conclusion that stromal ATP levels do not account for the observed suppression of leaf photosynthesis rates is problematic. Compelling evidence has been provided by Almalki (2014) and in this thesis for the following: the activity of the C3 cycle is severely suppressed by high T_{leaf} ; the supply of CO₂ to the chloroplast is not greatly affected; neither the enzymes that convert Ri5P to 3PGA nor stromal ATP levels are affected and at least this part of the C3 cycle remains fully functional; metabolite profiling has implicated carbon flow between Ri5P to 3PGA is compromised. Clearly, the last two statements are incompatible; one of these observations must be incorrect. The way forward to resolve this discrepancy would be to re-analyse the metabolite profiles of heat-stressed and control barley leaves to confirm the original analysis reported in Almalki (2014) was valid. Alternatively, a biochemical approach could be used to isolate and then assay each and every enzyme of the C3 cycle with the hope this would identify the site of thermal damage; this is a daunting challenge, many of the substrates for enzymes of the C3 cycle are not available commercially and some complex chemical synthesis would be required.

During the early days of research into the bioenergetics of chloroplasts it was common to isolate intact plastids and measure the rate of ATP synthesis directly using ^{32}P -labelled phosphate. An argument could be made that such an *in vitro* approach could be used here to confirm the role of ATP in heat-stressed leaves. Intact chloroplasts could be isolated from control leaves, placed in appropriate buffers and heat stressed *in vitro*; subsequently, the capacity of these chloroplasts to generate ATP could then be assessed using well established conventional methods. Although compelling, such an approach has its drawbacks. First, chloroplast preparations are rarely homogeneous and usually consist of a mixture of good intact and partially intact chloroplast, plus a variable amount of released thylakoid membranes from lysed plastids. Further, it is now well established that chloroplasts 'age' rapidly *in vitro*; some consider it pointless to make measurements on preparations that are over 60 minutes old (Dominy *et al.* 1981) and it would not be possible, therefore, to expose them to *in vitro* heat stress for 3 hours. For this reason, it is not recommended to use this approach.

One of the interesting observation to emerge from the Pseudo-Steady State measurements reported in Section 3.2 relates to the role of stomata. There is a tacit assumption that as air temperature increases and leaves begin to wilt, that stomata close to conserve water (Taiz and Zeiger 2010). Indeed, agronomists are well aware of 'midday closure' where g_s declines between *ca.* 11:00 and 14:00 causing a decline in photosynthesis rates (Lambers *et al.* 2005). Clearly these observations are real in a temperate arable setting where irradiance, T_{air} – and therefore T_{leaf} also

– are moderate. On closer consideration, however, this is not a sensible strategy for plants exposed to high irradiance and T_{air} as a high T_{leaf} will ensue and stomatal closure will make matters worse, potentially lethal. At moderate levels of light and T_{air} partial stomatal closure may raise T_{leaf} above T_{air} , but not to the extent that it exceeds the critical level of 36°C; in these conditions the plant is faced with two problems, potential leaf desiccation and potential thermal damage if T_{leaf} exceeds 36°C. In contrast plants exposed to very high irradiance and high T_{air} might result in T_{leaf} of 36°C; partial stomatal closure would result in less transpirational cooling and a further increase in T_{leaf} , beyond the critical threshold level for irreversible damage (Frolec et al. 2008). In these circumstances, leaves are faced with the same two problems, but keeping T_{leaf} below 38°C is imperative. Faced with the dilemma of conserving water or maintaining T_{leaf} , it appears that barley leaves do the latter; stomata open to apertures not normally observed in non-stressed leaves (above 1.0 mol m⁻² s⁻¹ cf. typical values of 0.3 – 0.5 for non-stressed leaves). The observations reported in Section 3.2 on the effects of high T_{leaf} on **gs** are novel and demonstrate that guard cells respond to high temperatures as well as the well documented stimuli of blue light, **Ca**, and water status

6.2 The Effects of Nitrogen Supply on the Growth and Development of Barley

In Chapters 4 and 5 a series of experiments are reported on the effects of nitrogen supply on barley. This represented a change in direction of the original aims of the project (to investigate the effects of high T_{leaf} on photosynthesis rates – see Chapter 3). The reasons for this change of direction were two-fold. First, it was felt the

studies on leaf temperature on photosynthesis rates had reached an impasse. All of the possible candidates explaining the metabolomics profiling results had been carefully discounted leaving the option of repeating the metabolomics experiments (and possibly incurring a similar error) or undertaking a major study of metabolite flux through the different sections of the C3 cycle. Second, one of the original objectives of this project was to assess the role of N-supply on the thermal suppression of photosynthesis; this was necessary because some of the earlier work from our lab was done on barley plants with abnormal phenotypes. Whilst undertaking these studies some unusual and very exciting observations were made. For these reasons, on one hand an impasse with the heat stress experiments, and on the other potentially very important observations on the effects of nitrogen status and nitrogen sinks on cereal productivity resulted in a re-focusing of the research direction.

To summarize briefly, measurements on A_{sat} and the carboxylation coefficient determined from A/C_i curves showed that unit leaf area photosynthesis rates increased with increasing N-supply. At the levels of N normally used in arable production in the Developed World there was clear evidence that photosynthesis rates were approximately half of those found in plants grown in high N-supply and that as a consequence grain yields in well fertilized soils are constrained by plant N-status.

Further studies revealed more interesting observations; barley appears to have two endogenous sensors of N-status. One seems to operate at N-supplies of around

300 μM ; below this threshold level plants develop a single culm that flowers (no tillers develop) but higher concentrations lead to a progressive increase in tiller number. The other sensor mechanism seems to operate at a higher endogenous N-status. Flowering continues and grain yield increases up to ca. 1.6 mM but then yield declines and flowering is progressively delayed; at 3 mM N-supply flowering is completely suppressed. The effects of plant N-status appears to be exerted on the crown vegetative and reproductive meristems. Low N-status suppresses tillering, that is the ability of the lateral crown meristems to produce lateral vegetative buds but when triggered undergoes a transition to a reproductive meristem generating floral buds. Higher levels of N-supply (up to 1.6 mM) promote profuse tillering and the transition to flower occurs when the appropriate signal is received. Beyond 1.6 mM N-supply, however, tillering becomes profuse but the meristem remains in the vegetative phase generating only vegetative buds.

For this reason, barley plants grown in hydroponic solutions containing a range of N-supply are morphologically very different and the explanation follows. Cereal crops are essentially wild grasses and despite domestication they still retain many of the strategies and traits ingrained by millions of years of evolution. One of these may be their response to N-supply. When N-supply is high members of the Poaceae family (which includes wheat, barley, oats and rye) could remain in the vegetative phase of growth indefinitely with the main shoot axis (the culm) and many secondary shoots (tillers). Below a critical threshold level (ca. 3 mM in barley), however, the VRN1 protein (which triggers flowering) accumulates in the crown meristem and the reproductive structures develop; below a second critical level (ca. 0.25 mM in barley) tillering is suppressed, the plant flowers but is 'uniculm'. Surprisingly, unlike animals

which reproduce when conditions are favourable, it appears that grasses tend to flower only when they are unfavourable (i.e. when they are N-stressed). This switch between vegetative and reproductive phases of growth in response to N-supply may be a good ecological strategy for wild plants, but it is not ideal for crop production – increasing N increases biomass but suppresses flowering. The implication of these findings is that in typical arable settings (0.3-0.5 mM soil N-supply) barley develops two or three flowering culms but photosynthesis rates are impaired by leaf protein levels (i.e. the abundance of the C3 Cycle enzymes).

These observations suggest that if leaf nitrogen status could be boosted an increase in ULA photosynthesis rates would occur leading to an increase in grain yield. To achieve these gains, however, barley would have to be modified in two ways. First, the mechanism(s), presumably located in the crown meristem, that sense nitrogen status in plants grown above 0.3 mM N-supply and result in the crown meristems undergoing tillering (*i.e.* nitrogen sinks) would have to be inactivated or at least modulated. This would lead to an increase in main stem nitrogen levels and higher ULA photosynthesis rates. Second, the mechanism(s), again probably located in the crown meristem, that sense the nitrogen status of plants grown above 1.6 mM N-supply and suppresses the vegetative-to-floral phase transition would have to be inactivated to ensure the gain in carbon assimilation would lead to a gain in grain yield.

In Chapter 4 the details of some experiments were provided where attempts were made to reduce tillering and hence sink strength. These included the mechanical removal of tillers and experiments with 'uniculm' mutants. Both of these approaches

failed. Mechanical removal of new tillers resulted in infection of the crown that was difficult to control. Further, the three 'uniculm' / 'low number of tillers' mutants tested showed very low fertility and it has not yet been possible to generate enough seed to undertake a set of experiments with the appropriate controls. It seems that whatever genetic lesions have resulted in a failure of the crown meristem of these plants to generate multiple vegetative buds (tillers), the same lesions have resulted in a failure of the same meristems to generate multiple florets after undergoing a vegetative-to-reproductive transition. Over twenty unculm mutants have been isolated in the Bowman background, and there are probably many others in different backgrounds. It is not clear whether all of these unculm mutants also show very low fertility, but the received wisdom is that they do (Prof Robbie Waugh, James Hutton Institute, per comm). To date, none of the mutations that cause the unculm phenotype has been mapped. A better understanding the mechanisms that control tillering in cereals is required as this may provide insight into how to suppress tillering without compromising flowering. Performing time course transcriptome profiling experiments on the vegetative crown meristem of developing (2-to-5 weeks old) plants may provide this insight, and exposure to a range of N-supply may help. It is recommended that these experiments are undertaken with some urgency, although the minute size of the crown meristem at this stage (<0.5 mm length) will make this approach challenging.

In Chapter 5 the results of transcriptome profiling experiments are reported on older barley plants (5-to-7 weeks old) where the crown meristem had already undergone a vegetative-to-reproductive transition. These experiments were designed to investigate why high levels of N-supply suppressed floral development at the 2-to-3

node stage. These experiments were hampered in part by the poor annotation of the barley sequences deposited in the public databases. A discussion is presented at the end of Chapter 5 on how this problem might be resolved. None-the-less, in the developing floral meristem high nitrogen status significantly ($p < 0.05$) suppressed nearly one thousand transcripts and up regulated nearly 300 transcripts by a factor of 3 or more. Manual interrogation of the public databases with each of these sequences revealed some annotation from which Gene Ontology (GO) classes could be determined for Metabolic and Biochemical function. Amongst those sequences that were down regulated by high nitrogen supply were transcription factors (including homologues of sequences involved in organ identity in other plants, ie.g. *SCARECROW*, *GAI*, and *APETELLA2*), regulators of flowering, suppressors of translation, and Expansins (that could be responsible for spike elongation). Sequences that were up regulated by high nitrogen included transcription factors, controllers of flowering, and various signalling components (kinases, *etc.*).

6.3 Future perspectives

In this study the direct effect of high temperatures on photosynthesis was assessed. All of the work presented in this thesis, and from others at Glasgow University, has indicated high T_{leaf} causes a decline in chloroplast ATP levels, and this impairs the synthesis of RuBP by Phosphoribulose Kinase, and hence photosynthesis rates. Unfortunately, it was not possible to demonstrate unequivocally a decrease in chloroplast ATP levels with heat stress. This might be due to the methods used to assess ATP levels in whole leaves (the luciferin-luciferase assay), and it might be

priuent to try alternative assays. Chromatographic separation and quantification of adenylates is one possibility and has the advantage that both ADP and ATP can be resolved, thereby providing a check as one form is converted to the other. The major limitation with these experiments, however, might be the inability to separate chloroplast adenylate levels from those in the rest of the cell. It is difficult to devise a method that can do this on attached leaves. Fractionation of chloroplasts from leaf tissue will inevitably lead to changes in the dynamic state of the adenylate pools during the preparation stage, rendering the results useless. One possibility might be attempting to resolve chloroplast ATP levels *in vivo* using ^{31}P NMR. This has been achieved with mitochondria in excised maize root tips (Roberts et al. 1984), but this approach has not been developed for routine analysis, and it is not clear how this could be achieved for an attached illuminated leaf. Further work is required to confirm the role of ATP levels on \mathbf{A}_{sat} in heat stressed attached leaves; particular attention could be given to resolving ATP biosynthesis and ATP consumption as both processes would lead to a change in the dynamic state of ATP/ADP ratios.

In a previous PhD study at Glasgow University no evidence was found for genotypic differences between C3 or C4 cereal crops and landraces that have been developed in tropical / sub-tropical and temperate latitudes. In all cases when \mathbf{T}_{leaf} rose above 38°C for an hours or more, \mathbf{A}_{sat} was severely and irreversibly inhibited (AlMalki 2014). None-the-less, there are endemic plants (agave, cactus, etc.,) which thrive in arid regions of the world that can tolerate \mathbf{T}_{leaf} of over 50°C . It is conceivable the photosynthetic apparatus in these species is inherently more tolerant of heat stress, and this opens the prospect of biongenieering these homologous proteins into cereal crops. The finding of the recent work on heat stress on barley undertaken at

Glasgow University has not identified specific proteins that cause thermal stress and so a transgenic approach to improve thermal tolerance in crops seems unlikely at present.

One possible cause for the remarkable thermal tolerance of the photosynthetic processes in plants such as agave is the presence of powerful repair mechanisms. This is generally attributable to Heat Shock Proteins (HSP) and an in-depth study of these in heat tolerant plants might be illuminating. For example, cotton (a moderately heat tolerant plant) shows a high induction of heat and thermal tolerance HSPs (Zhang et al. 2016). These include the accumulation of GHSP26, HSP101, HSC70 and HSFA but details of their exact role is sketchy. In barley HSP90, HSP70, HSP26 and the small HSPs (sHSP) have been implicated in refolding heat denatured proteins back to their functional forms. A full and detailed comparison at the level of the proteome of the HSP systems in heat tolerant and sensitive plants now seems timely.

The experiments reported in chapters 4 and 5 offer an opportunity for increasing cereal crop yields. These experiments provide a framework for more detailed time-series analyses on the changes in the transcriptome profiles of floral meristems from High and Moderate N-supply grown plants. These may provide some insight into how plant nitrogen status suppresses flower development and opens up the prospect of manipulating elite lines to produce higher yields in response to nitrogen applications. The effects of high N supply on the growth and development of spring barley requires further investigation. One avenue is to better understand the role of N-supply on tillering; tillers are nitrogen sinks and as such, are likely to reduce the

protein levels (and photosynthesis rates) in the main stem. Manipulation of tiller number (resource sinks) might lead to higher photosynthesis rates and higher yields. To address this, attempts were made to control tiller numbers by surgical removal with a scalpel, but problems with infection were encountered. Repeating these experiments under sterile or semi-sterile conditions may allow these experiments to be completed; cauterising scar tissue with dental wax might also work. Another approach that was attempted was the use of Uniculm mutants. Seeds from three Bowman lines that produce low tillers were procured and grown, but their inherently low fertility (2-3 seeds per plant per generation) has seriously hampered these experiments (approximately 100 seedlings will be required to undertake a full set of experiments over the full range of N-supply). Bulking up these seed may take six or seven harvests, but these experiments are underway. Another approach is to attempt to identify unicum mutants that have normal levels of fertility.

Manipulating the resource sink strength may boost protein levels in the main stem and result in increased photosynthesis rates, but this is unlikely to result in improved yields due to an increased suppression of flowering. The transcriptome profiling experiments reported in this study have identified a number of sequences in floral primordia meristems whose abundance is either highly increased or decreased in response to N-supply. What is not known at this stage are the molecular mechanisms that regulate these changes. The undifferentiated crown meristem produces leaf primordia; with increasing N-supply the meristem splits to generate two-or-more vegetative primordia that go on to produce tillers. When the signal to flower (VRN3) is translocated from the leaves to the crown, the vegetative meristems undergo a transition to the floral meristem. What is poorly understood

are the molecular mechanisms that regulate these changes; unravelling these mechanisms will provide a framework for controlling tillering at low nitrogen, whilst maintaining flowering at high nitrogen. The experiments reported here have provided some information on the role of N-supply on the suppression of flowering at the 2-3 node spike stage. What is now required are time-series transcriptome experiment over a range of N-supply, the results should allow models of vegetative and floral meristem development to be constructed for subsequent testing using classical loss-of-function and gain-of-function mutational analysis.

Undoubtedly, plant growth regulators (or hormones) will be involved in regulation of vegetative and reproductive stages in barley but these were not examined in this project. The roles of these hormones (which include auxins, cytokinins, and gibberellins) and their interaction with nitrogen require further study. The assessment of the concentrations of these compounds in tissues, however, is not trivial and few laboratories can perform these analyses with routine precision. Normally, ultra high performance liquid chromatography coupled with tandem mass spectrometry (UPLC-MS/MS) is required, along with experienced operators. To provide a full understanding of the role of these growth regulators on the development of the crown meristem, and understanding of the changes in the activity of the receptors, as well as changes in concentration of the hormones, will be required.

Appendixes

Appendix A-1. General Linear Model: Asat versus Temperature, Light Fig 3-1

Factor	Type	Levels	Values
Temp	fixed	6	25, 35, 36, 37, 38, 40
Light	fixed	2	Dark, Light

Analysis of Variance for AsatDat, using Adjusted SS for Tests

Source	DF	Seq SS	Adj SS	Adj MS	F	P
Temp	5	536.99	518.20	103.64	5.25	0.000
Light	1	0.59	0.00	0.00	0.00	0.989
Temp*Light	5	19.35	19.35	3.87	0.20	0.963
Error	61	1204.84	1204.84	19.75		
Total	72	1761.77				

S = 4.44427 R-Sq = 31.61% R-Sq(adj) = 19.28%

Grouping Information Using Tukey Method and 95.0% Confidence

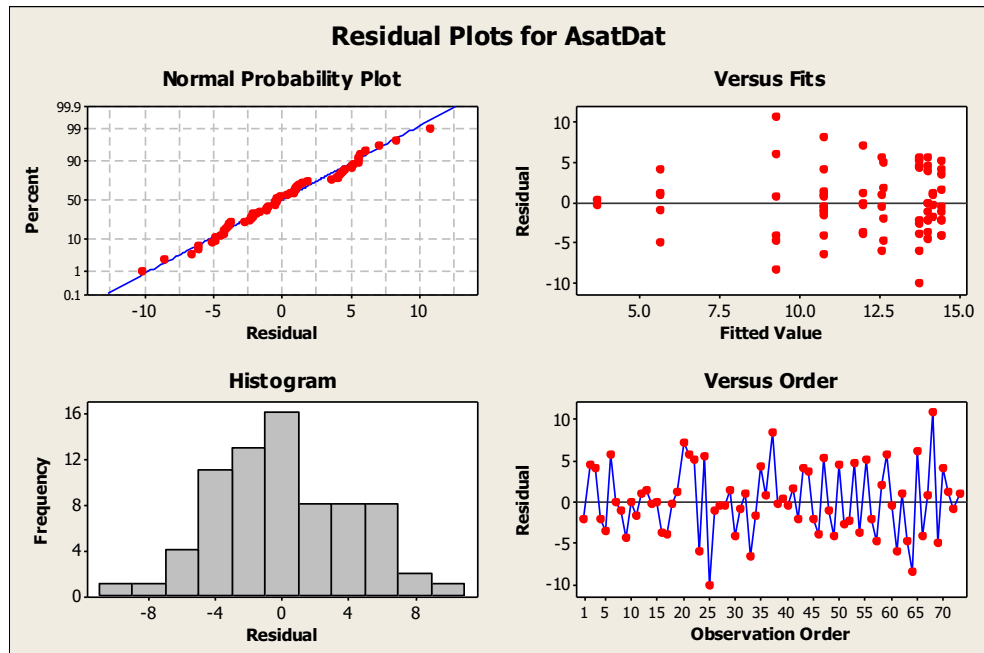
Temp	N	Mean	Grouping
25	20	14.2	A
35	9	13.9	A
37	9	13.1	A
36	10	12.3	A
38	18	10.0	A B
40	7	4.6	B

Means that do not share a letter are significantly different.

Grouping Information Using Tukey Method and 95.0% Confidence

Light	N	Mean	Grouping
Light	39	11.4	A
Temp	34	11.4	A

Means that do not share a letter are significantly different.



Appendix A-2 ETR vs Temp

Fig 3-2

General Linear Model: ETR Percent_1 versus ETRTemp1

Factor	Type	Levels	Values
ETRTemp1	fixed	5	25, 36, 37, 38, 40

Analysis of Variance for ETR Percent_1, using Adjusted SS for Tests

Source	DF	Seq SS	Adj SS	Adj MS	F	P
ETRTemp1	4	49133	49133	12283	46.15	0.000
Error	54	14373	14373	266		
Total	58	63506				

S = 16.3143 R-Sq = 77.37% R-Sq(adj) = 75.69%

Unusual Observations for ETR Percent_1

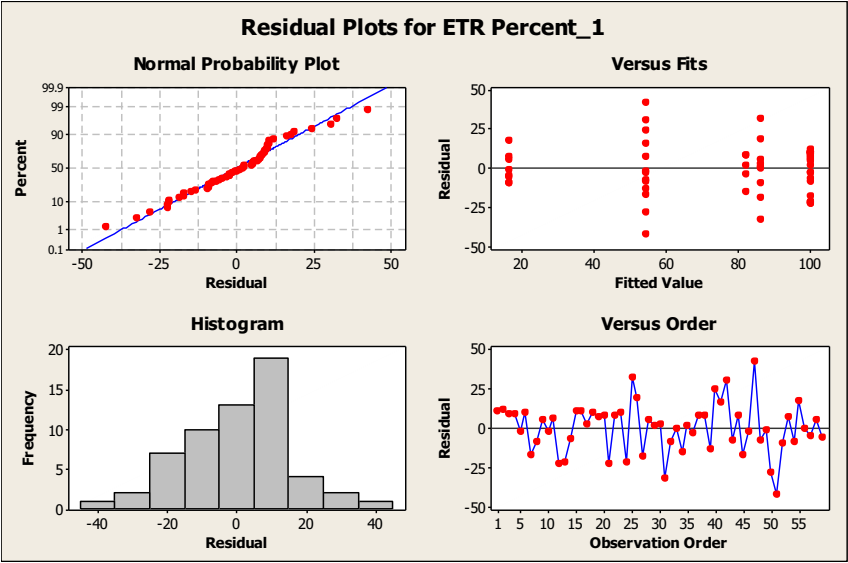
ETR						
Obs	Percent_1	Fit	SE Fit	Residual	St Resid	
25	118.397	86.098	5.438	32.299	2.10	R
31	53.511	86.098	5.438	-32.587	-2.12	R
47	97.138	54.547	4.525	42.591	2.72	R
51	11.916	54.547	4.525	-42.631	-2.72	R

R denotes an observation with a large standardized residual.

Grouping Information Using Tukey Method and 99.9% Confidence

ETRTemp1	N	Mean	Grouping
25	24	100.0	A
36	9	86.1	A
37	5	82.2	A B
38	13	54.5	B
40	8	16.6	C

Means that do not share a letter are significantly different.



Appendix A-3. General Linear Model: Log A_{sat} versus Temperature, Oxygen

Fig 3-7

Factor	Type	Levels	Values
PResTemp	fixed	4	25, 36, 38, 40
PResOxygen	fixed	2	1, 21

Analysis of Variance for LogPResDat, using Adjusted SS for Tests

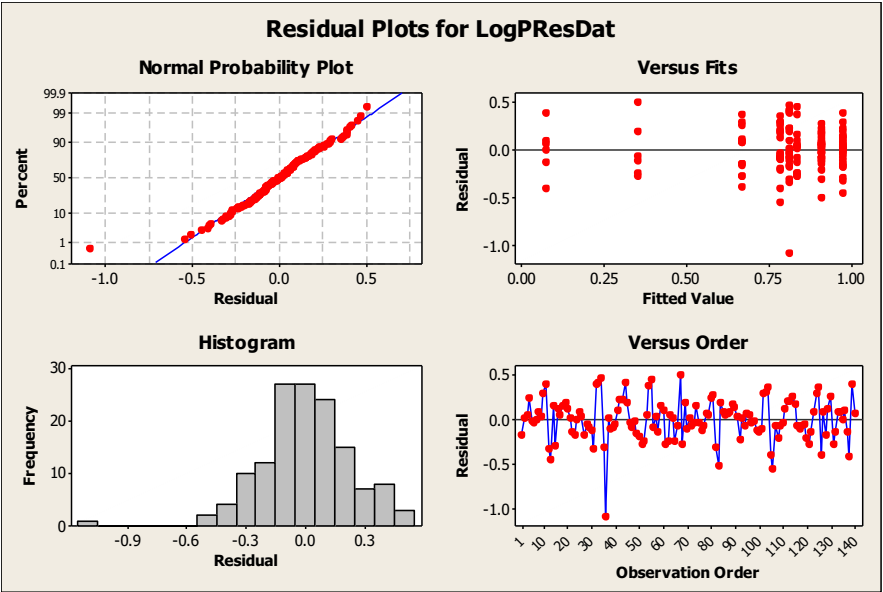
Source	DF	Seq SS	Adj SS	Adj MS	F	P
PResTemp	3	5.44767	5.44767	1.81589	32.92	0.000
PResOxygen	1	0.29512	0.44024	0.44024	7.98	0.005
PResTemp*PResOxygen	3	0.19265	0.19265	0.06422	1.16	0.326
Error	132	7.28226	7.28226	0.05517		
Total	139	13.21770				

S = 0.234880 R-Sq = 44.91% R-Sq(adj) = 41.98%

Grouping Information Using Tukey Method and 95.0% Confidence

PResTemp	PResOxygen	N	Mean	Grouping
25	1	30	1.0	A
25	21	30	0.9	A
38	1	14	0.8	A B
36	1	20	0.8	A B
36	21	20	0.8	A B
38	21	14	0.7	B C
40	1	6	0.4	C D
40	21	6	0.1	D

Means that do not share a letter are significantly different.



Appendix A-4. General Linear Model: LogATPLight versus

Fig 3-8

Factor Type Levels Values

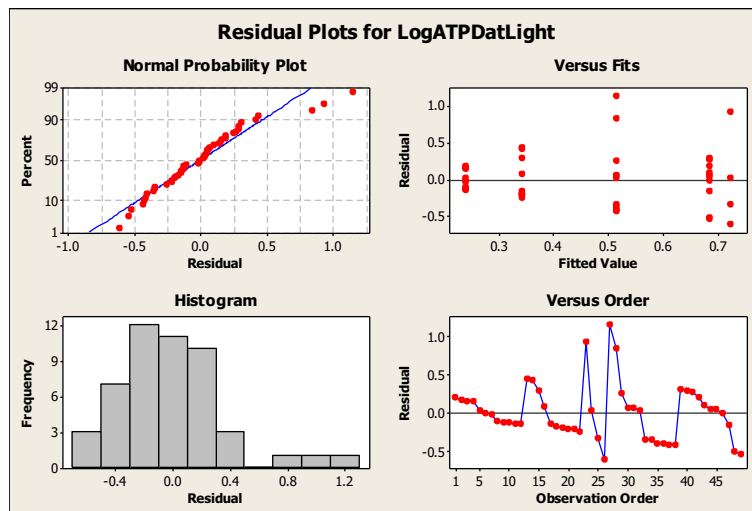
Covariance

Analysis of Variance for LogATPDatLight, using Adjusted SS for Tests

Source	DF	Seq SS	Adj SS	Adj MS	F	P
ATPTempLight	1	1.0900	1.0900	1.0900	7.63	0.008
Error	47	6.7112	6.7112	0.1428		
Total	48	7.8012				

S = 0.377878 R-Sq = 13.97% R-Sq(adj) = 12.14%

Term	Coef	SE Coef	T	P
Constant	-0.4383	0.3323	-1.32	0.194
ATPTempLight	0.026048	0.009428	2.76	0.008



General Linear Model: ATPDatDark versus ATPTempDark

Fig 3-8

Factor	Type	Levels	Values
ATPTempDark	fixed	5	25, 36, 37, 38, 40

Analysis of Variance for ATPDatDark, using Adjusted SS for Tests

Source	DF	Seq SS	Adj SS	Adj MS	F	P
ATPTempDark	4	2556.81	2556.81	639.20	7.05	0.000
Error	41	3717.99	3717.99	90.68		
Total	45	6274.80				

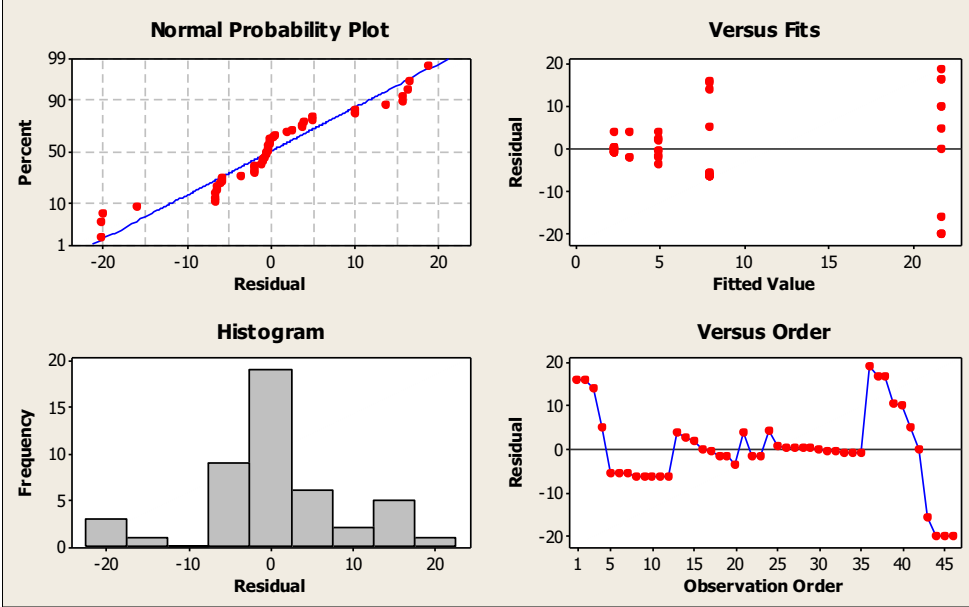
S = 9.52274 R-Sq = 40.75% R-Sq(adj) = 34.97%

Grouping Information Using Tukey Method and 95.0% Confidence

ATPTempDark	N	Mean	Grouping
40	11	21.6	A
25	12	7.9	B
36	8	4.8	B
37	3	3.2	B
38	12	2.3	B

Means that do not share a letter are significantly different.

Residual Plots for ATPDatDark



Appendix A-5. General Linear Model: Asat versus Temperature

Fig. 3-9

Factor	Type	Levels	Values
Temperature	fixed	9	25, 35, 37, 38, 39, 40, 41, 42, 43

Analysis of Variance for Asat, using Adjusted SS for Tests

Source	DF	Seq SS	Adj SS	Adj MS	F	P
Temperature	8	2110.76	2110.76	263.84	25.69	0.000
Error	87	893.52	893.52	10.27		
Total	95	3004.28				

S = 3.20474 R-Sq = 70.26% R-Sq(adj) = 67.52%

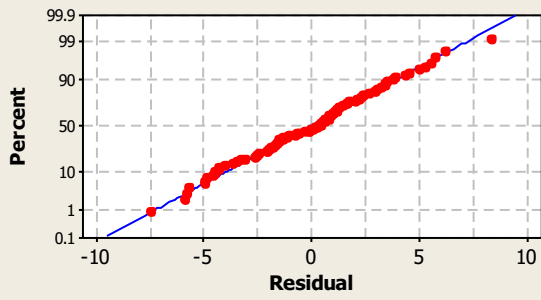
Grouping Information Using Tukey Method and 95.0% Confidence

Temperature	N	Mean	Grouping
25	12	16.4	A
35	5	15.5	A
38	3	14.9	A B
37	6	13.6	A B
39	11	13.1	A B
40	12	9.6	B C
41	20	7.3	C D
42	19	4.8	D E
43	8	1.5	E

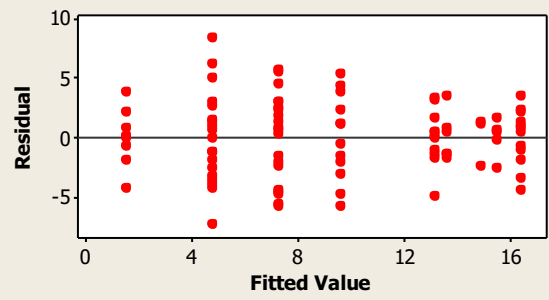
Means that do not share a letter are significantly different.

Residual Plots for Asat

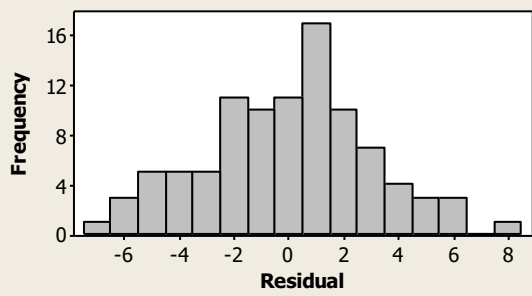
Normal Probability Plot



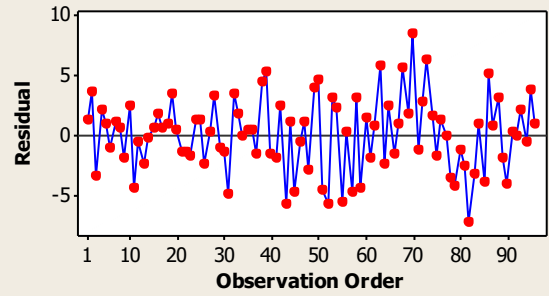
Versus Fits



Histogram



Versus Order



General Linear Model: LogStomata versus Temperature

Fig 3-9

Factor	Type	Levels	Values
Temperature	fixed	9	25, 35, 37, 38, 39, 40, 41, 42, 43

Analysis of Variance for LogStomata, using Adjusted SS for Tests

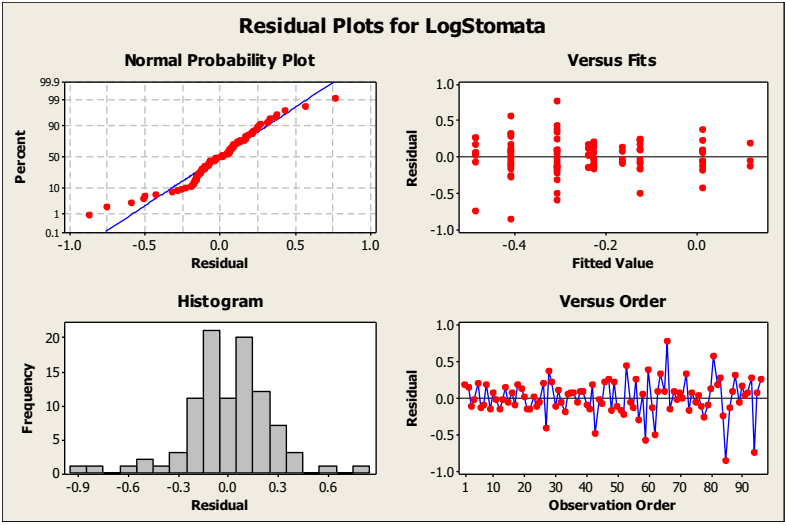
Source	DF	Seq SS	Adj SS	Adj MS	F	P
Temperature	8	2.37662	2.37662	0.29708	4.48	0.000
Error	87	5.77101	5.77101	0.06633		
Total	95	8.14763				

S = 0.257553 R-Sq = 29.17% R-Sq(adj) = 22.66%

Grouping Information Using Tukey Method and 95.0% Confidence

Temperature	N	Mean	Grouping
38	3	0.1	A
39	11	0.0	A
40	12	-0.1	A B
35	5	-0.2	A B
25	12	-0.2	A B
37	6	-0.2	A B
41	20	-0.3	A B
42	19	-0.4	B
43	8	-0.5	B

Means that do not share a letter are significantly different.



Appendix A-6. General Linear Model: Asat_2 versus N supply_2

Fig 4-3

Factor	Type	Levels	Values
N supply_2	fixed	6	0.08, 0.16, 0.32, 0.80, 1.60, 16.00

Analysis of Variance for Asat_2, using Adjusted SS for Tests

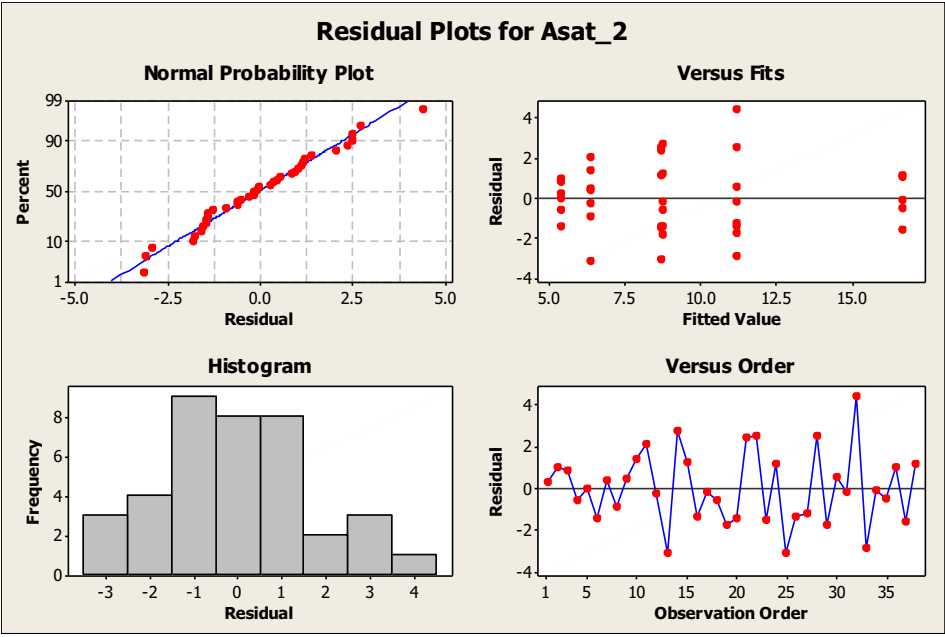
Source	DF	Seq SS	Adj SS	Adj MS	F	P
N supply_2	5	464.360	464.360	92.872	27.07	0.000
Error	32	109.791	109.791	3.431		
Total	37	574.151				

S = 1.85229 R-Sq = 80.88% R-Sq(adj) = 77.89%

Grouping Information Using Tukey Method and 95.0% Confidence

N supply_2	N	Mean	Grouping
16.00	5	16.7	A
1.60	8	11.2	B
0.32	6	8.7	B C
0.80	6	8.7	B C
0.16	7	6.3	C D
0.08	6	5.3	D

Means that do not share a letter are significantly different.



General Linear Model: Phi_2 versus N supply_2

Fig 4-3

Factor	Type	Levels	Values
N supply_2	fixed	6	0.08, 0.16, 0.32, 0.80, 1.60, 16.00

Analysis of Variance for Phi_2, using Adjusted SS for Tests

Source	DF	Seq SS	Adj SS	Adj MS	F	P
N supply_2	5	0.0093853	0.0093853	0.0018771	23.34	0.000
Error	32	0.0025736	0.0025736	0.0000804		
Total	37	0.0119588				

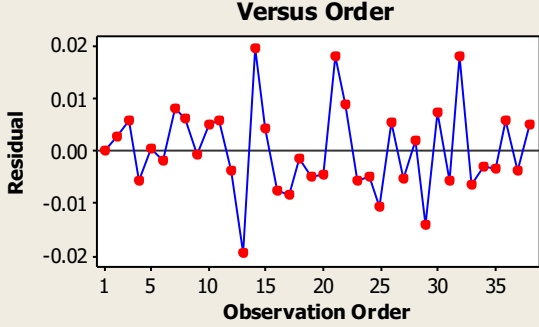
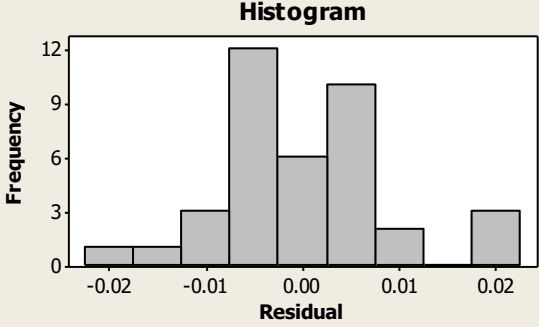
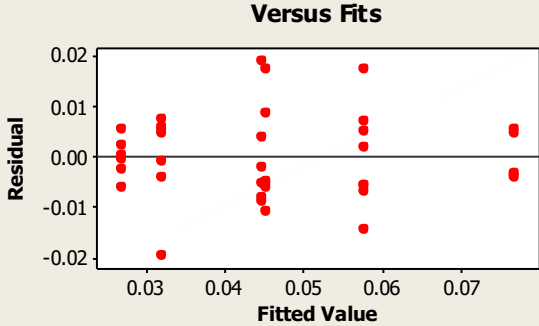
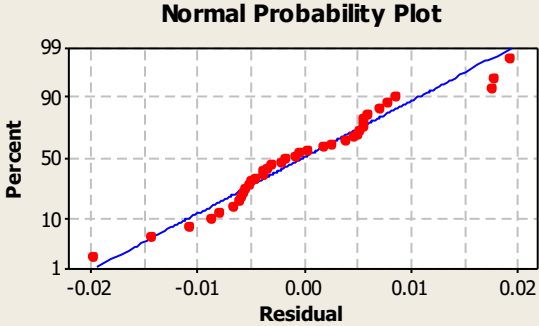
S = 0.00896799 R-Sq = 78.48% R-Sq(adj) = 75.12%

Grouping Information Using Tukey Method and 95.0% Confidence

N supply_2	N	Mean	Grouping
16.00	5	0.1	A
1.60	8	0.1	B
0.80	6	0.0	B C
0.32	6	0.0	B C
0.16	7	0.0	C D
0.08	6	0.0	D

Means that do not share a letter are significantly different.

Residual Plots for Phi_2



Appendix A-7. General Linear Model: Asat_1 versus N supply_1

Fig 4-4

Factor	Type	Levels	Values
N supply_1	fixed	6	0.08, 0.16, 0.32, 0.64, 3.20, 16.00

Analysis of Variance for Asat_1, using Adjusted SS for Tests

Source	DF	Seq SS	Adj SS	Adj MS	F	P
N supply_1	5	760.05	760.05	152.01	6.64	0.000
Error	40	915.05	915.05	22.88		
Total	45	1675.10				

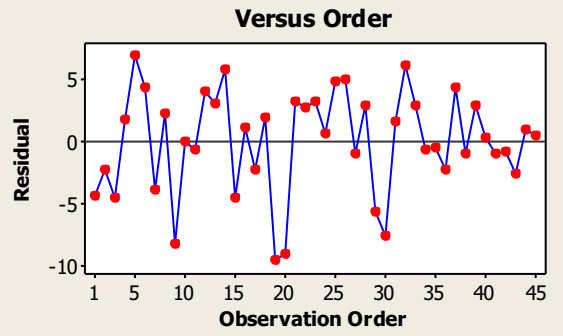
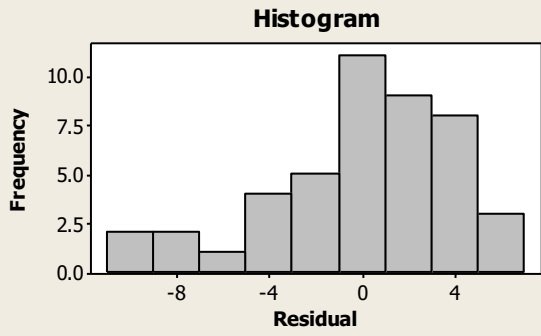
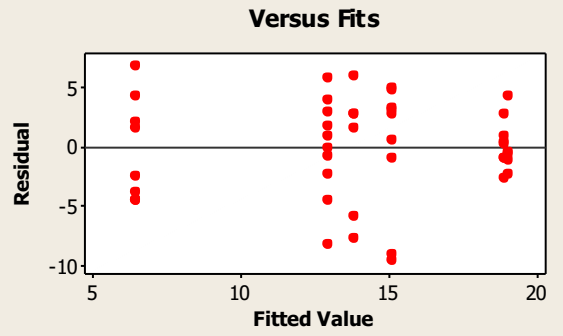
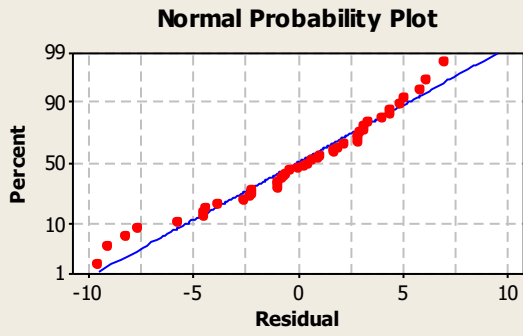
S = 4.78291 R-Sq = 45.37% R-Sq(adj) = 38.54%

Grouping Information Using Tukey Method and 95.0% Confidence

N supply_1	N	Mean	Grouping
3.20	5	19.0	A
16.00	7	18.9	A
0.64	6	13.8	A B
0.32	10	13.7	A B
0.16	10	12.9	A B
0.08	8	6.4	B

Means that do not share a letter are significantly different.

Residual Plots for Asat_1



General Linear Model: Phi_1 versus N supply_1

Fig 4-4

Factor	Type	Levels	Values
N supply_1	fixed	6	0.08, 0.16, 0.32, 0.64, 3.20, 16.00

Analysis of Variance for Phi_1, using Adjusted SS for Tests

Source	DF	Seq SS	Adj SS	Adj MS	F	P
N supply_1	5	0.0329317	0.0329317	0.0065863	9.24	0.000
Error	40	0.0285050	0.0285050	0.0007126		
Total	45	0.0614367				

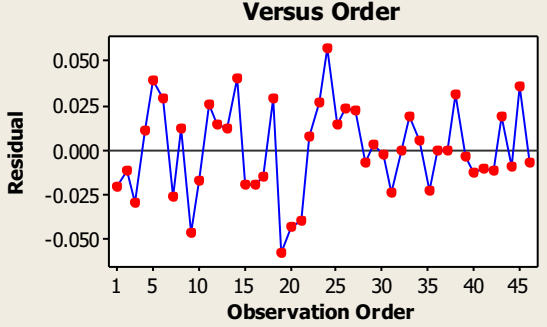
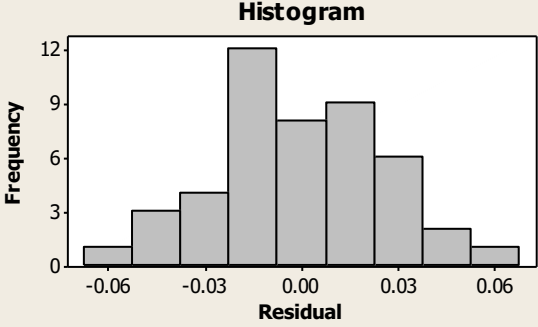
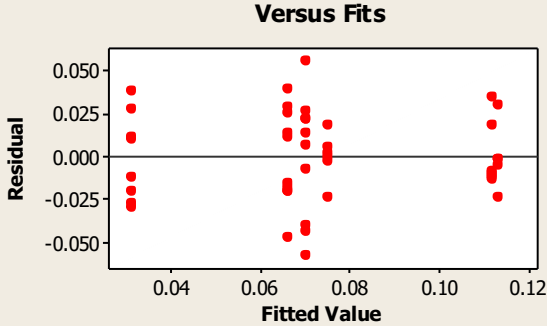
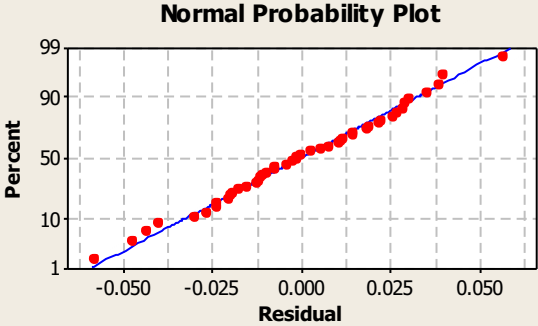
S = 0.0266950 R-Sq = 53.60% R-Sq(adj) = 47.80%

Grouping Information Using Tukey Method and 95.0% Confidence

N supply_1	N	Mean	Grouping
3.20	5	0.1	A
16.00	7	0.1	A
0.64	6	0.1	A B
0.32	10	0.1	A B
0.16	10	0.1	B C
0.08	8	0.0	C

Means that do not share a letter are significantly different.

Residual Plots for Phi_1



Appendix A-8. General Linear Model: ETR versus ETR N

Fig 4-5

Factor	Type	Levels	Values
ETR N	fixed	6	0.08, 0.16, 0.80, 1.60, 3.20, 16.00

Analysis of Variance for ETR, using Adjusted SS for Tests

Source	DF	Seq SS	Adj SS	Adj MS	F	P
ETR N	5	16029.9	16029.9	3206.0	26.49	0.000
Error	25	3026.0	3026.0	121.0		
Total	30	19055.8				

S = 11.0018 R-Sq = 84.12% R-Sq(adj) = 80.94%

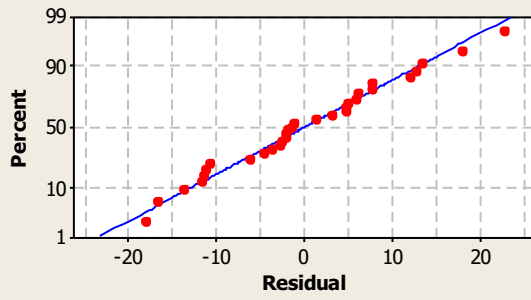
Grouping Information Using Tukey Method and 95.0% Confidence

ETR N	N	Mean	Grouping
16.00	4	123.0	A
1.60	5	93.4	B
3.20	4	93.3	B
0.80	8	81.3	B
0.16	5	53.9	C
0.08	5	53.0	C

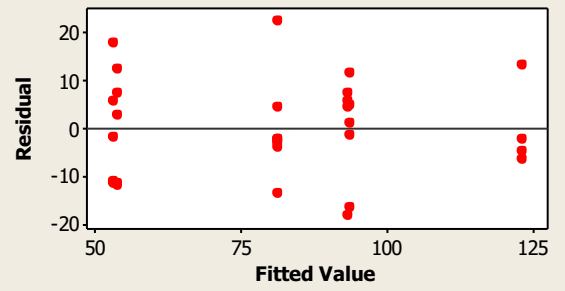
Means that do not share a letter are significantly different.

Residual Plots for ETR

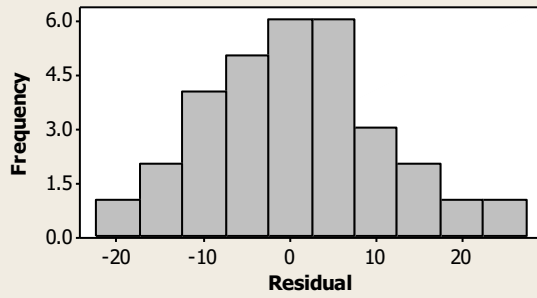
Normal Probability Plot



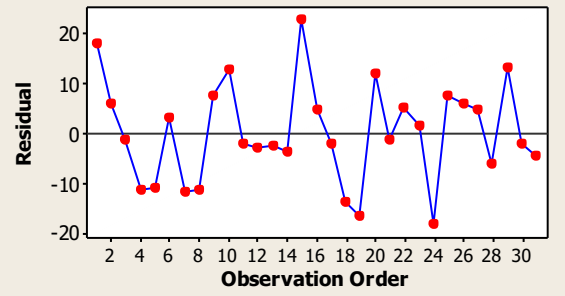
Versus Fits



Histogram



Versus Order



Appendix A-9. General Linear Model: Leaves/tiller versus nitrogen addition
Fig 4-7 A

Factor	Type	Levels	Values
nitrogen addition	fixed	5	0, 2, 10, 20, 47

Analysis of Variance for Leaves/tiller, using Adjusted SS for Tests

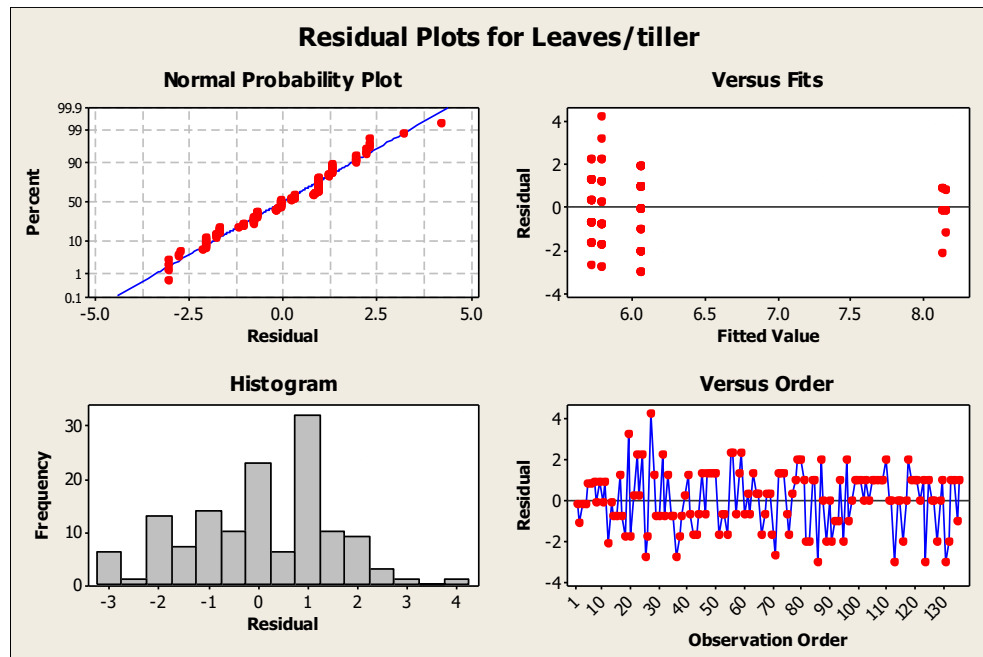
Source	DF	Seq SS	Adj SS	Adj MS	F	P
nitrogen addition	4	63.624	63.624	15.906	7.52	0.000
Error	131	276.934	276.934	2.114		
Total	135	340.559				

S = 1.45396 R-Sq = 18.68% R-Sq(adj) = 16.20%

Grouping Information Using Tukey Method and 95.0% Confidence

nitrogen			
addition	N	Mean	Grouping
0	6	8.2	A
2	7	8.1	A
47	59	6.1	B
10	27	5.8	B
20	37	5.7	B

Means that do not share a letter are significantly different.



Kruskal-Wallis Test: Leaves/tiller versus nitrogen addition

Kruskal-Wallis Test on Leaves/tiller

nitrogen

addition	N	Median	Ave Rank	Z
0	6	8.000	119.8	3.26
2	7	8.000	117.2	3.36
10	27	5.000	59.4	-1.35
20	37	6.000	58.3	-1.84
47	59	6.000	68.1	-0.11
Overall	136		68.5	

H = 24.81 DF = 4 P = 0.000

General Linear Model: Leaves/Tiller2 versus L/T2 N Level

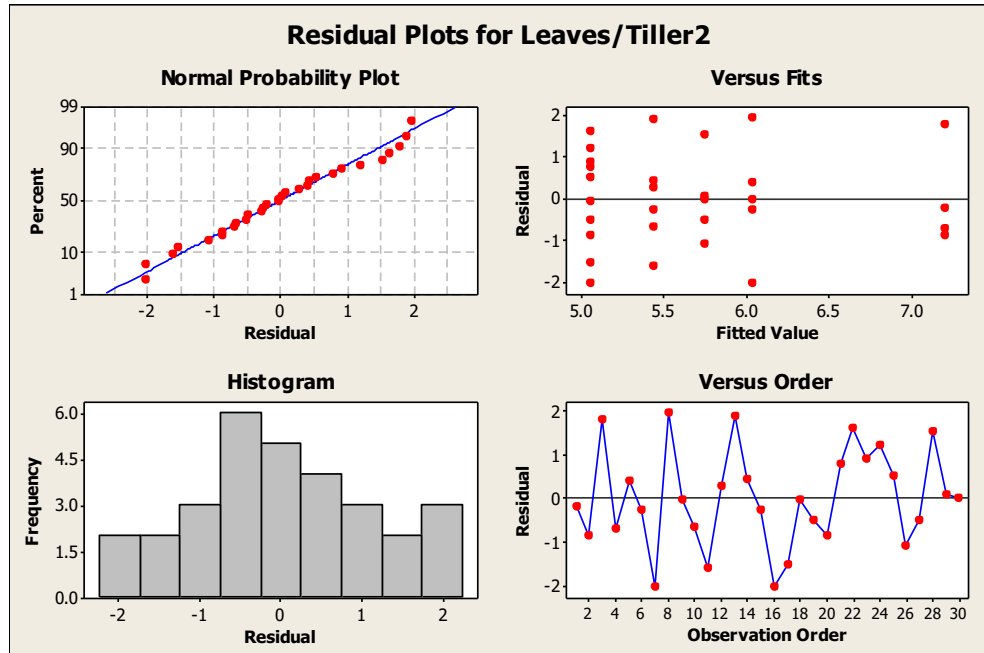
Fig 4-7 B

Factor	Type	Levels	Values
L/T2 N Level	fixed	5	0.08, 0.16, 0.64, 3.20, 16.00

Analysis of Variance for Leaves/Tiller2, using Adjusted SS for Tests

Source	DF	Seq SS	Adj SS	Adj MS	F	P
L/T2 N Level	4	14.402	14.402	3.601	2.43	0.074
Error	25	37.003	37.003	1.480		
Total	29	51.405				

S = 1.21660 R-Sq = 28.02% R-Sq(adj) = 16.50%



Kruskal-Wallis Test: Leaves/Tiller2 versus L/T2 N Level

Kruskal-Wallis Test on Leaves/Tiller2

L/T2 N Level	N	Median	Ave Rank	Z

0.08	4	6.750	25.5	2.44
0.16	5	6.000	18.2	0.75
0.64	6	5.429	13.3	-0.67
3.20	10	5.281	11.7	-1.67
16.00	5	5.738	15.0	-0.14
Overall	30		15.5	

H = 7.87 DF = 4 P = 0.096

Appendix A-10. General Linear Model: Tiller/ plant_1 versus T/P 1 N

Fig 4-8 A

Factor	Type	Levels	Values
T/P 1 N	fixed	5	0, 2, 10, 20, 47

Analysis of Variance for Tiller/ plant_1, using Adjusted SS for Tests

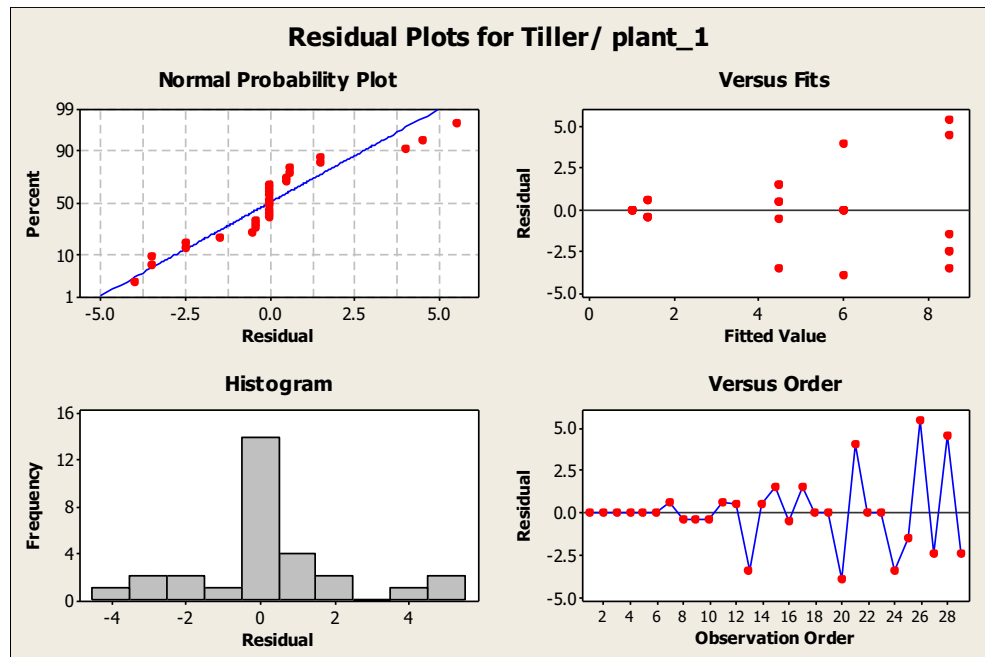
Source	DF	Seq SS	Adj SS	Adj MS	F	P
T/P 1 N	4	230.628	230.628	57.657	10.79	0.000
Error	24	128.200	128.200	5.342		
Total	28	358.828				

S = 2.31120 R-Sq = 64.27% R-Sq(adj) = 58.32%

Grouping Information Using Tukey Method and 95.0% Confidence

T/P	N	Mean	Grouping
1 N	6	8.5	A
47	6	6.0	A B
20	6	4.5	B C
10	6	1.4	C
2	5	1.0	C
0	6		

Means that do not share a letter are significantly different.



Kruskal-Wallis Test: Tiller/ plant_1 versus T/P 1 N

Kruskal-Wallis Test on Tiller/ plant_1

T/P 1 N	N	Median	Ave Rank	Z
0	6	1.000	5.5	-3.07
2	5	1.000	8.1	-1.99
10	6	5.000	15.8	0.24
20	6	6.000	20.8	1.88
47	6	6.500	23.7	2.80
Overall	29		15.0	

H = 19.83 DF = 4 P = 0.001

H = 21.17 DF = 4 P = 0.000 (adjusted for ties)

General Linear Model: LogT/P 2 versus T/P N 2

Fig 4-8 B

Factor	Type	Levels	Values
T/P N 2	fixed	6	0.08, 0.16, 0.32, 0.80, 1.60, 16.00

Analysis of Variance for LogT/P 2, using Adjusted SS for Tests

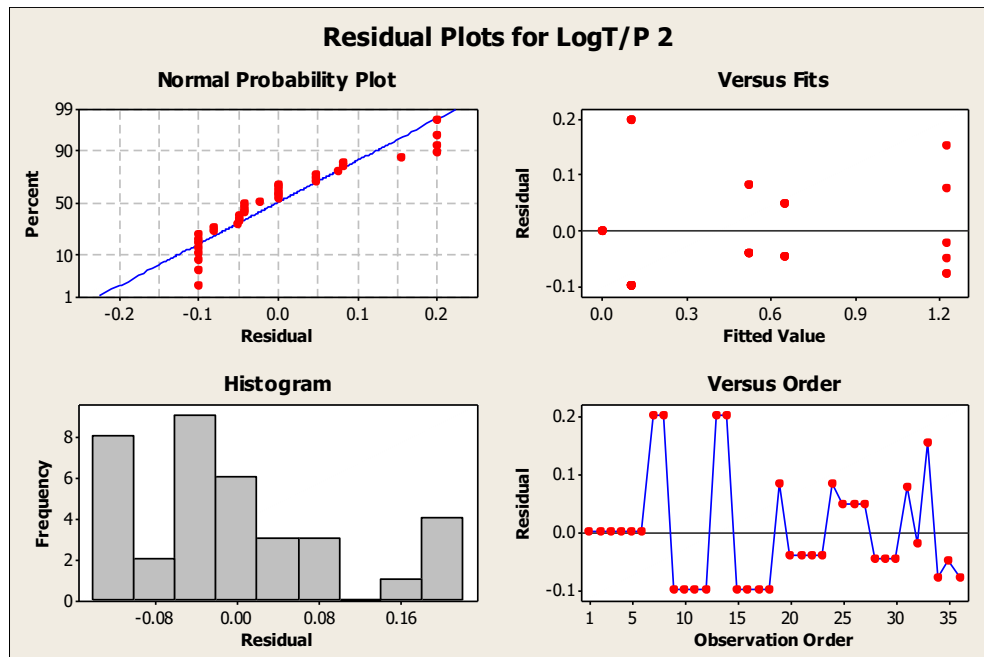
Source	DF	Seq SS	Adj SS	Adj MS	F	P
T/P N 2	5	6.5503	6.5503	1.3101	122.17	0.000
Error	30	0.3217	0.3217	0.0107		
Total	35	6.8720				

S = 0.103552 R-Sq = 95.32% R-Sq(adj) = 94.54%

Grouping Information Using Tukey Method and 95.0% Confidence

T/P N 2	N	Mean	Grouping
16.00	6	1.2	A
1.60	6	0.7	B
0.80	6	0.5	B
0.32	6	0.1	C
0.16	6	0.1	C
0.08	6	0.0	C

Means that do not share a letter are significantly different.



Kruskal-Wallis Test: Tiller/ plant_2 versus T/P N 2

Kruskal-Wallis Test on Tiller/ plant_2

T/P N 2	N	Median	Ave Rank	Z
0.08	6	1.000	7.5	-2.80
0.16	6	1.000	10.5	-2.04
0.32	6	1.000	10.5	-2.04
0.80	6	3.000	22.0	0.89
1.60	6	4.500	27.0	2.16
16.00	6	15.500	33.5	3.82
Overall	36		18.5	

H = 30.19 DF = 5 P = 0.000

General Linear Model: Tiller/ plant_3 versus T/P N 3

Fig 4-8 C

Factor	Type	Levels	Values
T/P N 3	fixed	5	0.08, 0.16, 0.64, 3.20, 16.00

Analysis of Variance for Tiller/ plant_3, using Adjusted SS for Tests

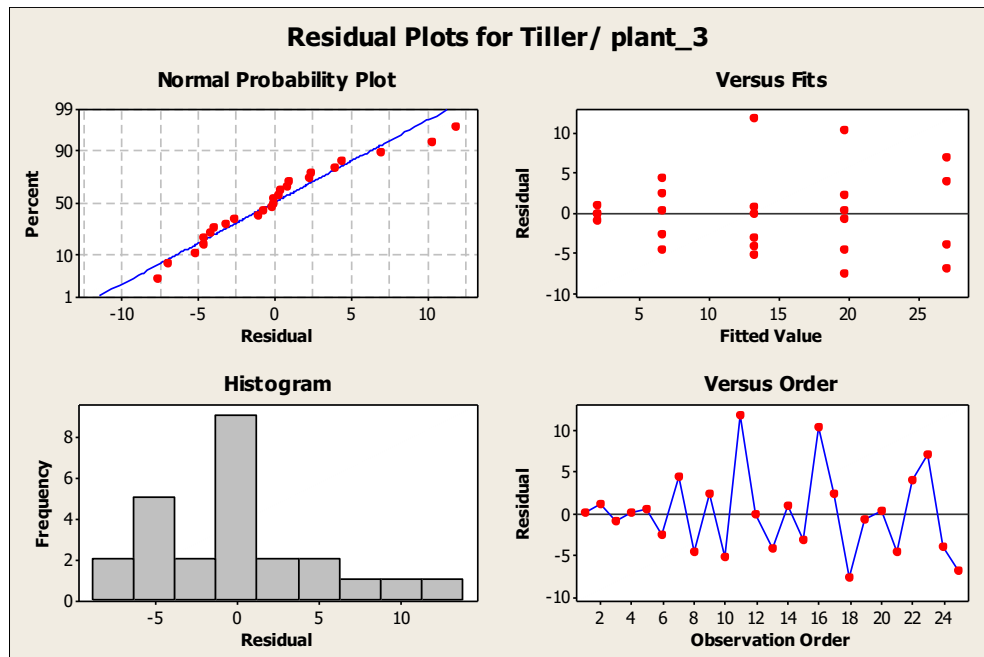
Source	DF	Seq SS	Adj SS	Adj MS	F	P
T/P N 3	4	1721.99	1721.99	430.50	15.02	0.000
Error	20	573.37	573.37	28.67		
Total	24	2295.36				

S = 5.35428 R-Sq = 75.02% R-Sq(adj) = 70.02%

Grouping Information Using Tukey Method and 95.0% Confidence

T/P N 3	N	Mean	Grouping
16.00	4	27.0	A
3.20	6	19.7	A B
0.64	6	13.2	B C
0.16	5	6.6	C D
0.08	4	2.0	D

Means that do not share a letter are significantly different.



Kruskal-Wallis Test: Tiller/ plant_3 versus T/P N 3

Kruskal-Wallis Test on Tiller/ plant_3

T/P N 3	N	Median	Ave Rank	Z
0.08	4	2.000	3.0	-2.96
0.16	5	7.000	7.5	-1.87
0.64	6	11.500	13.3	0.10
3.20	6	19.500	17.9	1.88
16.00	4	27.000	22.1	2.71
Overall	25		13.0	

H = 19.01 DF = 4 P = 0.001

H = 19.05 DF = 4 P = 0.001 (adjusted for ties)

Appendix A-11. General Linear Model: Spike versus Spike N

Fig 4-9

Factor	Type	Levels	Values
Spike N	fixed	8	0.08, 0.16, 0.32, 0.64, 0.80, 1.60, 3.20, 16.00

Analysis of Variance for Spike, using Adjusted SS for Tests

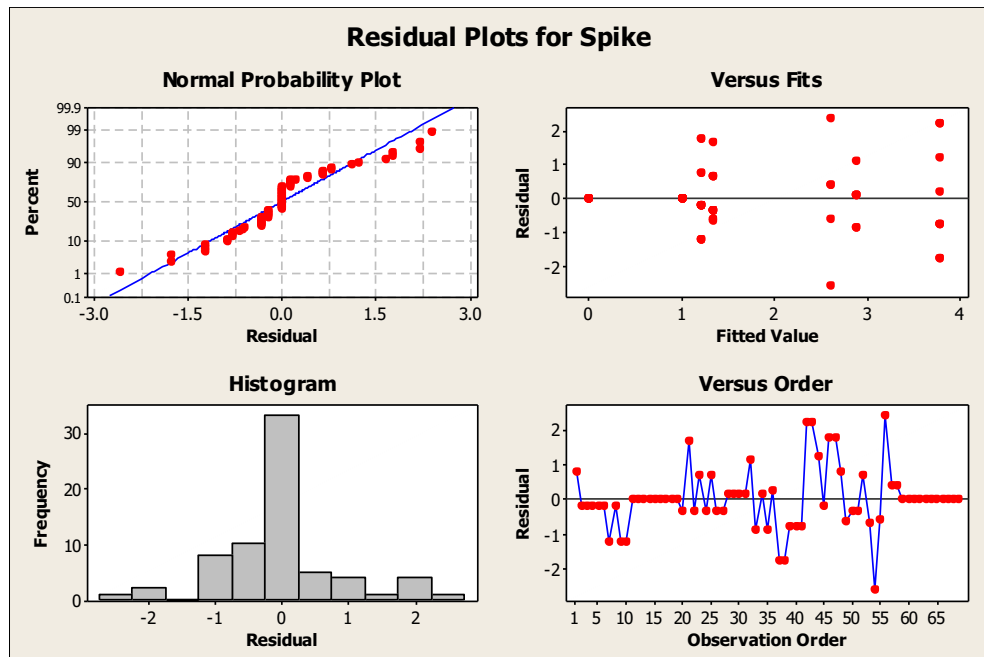
Source	DF	Seq SS	Adj SS	Adj MS	F	P
Spike N	7	94.943	94.943	13.563	15.41	0.000
Error	61	53.704	53.704	0.880		
Total	68	148.647				

S = 0.938294 R-Sq = 63.87% R-Sq(adj) = 59.73%

Grouping Information Using Tukey Method and 95.0% Confidence

Spike N	N	Mean	Grouping
1.60	9	3.8	A
0.80	8	2.9	A
0.64	5	2.6	A B
0.32	13	1.3	B C
0.08	14	1.2	B C
0.16	9	1.0	B C
16.00	5	0.0	C
3.20	6	-0.0	C

Means that do not share a letter are significantly different.



Kruskal-Wallis Test: Spike versus Spike N

Kruskal-Wallis Test on Spike

Spike N	N	Median	Ave Rank	Z
0.08	14	1.000000000	30.9	-0.87
0.16	9	1.000000000	29.0	-0.96
0.32	13	1.000000000	33.0	-0.39
0.64	5	3.000000000	46.8	1.37
0.80	8	3.000000000	55.1	3.01
1.60	9	3.000000000	58.9	3.83
3.20	6	0.000000000	8.0	-3.45
16.00	5	0.000000000	8.0	-3.12
Overall	69		35.0	

H = 43.94 DF = 7 P = 0.000

H = 46.59 DF = 7 P = 0.000 (adjusted for ties)

Appendix A-12. General Linear Model: Spike Length versus Spike Length N

Fig 4-10 A

Factor	Type	Levels	Values
Node Length N	fixed	5	0.08, 0.16, 0.64, 3.20, 16.00

Analysis of Variance for Spike Length, using Adjusted SS for Tests

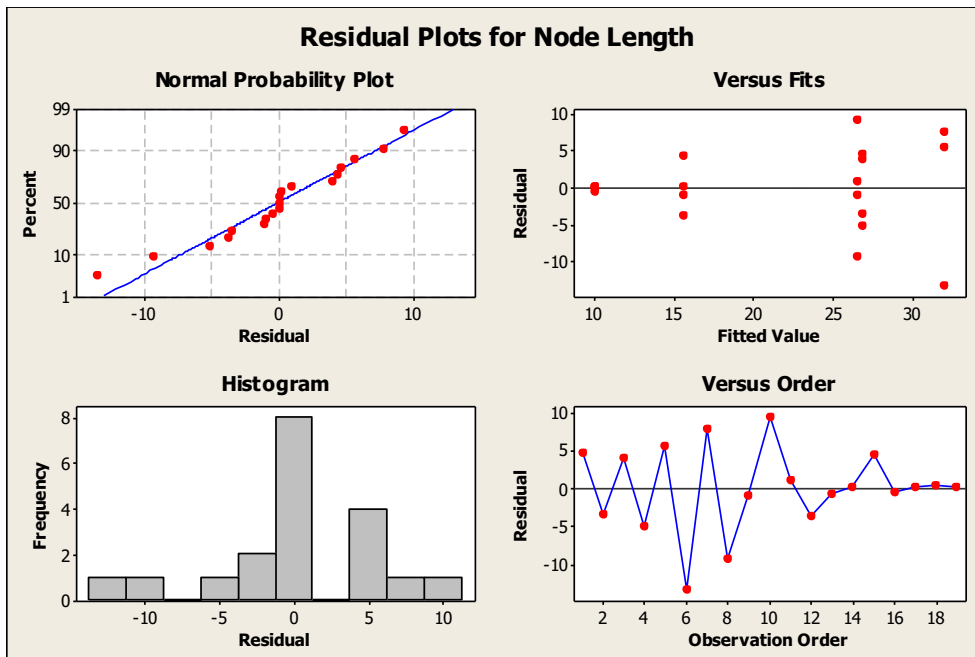
Source	DF	Seq SS	Adj SS	Adj MS	F	P
Spike Length N	4	1208.28	1208.28	302.07	7.59	0.002
Error	14	557.49	557.49	39.82		
Total	18	1765.77				

S = 6.31035 R-Sq = 68.43% R-Sq(adj) = 59.41%

Grouping Information Using Tukey Method and 95.0% Confidence

Node	Length N	N	Mean	Grouping
	0.16	3	32.0	A
	0.08	4	26.9	A B
	0.64	4	26.6	A B
	3.20	4	15.6	B C
	16.00	4	10.1	C

Means that do not share a letter are significantly different.



Kruskal-Wallis Test: Spike Length versus Spike Length N

Kruskal-Wallis Test on Spike Length

Spike

Length	N	Median	Ave Rank	Z
0.08	4	27.15	13.5	1.40
0.16	3	37.57	15.3	1.79
0.64	4	26.52	13.0	1.20
3.20	4	15.25	7.0	-1.20
16.00	4	10.16	2.5	-3.00
Overall	19		10.0	

H = 13.62 DF = 4 P = 0.009

General Linear Model: Num Nodes versus Num Node N

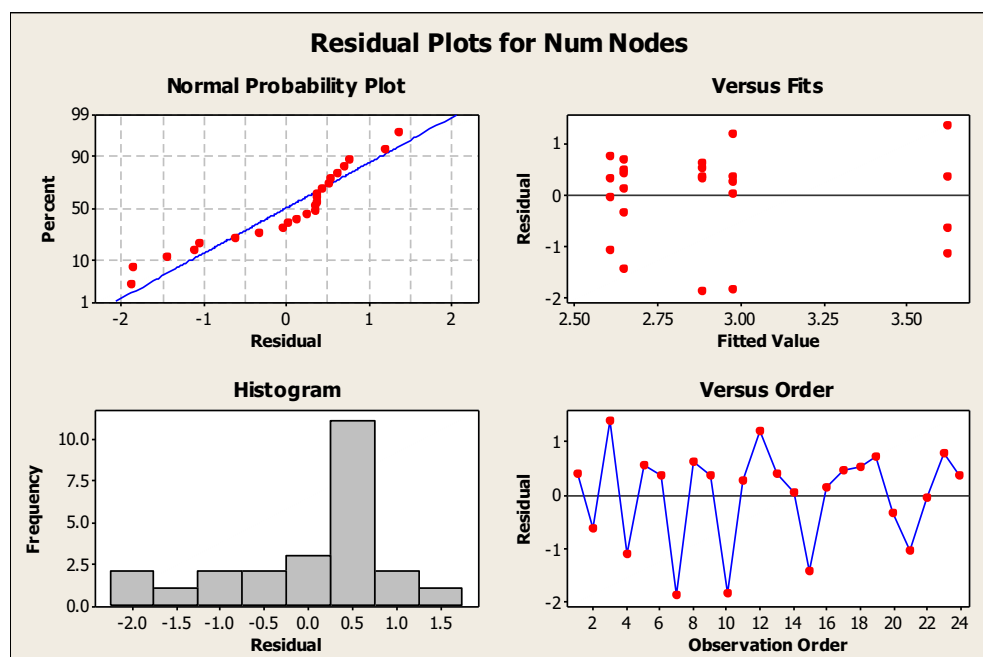
Fig 4-10 B

Factor	Type	Levels	Values
Num Node N	fixed	5	0.08, 0.16, 0.64, 3.20, 16.00

Analysis of Variance for Num Nodes, using Adjusted SS for Tests

Source	DF	Seq SS	Adj SS	Adj MS	F	P
Num Node N	4	2.8577	2.8577	0.7144	0.75	0.573
Error	19	18.2146	18.2146	0.9587		
Total	23	21.0723				

S = 0.979115 R-Sq = 13.56% R-Sq(adj) = 0.00%



Kruskal-Wallis Test: Num Nodes versus Num Node N

Kruskal-Wallis Test on Num Nodes

Num Node N	N	Median	Ave Rank	Z
0.08	4	3.500	15.6	0.97
0.16	5	3.250	14.4	0.68
0.64	5	3.231	13.7	0.43

3.20	6	2.928	9.7	-1.13
16.00	4	2.754	9.8	-0.85
Overall	24		12.5	

H = 2.85 DF = 4 P = 0.582

H = 2.86 DF = 4 P = 0.582 (adjusted for ties)

Appendix A-13. General Linear Model: Spike Length 2 versus Spike N 2

Fig 4-11 A

Factor	Type	Levels	Values
Spike N 2	fixed	5	0.08, 0.16, 0.64, 3.20, 16.00

Analysis of Variance for Spike Length 2, using Adjusted SS for Tests

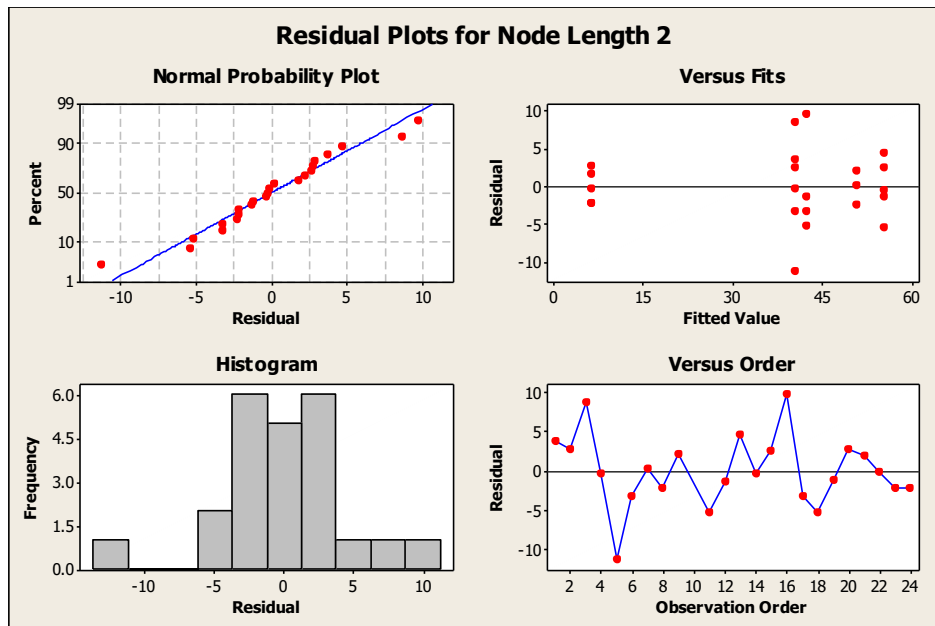
Source	DF	Seq SS	Adj SS	Adj MS	F	P
Spike N 2	4	7168.7	7168.7	1792.2	70.09	0.000
Error	18	460.3	460.3	25.6		
Total	22	7629.0				

S = 5.05662 R-Sq = 93.97% R-Sq(adj) = 92.63%

Grouping Information Using Tukey Method and 95.0% Confidence

Spike N 2	N	Mean	Grouping
0.64	5	55.4	A
0.16	3	50.8	A B
3.20	4	42.3	B
0.08	6	40.3	B
16.00	5	6.2	C

Means that do not share a letter are significantly different.



Kruskal-Wallis Test: Node Length 2 versus Node N 2

23 cases were used

Kruskal-Wallis Test on Spike Length 2

Spike N 2	N	Median	Ave Rank	Z
0.08	6	41.500	10.6	-0.60
0.16	3	51.000	16.7	1.28
0.64	5	55.000	20.4	3.13
3.20	4	40.000	11.4	-0.20
16.00	5	6.000	3.0	-3.35
Overall	23		12.0	

H = 18.19 DF = 4 P = 0.001

H = 18.21 DF = 4 P = 0.001 (adjusted for ties)

General Linear Model: Num Nodes 2 versus Node N 2

Fig 4-11 B

Factor	Type	Levels	Values
Node N 2	fixed	5	0.08, 0.16, 0.64, 3.20, 16.00

Analysis of Variance for Num Nodes 2, using Adjusted SS for Tests

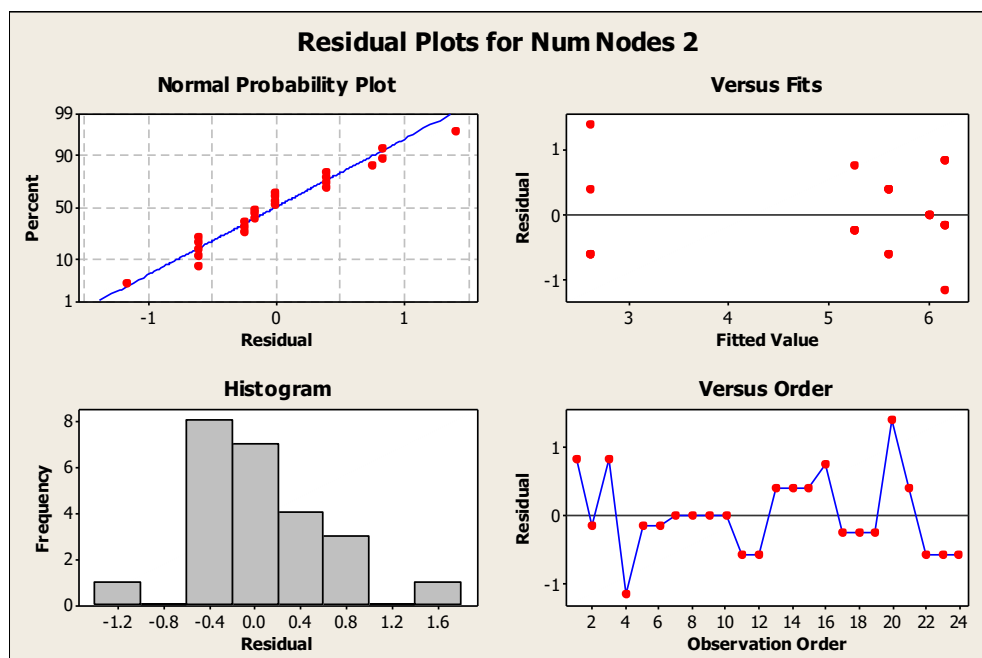
Source	DF	Seq SS	Adj SS	Adj MS	F	P
Node N 2	4	42.642	42.642	10.660	25.37	0.000
Error	19	7.983	7.983	0.420		
Total	23	50.625				

S = 0.648209 R-Sq = 84.23% R-Sq(adj) = 80.91%

Grouping Information Using Tukey Method and 95.0% Confidence

Node N 2	N	Mean	Grouping
0.08	6	6.2	A
0.16	4	6.0	A
0.64	5	5.6	A
3.20	4	5.3	A
16.00	5	2.6	B

Means that do not share a letter are significantly different.



Kruskal-Wallis Test: Num Nodes 2 versus Node N 2

Kruskal-Wallis Test on Num Nodes 2

Node N 2	N	Median	Ave Rank	Z
0.08	6	6.000	17.8	2.10
0.16	4	6.000	17.0	1.39
0.64	5	6.000	13.6	0.39
3.20	4	5.000	10.6	-0.58
16.00	5	2.000	3.0	-3.38
Overall	24		12.5	

H = 14.35 DF = 4 P = 0.006

H = 16.18 DF = 4 P = 0.003 (adjusted for ties)

Appendix A-14. General Linear Model: 1000 g wt Soil versus Grain N Soil
Fig 4-12 A

Factor	Type	Levels	Values
Grain N Soil	fixed	5	0, 2, 10, 20, 47

Analysis of Variance for 1000 g wt Soil, using Adjusted SS for Tests

Source	DF	Seq SS	Adj SS	Adj MS	F	P
Grain N Soil	4	11985.0	11985.0	2996.2	99.08	0.000
Error	25	756.0	756.0	30.2		
Total	29	12740.9				

S = 5.49903 R-Sq = 94.07% R-Sq(adj) = 93.12%

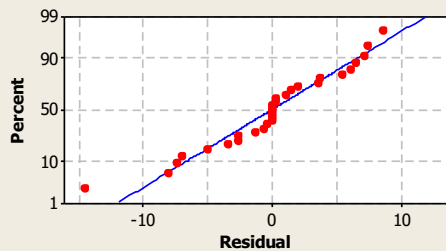
Grouping Information Using Tukey Method and 95.0% Confidence

Grain			
N Soil	N	Mean	Grouping
2	6	59.5	A
0	6	46.5	B
20	6	35.2	C
10	6	28.3	C
47	6	-0.0	D

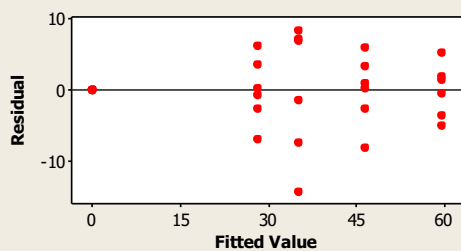
Means that do not share a letter are significantly different.

Residual Plots for 1000 g wt Soil

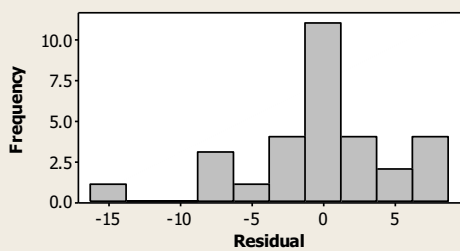
Normal Probability Plot



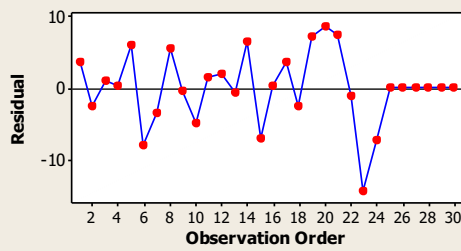
Versus Fits



Histogram



Versus Order



General Linear Model: 1000 g wt Hyd versus Grain N Hyd
Fig 4-12 B

Factor	Type	Levels	Values
Grain N Hyd	fixed	6	0.08, 0.16, 0.32, 0.64, 1.60, 16.00

Analysis of Variance for 1000 g wt Hyd, using Adjusted SS for Tests

Source	DF	Seq SS	Adj SS	Adj MS	F	P
Grain N Hyd	5	6838.1	6838.1	1367.6	11.04	0.000
Error	45	5574.3	5574.3	123.9		
Total	50	12412.4				

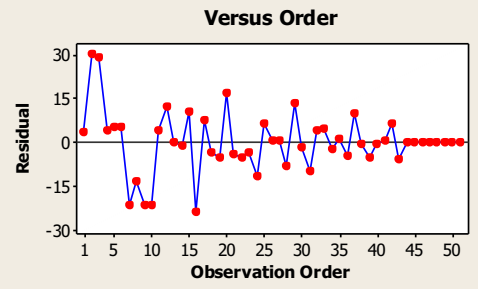
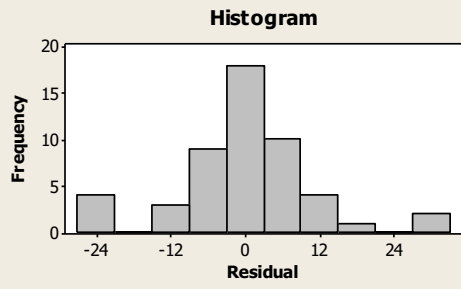
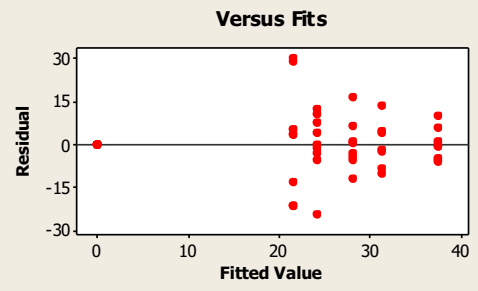
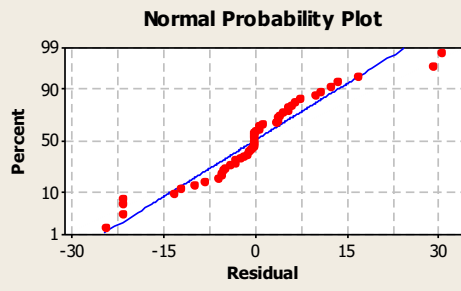
S = 11.1299 R-Sq = 55.09% R-Sq(adj) = 50.10%

Grouping Information Using Tukey Method and 95.0% Confidence

Grain			
N Hyd	N	Mean	Grouping
1.60	9	37.5	A
0.64	7	31.4	A B
0.32	8	28.2	A B
0.16	9	24.3	A B
0.08	10	21.6	B
16.00	8	0.0	C

Means that do not share a letter are significantly different.

Residual Plots for 1000 g wt Hyd



General Linear Model: Grain Num Soil versus Grain N Soil

Fig 4-12 C

```
actor          Type  Levels  Values
Grain N Soil  fixed          5  0, 2, 10, 20, 47
```

Analysis of Variance for Grain Num Soil, using Adjusted SS for Tests

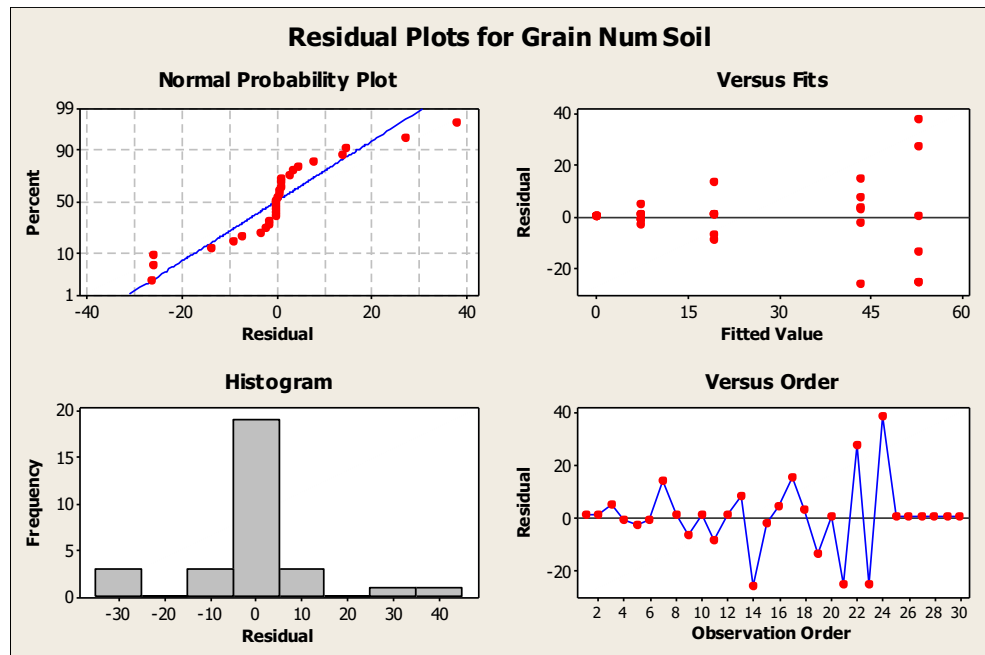
Source	DF	Seq SS	Adj SS	Adj MS	F	P
Grain N Soil	4	12485.1	12485.1	3121.3	15.36	0.000
Error	25	5080.3	5080.3	203.2		
Total	29	17565.5				

S = 14.2553 R-Sq = 71.08% R-Sq(adj) = 66.45%

Grouping Information Using Tukey Method and 95.0% Confidence

Grain			
N Soil	N	Mean	Grouping
20	6	52.8	A
10	6	43.3	A
2	6	19.2	B
0	6	7.3	B
47	6	0.0	B

Means that do not share a letter are significantly different.



Kruskal-Wallis Test: Grain Num Soil versus Grain N Soil

Kruskal-Wallis Test on Grain Num Soil

Grain N

Soil	N	Median	Ave Rank	Z
0	6	7.000000000	9.8	-1.79
2	6	2.00000E+01	16.3	0.23
10	6	4.65000E+01	23.5	2.49
20	6	4.60000E+01	24.5	2.80
47	6	0.000000000	3.5	-3.73
Overall	30		15.5	

H = 24.98 DF = 4 P = 0.000

H = 25.22 DF = 4 P = 0.000 (adjusted for ties)

General Linear Model: Grain Num Hyd versus Grain N Hyd
Fig 4-12 D

Factor	Type	Levels	Values
Grain N Hyd	fixed	6	0.08, 0.16, 0.32, 0.64, 1.60, 16.00

Analysis of Variance for Grain Num Hyd, using Adjusted SS for Tests

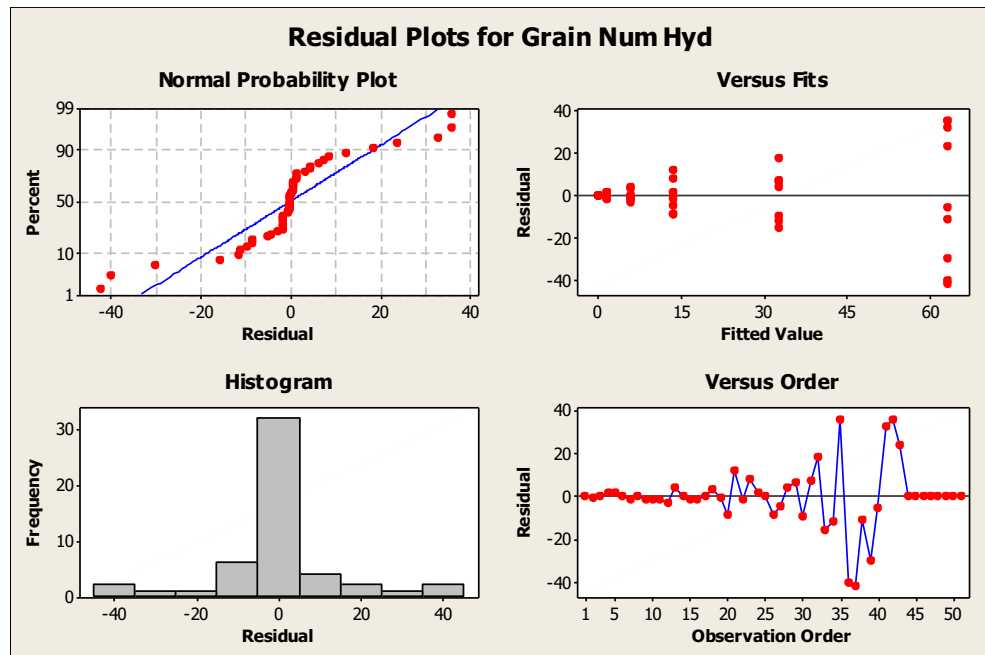
Source	DF	Seq SS	Adj SS	Adj MS	F	P
Grain N Hyd	5	26593.9	26593.9	5318.8	23.82	0.000
Error	45	10047.1	10047.1	223.3		
Total	50	36641.0				

S = 14.9422 R-Sq = 72.58% R-Sq(adj) = 69.53%

Grouping Information Using Tukey Method and 95.0% Confidence

Grain			
N Hyd	N	Mean	Grouping
1.60	9	63.1	A
0.64	7	32.6	B
0.32	8	13.5	B C
0.16	9	5.7	C
0.08	10	1.5	C
16.00	8	0.0	C

Means that do not share a letter are significantly different.



Kruskal-Wallis Test: Grain Num Hyd versus Grain N Hyd

Kruskal-Wallis Test on Grain Num Hyd

Grain N Hyd	N	Median	Ave Rank	Z
0.08	10	2.000000000	12.4	-3.23
0.16	9	5.000000000	24.1	-0.43
0.32	8	1.30000E+01	31.2	1.07
0.64	7	3.70000E+01	40.3	2.74
1.60	9	5.80000E+01	45.1	4.25
16.00	8	0.000000000	6.0	-4.14
Overall	51		26.0	

H = 45.31 DF = 5 P = 0.000

Appendix A-15. General Linear Model: Chlorophyll versus Chl N
Fig 4-15

Factor	Type	Levels	Values
Chl N	fixed	5	0.08, 0.16, 0.32, 0.64, 16.00

Analysis of Variance for Chlorophyll, using Adjusted SS for Tests

Source	DF	Seq SS	Adj SS	Adj MS	F	P
Chl N	4	280.622	280.622	70.155	9.95	0.000
Error	45	317.405	317.405	7.053		
Total	49	598.026				

S = 2.65583 R-Sq = 46.92% R-Sq(adj) = 42.21%

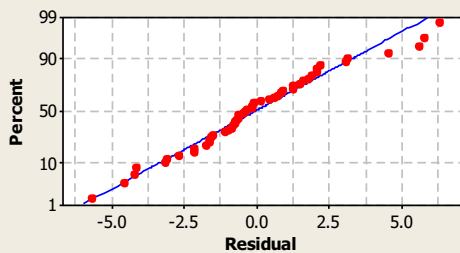
Grouping Information Using Tukey Method and 95.0% Confidence

Chl N	N	Mean	Grouping
16.00	10	10.8	A
0.64	10	8.0	A B
0.32	10	5.5	B C
0.16	10	4.8	B C
0.08	10	4.5	C

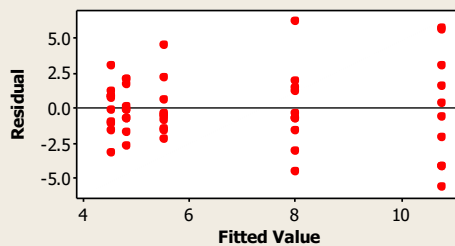
Means that do not share a letter are significantly different.

Residual Plots for Chlorophyll

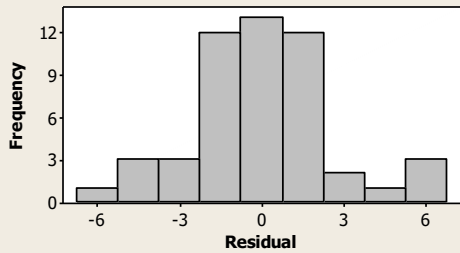
Normal Probability Plot



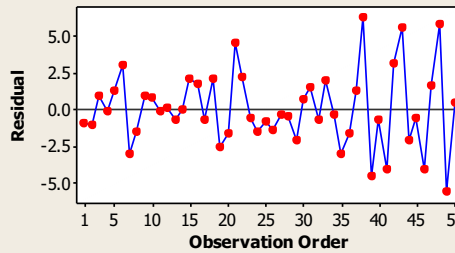
Versus Fits



Histogram



Versus Order



Appendix A-16. General Linear Model: Protein versus Protein N

Fig. 4-16

Factor	Type	Levels	Values
Protein N	fixed	4	0.16, 0.32, 0.80, 16.00

Analysis of Variance for Protein, using Adjusted SS for Tests

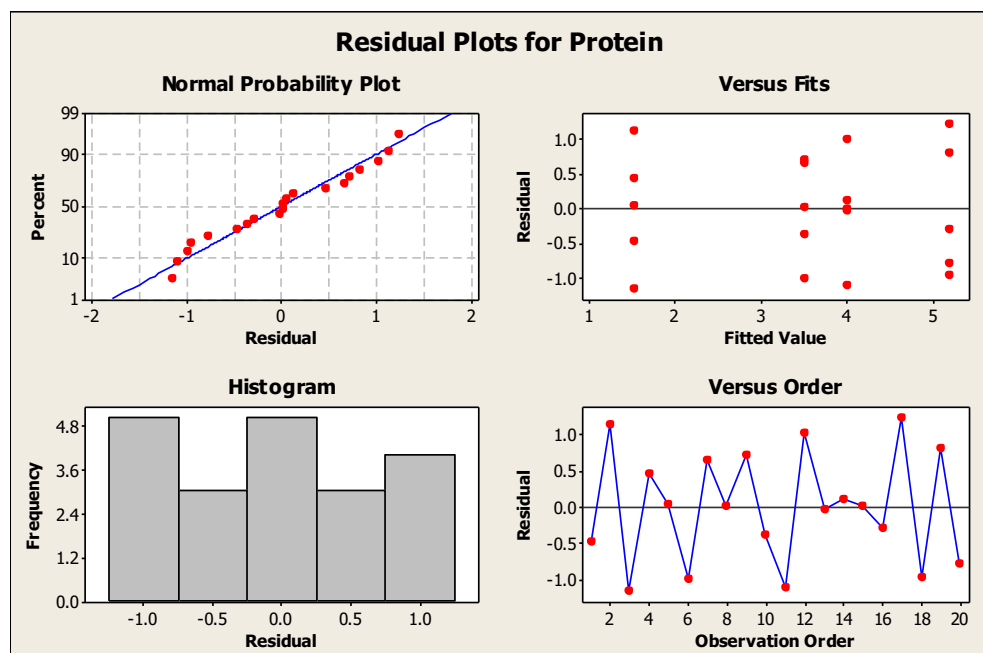
Source	DF	Seq SS	Adj SS	Adj MS	F	P
Protein N	3	34.960	34.960	11.653	16.50	0.000
Error	16	11.298	11.298	0.706		
Total	19	46.258				

S = 0.840298 R-Sq = 75.58% R-Sq(adj) = 71.00%

Grouping Information Using Tukey Method and 95.0% Confidence

Protein N	N	Mean	Grouping
16.00	5	5.2	A
0.80	5	4.0	A B
0.32	5	3.5	B
0.16	5	1.5	C

Means that do not share a letter are significantly different.



Appendix A-17 .General Linear Model: Num Chloroplasts versus Chloroplast N

Fig 4-17

Factor	Type	Levels	Values
Chloroplast N	fixed	6	0.08, 0.16, 0.32, 0.80, 1.60, 16.00

Analysis of Variance for Num Chloroplasts, using Adjusted SS for Tests

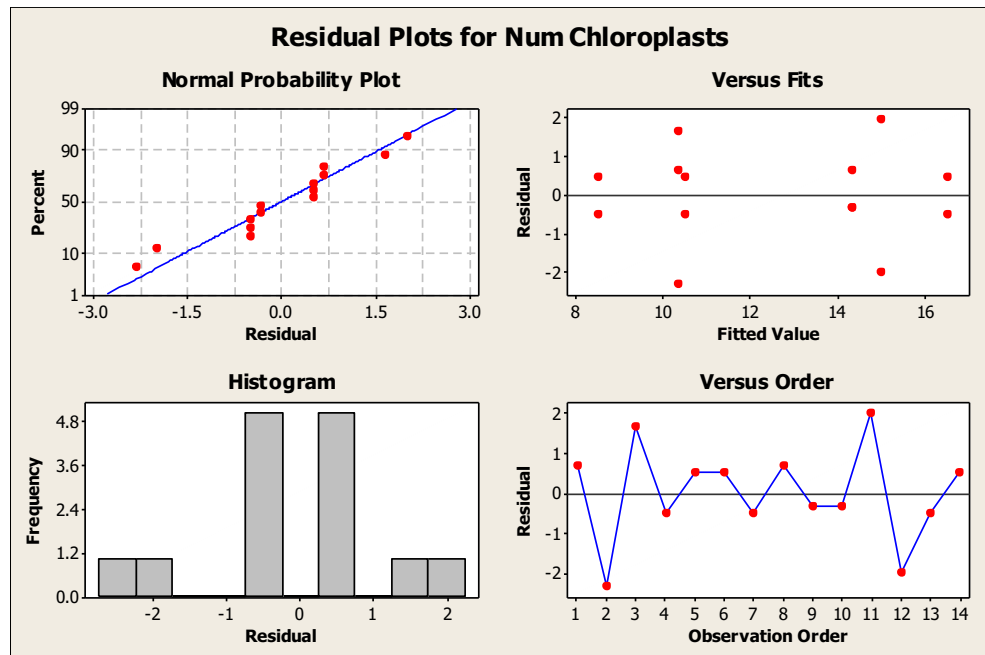
Source	DF	Seq SS	Adj SS	Adj MS	F	P
Chloroplast N	5	108.667	108.667	21.733	9.23	0.004
Error	8	18.833	18.833	2.354		
Total	13	127.500				

S = 1.53433 R-Sq = 85.23% R-Sq(adj) = 76.00%

Grouping Information Using Tukey Method and 95.0% Confidence

Chloroplast N	N	Mean	Grouping
16.00	2	16.5	A
1.60	2	15.0	A B
0.80	3	14.3	A B
0.16	2	10.5	B C
0.08	3	10.3	B C
0.32	2	8.5	C

Means that do not share a letter are significantly different.



Kruskal-Wallis Test: Num Chloroplasts versus Choroplast N

Kruskal-Wallis Test on Num Chloroplasts

Choroplast N	N	Median	Ave Rank	Z
0.08	3	11.000	4.7	-1.32
0.16	2	10.500	4.8	-1.00
0.32	2	8.500	2.3	-1.92
0.80	3	14.000	10.0	1.17
1.60	2	15.000	10.8	1.19
16.00	2	16.500	12.8	1.92
Overall	14		7.5	

H = 10.82 DF = 5 P = 0.055

H = 10.92 DF = 5 P = 0.053 (adjusted for ties)

Appendix A-18. General Linear Model: Leaf thickness versus Leaf Th N
Fig 4-18

Factor	Type	Levels	Values
Leaf Th N	fixed	5	0.08, 0.16, 0.32, 0.80, 16.00

Analysis of Variance for Leaf thickness, using Adjusted SS for Tests

Source	DF	Seq SS	Adj SS	Adj MS	F	P
Leaf Th N	4	8052.1	8052.1	2013.0	7.97	0.001
Error	17	4293.3	4293.3	252.5		
Total	21	12345.5				

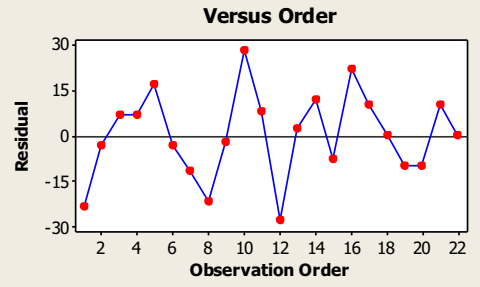
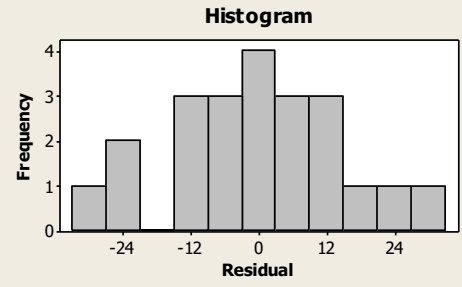
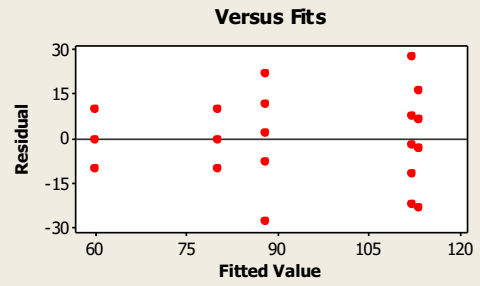
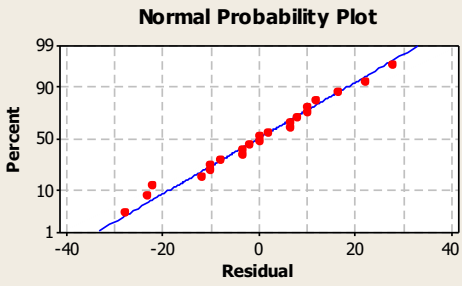
S = 15.8918 R-Sq = 65.22% R-Sq(adj) = 57.04%

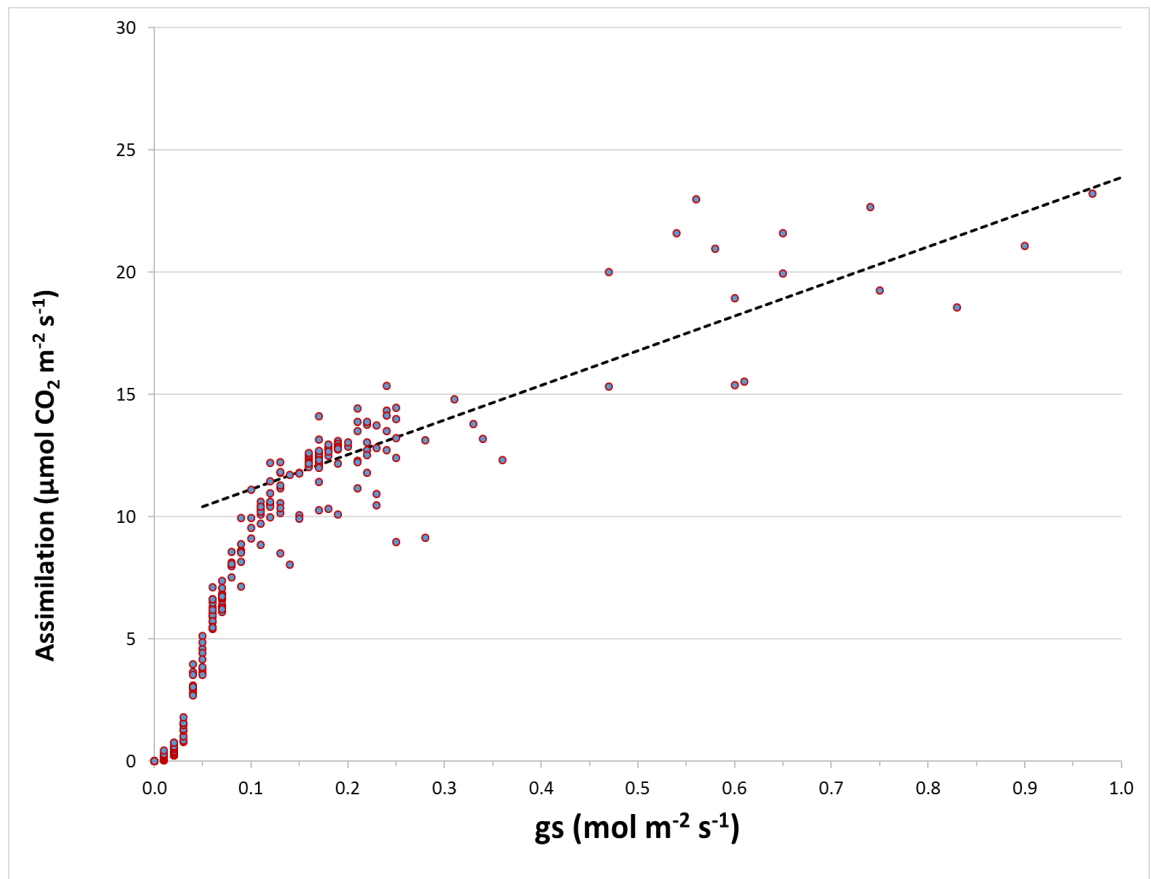
Grouping Information Using Tukey Method and 95.0% Confidence

Leaf Th N	N	Mean	Grouping
16.00	6	113.3	A
0.80	5	112.0	A
0.32	5	88.0	A B
0.16	3	80.0	A B
0.08	3	60.0	B

Means that do not share a letter are significantly different.

Residual Plots for Leaf thickness





A 19. Plot of A_{sat} Against Stomatal Conductance (g_s) of Barley Leaves

A_{sat} and g_s were measured from unstressed attached barley leaves exposed to saturating levels of PAR ($580 \mu\text{mol m}^{-2} \text{s}^{-1}$) in normal air ($\sim 380 \mu\text{mol CO}_2 \text{mol}^{-1}$ Air) at different times of the day. The data show that g_s has a profound effect on A_{sat} below $0.25 - 0.30 \text{ mol m}^{-2} \text{s}^{-1}$, but above that threshold level other factors dominate.

**Table A-1 List of Highly Abundant Sequences in Floral Primodia of Barley
Grown in 0.6 mM Nitrogen**

In the supplemented DVD.

**Table A- 2. List of Highly Abundant Sequences in Floral Primodia of Barley
Grown in 16 mM Nitrogen**

In the supplemented DVD.

References:

- Aasland R, Stewart AF, Gibson T. The SANT domain: A putative DNA binding domain in the SWI-SNF and ADA complexes, the transcriptional co-repressor N-CoR and TFIIIB. *Trends Biochem. Sci.* 1996. p. 87–8.
- Albacete A, Ghanem ME, Martinez-Andujar C, Acosta M, Sanchez-Bravo J, Martinez V, et al. Hormonal changes in relation to biomass partitioning and shoot growth impairment in salinized tomato (*Solanum lycopersicum* L.) plants. *J Exp Bot.* 2008;59(15):4119–31.
- Alemayehu FR, Frenck G, van der Linden L, Mikkelsen TN, Jørgensen RB. Can barley (*Hordeum vulgare* L. s.l.) adapt to fast climate changes? A controlled selection experiment. *Genet Resour Crop Evol.* 2014;61(1):151–61.
- Allahverdiyeva Y, Suorsa M, Tikkanen M, Aro E-M. Photoprotection of photosystems in fluctuating light intensities. *J Exp Bot.* 2015;66(9):2427–36.
- Allen-stevens T. *Winter Barley Maximising Margins- Growing for Yield.* Cambridge; 2013.
- Alley MM, Pidgen TH, Brann DE, Hammons JL, Mulford RL. Nitrogen fertilization of winter barley - Principles and recommendations. *Virginia Coop Ext.* 2009;(424–801):1–4.
- Almalki NA. *High temperature stress on cereal photosynthesis: a re-evaluation.* University of Glasgow; 2014.
- Almenaie HS, Mahgoub HS, Al-Ragam O, Al-Dosery N, Mathew M, Suresh N. Performance and Yield Components of Forage Barley Grown Under Harsh Environmental Conditions of Kuwait. In: Zhang G, Li C, Liu X, editors. *Adv*

- Barley Sci Proc 11th Int Barley Genet Symp. Dordrecht: Springer Netherlands; 2013. p. 367–74.
- Archontoulis S V, Yin X, Vos J, Danalatos NG, Struik PC. Leaf photosynthesis and respiration of three bioenergy crops in relation to temperature and leaf nitrogen: how conserved are biochemical model parameters among crop species? *J Exp Bot.* 2012;63(2):895–911.
- Ashoub A, Baeumlisberger M, Neupaertl M, Karas M, Bruggemann W. Characterization of common and distinctive adjustments of wild barley leaf proteome under drought acclimation, heat stress and their combination. *Plant Mol Biol.* 2015;87(4–5):459–71.
- Avicé J-C, Etienne P. Leaf senescence and nitrogen remobilization efficiency in oilseed rape (*Brassica napus* L.). *J Exp Bot.* 2014 Jul;65(14):3813–24.
- Bai X, Huang Y, Mao D, Wen M, Zhang L, Xing Y. Regulatory role of FZP in the determination of panicle branching and spikelet formation in rice. *Sci Rep.* Nature Publishing Group; 2016 Jan 8;6(19022):1–11.
- Baker NR. Chlorophyll Fluorescence: A Probe of Photosynthesis In Vivo. *Annu Rev Plant Biol.* 2008;59(1):89–113.
- Balazadeh S, Schildhauer J, Araújo WL, Munné-Bosch S, Fernie AR, Proost S, et al. Reversal of senescence by N resupply to N-starved *Arabidopsis thaliana*: transcriptomic and metabolomic consequences. *J Exp Bot.* 2014;65(14):3975–92.
- Barkan A, Small I. Pentatricopeptide Repeat Proteins in Plants. *Annu Rev Plant Biol.* 2014 Apr 29;65(1):415–42.
- Barrett CB. Measuring food insecurity. *Science.* 2010;327(5967):825–8.

- Bassett TJ. Reducing hunger vulnerability through sustainable development. *Proc Natl Acad Sci U S A*. 2010;107(13):5697–8.
- Beddington J. Food security: contributions from science to a new and greener revolution. *Philos Trans R Soc B Biol Sci*. 2010;365(1537):61–71.
- Benson A a. Identification of Ribulose C14 O2 Photosynthesis Products. *J Am Chem Soc*. 1951;73(6):2971–2.
- Benson AA, Calvin M. The Path of Carbon in Photosynthesis. *J Exp Bot*. 1950;1(1):63–8.
- Blankenberg D, Gordon A, Von Kuster G, Coraor N, Taylor J, Nekrutenko A, et al. Manipulation of FASTQ data with galaxy. *Bioinformatics*. 2010;26(14):1783–5.
- Boden S a, Weiss D, Ross JJ, Davies NW, Trevaskis B, Chandler PM, et al. EARLY FLOWERING3 Regulates Flowering in Spring Barley by Mediating Gibberellin Production and FLOWERING LOCUS T Expression. *Plant Cell*. 2014;26(4):1557–69.
- Bolger AM, Lohse M, Usadel B. Trimmomatic: a flexible trimmer for Illumina sequence data. *Bioinformatics*. 2014;30(15):2114–20.
- Borlaug NE. Sixty-two years of fighting hunger: personal recollections. *Euphytica*. 2007;157(3):287–97.
- Bray NL, Pimentel H, Melsted P, Pachter L. Near-optimal probabilistic RNA-seq quantification. *Nat Biotechnol*. 2016;34(5):525–7.
- Buckley TN, Mott KA. Modelling stomatal conductance in response to environmental factors. *Plant Cell Environ*. 2013 Sep;36(9):1691–9.
- Bukhov NG, Carpentier R. Heterogeneity of photosystem II reaction centers as

- influenced by heat. *Physiol Plant*. 2000;110:279–85.
- von Caemmerer S. Steady-state models of photosynthesis. *Plant Cell Environ*. 2013;36(9):1617–30.
- Čajánek M, Štroch M, Lachetová I, Kalina J, Spunda V. Characterization of the photosystem II inactivation of heat-stressed barley leaves as monitored by the various parameters of chlorophyll a fluorescence and delayed fluorescence. *J Photochem Photobiol B Biol*. 1998;47(1):39–45.
- van Campen J, Yaapar MN, Narawatthana S, Lehmeier C, Wanchana S, Thakur V, et al. Combined Chlorophyll Fluorescence and Transcriptomic Analysis Identifies the P3/P4 Transition as a Key stage in Rice Leaf Photosynthetic Development. *Plant Physiol*. 2016;170(March):1655–74.
- Cano FJ, Sánchez-Gómez D, Rodríguez-Calcerrada J, Warren CR, Gil L, Aranda I. Effects of drought on mesophyll conductance and photosynthetic limitations at different tree canopy layers. *Plant Cell Environ*. 2013;36(11):1961–80.
- Carmo-Silva a. E, Gore M a., Andrade-Sanchez P, French AN, Hunsaker DJ, Salvucci ME. Decreased CO₂ availability and inactivation of Rubisco limit photosynthesis in cotton plants under heat and drought stress in the field. *Environ Exp Bot*. Elsevier B.V.; 2012 Nov;83:1–11.
- Carmo-Silva a E, Salvucci ME. The temperature response of CO₂ assimilation, photochemical activities and Rubisco activation in *Camelina sativa*, a potential bioenergy crop with limited capacity for acclimation to heat stress. *Planta*. 2012;236(5):1433–45.
- Carmo-Silva AE, Salvucci ME. The regulatory properties of Rubisco activase differ among species and affect photosynthetic induction during light transitions.

- Plant Physiol. 2013;161(4):1645–55.
- Cen Y, Sage R. The regulation of Rubisco activity in response to variation in temperature and atmospheric CO₂ partial pressure in sweet potato. *Plant Physiol.* 2005;139:979–90.
- Cenci A, Rouard M. Evolutionary Analyses of GRAS Transcription Factors in Angiosperms. *Front Plant Sci.* 2017;8(March):273.
- Chandler PM, Harding CA. “Overgrowth” mutants in barley and wheat: New alleles and phenotypes of the “Green Revolution” *della* gene. *J Exp Bot.* 2013;64(6):1603–13.
- Chang S, Chang T, Song Q, Zhu X-G, Deng Q. Photosynthetic and agronomic traits of an elite hybrid rice Y-Liang-You 900 with a record-high yield. *F Crop Res.* Elsevier B.V.; 2016 Feb;187:49–57.
- Chauvet A, Jankowiak R, Kell A, Picorel R, Savikhin S. Does the Singlet Minus Triplet Spectrum with Major Photobleaching Band Near 680–682 nm Represent an Intact Reaction Center of Photosystem II? *J Phys Chem B.* 2015 Jan 15;119(2):448–55.
- Chen A, Li C, Hu W, Lau MY, Lin H, Rockwell NC, et al. PHYTOCHROME C plays a major role in the acceleration of wheat flowering under long-day photoperiod. *Proc Natl Acad Sci U S A.* 2014;111(28):10037–44.
- Cheng H, Qin L, Lee S, Fu X, Richards DE, Cao D, et al. Gibberellin regulates *Arabidopsis* floral development via suppression of DELLA protein function. *Development.* 2004;131(5):1055–64.
- Clarke JE, Johnson GN. In vivo temperature dependence of cyclic and pseudocyclic electron transport in barley. *Planta.* 2001;212(5–6):808–16.

- Cohu CM, Muller O, Adams WW, Demmig-Adams B. Leaf anatomical and photosynthetic acclimation to cool temperature and high light in two winter versus two summer annuals. *Physiol Plant*. 2014;152(1):164–73.
- Consortium IBGS. A physical, genetic and functional sequence assembly of the barley genome. *Nature*. Nature Publishing Group; 2012 Oct 17;491(7426):711–6.
- Cornic G, Baker NR. Electron Transport in Leaves: A Physiological Perspective. In: Eaton-Rye JJ, Tripathy BC, Sharkey TD, editors. *Photosynth Plast Biol Energy Convers Carbon Assim Adv Photosynth Respir*. Springer; 2012. p. 591–605.
- Cosgrove DJ. Plant expansins: Diversity and interactions with plant cell walls. *Curr Opin Plant Biol*. Elsevier Ltd; 2015;25:162–72.
- Crafts-Brandner SJ, Salvucci ME. Rubisco activase constrains the photosynthetic potential of leaves at high temperature and CO₂. *Proc Natl Acad Sci*. 2000 Nov 21;97(24):13430–5.
- Crafts-Brandner SJ, Salvucci ME. Sensitivity of photosynthesis in a C₄ plant, maize, to heat stress. *Plant Physiol*. 2002;129(4):1773–80.
- Curtis T, Halford NG. Food security: the challenge of increasing wheat yield and the importance of not compromising food safety. *Ann Appl Biol*. 2014;164(3):354–72.
- Dechorgnat J, Nguyen CT, Armengaud P, Jossier M, Diatloff E, Filleur S, et al. From the soil to the seeds: the long journey of nitrate in plants. *J Exp Bot*. 2011 Feb 1;62(4):1349–59.
- Ding X, Cao Y, Huang L, Zhao J, Xu C, Li X, et al. Activation of the Indole-3-Acetic Acid-Amido Synthetase GH3-8 Suppresses Expansin Expression and

- Promotes Salicylate- and Jasmonate-Independent Basal Immunity in Rice. *Plant Cell Online*. 2008;20(1):228–40.
- Dominy PJ, Williams WP. The role of respiratory electron flow in the control of excitation energy distribution in blue-green algae. *Biochim Biophys Acta - Bioenerg*. 1987;892(3):264–74.
- Dreni L, Zhang D. Flower development: the evolutionary history and functions of the AGL6 subfamily MADS-box genes. *J Exp Bot*. 2016 Mar;67(6):1625–38.
- Dubin MJ. The Application of Next Generation Sequencing Techniques to Plant Epigenomics. In: Sablok G, Kumar S, Ueno S, Kuo J, Varotto C, editors. *Adv Underst Biol Sci Using Next Gener Seq Approaches*. Cham: Springer International Publishing; 2015. p. 13–31.
- Eberhard S, Finazzi G, Wollman F-A. The dynamics of photosynthesis. *Annu Rev Genet*. 2008;42(1):463–515.
- Egorova EA, Bukhov NG. Effect of Elevated Temperatures on the Activity of Alternative Pathways of Photosynthetic Electron Transport in Intact Barley and Maize Leaves. *Russ J Plant Physiol*. 2002;49(5):645–55.
- Emebiri LC. Breeding malting barley for consistently low grain protein to sustain production against predicted changes from global warming. *Mol Breed*. 2015;35(1):18.
- Endo T, Asada K. Photosystem I and Photoprotection: Cyclic Electron Flow and Water-Water Cycle. In: Demmig-adams B, Adams WW, Mattoo AK, editors. *Photoprotection, Photoinhibition, Gene Regul Environ*. springer; 2008. p. 205–21.
- Epron D, Godard D, Cornic G, Genty B. Limitation of net CO₂ assimilation rate by

- internal resistances to CO₂ transfer in the leaves of two tree species (*Fagus sylvatica* L. and *Castanea sativa* Mill.). *Plant, Cell Environ.* 1995;18(1):43–51.
- Essemine J, Qu M, Mi H, Zhu X-G. Response of Chloroplast NAD(P)H Dehydrogenase-Mediated Cyclic Electron Flow to a Shortage or Lack in Ferredoxin-Quinone Oxidoreductase-Dependent Pathway in Rice Following Short-Term Heat Stress. *Front Plant Sci.* 2016;7:1–15.
- Evans JR. Improving photosynthesis. *Plant Physiol.* 2013;162(4):1780–93.
- Fan M, Shen J, Yuan L, Jiang R, Chen X, Davies WJ, et al. Improving crop productivity and resource use efficiency to ensure food security and environmental quality in China. *J Exp Bot.* 2012;63(1):13–24.
- FAO. FAO Stat [Internet]. 2016 [cited 2016 Jul 27]. Available from: http://faostat3.fao.org/browse/D/*/E
- Farquhar GD, Sharkey TD. Stomatal Conductance and Photosynthesis. *Annu Rev Plant Physiol.* 1982;33(1):317–45.
- Fischer RA (Tony), Edmeades GO. Breeding and Cereal Yield Progress. *Crop Sci.* 2010;50(Supplement_1):S85–95.
- Fjellheim S, Boden S, Trevaskis B. The role of seasonal flowering responses in adaptation of grasses to temperate climates. *Front Plant Sci.* 2014;5(431):1–15.
- Flexas J, Carriquí M, Coopman RE, Gago J, Galmés J, Martorell S, et al. Stomatal and mesophyll conductances to CO₂ in different plant groups: Underrated factors for predicting leaf photosynthesis responses to climate change? *Plant Sci.* 2014;226:41–8.

- Forde BG, Lea PJ. Glutamate in plants: metabolism, regulation, and signalling. *J Exp Bot.* 2007;58(9):2339–58.
- Froese A, Sehon AH. Kinetics of antibody--hapten reactions. *Contemp Top Mol Immunol.* 1975;4(2):23–54.
- Frolec J, Ilík P, Krchňák P, Sušila P, Nauš J. Irreversible changes in barley leaf chlorophyll fluorescence detected by the fluorescence temperature curve in a linear heating/cooling regime. *Photosynthetica.* 2008;46(4):537–46.
- Fukayama H, Ueguchi C, Nishikawa K, Katoh N, Ishikawa C, Masumoto C, et al. Overexpression of Rubisco Activase Decreases the Photosynthetic CO₂ Assimilation Rate by Reducing Rubisco Content in Rice Leaves. *Plant Cell Physiol.* 2012;53(6):976–86.
- Galmés J, Andralojc PJ, Kapralov M V, Flexas J, Keys AJ, Molins A, et al. Environmentally driven evolution of Rubisco and improved photosynthesis and growth within the C₃ genus *Limonium* (Plumbaginaceae). *New Phytol.* 2014;203(3):989–99.
- Gandin A, Koteyeva NK, Voznesenskaya E V, Edwards GE, Cousins AB. The acclimation of photosynthesis and respiration to temperature in the C₃-C₄ intermediate *Salsola divaricata*: induction of high respiratory CO₂ release under low temperature. *Plant Cell Environ.* 2014 Nov;37(11):2601–12.
- Gardestrom P. Metabolite levels in the chloroplast and extrachloroplast compartments of barley leaf protoplasts during the initial phase of photosynthetic induction. *BBA - Bioenerg.* 1993;1183(2):327–32.
- Ghanem ME, Albacete A, Smigocki AC, Frebort I, Pospisilova H, Martinez-Andujar C, et al. Root-synthesized cytokinins improve shoot growth and fruit yield in

- salinized tomato (*Solanum lycopersicum* L.) plants. *J Exp Bot.* 2011;62(1):125–40.
- Gillon JS, Yakir D. Internal conductance to CO₂ diffusion and C₁₈O₂ discrimination in C₃ leaves. *Plant Physiol.* 2000;123(1):201–14.
- Gontero B, Salvucci ME. Regulation of photosynthetic carbon metabolism in aquatic and terrestrial organisms by Rubisco activase, redox-modulation and CP12. *Aquat Bot.* 2014;118:14–23.
- Gu J, Yin X, Stomph T-J, Struik PC. Can exploiting natural genetic variation in leaf photosynthesis contribute to increasing rice productivity? A simulation analysis. *Plant Cell Environ.* 2014 Jan;37(1):22–34.
- Haas BJ, Papanicolaou A, Yassour M, Grabherr M, Blood PD, Bowden J, et al. De novo transcript sequence reconstruction from RNA-seq using the Trinity platform for reference generation and analysis. *Nat Protoc.* 2013;8(8):1494–512.
- Hall AJ, Savin R, Slafer GA. Is time to flowering in wheat and barley influenced by nitrogen?: A critical appraisal of recent published reports. *Eur J Agron. Elsevier B.V.*; 2014;54:40–6.
- Hedden P. The genes of the Green Revolution. *Trends Genet.* 2003;19(1):5–9.
- Henderson JN, Hazra S, Dunkle AM, Salvucci ME, Wachter RM. Biophysical characterization of higher plant Rubisco activase. *Biochim Biophys Acta.* 2013;1834(1):87–97.
- Hepworth J, Dean C. Flowering Locus C's Lessons: Conserved Chromatin Switches Underpinning Developmental Timing and Adaptation. *Plant Physiol.* 2015;168(4):1237–45.

- Hirsch S, Oldroyd GED. GRAS-domain transcription factors that regulate plant development. *Plant Signal Behav.* 2009;4(8):698–700.
- Hu Z, Xu F, Guan L, Qian P, Liu Y, Zhang H, et al. The tetratricopeptide repeat-containing protein slow green1 is required for chloroplast development in *Arabidopsis*. *J Exp Bot.* 2014;65(4):1111–23.
- Hussain I, Khan MA, Khan EA. Bread wheat varieties as influenced by different nitrogen levels. *J Zhejiang Univ Sci B.* 2006;7(1):70–8.
- Hüve K, Bichele I, Rasulov B, Niinemets U. When it is too hot for photosynthesis: heat-induced instability of photosynthesis in relation to respiratory burst, cell permeability changes and H₂O₂ formation. *Plant Cell Environ.* 2011;34(1):113–26.
- Jones D. Wheat yield world record shattered in Lincolnshire [Internet]. *Farmers Wkly.* 2015 [cited 2016 Jul 28]. Available from: <http://www.fwi.co.uk/arable/wheat-yield-world-record-shattered-in-lincolnshire.htm>
- Kaa R, Kotabov E, Pril O. Acceleration of plastoquinone pool reduction by alternative pathways precedes a decrease in photosynthetic CO₂ assimilation in preheated barley leaves. *Physiol Plant.* 2008;133(4):794–806.
- Kalaji HM, Jajoo A, Oukarroum A, Brestic M, Zivcak M, Samborska IA, et al. Chlorophyll a fluorescence as a tool to monitor physiological status of plants under abiotic stress conditions. *Acta Physiol Plant.* 2016 Apr 29;38(102):1–11.
- Khush GS. Strategies for increasing the yield potential of cereals: case of rice as an example. Gupta P, editor. *Plant Breed.* 2013;132(5):433–6.
- Kiba T, Kudo T, Kojima M, Sakakibara H. Hormonal control of nitrogen acquisition:

- roles of auxin, abscisic acid, and cytokinin. *J Exp Bot.* 2011;62(4):1399–409.
- Kim T-H, Böhmer M, Hu H, Nishimura N, Schroeder JI. Guard Cell Signal Transduction Network: Advances in Understanding Abscisic Acid, CO₂, and Ca²⁺ Signaling. *Annu Rev Plant Biol.* 2010;61(1):561–91.
- Kirschbaum MUF. Does Enhanced Photosynthesis Enhance Growth? Lessons Learned from CO₂ Enrichment Studies. *PLANT Physiol.* 2011;155(1):117–24.
- Kishore GM, Shewmaker C. Biotechnology: Enhancing human nutrition in developing and developed worlds. *Proc Natl Acad Sci.* 1999;96(11):5968–72.
- Komatsu M, Tobita H, Watanabe M, Yazaki K, Koike T, Kitao M. Photosynthetic downregulation in leaves of the Japanese white birch grown under elevated CO₂ concentration does not change their temperature-dependent susceptibility to photoinhibition. *Physiol Plant.* 2013;147(2):159–68.
- Kosová K, Vítámvás P, Prášil IT. Proteomics of stress responses in wheat and barley-search for potential protein markers of stress tolerance. *Front Plant Sci.* 2014;5(711):1–14.
- Krogan NT, Hogan K, Long JA. APETALA2 negatively regulates multiple floral organ identity genes in Arabidopsis by recruiting the co-repressor TOPLESS and the histone deacetylase HDA19. *Development.* 2012;139(22):4180–90.
- Krömer S, Stitt M, Heldt HW. Mitochondrial oxidative phosphorylation participating in photosynthetic metabolism of a leaf cell. *FEBS Lett.* 1988;226(2):352–6.
- Kubien DS, Sage RF. The temperature response of photosynthesis in tobacco with reduced amounts of Rubisco. *Plant, Cell Environ.* 2008;31(4):407–18.
- Kudoyarova GR, Korobova A V., Akhiyarova GR, Arkhipova TN, Zaytsev DY,

- Prinsen E, et al. Accumulation of cytokinins in roots and their export to the shoots of durum wheat plants treated with the protonophore carbonyl cyanide *m*-chlorophenylhydrazone (CCCP). *J Exp Bot.* 2014;65(9):2287–94.
- Laanemets K, Brandt B, Li J, Merilo E, Wang Y-F, Keshwani MM, et al. Calcium-Dependent and -Independent Stomatal Signaling Network and Compensatory Feedback Control of Stomatal Opening via Ca²⁺ Sensitivity Priming. *PLANT Physiol.* 2013;163(2):504–13.
- Lambers H, Robinson SA, Ribas-Carbo M. Regulation of Respiration In Vivo. In: Lambers H, Ribas-Carbo M, editors. *Plant Respir.* Berlin/Heidelberg: Springer-Verlag; 2005. p. 1–15.
- Lawlor DW. Limitation to Photosynthesis in Water-stressed Leaves: Stomata vs. Metabolism and the Role of ATP. *Ann Bot.* 2002 Jun 15;89(7):871–85.
- Lawlor DW, Khanna-Chopra R. Regulation of Photosynthesis During Water Stress. In: Sybesma C, editor. *Adv Photosynth Res.* Dordrecht: Springer Netherlands; 1984. p. 379–82.
- Lazár D, Ilík P. High-temperature induced chlorophyll fluorescence changes in barley leaves: Comparison of the critical temperatures determined from fluorescence induction and from fluorescence temperature curve. *Plant Sci.* 1997;124(2):159–64.
- Li D, Tian M, Cai J, Jiang D, Cao W, Dai T. Effects of low nitrogen supply on relationships between photosynthesis and nitrogen status at different leaf position in wheat seedlings. *Plant Growth Regul.* 2013;70(3):257–63.
- Li S, Zhao Y, Zhao Z, Wu X, Sun L, Liu Q, et al. Crystal Structure of the GRAS Domain of SCARECROW-LIKE7 in *Oryza sativa*. *Plant Cell.* 2016;28(5):1025–

34.

Li T, Heuvelink E, Dueck T a, Janse J, Gort G, Marcelis LFM. Enhancement of crop photosynthesis by diffuse light: quantifying the contributing factors. *Ann Bot.* 2014a;114(1):145–56.

Li X, Han B, Xu M, Han L, Zhao Y, Liu Z, et al. Plant growth enhancement and associated physiological responses are coregulated by ethylene and gibberellin in response to harpin protein Hpa1. *Planta.* 2014b;239(4):831–46.

Li Y, Krouk G, Coruzzi GM, Ruffel S. Finding a nitrogen niche: a systems integration of local and systemic nitrogen signalling in plants. *J Exp Bot.* 2014c;65(19):5601–10.

Liu J, Last RL. A land plant-specific thylakoid membrane protein contributes to photosystem II maintenance in *Arabidopsis thaliana*. *Plant J.* 2015;82(5):731–43.

Lobell DB, Asner GP. Climate and Management Contributions to Recent Trends in U.S. Agricultural Yields. *Science.* 2003;299(5609):1032–1032.

Lorimer GH. The Carboxylation and Oxygenation of Ribulose 1,5-Bisphosphate: The Primary Events in Photosynthesis and Photorespiration. *Annu Rev Plant Physiol.* 1981;32:349–83.

Losh JL, Young JN, Morel FMM. Rubisco is a small fraction of total protein in marine phytoplankton. *New Phytol.* 2013;198(1):52–8.

Love MI, Huber W, Anders S. Moderated estimation of fold change and dispersion for RNA-seq data with DESeq2. *Genome Biol.* 2014;15(12):550–70.

Makino a, Nakano H, Mae T, Shimada T, Yamamoto N. Photosynthesis, plant

- growth and N allocation in transgenic rice plants with decreased Rubisco under CO₂ enrichment. *J Exp Bot.* 2000;51(February):383–9.
- Makino A, Harada M, Sato T, Nakano H, Mae T. Growth and N Allocation in Rice Plants under CO₂ Enrichment. *Plant Physiol.* 1997;115(1):199–203.
- Malnoe A, Wang F, Girard-Bascou J, Wollman F-A, de Vitry C. Thylakoid FtsH Protease Contributes to Photosystem II and Cytochrome b₆f Remodeling in *Chlamydomonas reinhardtii* under Stress Conditions. *Plant Cell.* 2014;26(1):373–90.
- Mann CC. Crop Scientists Seek a New Revolution. *Science.* 1999;283(5400):310–4.
- Marín IC, Loeffler I, Bartetzko L, Searle I, Coupland G, Stitt M, et al. Nitrate regulates floral induction in *Arabidopsis*, acting independently of light, gibberellin and autonomous pathways. *Planta.* 2011;233(3):539–52.
- Marowa P, Ding A, Kong Y. Expansins: roles in plant growth and potential applications in crop improvement. *Plant Cell Rep.* Springer Berlin Heidelberg; 2016;35(5):949–65.
- Marschner P, Rengel Z. Nutrient Availability in Soils. *Marschner's Miner Nutr High Plants.* Elsevier; 2012. p. 315–30.
- Matías-hernández L, Aguilar-jaramillo AE, Cigliano RA, Sanseverino W, Pelaz S. Flowering and trichome development share hormonal and transcription factor regulation. *J Exp Bot.* 2016;67(5):1209–19.
- Medici A, Krouk G. The Primary Nitrate Response: a multifaceted signalling pathway. *J Exp Bot.* 2014;65(19):5567–76.

- Mehler AH. Studies on reactions of illuminated chloroplasts. II. Stimulation and inhibition of the reaction with molecular oxygen. *Arch Biochem Biophys.* 1951;34(2):339–51.
- Miller AJ, Fan X, Orsel M, Smith SJ, Wells DM. Nitrate transport and signalling. *J Exp Bot.* 2007;58(9):2297–306.
- Munekage Y, Hashimoto M, Miyake C, Tomizawa K, Endo T, Tasaka M, et al. Cyclic electron flow around photosystem I is essential for photosynthesis. *Nature.* 2004;429(6991):579–82.
- Nakano H, Makino A, Mae T. The effect of elevated partial pressures of CO₂ on the relationship between photosynthetic capacity and N content in rice leaves. *Plant Physiol.* 1997;115(1):191–8.
- Nanopore Technology. Nanopore Tech. [Internet]. Nanopore. 2016. Available from: <https://nanoporetech.com/products>
- Nickelsen J, Rengstl B. Photosystem II assembly: from cyanobacteria to plants. *Annu Rev Plant Biol.* 2013;64:609–35.
- Nixon PJ, Rich PR. Chlororespiratory Pathways and Their Physiological Significance. In: Wise RR, Hooper JK, editors. *Struct Funct Plast.* springer; 2007. p. 237–51.
- Ocheltree TW, Nippert JB, Prasad PV V. Stomatal responses to changes in vapor pressure deficit reflect tissue-specific differences in hydraulic conductance. *Plant Cell Environ.* 2014;37(1):132–9.
- Ogren WL, Bowes G. Ribulose diphosphate carboxylase regulates soybean photorespiration. *Nat New Biol.* 1971 Mar 31;230(13):159–60.

- Oliver SN, Finnegan EJ, Dennis ES, Peacock WJ, Trevaskis B. Vernalization-induced flowering in cereals is associated with changes in histone methylation at the VERNALIZATION1 gene. *Proc Natl Acad Sci U S A*. 2009;106(20):8386–91.
- Ongaro V, Leyser O. Hormonal control of shoot branching. *J Exp Bot*. 2008;59(1):67–74.
- Ozgun R, Uzilday B, Sekmen a. H, Turkan I. The effects of induced production of reactive oxygen species in organelles on endoplasmic reticulum stress and on the unfolded protein response in arabidopsis. *Ann Bot*. 2015;116(4):541–53.
- Pandey S, Kushwaha R. Leaf anatomy and photosynthetic acclimation in *Valeriana jatamansi* L. grown under high and low irradiance. *Photosynthetica*. 2005;43(1):85–90.
- Paul MJ, Knight JS, Habash D, Parry MAJ, Lawlor DW, Barnes SA, et al. Reduction in phosphoribulokinase activity by antisense RNA in transgenic tobacco: effect on CO₂ assimilation and growth in low irradiance. *Plant J*. 1995;7(4):535–42.
- Peeva VN, Tóth SZ, Cornic G, Ducruet JM. Thermoluminescence and P700 redox kinetics as complementary tools to investigate the cyclic/chlororespiratory electron pathways in stress conditions in barley leaves. *Physiol Plant*. 2012;144(1):83–97.
- Peltier G, Aro E-M, Shikanai T. NDH-1 and NDH-2 Plastoquinone Reductases in Oxygenic Photosynthesis. *Annu Rev Plant Biol*. 2016;67(1):55–80.
- Peltier G, Cournac L. Chlororespiration. *Annu Rev Plant Biol*. 2002;53(1):523–50.
- Pick TR, Bräutigam A, Schulz M a, Obata T, Fernie AR, Weber APM. PLGG1, a plastidic glycolate glycerate transporter, is required for photorespiration and

defines a unique class of metabolite transporters. *Proc Natl Acad Sci U S A*. 2013;110(8):3185–90.

Pimentel D, Huang X, Cordova A, Pimentel M. *Impact of Population Growth on Food Supplies and Environment*. *Popul Environ*. Kluwer Academic Publishers-Plenum Publishers; 1997;19(1):9–14.

Portis AR, Li C, Wang D, Salvucci ME. Regulation of Rubisco activase and its interaction with Rubisco. *J Exp Bot*. 2007;59(7):1597–604.

Pretty J. Agricultural sustainability: concepts, principles and evidence. *Philos Trans R Soc B Biol Sci*. 2008;363(1491):447–65.

Pribil M, Labs M, Leister D. Structure and dynamics of thylakoids in land plants. *J Exp Bot*. 2014;65(8):1955–72.

Prins A, Orr DJ, Andralojc PJ, Reynolds MP, Carmo-Silva E, Parry MAJ. Rubisco catalytic properties of wild and domesticated relatives provide scope for improving wheat photosynthesis. *J Exp Bot*. 2016;67(6):1827–38.

Rakshit R, Patra a. K, Pal D, -Kumar M, Singh R. Effect of Elevated CO₂ and Temperature on Nitrogen Dynamics and Microbial Activity During Wheat (*Triticum aestivum* L.) Growth on a Subtropical Inceptisol in India. *J Agron Crop Sci*. 2012;198(6):452–65.

Robertson LD, Stark JC. Idaho Spring Barley Production Guide [Internet]. Idaho Spring Barley Prod. Guid. 2003. p. 1–57. Available from: https://barley.idaho.gov/pdf/spring_barley_production_guide.pdf

Rollins JA, Habte E, Templer SE, Colby T, Schmidt J, Von Korff M. Leaf proteome alterations in the context of physiological and morphological responses to drought and heat stress in barley (*Hordeum vulgare* L.). *J Exp Bot*.

2013;64(11):3201–12.

Ruffel S, Gojon A, Lejay L. Signal interactions in the regulation of root nitrate uptake.

J Exp Bot. 2014;65(19):5509–17.

Sage RF, Way DA, Kubien DS. Rubisco, Rubisco activase, and global climate change. J Exp Bot. 2008;59(7):1581–95.

Salvucci ME. Relationship between the Heat Tolerance of Photosynthesis and the Thermal Stability of Rubisco Activase in Plants from Contrasting Thermal Environments. Plant Physiol. 2004;134(4):1460–70.

Salvucci ME, Crafts-Brandner SJ. Mechanism for deactivation of Rubisco under moderate heat stress. Physiol Plant. 2004;122(4):513–9.

Sambrook J, W Russell D. Molecular Cloning: A Laboratory Manual. 3rd ed. New York: Cold Spring Harbor Laboratory Press; 2001. p. 7.1-7.92.

Schmitz-Linneweber C, Small I. Pentatricopeptide repeat proteins: a socket set for organelle gene expression. Trends Plant Sci. 2008;13(12):663–70.

Schrader SM, Wise RR, Wacholtz WF, Ort DR, Sharkey TD. Thylakoid membrane responses to moderately high leaf temperature in Pima cotton. Plant, Cell Environ. 2004 Jun;27(6):725–35.

Schwarz P, Li Y. Malting and Brewing Uses of Barley. In: Ullrich SE, editor. Barley Prod Improv Uses. 2011. p. 478–521.

Shahwani MN. Studies on Abiotic Stress Tolerance in *Hordeum vulgare* L . Genotypes from Arid and Temperate Regions. University of Glasgow; 2011.

Sharkey TD, Badger MR. Effects of water stress on photosynthetic electron transport, photophosphorylation, and metabolite levels of *Xanthium strumarium*

mesophyll cells. *Planta*. 1982;156(3):199–206.

Sharkey TD, Seemann JR. Mild Water Stress Effects on Carbon-Reduction-Cycle Intermediates, Ribulose Bisphosphate Carboxylase Activity, and Spatial Homogeneity of Photosynthesis in Intact Leaves. *PLANT Physiol*. 1989;89(4):1060–5.

Sharkey TD, Zhang R. High Temperature Effects on Electron and Proton Circuits of Photosynthesis. *J Integr Plant Biol*. 2010;52(8):712–22.

Sharma DK, Andersen SB, Ottosen C-O, Rosenqvist E. Wheat cultivars selected for high F_v / F_m under heat stress maintain high photosynthesis, total chlorophyll, stomatal conductance, transpiration and dry matter. *Physiol Plant*. 2014;284–98.

Shikanai T. Chapter 22 Regulation of Photosynthetic Electron Transport. In: Rebeiz CA, Benning C, Bohnert HJ, Daniell H, Hooper JK, Lichtenthaler HK, et al., editors. *Chloroplast Basics Appl*. Dordrecht: Springer Netherlands; 2010. p. 347–62.

Shikanai T. Central role of cyclic electron transport around photosystem I in the regulation of photosynthesis. *Curr Opin Biotechnol*. Elsevier Ltd; 2014;26:25–30.

Shin J-H, Jeong D-H, Park MC, An G. Characterization and transcriptional expression of the alpha-expansin gene family in rice. *Mol Cells*. 2005;20(2):210–8.

Sinclair TR, Ruffy TW. Nitrogen and water resources commonly limit crop yield increases, not necessarily plant genetics. *Glob Food Sec*. 2012 Dec;1(2):94–8.

Sinclair TR, Sinclair CJ. Bread, beer and the seeds of change: Agriculture's imprint

- on world history. Sinclair TR, Sinclair CJ, editors. Wallingford: CABI; 2010.
- Singh J, Pandey P, James D, Chandrasekhar K, Achary VMM, Kaul T, et al. Enhancing C3 photosynthesis: an outlook on feasible interventions for crop improvement. *Plant Biotechnol J*. 2014;12(9):1217–30.
- Solhaug KA, Xie L, Gauslaa Y. Unequal Allocation of Excitation Energy between Photosystem II and I Reduces Cyanolichen Photosynthesis in Blue Light. *Plant Cell Physiol*. 2014;55(8):1404–14.
- Song YH, Shim JS, Kinmonth-Schultz H a, Imaizumi T. Photoperiodic Flowering: Time Measurement Mechanisms in Leaves. *Annu Rev Plant Biol*. 2015;66:441–64.
- Sulpice R, Tschoep H, VON Korff M, Büssis D, Usadel B, Höhne M, et al. Description and applications of a rapid and sensitive non-radioactive microplate-based assay for maximum and initial activity of D-ribulose-1,5-bisphosphate carboxylase/oxygenase. *Plant Cell Environ*. 2007 Sep;30(9):1163–75.
- Sun T, Gubler F. Molecular mechanism of gibberellin signaling in plants. *Annu Rev Plant Biol*. 2004;55(1):197–223.
- Sun X, Xie Z, Zhang C, Mu Q, Wu W, Wang B, et al. A characterization of grapevine of GRAS domain transcription factor gene family. *Funct Integr Genomics. Functional & Integrative Genomics*; 2016;347–63.
- Sung S, Amasino RM. Vernalization and epigenetics: How plants remember winter. *Curr Opin Plant Biol*. 2004;7(1):4–10.
- Szűcs P, Skinner JS, Karsai I, Cuesta-Marcos A, Haggard KG, Corey AE, et al. Validation of the VRN-H2/VRN-H1 epistatic model in barley reveals that intron length variation in VRN-H1 may account for a continuum of vernalization

- sensitivity. *Mol Genet Genomics*. 2007 Feb 28;277(3):249–61.
- Tabuchi M, Abiko T, Yamaya T. Assimilation of ammonium ions and reutilization of nitrogen in rice (*Oryza sativa* L.). *J Exp Bot*. 2007;58(9):2319–27.
- Taiz L, Zeiger E. *Plant Physiology*. 4th ed. Sunderland, MA, USA: Sinauer Associates; 2006.
- Taiz L, Zeiger E. *Plant Physiology (Fifth Edition)*. Sinauer Assoc. 2010.
- Takatani N, Ito T, Kiba T, Mori M, Miyamoto T, Maeda S -i., et al. Effects of High CO₂ on Growth and Metabolism of Arabidopsis Seedlings During Growth with a Constantly Limited Supply of Nitrogen. *Plant Cell Physiol*. 2014;55(2):281–92.
- Tavakkoli E, Fatehi F, Rengasamy P, McDonald GK. A comparison of hydroponic and soil-based screening methods to identify salt tolerance in the field in barley. *J Exp Bot*. 2012;63(10):3853–67.
- Tezara W, Mitchell VJ, Driscoll SD, Lawlor DW. Water stress inhibits plant photosynthesis by decreasing coupling factor and ATP. *Nature*. 1999;401(6756):914–7.
- Timm S, Wittmiß M, Gamlien S, Ewald R, Florian A, Frank M, et al. Mitochondrial Dihydrolipoyl Dehydrogenase Activity Shapes Photosynthesis and Photorespiration of Arabidopsis thaliana. *Plant Cell*. 2015;27(7):1968–84.
- Toenniessen GH, O'Toole JC, DeVries J. Advances in plant biotechnology and its adoption in developing countries. *Curr Opin Plant Biol*. 2003;6(2):191–8.
- Tsutsumi K, Konno M, Miyazawa S-I, Miyao M. Sites of Action of Elevated CO₂ on Leaf Development in Rice: Discrimination between the Effects of Elevated CO₂

- and Nitrogen Deficiency. *Plant Cell Physiol.* 2014;55(2):258–68.
- Uematsu K, Suzuki N, Iwamae T, Inui M, Yukawa H. Increased fructose 1,6-bisphosphate aldolase in plastids enhances growth and photosynthesis of tobacco plants. *J Exp Bot.* 2012;63(8):3001–9.
- Ullrich SE. Significance, Adaptation, Production, and Trade of Barley. In: Ullrich SE, editor. *Barley Prod Improv Uses.* Oxford, UK: Wiley-Blackwell; 2011. p. 3–13.
- UNFCCC. Kuwait's Initial National Communications under the United Nations Framework Convention on Climate Change. 2012.
- Velitchkova M, Doltchinkova V, Lazarova D, Mihailova G, Doncheva S, Georgieva K. Effect of high temperature on dehydration-induced alterations in photosynthetic characteristics of the resurrection plant *Haberlea rhodopensis*. *Photosynthetica.* 2013;51(4):630–40.
- Ventrella A, Catucci L, Agostiano A. Effect of aggregation state, temperature and phospholipids on photobleaching of photosynthetic pigments in spinach Photosystem II core complexes. *Bioelectrochemistry.* 2008;73(1):43–8.
- Vermeulen SJ, Campbell BM, Ingram JSI. Climate Change and Food Systems. *Annu Rev Environ Resour.* 2012;37(1):195–222.
- Voss I, Sunil B, Scheibe R, Raghavendra S. Emerging concept for the role of photorespiration as an important part of abiotic stress response. Weber A, editor. *Plant Biol.* 2013;15(4):713–22.
- Walker B, Ariza LS, Kaines S, Badger MR, Cousins AB. Temperature response of in vivo Rubisco kinetics and mesophyll conductance in *Arabidopsis thaliana*: comparisons to *Nicotiana tabacum*. *Plant Cell Environ.* 2013;36(12):2108–19.

- Walker BJ, Strand DD, Kramer DM, Cousins AB. The Response of Cyclic Electron Flow around Photosystem I to Changes in Photorespiration and Nitrate Assimilation. *PLANT Physiol.* 2014;165(1):453–62.
- Walker BJ, VanLoocke A, Bernacchi CJ, Ort DR. The Costs of Photorespiration to Food Production Now and in the Future. *Annu Rev Plant Biol.* 2016;67(1):107–29.
- Wang D, Li X-F, Zhou Z-J, Feng X-P, Yang W-J, Jiang D-A. Two Rubisco activase isoforms may play different roles in photosynthetic heat acclimation in the rice plant. *Physiol Plant.* 2010;139(1):55–67.
- Wei K, Han P. Pentatricopeptide repeat proteins in maize. *Mol Breed. Molecular Breeding*; 2016;36(12):170.
- Wellmer F, Riechmann JL. Gene networks controlling the initiation of flower development. *Trends Genet.* 2010;26(12):519–27.
- Werner T, Holst K, Pors Y, Guivarc'h A, Mustroph A, Chriqui D, et al. Cytokinin deficiency causes distinct changes of sink and source parameters in tobacco shoots and roots. *J Exp Bot.* 2008;59(10):2659–72.
- White AC, Rogers A, Rees M, Osborne CP. How can we make plants grow faster? A source–sink perspective on growth rate. *J Exp Bot.* 2016;67(1):31–45.
- Wiczarz M, Gubernator B, Kruk J, Niewiadomska E. Enhanced chloroplastic generation of H₂O₂ in stress-resistant *Thellungiella salsuginea* in comparison to *Arabidopsis thaliana*. *Physiol Plant.* 2015;153(3):467–76.
- de Wit M, Galvão VC, Fankhauser C. Light-Mediated Hormonal Regulation of Plant Growth and Development. *Annu Rev Plant Biol.* 2016 Apr 29;67(1):513–37.

- Wu F, Shi X, Lin X, Liu Y, Chong K, Theißen G, et al. The ABCs of flower development: mutational analysis of AP1 / FUL -like genes in rice provides evidence for a homeotic (A)-function in grasses. *Plant J.* 2017;89(2):310–24.
- Xu G, Fan X, Miller AJ. Plant Nitrogen Assimilation and Use Efficiency. *Annu Rev Plant Biol.* 2012;63(1):153–82.
- Xu Q, Krishnan S, Merewitz E, Xu J, Huang B. Gibberellin-Regulation and Genetic Variations in Leaf Elongation for Tall Fescue in Association with Differential Gene Expression Controlling Cell Expansion. *Sci Rep.* Nature Publishing Group; 2016;6(1):30258.
- Yamamoto Y, Kai S, Ohnishi A, Tsumura N, Ishikawa T, Hori H, et al. Quality Control of PSII: Behavior of PSII in the Highly Crowded Grana Thylakoids Under Excessive Light. *Plant Cell Physiol.* 2014;55(7):1206–15.
- Yamori W, von Caemmerer S. Effect of Rubisco activase deficiency on the temperature response of CO₂ assimilation rate and Rubisco activation state: insights from transgenic tobacco with reduced amounts of Rubisco activase. *Plant Physiol.* 2009;151(4):2073–82.
- Yamori W, Shikanai T. Physiological Functions of Cyclic Electron Transport Around Photosystem I in Sustaining Photosynthesis and Plant Growth. *Annu Rev Plant Biol.* 2016;67(1):81–106.
- Yan K, Chen P, Shao H, Zhang L, Xu G. Effects of Short-Term High Temperature on Photosynthesis and Photosystem II Performance in Sorghum. *J Agron Crop Sci.* 2011;197(5):400–8.
- Yin X. Improving ecophysiological simulation models to predict the impact of elevated atmospheric CO₂ concentration on crop productivity. *Ann Bot.*

2013;112(3):465–75.

Yuan L. Progress in super-hybrid rice breeding. *Crop J.* Elsevier B.V.; 2017 Feb;(http://dx.doi.org/10.1016/j.cj.2017.02.001):1–4.

Zadoks JC, Chang TT, Konzak CF. A Decimal Code for the Growth Stages of Cereals. *Weed Res.* 1974;14(6):415–21.

Zhang D, Yuan Z. Molecular Control of Grass Inflorescence Development. *Annu Rev Plant Biol.* 2014;65(1):553–78.

Zhang L, Melø TB, Li H, Naqvi KR, Yang C. The inter-monomer interface of the major light-harvesting chlorophyll *a/b* complexes of photosystem II (LHCII) influences the chlorophyll triplet distribution. *J Plant Physiol.* 2014;171(5):42–8.

Zhang M, Wang C, Lin Q, Liu A, Wang T, Feng X, et al. A tetratricopeptide repeat domain-containing protein SSR1 located in mitochondria is involved in root development and auxin polar transport in *Arabidopsis*. *Plant J.* 2015;83(4):582–99.

Zhang SX, Babovic V. A real options approach to the design and architecture of water supply systems using innovative water technologies under uncertainty. *J Hydroinformatics.* 2012 Jan;14(1):13–29.

Zhang XC, Yu XF, Ma YF. Effect of nitrogen application and elevated CO₂ on photosynthetic gas exchange and electron transport in wheat leaves. *Photosynthetica.* 2013;51(4):593–602.

Zhou Y, Tol RSJ. Evaluating the costs of desalination and water transport. *Water Resour Res.* 2005 Mar;41(3):1–10.

Zhu XG, Long SP, Ort DR. Improving photosynthetic efficiency for greater yield.

Annu Rev Plant Biol. 2010;61:235–61.